University of Alberta

A Study of the Relative Contributions of HSV-1 Proteins to the Process of Host Shutoff

by

Leslie Jill Shai

A thesis submitted to the Faculty of Graduate Studies and Research in partial fulfillment of the

requirements for the degree of Master of Science

in

Virology

Department of Medical Microbiology & Immunology

Edmonton, Alberta

Fall 2004

Library and Archives Canada
Published Heritage Branch
395 Wellington Street
Ottawa ON K1A 0N4
Canada

Bibliothèque et Archives Canada
Direction du Patrimoine de l'édition
395, rue Wellington
Ottawa ON K1A 0N4
Canada

Your file Votre référence
ISBN: 0-612-95849-3
Our file Notre référence
ISBN: 0-612-95849-3

The author has granted a non-exclusive license allowing the Library and Archives Canada to reproduce, loan, distribute or sell copies of this thesis in microform, paper or electronic formats.

L'auteur a accordé une licence non exclusive permettant à la Bibliothèque et Archives Canada de reproduire, prêter, distribuer ou vendre des copies de cette thèse sous la forme de microfiche/film, de reproduction sur papier ou sur format électronique.

The author retains ownership of the copyright in this thesis. Neither the thesis nor substantial extracts from it may be printed or otherwise reproduced without the author's permission.

L'auteur conserve la propriété du droit d'auteur qui protège cette thèse. Ni la thèse ni des extraits substantiels de celle-ci ne doivent être imprimés ou aturement reproduits sans son autorisation.

In compliance with the Canadian Privacy Act some supporting forms may have been removed from this thesis.

While these forms may be included in the document page count, their removal does not represent any loss of content from the thesis.

Conformément à la loi canadienne sur la protection de la vie privée, quelques formulaires secondaires ont été enlevés de cette thèse.

Bien que ces formulaires aient inclus dans la pagination, il n'y aura aucun contenu manquant.

Canada

Abstract

Host mRNAs decrease in abundance during HSV-1 infection, but the extent to which this occurs is unknown. Our results confirmed that most host mRNAs are downregulated during HSV-1 infection. Our results also suggest that unpolyadenylated RNAs are stable over HSV-1 infection. Vhs, ICP22 and ICP27 have all been implicated in the host shutoff process. We did not observe a requirement for ICP22 in RNA level host shutoff. Ljs1, a vhs$^-$/ICP27$^-$ HSV-1 mutant was generated in order to determine the relative contributions of vhs, ICP27, and other viral proteins to RNA level and protein level host shutoff. We observed that vhs and ICP27 contributed independently to the host shutoff process at both of these levels, though vhs contribution at the protein level was minor. In addition, we noted that ICP27 is not critical for mediating shutoff of some host mRNAs.

TABLE OF CONTENTS

Abstract .....
List of Tables .....
List of Figures .....
List of Abbreviations .....
1 INTRODUCTION 1
1.1 Herpesviridae family 1
1.1.1 Defining characteristics 1
1.1.2 Phylogeny of the Herpesviridae family 1
1.1.2.1 Herpes simplex viruses 1 & 2 3
1.2 The life cycle of HSV 6
1.3 Stages in the HSV-1 lytic cycle 7
1.3.1 Virion attachment, membrane fusion and nucleocapsid delivery into a host cell 7
1.3.2 The tegument and its proteins 7
1.3.3 Delivery of the HSV-1 genome to the nucleus 10
1.3.4 IE proteins and their functions 10
1.3.4.1 ICP0 10
1.3.4.2 ICP4 11
1.3.4.3 ICP22 12
1.3.4.4 ICP27 14
1.3.4.5 ICP47 16
1.3.5 E proteins and their genome replication activities. 17
1.3.5.1 HSV-1 genome 17
1.3.5.2 HSV-1 DNA replication 17
1.3.6 Late proteins and their roles in capsid structure, tegumentation, envelopment, virion maturation, and viron egress as well as modulation of host anti-viral responses 19
1.4 Cell cycle arrest induced by HSV-1 23
1.5 Host shutoff during HSV-1 infection 23
1.5.1 Primary & secondary shutoff 24
1.5.2 Primary host shutoff 24
1.5.2.1 Initially-delivered vhs 25
1.5.2.1.1 Vhs substrate specificity: 26
1.5.2.1.2 Enzymatic characteristics of vhs: What we learned about vhs from *in vitro* assays 26
1.5.2.1.3 VP16 tempering of vhs activity 29
1.5.2.2 Vhs requirements *in vivo* 30
1.5.3 Secondary host shutoff 31
1.5.3.1 Arrest of host transcription 31
1.5.3.2 ICP27-mediated splicing inhibition 33
1.5.3.3 Host translation arrest 35
1.5.4 Indirect shutoff effecter mechanisms: Modulators of other shutoff processes 37
1.5.5 Early studies of host mRNA levels during HSV infection 38
1.6 Study of global effects on mRNA levels with microarray analysis 39
1.7 Herpes microarray studies 42
1.8 Interpretation of fluorescence intensities from our microarray analysis 46

1.9 Extracellular matrix 50
1.10 Project rationale 53
2 MATERIALS AND METHODS 54
2.1 Cell and virus culture 54
2.1.1 Cell lines 54
2.1.2 Cell maintenance 55
2.1.3 Cryopreservation of cells 55
2.1.4 Virus strains 56
2.1.5 Generation of virus stocks: Isolation of cell-associated virus 57
2.1.6 Titration of virus stocks 58
2.1.7 Experimental infection 58
2.1.8 Monitoring viral plaque growth 59
2.2 Molecular biology techniques 59
2.2.1 Electrophoresis of DNA 60
2.2.2 Monitoring mRNA levels with Northern analysis 60
2.2.2.1 Isolation and quantitation of total RNA 60
2.2.2.2 Isolation of the poly A^+ fraction from total RNA 61
2.2.2.3 Electrophoresis, transfer, and immobilization of RNA 62
2.2.2.4 Detection of specific mRNAs 62
2.2.2.4.1 Generation and use of random prim- labeled probes 62
2.2.2.4.2 Generation and use of 5'end-labeled oligonucleotide probes 65
2.2.2.5 Imaging and quantitation of mRNA signal 66
2.2.3 Monitoring protein levels with Western analysis 66
2.2.3.1 Preparation of cell extracts for SDS-PAGE 66
2.2.3.2 Electrophoresis and transfer of total protein 66
2.2.3.3 Detection of vhs by Western blot 67
2.2.3.3.1 Pre-clearing the vhs antiserum 67
2.2.3.3.2 Western blot analysis 67
2.2.4 Analysis of metabolically labeled proteins 68
2.3 Generation of a $vhs^-/ICP27^-$ HSV-1 double mutant 69
2.3.1 Coinfection 70
2.3.1.1 Screening for the $vhs^-/ICP27^-$ double mutant from 5dl1.2 / vhsA coinfection 70
2.3.1.2 Screening for the $vhs^-/ICP27^-$ double mutant from 5dl1.2/ΔSma coinfection 71
3 RESULTS 74
3.1 Northern analysis of cluster 16 mRNAs 74
3.2 Northern analysis of "highly expressed and unchanged" group A mRNAs 79
3.3 Attempt to adjust microarray calibration 93
3.4 Host mRNA profile in HSV-1 infection of HEL cells 99
3.5 GAPDH, β-actin & collagen mRNA profiles over HSV-1 infection. 102
3.6 Vhs levels in KOS and 5dl1.2 infections 121
3.7 Collagen, GAPDH, β-actin, fibronectin & exostoses mRNA profiles over IE mutant and UV-irradiated IE mutant infections 124
3.8 Generation of a $vhs^-/ICP27^-$ double mutant of HSV-1 138
3.8.1 Screening for the $vhs^-/ICP27^-$ double mutant from 5dl1.2/ΔSma coinfection 143
3.9 Comparison of ljs1 with with parental strains ΔSma and 5dl1.2 148
3.9.1 Growth of ljs1 on V27 cells 148

3.9.2 Collagen and GAPDH mRNA profiles over ljs1, ΔSma, 5dl1.2, and KOS infections 150
3.9.3 HSV-1 induced host protein level shutoff by ljs1, ΔSma, 5dl1,2, and KOS 159
4 DISCUSSION 164
4.1 Evaluating the quantitation of our microarray analysis 164
4.2 Northern analysis of Alu transcripts & unpolyadenylated RNAs in HSV-1 infection 165
4.2.1 Why may polyA⁻ RNAs not be destabilized by vhs? 167
4.3 Detailed analysis of collagen, β-actin and GAPDH mRNAs in KOS, UV-irradiated KOS and ΔSma infections 169
4.3.1 Assessing mRNA destabilization/degradation activities of KOS, UV-irradiated KOS, and ΔSma infections 170
4.4 Detailed analysis of collagen, fibronectin, exostoses, β-actin and GAPDH mRNAs in IE mutant infections 170
4.5 Host shutoff studies conducted with the vhs⁻/ICP27⁻ double mutant, ljs1 175
4.6 Do vhs and ICP27 function in host shutoff independently? 178
4.7 Major conclusions from this work 179
5 BIBLIOGRAPHY 181

List of Tables

1	Most extensively downregulated mRNAs : cluster 16	49
2	Quantitation of cluster 16 mRNAs over the course of infection	78
3	Prevalence of *Alu* repeat element sequences in group A clones	87
4	Quantitation of a series of mRNAs over mock, IE deletion mutant infections, and UV-irradiated IE deletion mutant infections	133

List of Figures

1	Patterns of mRNA-level expression for 20 mRNA cohorts during infection as determined by microarray analysis.	47
2	Northern analysis of cluster 16 mRNAs	75
3	Northern analysis of group A mRNAs	81
4	Northern analysis of *Alu* element-containing group A mRNAs	82
5	Total and polyA$^+$ RNA signal intensities of group A RNAs over infection.	92
6	Northern analysis of total and polyA$^+$ RNA for cluster 16 and group A mRNAs	95
7	mRNA profiles for two cluster 16 mRNAs and one group A RNA	98
8	Northern analysis of ICP27 mRNA to verify transcriptional arrest in UV-irradiated and actD-treated infections	101
9	Northern analysis showing size determination for bands detected by probes for collagen and GAPDH mRNAs	104
10	Northern analysis identifying polyadenylated collagen mRNA species, and monitoring mock treatment effects	107
11	Northern analysis of GAPDH mRNA over the course of infection	110
12	Northern analysis of β-actin mRNA over the course of infection	111
13	Northern analysis of collagen mRNA over the course of infection	112
14	Western analysis illustrating vhs protein levels in 5dl1.2 and KOS infections	123
15	Northern analysis of a series of mRNAs over mock, IE mutant infections, and UV-irradiated IE mutant infections	125
16	Collagen mRNA profiles over IE mutant infections and UV-irradiated IE mutant infections	128
17	Fibronectin mRNA profiles over IE mutant infections and UV-irradiated IE mutant infections	129

18	Exostoses mRNA profiles over IE mutant infections and UV-irradiated 5dl1.2 (ICP 27$^-$) infections	130
19	GAPDH mRNA profiles over IE mutant infections and UV-irradiated IE mutant infections	131
20	β-actin mRNA profiles over IE mutant infections and UV-irradiated IE mutant infections	132
21	RNA profiles for different RNA species are distinct in 5dl1.2 (ICP27$^-$) infection	137
22	Scaled diagram illustrating vhs and ICP27 genes in the HSV-1 genome	140
23	Schematic diagram (not to scale) of desired crossover event to generate vhs$^-$ / ICP27$^-$ HSV-1 double mutant (ljs1) from ΔSma and 5dl1.2 parental strains	142
24	PCR analysis used in screening for vhs ΔSma truncation in potential vhs$^-$ /5dl1.2$^-$ HSV-1 strains	144
25	Southern analysis of the vhs locus in ljs1 and parental strains	146
26	Southern analysis of the ICP27 locus in ljs1 and parental strains	147
27	Comparison of ljs1 plaque size with that of KOS and parental strains, ΔSma, and 5dl1.2	149
28	Northern analysis of collagen and GAPDH mRNA over UV-irradiated KOS, KOS, ΔSma, 5dl1.2, and ljs1 infections	151
29	Quantitation of collagen and GAPDH mRNA over UV-irradiated KOS, KOS, ΔSma, 5dl1.2, and ljs1 infections	153
30	Northern analysis of collagen mRNA over UV-irradiated KOS, KOS, ΔSma, 5dl1.2, and ljs1 infections	156
31	Quantitation of of collagen mRNA over ljs1 and parental strain infections	157
32	Metabolic labeling comparison of KOS, ljs1, and ljs1 parental infections	160

List of Abbreviations

actD	actinomycin D
APS	ammonium persulfate
ATCC	American Type Culture Collection
β-gal	beta-galactosidase
BVH-1	bovine herpesvirus 1
cdc2/cdk1	cyclin dependent kinase 1
CDKI2C	cyclin dependent kinase inhibitor 2C
CstF	cleavage stimulation factor
CTGF	connective tissue growth factor
DEPC	diethylpyrocarbonate
DMEM	Dulbecco's modified Eagle medium
DMSO	dimethyl sulfoxide
DTT	dithiothreitol
E	early
EBV	Epstein-Barr virus
ECM	extracellular matrix
eIF	eukaryotic initiation factor
EST	expressed sequence tag
g	glycoprotein
GAPDH	glyceraldehyde-3-phosphate dehydrogenase
GFAP	glial fibrillary acidic protein
h.p.i.	hours post infection
HCMV	human cytomegalovirus
HFF	human foreskin fibroblast
HHV-1	human herpesvirus 1
HI-FBS	heat inactivated fetal bovine serum
HIV	human immunodefficiency virus
hnRNP K	heterogeneous nuclear ribonucleoprotein K
HSP	heat shock protein
HSV-1	Herpes simplex virus 1
HSV-2	herpes simplex virus 2
HVEM	herpesvirus entry mediator
ICP	infected cell protein
IE	immediate early
IRES	internal ribosome entry site
KSHV	Kaposi's sarcoma associated herpesvirus
L	late
LATs	latency associated transcripts
LL	leaky late
MOI	multiplicity of infection
MOPS	3-(N-Morpholino) propanesulfonic acid
NCBI	National Center for Biotechnology Information
NMOPS	Northern MOPS
O.D.	optical density
P	prototype isoform
p.f.u.	plaque forming units
PABP	polyA binding protein
PCR	polymerase chain reaction
PML	promyelocytic leukemia
REF	RNA and export factor binding proteins
RRL	rabbit reticulocyte lysate
SEM infection	skin, eyes and mouth infection
SF	serum free
snRNP	small nuclear ribonuclear protein
TIF	Translation initiation factor
TL	true late
TRIM	tripartite motif containing protein
TR_L	terminal repeat long
TR_S	terminal repeat short
UL	unique long
US	unique short
UV	ultra violet
vhs	virion host shutoff protein
VZV	varicella-zoster virus

1 INTRODUCTION

1.1 Herpesviridae family

1.1.1 Defining characteristics

Several defining structural features are common to all Herpesviridae family members (reviewed in (267, 269)). All herpesvirus genomes are composed of linear double stranded DNA that is packaged into icosahedral capsids. Surrounding the capsid structure is the tegument, a proteinaceous layer that can vary in thickness and appear amorphous (365). All herpesviruses have an envelope that is derived from host cell membranes, and that contains viral glycoproteins (319).

A fascinating and distinct feature of herpesviruses is their capacity to undergo latent infection, where no viral progeny are produced. Few viral proteins are produced in some latent herpes virus infections, and in others, no viral protein products are detected at all. The latent state is effectively maintained for the lifetime of the host. Reactivations from latency occur in fully immunocompetent hosts and serve as a reservoir of progeny for further transmission.

1.1.2 Phylogeny of the Herpesviridae family

The breadth of herpesvirus diversity is exemplified by the fact that many vertebrate organisms and at least one invertebrate organism are infected with herpes viruses. Herpes infection is species specific, indicating exquisite adaptation of herpesviruses through extensive coevolution with their hosts. While the Herpesviridae family is highly diverse, there are still some features of herpes viruses that effectively serve to categorize them into three subfamilies (phylogeny reviewed in (59)). These subfamilies, *Alphaherpesvirinae*, *Betaherpesvirinae* and *Gammaherpesvirinae*, are defined by the degree of host specificity, tissue tropism and rate of infection progress of their members. Herpes viruses are similarly categorized by phenotypic classification and molecular phylogenetic studies.

Alpha herpesviruses are able to infect a diverse range of host species, have a rapid life cycle and readily lytically infect in cell culture. A defining feature of the *Alphaherpesvirinae* family is the propensity to latently infect neural tissue. Herpes simplex virus 1 (HSV-1) / human herpesvirus 1 (HHV-1) and herpes simplex virus 2 (HSV-2) / human herpesvirus 2 (HHV-2) are two clinically relevant alphaherpesviruses from the genera Simplexvirus that will be discussed further below. Varicella-zoster virus (VZV) / HHV-3, a member of the Varicellovirus genera, is another clinically relevant alphaherpesvirus. VZV causes chicken pox in children and zosteriform lesions (shingles) upon reactivation in older adults (reviewed in (46, 285)).

Betaherpesviruses are characterized by their slow life cycle, narrow host range and slow progression of infection in cell culture. Two clinically relevant betaherpesviruses of the genera Roseolovirus, HHV-6 and HHV-7, generally cause acute febrile illness in young children, and sometimes cause a characteristic roseola rash (reviewed in (13, 135)). Human cytomegalovirus (HCMV), another clinically relevant herpes virus from the genera Cytomegalovirus, causes inapparent or mild flu-like symptoms in most infections (reviewed in (257, 336)). HCMV is harmful in congenital infections, causing sequelae in approximately 1 in 500 births (318).

Gammaherpesviruses replicate in lymphoblastoid cells *in vitro*, generally infect T and B cell lymphocytes and often latently infect lymphoid tissue. There are two known clinically relevant gammaherpesviruses. A Rhadnovirus genera member, Kaposi's sarcoma associated herpesvirus (KSHV) / HHV-8), is associated with several cancers: Kaposi's sarcoma, primary effusion lymphoma and the plasma cell variant of Multicentric Castleman's Disease (reviewed in (287)). Infection with a Lymphocryptovirus genera member, Epstein-Barr virus (EBV), is asymptomatic if acquired early in life, but often manifests as infectious mononucleosis if acquired later on. EBV has also been associated with lymphoproliferative disorders through transformation of B-lymphocytes: Burkitt's lymphoma, X-linked lymphoproliferative syndrome, and Hodgkin's disease (reviewed in (183)).

1.1.2.1 Herpes simplex viruses 1 & 2

HSV-1 and HSV-2 are both introduced into a host through mucosal surfaces or abraded skin, but have different tissue tropisms (clinical Simplexvirus infections reviewed in (354, 362)). HSV-1 generally infects epithelial cells at oral and pharyngeal sites through salivary secretions, producing lesions on the buccal or gingival mucosa, and then latently infects the trigeminal ganglia. HSV-1 reactivation generally results in lesions on the vermillion border of the lip. HSV-2 generally infects at genital sites through genital secretions and then latently infects the sacral ganglia. HSV-1 and HSV-2 are both capable of infecting both orally and genitally. Less commonly, HSV can infect other sites and produce other clinical manifestations. For example, herpes keratitis manifests as clouding of the cornea, after infection of the optical nerve with HSV. Herpetic whitlow, erythema multiforme, and herpes gladiatorum are three forms of HSV skin infection. HSV can cause fatal encephalitis. Neonates can also be infected with herpes simplex viruses, sometimes with severe sequelae. Neonates can be infected in the skin, eyes and mouth (SEM infection), have encephalitis with possible cognitive sequelae, or be infected systemically, possibly resulting in organ failure.

HSV-1 is endemic to the human population. Seroconversion to HSV-1 occurs earlier in life in developing countries than in developed countries; however by the age of 40, seroprevalence in all socioeconomic conditions is around 70-80% of the population (reviewed in (355)). HSV-1 prevalence generally increases with age, and plateaus after the age of 30 (308). In the United States, seropositivity reaches levels of 90% for the population over 70 years of age (360).

HSV-2 seroprevalence in the United States is 26% and 18% for females and males respectively (reviewed in (308)). HSV-2 infection is on the rise in the United States, where there was a 30% increase in HSV-2 prevalence between the late 1970's and early 1990's.

A significant recent change has been noted in the epidemiology of HSV. An increase in the prevalence of genital HSV-1 infection has been noted in the British Isles,

Scandinavia, and Germany. In some countries, it appears that the majority of first clinical episodes of genital herpes in young women are now due to HSV-1 (178).

Herpes infections can be treated, though not cured, with (reviewed in (352)) antiviral drugs. Acyclovir, penciclovir, and famciclovir are chain terminators that selectively act as substrates for the viral thymidine kinase. Both foscarnet and cifidovir (also a chain terminator) inhibit the viral DNA polymerase. New drugs are being generated to target other viral processes. For example, BAY 57-1293, a helicase-primase inhibitor, is being investigated for use in treatment of HSV (19).

Drug resistant HSV strains were not predicted to rapidly develop because, unlike human immunodeficiency virus (HIV), HSV does not have an extremely high mutagenic rate. Nonetheless, the development of acyclovir resistant HSV strains has been reported (213). Acyclovir resistance mutations occurred most frequently in the viral thymidine kinase gene, and rarely, in the gene coding for viral DNA polymerase. The risk of generating a drug-resistant HSV strain in treatment of an immunocompetent host is quite low. Most of the drug-resistance mutations were generated in immunocompromised hosts. Other antiviral drugs that act on the thymidine kinase gene, penciclovir, and famciclovir are often similarly ineffective in treating acyclovir-resistant strains, but drugs that work via alternate mechanisms, such as foscarnet and cifidovir, are still useful in treatment of such cases.

Protection with vaccines tested so far was found to be partial and transient, i.e., trials of potential HSV vaccines have proven to be generally unsuccessful (reviewed in (157)). The relatively higher efficacy of prophylactic HSV-2 vaccines in women may indicate that mucosal antibody responses from cervical secretions may be clinically important. There are several HSV vaccine protocols in phase I clinical trials, the potential of which is yet to be determined.

Neonatal infection occurs with an incidence ranging from 1 in 3500 to 1 in 20 000 births (reviewed in (150, 152)). Very significant improvements have been made in the last 25 years in treatment of these infections. PCR detection allows central nervous system infection to be detected before neurological sequelae develop and facilitates the detection of neonatal infections that do not present with obvious skin lesions. The risk of

lesion production and asymptomatic shedding at birth has been reduced by the prophylactic use of antivirals in at-risk pregnant mothers in the last month of gestation (291). When the mother shows evidence of infection, caesarian section effectively reduces the risk of transmission of HSV to the neonate in the birth canal (30). Acyclovir is successfully used in the treatment of recognized HSV neonatal infection as well as in prophylactic treatment of exposed neonates.

The increase in HSV-1 genital infection prevalence creates a problematic scenario for the prevention of neonatal herpes infection. As HSV-1 genital infections are often asymptomatic, there is often no clinical history to indicate prophylactic antiviral treatments before birth, nor do lesions present at birth to indicate caesarian section. Serology cannot be used to identify HSV-1 genital infection as seropositivity due to oral infection is so prevalent in the population. The only way to prevent neonatal HSV-1 infection in the absence of maternal symptom presentation is to systematically conduct rapid tests for genital asymptomatic shedding of HSV-1 during labour, and conduct ceasarian section, or post partum prophylactic acyclovir treatment of neonates as necessary.

Currently, clinical trials are underway to harness HSV-1's lytic activity for the treatment of malignant gliomas (reviewed in (289)). Glioma cells actively replicate in adult brain tissue, where normal brain cells do not. Replicating cells in brain tissue are selectively targeted by HSV-1 in these therapies. There are many benefits to this type of treatment, including the possibility that the "drug" can perpetuate and disseminate itself within the tumour for as long as tumour cells remain. The thymidine kinase negative *dl*sptK HSV-1 strain was first developed as a potential oncolytic virus (188). Unfortunately, *dl*sptK had excessive toxicity at high titers, and was therefore not used in phase I clinical trials. More recently G207, a HSV-1 strain with deletions in both copies of γ34.5 as well as a *lacZ* insertion in the UL39 locus, has been tested for oncolytic potential in phase I clinical trials (185). G207 successfully decreased the growth of some subcutaneous U87-MG tumours in nude mice and prolonged survival of some nude mice with intracranial U87-MG tumours (209). G207 is hypersensitive to ganciclovir and can

therefore likely be inactivated with standard anti-HSV therapies if adverse effects of cancer treatment with this virus occur (209).

1.2 The life cycle of HSV

HSV initially associates with its host cell via interactions between viral glycoprotein C and cell surface herparan sulfate moieties (reviewed in (268)). Further interactions between other viral surface glycoproteins and host cell receptors mediate viral envelope-plasma membrane fusion and release of the capsid into the cytoplasm. Upon release of the capsid into the cytoplasm, some tegument proteins are released from the capsid surface and mediate their activities. The capsid is transported to the nucleus on a microtubule, dyneine-like structure. The HSV genome is delivered to the nucleus. Viral genes are transcribed in a cascade of immediate early (IE), early (E), and late (L) gene expression. Immediate early proteins are largely transcriptional factors required to induce the expression of early and late genes. Early genes generally encode proteins used for the replication of viral DNA. Late genes generally encode structural components of the virion. True late (TL) proteins are only expressed after viral DNA replication proceeds. Leaky late (LL) proteins are expressed at low levels before viral DNA replication and are then expressed at high levels once viral DNA replication proceeds. Virions are assembled and are released from infected cells through the fusion of Golgi and plasma membranes or upon cell lysis. Neurons innervating HSV-infected sites become infected with HSV. Herpes simplex viruses are transported to neuronal cell bodies via retrograde axonal transport, whereupon, they latently infect the neuronal cells. In latent infection, latency-associated transcripts (LATs) are synthesized, but no viral protein synthesis has been confirmed. Various stress stimuli, such as UV-light, menstruation, and illness, trigger reactivation from latency by mechanisms that are not well understood. HSV virions are generated in latently infected neurons and again are transported along neuronal axons to sites innervated by the infected neuron. Reactivation lytic infection ensues, with or without the formation of clinically apparent lesions.

1.3 Stages in the HSV-1 lytic cycle

1.3.1 Virion attachment, membrane fusion and nucleocapsid delivery into a host cell

HSV-1 entry into the host cell occurs through fusion of the viral envelope with the host cell membrane and is mediated by viral envelope glycoproteins (reviewed in (297, 314)). Viral glycoproteins gB, gD, gH, and gL must be present and must be expressed on the same membrane in order to mediate this fusion (31, 342). Their functions are described below.

Initial tethering of the virion to the host cells is mediated by interactions between cell surface heparan sulfate and viral glycoproteins gB and gC (293, 359). gB is necessary for tethering, while gC greatly increases the efficiency of HSV-1 binding to cells, but is not absolutely required (123).

Tethering to heparan sulfate alone is not sufficient to mediate entry of HSV-1 virions into cells. Rather, interactions between viral gD and cell surface receptors are necessary to mediate fusion of the viral envelope and cell plasma membrane, so that the capsid and tegument can be released into the infected cell. gD can associate with the infected cell through 3 different kinds of receptors: a TNF receptor family member, herpesvirus entry mediator A (HveA) (212), two immunoglobulin family members, nectins 1 (HveC) (104) and 2 (HveB) (350), and some 3-0-sulfotransferase - modified heparan sulfate molecules (296). gH and gL form a heterodimer (95) that is required, along with gD (174) and gB (35), to mediate membrane fusion. The mechanism of the fusion event is not well understood. Recently, Browne *et al.*, through studies with modified gD molecules, suggested that gD must be anchored into both leaflets of a lipid bilayer to mediate fusion (32).

1.3.2 The tegument and its proteins

The mature tegument may appear amorphous, due to varying thickness of its composite layers, but it is actually a significantly structured entity (365). Cryoelectron microscope analyses indicate that the innermost layer of the tegument exhibits

icosahedral symmetry (365). Tegument assembly is described further below. Tegument proteins have pleiotropic effects on infected cells. They make the host cell hospitable for the entering nucleocapsid by modulation host cell metabolism, immune function, etc.

ICP1/2, a phosphoprotein encoded by UL 36 (204, 205), forms the first tegument layer surrounding the capsid (365) and complexes with a 140kDa protein that binds a-sequence DNA. ICP1/2 is not involved in cleavage or packaging of newly synthesized DNA (65). The viral genome, VP5 and ICP1/2 form a complex. ICP1/2 localizes to the nuclear envelope of infected cells (214), and likely chaperones the HSV capsid to the nuclear pore through this localization. ICP1/2 may be necessary to target capsids to the correct maturation pathway as virion maturation and egress is abrogated in the absence of ICP1/2 (65).

UL 37 is the largest open reading frame of HSV-1. UL37 encodes a phosphoprotein (11) that interacts with ICP1/2 that is thought to form the second layer of the tegument and that is postulated to be necessary for an early step in tegumentation (154).

VP13/14, encoded by UL47 (356), are tegument phosphoproteins that are believed to be posttranslationally-modified forms of the same protein (172). VP13/14 is targeted efficiently to the nucleus in numerous punctuate domains and is capable of shuttling between the nucleus and cytoplasm of the cell (75, 214).

VP22, a 38kDa major virion phosphoprotein (79) encoded by UL49, is necessary for efficient spread of HSV-1 from cell to cell during the course of productive infection (245). It localizes to the cell nucleus at late times in infection (246). The nuclear localization of VP22 is facilitated by microtubule reorganization during infection (159). Van Leeuwen *et al.* have suggested that VP22 may inhibit nucleosome deposition on the HSV-1 genome through inhibitory interactions with template activating factor I, which promotes ordered transfer of nucleosomes to naked DNA (345). Perhaps this process prevents silencing of the HSV-1 genome in initiation of lytic infection. A role for VP22 in tegumentation or final envelopment is suggested by its ability to target membranes of acidic compartments that may be derived from the trans-Golgi network (26).

US11 is a multifunctional protein. US11 is thought to mediate transport of nucleocapsids in anteretrograde axonal transport in neurons through its association with the human ubiquitous kinesin heavy chain, a microtubule-dependent motor protein (69). US11's ability to inhibit the PKR pathway was recognized (221) through the discovery that γ34.5$^-$ mutations can be complemented by second-site mutations (211) that induce premature expression of L US11 protein at early times post infection. US11 binds double stranded RNA and inhibits the activity of PKR by preventing the phosphorylation of eIF2α (43). A 68 amino acid fragment of US11 that binds RNA and associates with ribosomes can inhibit activation of the PKR kinase in a cell-free system, implicating these two affinities in the inhibition of PKR (247).

UL13 kinase is a serine-threonine protein kinase that phosphorylates many viral and cellular proteins and thus modifies their activities (252, 253). Its activity, along with that of host kinases, is thought to mediate dissociation of the tegument upon release into the host cell (215).

VP16 is an abundant tegument 65kDa phosphoprotein (214) that participates in several infection processes (reviewed in (269)). VP16 localizes to the nucleus (214), and therein, is a potent transactivator of viral IE gene expression (37, 315). In association with host cell factor HCF-1, VP16 binds TAATGARAT sequences in HSV-1 immediate early promoters complexed with the Oct-1 transcription factor, thereupon initiating IE gene transcription (reviewed in (124)). VP16 transactivation of IE genes is only necessary to initiate IE viral gene expression in low MOI infections (5). The C-terminal acidic transcriptional activation domain is required to mediate IE gene transactivation (4, 306).

Weinheimer *et al.* (353) observed that VP16 null mutants failed to efficiently package viral DNA and also failed to produce extracellular virions, perhaps through some defect in virion egress. Mossman *et al.* (219) postulated that these effects might be due to the extensive impairment of viral protein synthesis in VP16 null mutant infection, resulting in a simple lack of viral components to undergo the above processes. Mossman *et al.*, however, determined that a VP16$^-$/vhs$^-$ mutant infection that effectively enabled increased viral protein synthesis at late times post infection was still inhibited in some

viral egress activity post initial virion envelopment. Thus, VP16 does appear to be necessary for efficient egress.

VP16 and vhs, another tegument protein, participate in the process of host shutoff, as described in detail further below.

1.3.3 Delivery of the HSV-1 genome to the nucleus

The HSV-1 capsid is transported to the nucleus along microtubules (309), propelled by dynein (74). Dynactin is required for HSV-1 capsid transport as well (74). Capsids rapidly inject viral DNA upon binding to the nuclear pore complex in a process that requires importin-β (231).

1.3.4 IE proteins and their functions

Four of the five IE genes: ICP0, ICP4, ICP22 and ICP27 encode proteins involved in transcriptional regulation of infection. Many of these IE proteins have diverse pleiotropic functions in HSV-1 infection. The fifth IE protein, ICP47, is immunomodulatory. IE proteins and their functions are described below.

1.3.4.1 ICP0

ICP0 (reviewed in (81, 82)) is a protein that mediates pleiotropic effects during infection. It is a viral and cellular transcription regulator, a governor of latency, a protector from the interferon response, and a ubiquitin ligase. The activities of ICP0 are described below.

ICP0 mutants exhibit impaired growth in low MOI infections (83, 275, 327), but elicit wildtype-like infection at high MOI. ICP0 is critical for efficient infection initiated with HSV DNA alone, in the absence of tegument proteins (36). ICP0 and ICP4 can both activate viral transcription, and act synergistically (reviewed in (86)). ICP0 is a promiscuous viral transcriptional activator, and also upregulates transcription of some host mRNAs. It does not, however, appear to activate transcription by conventional means, through interaction with promoter sequences, as no specific promoter sequence required for its activity could be defined. Instead, ICP0 targets a host cell repression

mechanism to permit the initiation of the viral lytic cycle (reviewed in (82)). ICP0 localizes to, and disrupts ND10 sites (191), which are sites of chromatin repression and are involved in regulation of host cell transcription. The ND10 sites are disrupted by degradation of promyelocytic leukemia (PML) proteins targeted for degradation by ICP0's E3 ubiquitin ligase activity (84, 85). Other proteins that allegedly function in chromatin repression, such as Sp100, are also targeted for degradation by ICP0. (ICP0's ubiquitin ligase activity can target the degradation of many non-ND10 proteins in the cell, eliciting unknown pleiotropic effects in infection.) Everett suggests that high MOI infections (which introduce a high input of viral genomes) may be capable of saturating the ND10 inhibitory mechanism. This may serve to explain the different infection patterns of ICP0$^-$ infections at low and high MOIs.

ICP0$^-$ infection proceeds with differential permissivity in different cell lines. ICP0$^-$ mutants can infect U2OS cells, which are immortalized, as efficiently as wildtype virus. Vero cells are intermediately permissive, and non-immortalized fibroblast cells are the most restrictive. The mechanism by which U2OS cells can complement ICP0$^-$ infection is not known. It is possible that the antiviral biological function that ICP0 normally disrupts is not present in U2OS cells. Alternatively, U2OS cells may contain a self-suppressing activity that effectively substitutes for ICP0.

ICP0 mutants are hypersensitive to interferon, and fail to transcribe viral mRNAs in the presence of interferon (220). ICP0 may inhibit some interferon-stimulated responses by targeting some ND10 interferon-induced proteins to the proteasome for degradation.

1.3.4.2 ICP4

ICP4 is a 175kDa phosphoprotein that exists in solution as a homodimer and localizes to the nucleus during infection. In ICP4$^-$ infection, IE proteins and E ICP6 are overproduced while other E and all L proteins are not synthesized (63, 71). Thus, ICP4 is required for expression of most early and all late genes and is also required for downregulation of immediate early gene expression. ICP4 increases E and L mRNA levels by facilitating efficient E and L gene transcription (108, 116, 351). ICP4 is not

targeted to activate E and L genes through obvious sequence specificity. A TATA box alone is sufficient to direct ICP4 to act on its substrate for the purpose of activating transcription (116). ICP4 mediates viral transcriptional activation by enhancing the binding of TFIID to DNA, thus promoting transcription pre-initiation complex formation (115). ICP4 autoregulates its own expression through binding a negative autoregulatory response element in its own promoter (103, 230, 266). ICP4's affinity for different substrates and subsequent activity may vary according to its phosphorylation state. Dephosphorylated forms of ICP4 bind IE promoters, while phosphorylated forms bind E and L promoters (239). ICP4, ICP27 and the viral DNA OriS sequence are necessary to localize viral transcription to ND10 sites (335).

1.3.4.3 ICP22

ICP22 is a 68kDa guanylated, adenylated (22, 210) and phosphorylated (252, 253) protein. ICP22 is required for optimal replication in some primary human cell strains, as well as in rodent-derived cell lines (288). Prod'hon *et al.* (251) reported that unphosphorylated ICP22 downregulates the expression of CAT expression constructs under the control of IE promoters, including the ICP22 promoter itself, and that UL13 kinase, which is known to phosphorylate ICP22, partially reverses this inhibition. The putative repression of IE genes by ICP22 appears similar in cell types that differentially support the growth of ICP22 mutants (251, 288). Thus, putative IE gene downregulation does not explain the cell type - specific requirement for ICP22 in infection.

ICP22 is required to induce the modifications in the large subunit of host RNA polymerase II seen in HSV-1 infection (180, 260). Specifically, ICP22 is required for the depletion of the IIA RNA polymerase II isoform, which is hypophosphorylated and is involved in normal transcription initiation. ICP22 is also required for the formation of a novel intermediately phosphorylated RNA polymerase II isoform, IIi, which is capable of transcribing viral RNA. ICP22 is not however, necessary for the depletion of IIO, the hyperphosphorylated RNA polymerase II isoform that is involved in normal transcriptional elongation (180, 260, 261). The downstream effects of these post-translational modifications are not well understood, but are thought to possibly redirect

transcription machinery to the task of generating viral mRNA, and possibly contribute to the arrest of host transcription that occurs in host shutoff (described in section 1.5.3.1). Rice *et al.* determined that ICP22-dependent modification of the large subunit of RNA polymerase II occurred in ICP22$^+$ permissive and ICP22$^-$ non-permissive cell lines (260). This phenomenon therefore does not explain the cell-type dependent differences in ICP22$^-$ infection either.

In some primary human cells, and in some animal cell lines, ICP22 is necessary for the efficient expression of several true late gene mRNAs and their encoded proteins such as US11, VP19C and vhs (252, 288). Advani *et al.* (9) propose that ICP22 facilitates the expression of true late genes by enabling the unwinding of newly synthesized viral DNA templates, making them accessible for transcription. ICP22's effects in this process are not direct. ICP22 stabilizes cyclin dependent kinase 1 / cdc2 (cdk1), and facilitates the degradation of its cyclin partner, cyclin B (8). Advani *et al.* determined that functional cdk1 was necessary for the expression of one true late protein, US11(10). The viral DNA polymerase processivity factor, UL42 binds the remaining cdk1 in a stable complex that does have kinase activity, effectively substituting for cyclin B, and possibly redirecting the kinase to alternative substrates. This complex binds a phosphorylated form of host topoisomerase IIα that is thought to untangle newly synthesized viral DNA, making this DNA template accessible for late gene transcription (9). Advani *et al.* did not verify if this phenomenon was cell type specific.

UL13 kinase is also necessary for several of the processes mentioned above, including: alleviation of IE promoter inhibition (251) , stabilization and increasing the activity of cdk1 (8), destabilization of cyclin B (8) and RNA polymerase II modification (180). As UL13 kinase phosphorylates ICP22 (253) (ICP22 is the major substrate for UL13 kinase.), it is likely that UL13 participates in these processes indirectly through the post-translational modification of ICP22.

US1.5's transcription unit resides within that of ICP22. US1.5 is colinear with 2/3rds of the C-terminal portion of ICP22, and is expressed as an IE protein (42). US1.5 has functions which overlap with those of ICP22's C-terminal portion and is also phosphorylated by UL13 kinase (229).

The effects of ICP22 and UL13 kinase on host shutoff will be described in the host shutoff section.

1.3.4.4 ICP27

ICP27 is a 63kDa essential IE viral phosphoprotein (6) that has pleiotropic effects during infection. ICP27 is necessary for efficient regulation of the viral gene expression cascade. ICP27 improves the use of weak polyadenylation sites on several viral L mRNAs (199-201). ICP27 shuttles between the nucleus and the cytoplasm (206, 241, 278, 310), associates with unspliced viral mRNAs, and is thought to mediate export of unspliced viral mRNAs to the cytoplasm (278, 310). ICP27 is necessary to mediate host shutoff and is thought to contribute to the process both by arresting host transcription, and inhibiting host mRNA splicing (34, 118, 119, 175). ICP27 is also involved in the post-translational modification and relocalization of RNA polymerase II during infection. These ICP27 activities are described below. ICP27 shutoff activities are described in Introduction section 1.5.3.

ICP27 is required for downregulating the synthesis of 2 IE proteins, ICP4 and ICP27(274). Reports indicate that ICP27 is required for the expression of some E genes. Some work indicates that viral DNA replication is ICP27 dependent.. Sacks *et al.* reported that ICP27 mutants are able to mediate E protein (ICP6, ICP8, glycoprotein B, ICP36) synthesis and viral DNA replication (274). Uprichard and Knipe (343) showed that a different subset of E proteins (including UL5, UL8, UL52, UL9, UL42 and UL 30) are poorly expressed in the absence of ICP27 and that the E gene expression impairment occurs at the levels of mRNA accumulation. These two reports did not report conflicting results for any particular E protein and both groups agreed that ICP8 is efficiently expressed in ICP27$^-$ infection. In contrast to the report by Sacks *et al.* (274), several groups reported that impaired expression of a subset of E proteins in ICP27$^-$ infection manifests in an impairment of viral DNA replication (195, 259, 262).

TL protein (ICP1/2, ICP48, glycoprotein C) synthesis is greatly reduced in ICP27 mutant infections (274). LL protein (ICP15 and ICP19) expression is also drastically reduced in ICP27 mutant infections (274). ICP27 appears to be necessary for the

transcriptional upregulation of at least two late genes, glycoprotein C and UL47, as was demonstrated by comparison of RNA synthesis rates by pulse-labeling (138).

A link between ICP27 and activation of weak polyadenylation sites was first suggested in transfection studies conducted by Sandri-Golidin and Mendoza (282). They reported that transfected ICP27 (in the presence of ICP0 and ICP4) increased the protein expression of cotransfected plasmids encoding CAT mRNAs with weak polyadenylation sites that have an AATAAA recognition signal, but no G/U box (282). McLauchlan *et al.* (200, 201) reported similar results for transfected CAT constructs where the weak polyadenylation site came from the L UL38 gene. Through ICP27 mutant infections, and cotransfections with ICP27, McLauchlan *et al.* determined that the protein responsible for the increased 3' processing of these weak polyadenylation sites was ICP27. Transfected ICP27 was sufficient to induce the weak polyadenylation site use. Thus, ICP27 facilitates the use of weak polyadenylation sites, facilitating the expression of L genes that are otherwise poorly expressed. McGregor *et al.* (199) verified this phenomenon, and the necessity for ICP27 to mediate this phenomenon *in vitro*. McGregor *et al.* also determined that infection causes enhanced binding of the 64kDa component of cleavage stimulation factor (CstF) to polyA sites, and that ICP27 expression was necessary for this effect. Thus CstF recruitment may be a mechanism by which 3' processing is improved by ICP27.

Given that ICP27 has been implicated in both arrest of host transcription (316) and transcriptional activation of at least two L genes (138), it comes as no surprise that ICP27 has been found to associate with host RNA polymerase II. Small amounts of ICP27 associate with RNA polymerase II-general transcription factor complexes of low molecular mass (141). Zhou & Knipe (364) have verified the association of ICP27 with RNA polymerase II by reciprocal immunoprecipitations. At least a portion of this interaction is due to direct protein-protein interactions as RNAse treatment does not abolish the interaction. ICP27 was also found to be necessary to facilitate the association of ICP8 with RNA polymerase II. Whether ICP27 actually bridges the interaction, or increases RNA polymerase II affinity for ICP8 through alterations of RNA polymerase II

has not been determined. Whether these associations are involved in host transcriptional arrest and/or L gene transcription has not been resolved.

ICP27 is required for the nuclear export of intronless viral mRNAs (278, 310). The mechanism by which this occurs is still being resolved. ICP27 binds nuclear and cytoplasmic polyA$^+$ mRNA *in vivo* and this binding appears to be specific to unspliced RNA as 5 unspliced viral mRNAs were found to associate with ICP27, while two spliced viral mRNAs were not (279). Koffa *et al.* studied the mechanism of ICP27 mediated transport of unspliced viral mRNAs by microinjection of ICP27 into *Xenopus laevis* oocytes (158). ICP27 dramatically stimulated nuclear export of viral RNA. Koffa *et al.* proposed that ICP27 facilitates viral mRNA export via the TAP-mediated export pathway by recruiting REF (RNA and export factor binding proteins) directly, and then the TAP/NXF1 complex indirectly. They based this suggestion on the following observations. ICP27 complexes with REF and with TAP. Both REF and TAP are necessary to mediate unspliced viral mRNA export. ICP27 associates with heterogeneous nuclear ribonucleoprotein K (hnRNP K) (348). hnRNP K has homology to REFs, is capable of shuttling between the nucleus and the cytoplasm, may have a role in the processing and transport of pre-mRNA, and may be used by ICP27 to facilitate the export of unspliced viral mRNAs. Aly/Ref, the metazoan homologue of the yeast export factor Yra1p, interacts with TAP directly, and also interacts with ICP27 (46, 173). Deletions in ICP27 that abrogate Aly-Ref binding also abrogate viral unspliced mRNA export. These results are consistent with the idea that Aly/Ref is also important in ICP27 mediated mRNA-export.

1.3.4.5 ICP47

ICP47 is the only IE protein that has not been found to be involved in regulating HSV's gene expression cascade. ICP47 is an immunomodulatory protein. ICP47 prevents the presentation of HSV-1 antigens to immune cells by binding and inhibiting the activity of the TAP transporter (97, 126). Antigenic peptides therefore do not enter the endoplasmic reticulum. In the absence of antigenic peptides, MHC molecules are not stably complexed, nor do they come to be presented on the cell surface with viral antigen.

1.3.5 E proteins and their genome replication activities.

The HSV-1 genome is first described here in order to introduce its components and arrangement so that the process of genome replication described below is clear.

1.3.5.1 HSV-1 genome

The HSV-1 genome is G-C rich (68% G+C content), linear, 152 k.b.p.'s in length, and consists of two unique regions, unique long (UL), and unique short (US) respectively (reviewed in (24, 171), prototype genome sequence available through NCBI code NC_001806 or (3)). Each of these unique regions are flanked by repeat sequences termed terminal repeat long (TR_L), and terminal repeat short (TR_S) respectively, and in between UL, and US regions by the internal repeat long IR_L, and internal repeat short IR_S repeat sequences. Both genome strands direct synthesis of transcripts that encode viral proteins, and some open reading frames overlap. The A sites within the repeat sequences facilitate recombination between the viral repeat sequences such that the UL and US regions can invert relative to each other, yielding 4 HSV genome isoforms. HSV genome recombination is not required to maintain viral viability in cell culture (140, 244). HSV-1 genes are named for the position of their open reading frame along the UL, and US regions in the prototype (P) genome isoform.

1.3.5.2 HSV-1 DNA replication

Viral DNA replication occurs in distinct viral replication compartments that are close to or associated with ND10 sites in the nucleus (134, 192, 313).

The mechanism by which viral DNA replication is though to occur is described below (reviewed in (24, 171, 280)). Generally, E genes encode proteins that participate in this process, and their DNA replication functions are described below.

Poffenberger and Roizman (243) determined that HSV-1 genomes are either joined head to tail in the virion or are circularized upon release into in infected cell. This observation suggests the possibility that HSV-1 DNA replication occurs through a rolling circle mechanism. Deshmane et al. (66) conducted field inversion gel electrophoresis studies of viral DNA, in which genome length and well-associated viral DNA was

detected. The well-associated DNA was processed to 150kb genome unit lengths. There was a high ratio of joint to terminal fragments (2.5) as compared to virion DNA. This result suggests that HSV-1 DNA may be in concatameric form in the order of 1-2 genome lengths and that the association of the DNA to the wells in FIGE studies could be due to conformation rather than genome length (66). (This result could also be explained by a heavily branched multiple-genome DNA structure.) Additional evidence for the rolling circle DNA replication mechanism came from the observation by Skaliter et al. (299) of duplex circles with multi-unit linear appendages in electron microscopy studies. Skaliter et al. (299) proposed that HSV-1 DNA replication initiates as a theta replication, and then transfers to a rolling-circle genome replication mechanism to yield concatemeric HSV-1 DNA. (Direct evidence for theta replication intermediates had not been found.)

Jackson and DeLuca (136), however, recently found evidence to contest these postulates (reviewed in (280)). The strength of the rolling circle replication postulate depended on the putative presence of circularized genome templates in replicating cells. Jackson and DeLuca, however determined that circularized genomes were not found in replicating cells, but rather, were found in quiescent infections, approximating the latent state. Additionally, Jackson and DeLuca determined that circular genomes are only present in infection where ICP0 is not expressed, further linking the circularized genome to another feature of latently infected cells. HSV-1 genome replication is now postulated to occur through generation of heavily branched concatameric genome structures from which individual genomes can be isolated by recombination events. Other mechanisms may be considered in future. Despite debate about the macromolecular structure of HSV-1 DNA replication, some HSV-1 DNA replication processes are understood and are described below.

The viral genome contains 3 origins of replication: ori_L that is in the UL region, and ori_S, of which there are two copies, one in each of the repeats flanking the US region. Wu *et al.* (358) demonstrated that 7 HSV-1 genes (reviewed in (24)), when co-expressed in transfection studies, could reconstitute DNA replication on a plasmid containing a HSV origin of replication. UL9 recognizes, and binds a HSV ori sequence (77, 78, 232) as a homodimer (170). UL9 has nucleoside triphosphatase, and 3'-5' helicase activities

(23, 33, 72, 93) which make the genome accessible to the DNA replication machinery. UL9's processivity increases when it is complexed with the single stranded DNA binding protein, ICP8 (23). ICP8 also maintains unwound DNA in a single-stranded state (184, 273). A HSV DNA helicase-primase composed of subunits encoded by UL5, UL52, and UL8 (198) unwinds the HSV DNA at the replication fork, and primes DNA replication on the lagging strand (56, 57). A HSV DNA polymerase, two subunits of which are encoded by UL30 andUL42 respectively, replicates HSV DNA (100, 346). The polymerase also has 3'-5' exonuclease activity for the purpose of proofreading during replication, as well as RNaseH activity that likely degrades Okazaki fragments (55). HSV-1 encodes DNA replication proteins that are not necessary for growth in cell culture, but that may be necessary for replication of HSV DNA in non-replicating cells (such as neurons in reactivation from latency): alkaline endo-exonuclease (UL12) (117, 197), uracil DNA glycosylase (UL2) (38, 40, 197), deoxyuridine triphosphatase (UL50) (21, 39, 197, 357), thymidine kinase (ICP36) (28, 47, 48), and ribonucleotide reductase (14, 132, 197) (The large subunit is ICP6 and the small subunit is UL40.).

Concatamers containing multiple copies of the HSV-1 genome are generated during genome replication and are then cleaved into unit length at the Pac / DNA packaging signal. The following HSV proteins are necessary for viral DNA concatamer cleavage into unit-length genomes and for packaging of HSV DNA into capsids: UL15 (15), UL28 (7, 337), UL6 (166), UL33 (12), VP22A (292), VP5 (64), VP23 (64), UL12 (187, 290),.UL25 (203, 326), UL32 (167, 326), and ICP35 (167).

1.3.6 Late proteins and their roles in capsid structure, tegumentation, envelopment, virion maturation, and viron egress as well as modulation of host anti-viral responses

L HSV-1 genes generally encode structural proteins of the virion. The L proteins and their roles in the process of virion assembly and egress are described below. Capsid assembly is initiated via inter-subunit associations. The order in which these subassembly events occur is unknown. We do understand, however that viral DNA concatamer cleavage, viral DNA packaging, and capsid maturation are mechanistically

linked. Mature nucleocapsids then undergo tegumentation and envelopment events. Below, capsid structures are described. The various capsid forms, and when they occur are also noted. Further processes in the development of the mature virion are described.

Mature HSV-1 capsids have icosahedral symmetry (365) (capsid structure and assembly reviewed in (105, 263, 323)). The triangulation number of HSV-1 capsids, T=16, represents the fact that each triangular face of the HSV-1 capsid surface is composed of 16 substructural units whose central points approximate the subdivision of the triangular face into 16 equivalent subunits. Each of these subunits is composed of a VP5 multimer / capsomer. The VP5 capsomers at the face vertices are pentamers of VP5 (224). The remaining capsomers on the face center and edges are hexamers of VP5 (366). Triplexes of VP23 and VP19C, complexed at a ratio of 2:1 (224, 366), form the scaffold that connects the capsomers to each other (317, 366). VP26 molecules are complexed with VP5 molecules at a 1:1 ratio on the outer surface of hexamers (341).

Inside the capsid surface structure there is an internal scaffold or core formed from viral proteins VP22a (the major core protein), VP21, and VP24. VP22 is known to associate with chromatin and is likely associated with HSV-1 DNA that is packaged in the capsid as a toroid (99). UL26 is a self-cleaving viral protease that, upon self cleavage, generates both VP21 and VP24 (101, 341). VP24 is the viral protease responsible for cleavage of the internal scaffold, and facilitates viral DNA packaging (101, 250, 265).

Capsid designations correlate with different capsid maturation steps (capsid maturation reviewed in (324)) and are determined on the basis of their appearance in electron microscopy (EM) studies (106). "A" capsids, which lack viral, DNA have all the core components described above (366). "B" capsids contain viral DNA, as well as some proteins from the core (107). "C" capsids are mature capsids that contain condensed viral DNA, which has been completely packaged, and a mature core.

In immature virions, the capsomers do not have direct associations with each other, but rather are connected with each other only through web-like interactions with the triplex proteins (340). HSV-1 DNA is internalized through a channel passing though only one capsomer on any given capsid. UL6, in an oligomeric state of 12, forms a ring

through which DNA can pass, was determined to bind at only one vertex on any given virion, and likely forms the portal of entry for HSV-1 DNA (223). The encapsidation of viral DNA then triggers the removal of VP22a and VP21 from the core by VP24 proteolysis. Structural rearrangement of the capsid subunits to form the mature capsomer ensues (101). The capsomer channels become more narrow, VP5 capsomers undergo rotation such that the surface of the capsid is more contiguous, and the contacts between the capsomers are direct (125, 340).

Many aspects of the processes of primary tegument and envelope acquisition, de-envelopment, secondary (final) tegument and envelope acquisition and virion egress (reviewed in (144, 207, 300)) have been clarified only recently. Until recently, the mechanism by which the viral envelope is acquired was debated. One possible mechanism that had been proposed was that of the luminal pathway (80), in which the viral envelope was acquired when the virus budded through the inner nuclear membrane. The enveloped virions would pass through the ER secretory pathway and be released into the extracellular space. Evidence in support of this postulate included the prevalence of cytoplasmic viral particles that were enveloped in vesicles (80). Another mechanism proposed was that of the re-envelopment pathway, where a primary envelope is acquired when a capsid buds into the inner lamellae of the nuclear membrane, but is lost as the virion buds out the outer lamellae, releasing nucleocapsids into the cytoplasm. The capsid would then be re-enveloped as it buds into the trans-Golgi network, and then would be released from the cell upon fusion of this compartment with the plasma membrane. Evidence in support for the reenvelopment pathway includes the presence of naked capsids in the cytoplasm of HSV-infected cells (298) and the differences in phospholipid composition of the nuclear membrane and the mature virion envelope (344).

Skepper et al. (300) definitively showed that virion egress occurs through the envelopment, deenvelopment, reenvelopment pathway. Skepper et al. engineered a modified glycoprotein (gD) molecule that was ER-retrieved (and therefore targeted to the inner and outer nuclear membranes). This modified glycoprotein was present in peri-nuclear virion envelopes, but was not present in the envelopes of mature extracellular virions. This result indicated that the primary envelope had been shed and that the

mature virion envelope was acquired from a post-ER cytoplasmic compartment. There are still many questions pertaining to these processes that remain unresolved.

The tegument is also thought to be formed in two steps, with both a primary and secondary (mature) tegument being formed. The mature capsid is transported towards the nuclear membrane, and acquires a primary tegument protein layer. Both UL31 and UL34 are required for efficient primary tegument acquisition and primary envelopment and are found in the nuclear membrane, though their precise arrangement in the primary virion is not definitively known (44, 98, 155, 258, 270). The nucleocapsid acquires its primary envelope as it buds into the inner lamellae of the nuclear membrane (347). As described above, after passing through the perinuclear space the primary virion loses it primary envelope as it fuses with the outer nuclear membrane. UL31 and UL34 apparently do not remain associated with the capsid, as they are not components of the mature tegument (98, 300).

On the capsid surface, UL36 / ICP1/2 associates with capsid pentons to form the first tegument layer (205). This first layer actually maintains icosahedral symmetry (365). Klupp *et al.* (154) suggest that in pseudorabies virus tegument formation, UL37 forms the second tegument layer. While some tegument protein-protein interactions have been recognized, the rest of the tegument overall structure is not known at high resolution, and may be amorphous (365).

L particles are naturally-occurring membranous structures that contain viral envelope proteins, all known tegument proteins, but no capsid (264). We therefore know that tegument formation inclusive of all tegument proteins is possible with tegument assembly initiation at the site of envelopment. As to whether this tegument would have any or all required sub-structural arrangement has not been determined. *In vivo*, it is likely that some of the tegument is acquired as the nucleocapsid passes through the cytoplasm, and that some of it is acquired simultaneously with viral reenvelopment.

Reenvelopment is now understood to occur as the nucleocapsid buds into a Golgi complex vesicle (49, 67, 112, 143). Budding of virions into Golgi vesicles is facilitated by the gE-gI complex, which localizes to the trans-Golgi network (202). The viral surface glycoproteins mature as the virion passes through the Golgi compartments (67,

68) (320). Upon fusion of Golgi vesicles with the cell plasma membrane, or upon lysis of the host cell, mature virions are released into the extracellular space, ready to initiate infection on a new host cell. Alternatively, virions remain cell associated, and are transferred across cell junctions to neighbouring cells in a process which requires the gE-gI complex and in a manner resistant to neutralizing antibodies (70). The gE-gI complex sorts virions to the lateral surfaces (and not apical surfaces) of polarized infected cells (145).

γ34.5 is a multifunctional non-structural late protein. γ34.5 abrogates global translational arrest in an infected cell that would normally mediated through the PKR pathway. γ34.5 regulates protein phosphatase 1 such that it dephosphorylates the translation initiation factor eIF2α. eIF2α is thus maintained in a non-phosphorylated state that permits translation, despite induction of the cellular protein kinase PKR (double stranded RNA-activated) pathway that occurs is response to infection (52) (120). γ34.5 inhibits an interferon-induced antiviral pathway in U2OS cells at a post-transcriptional level (220).

1.4 Cell cycle arrest induced by HSV-1

HSV-1 induces arrest of the cell cycle at the G1 stage (reviewed in (94)). Interestingly, some elements of the cell cycle machinery are upregulated during infection, indicating that HSV-1 selectively maintains elements of the host cell cycle that facilitate HSV-1 replication. L particles are able to block cell growth; thus initially-delivered tegument proteins can mediate host cell growth arrest (58). ICP0, an IE protein packaged in the virion, is capable of arresting cell growth (128, 179). Another viral protein (other than ICP0) is capable of inducing cell cycle arrest (179). ICP27 is necessary for the inhibition of G1-phase functions (311).

1.5 Host shutoff during HSV-1 infection

During HSV-1 infection host mRNAs decrease in abundance (See Introduction section 01.5.5 for literature survey of reports on this subject.), polyribosomes are disrupted (227, 332, 333) and host translation is arrested (130, 133, 226, 248). The net

result of these processes is the general abrogation of host protein synthesis, and the redirection of the host metabolic apparatii to the generation of viral products. These processes constitute what is defined as HSV-1 induced host shutoff.

1.5.1 Primary & secondary shutoff

Two distinct shutoff phases: early / primary shutoff, and delayed / secondary shutoff were demonstrated in the following study (89). The HSV-1 mutant strain tsB7 has a temperature sensitive ability to deliver its genome to the nucleus. At the permissive temperature, tsB7 could mediate translational arrest, regardless of whether or not cell transcription was arrested. At the non-permissive temperature, however, tsB7 could mediate host translational arrest only if host transcription was arrested. Thus, there are elements of primary shutoff that can occur in the absence of *de novo* viral gene expression. There are also secondary shutoff processes that minimally require the transport of the viral genome to the nucleus and likely require the synthesis of new viral gene products.

1.5.2 Primary host shutoff

The term "virion host shutoff" is used to describe the shutoff activities that occur in the absence of viral gene expression that can be attributed exclusively to incoming virion components. HSV-1 and HSV-2 *virions alone* can induce the degradation of host mRNA in the absence *of de novo* viral gene expression (90-92, 283, 330). The studies cited above were conducted using several methods to prevent *de novo* viral gene expression, namely: UV-irradiation of virus, treatment of infections with actinomycin D or treatment of infections with cycloheximide. In transcriptionally arrested cells, the virion host shutoff effects appear to be sufficient to induce host shutoff at the protein level.

Hill *et al.* (127) acknowledged that while HSV-2 infection transcriptionally arrested by either UV irradiation or actinomycin D was able to induce translational arrest, UV-irradiated HSV-1 was not. However, it is worthwhile to note that many investigators did not distinguish between shutoff effects that occurred where only viral transcription

was arrested (UV-irradiation) and contexts where both virus and host were rendered transcriptionally incompetent. The results of Hill *et al.* expressly indicated that HSV-1 primary shutoff activities do not actually induce host translational arrest in a transcriptionally competent host cell. (The differences in primary shutoff potency between HSV-1 and HSV-2 have since been ascribed to different activities of their respective vhs proteins (87).)

1.5.2.1 Initially-delivered vhs

The virion host shutoff protein (vhs) (reviewed in (190, 307)) is a leaky late viral protein that is incorporated into the tegument. Vhs was identified as the mediator of virion host shutoff in studies described below.

Powell & Courtney (248) determined that HSV-2 shuts off host protein synthesis more rapidly and efficiently than HSV-1. Morse *et al.* (216) used this difference in host protein synthesis shutoff phenotype between HSV-1 and HSV-2 and a series of HSV-1 X HSV-2 intertypic recombinant to map the activity to the segment (between 0.52 & 0.59 mapping units) of the HSV-2 prototype genome. Kwong *et al.* (164) mapped the genetic location of the vhs function at higher resolution to between mapping units 0.604 to 0.606. Based on the mapping of the vhs1 primary shutoff defective mutation to the UL41 ORF, Smibert *et al.* (302) generated an antibody directed to amino acids 333-347 of the putative encoded protein. This antibody was used to identify vhs, whis was determined to be a 58kDa protein. Read *et al.* (256) found two forms of vhs, whose molecular masses are 58kDa and 59.5kDa respectively. Both forms of vhs are phosphorylated, but only the 58kDa form is incorporated into virions (256). There is an 8 to 16 fold enrichment of vhs protein in a partially purified virion extract relative to crude cell lysates, suggesting that the vhs protein is a virion component (302).

In assays where vhs-expressing plasmids were cotransfected with reporter gene constructs, 40 fold less HSV-2 vhs plasmid mediated the same shutoff activity as HSV-1 plasmid (87). Thus HSV-2 vhs is more catalytically potent than HSV-1 vhs. Additionally, in generating, and similarly testing HSV-1 and HSV-2 vhs chimeras, it was

found that amino acids 1 through 135, 210 through 245, and 369 through 492 could confer the increased HSV-2 vhs activity onto HSV-1 vhs (87).

1.5.2.1.1 Vhs substrate specificity:

Vhs does not have any known sequence specificity associated with it's nuclease activity. Viral mRNA does not escape its grasp. IE protein synthesis occurs at higher levels, and continues later into the time course of a shutoff-defective vhs1 mutant infection (255). In an effort to understand what caused the poor gene expression phase transition, Oroskar & Read (234) monitored the levels of ICP0, ICP4, and ICP27 mRNAs throughout infection. In WT HSV-1 infection, these mRNAs are expressed transiently and then degraded. However in vhs1 primary shutoff-defective infection, IE mRNAs were not degraded. Vhs is therefore necessary for IE mRNA turnover and timely progression through the viral gene expression cascade. Kwong & Frenkel (163) similarly verified the dependence of ICP4, ICP22, and ICP47 mRNA turnover on normal vhs function delivered in virions. Using translational read-outs, Kwong & Frenkel also interpolated that early and late gene mRNA turnover similarly depended on normal vhs function, and did not occur with the vhs-1 mutant. Oroskar & Read (233) directly monitored the half-lives of 10 viral mRNAs from among all viral kinetic classes. Functional vhs was also necessary for E and L gene downregulation at the mRNA level.

1.5.2.1.2 Enzymatic characteristics of vhs: What we learned about vhs from in vitro assays

Krikorian & Read (161) showed that vhs degradation activities were specific to mRNA, and did not occur with endogenous or with added 28S rRNA. The *in vitro* vhs activity was insensitive to micrococcal nuclease, indicating that vhs was not likely to be a ribonucleoprotein. The *in vitro* assay was dependent on added magnesium, but not on any energy-generating systems such as added ATP, GTP, creatine phosphate, or creatine phosphokinase.

Several groups asked the question: Does vhs function in the absence of other viral proteins? Zelus *et al.* (363) assayed mRNA degradation activities directly from crude

virion extracts and also developed an assay for vhs where it was *in vitro* translated in the absence of other viral products. The vhs was *in vitro* translated and assayed in rabbit reticulocyte lysate (RRL). mRNA degradation was induced by both KOS virions and *in vitro* translated WT vhs. Vhs can therefore mediate mRNA degradation independently of other viral proteins. (Since vhs was not purified to homogeneity, the existence of cellular vhs cofactors was not ruled out.) Similarly, Jones *et al.* (146) confirmed the ability of a transfected vhs gene to downregulate the synthesis of a protein (β-gal) encoded by a cotransfected plasmid, indicating that vhs functions independently of other viral proteins with respect to its ability to induce arrest of a host protein translation. Thus, vhs does degrade mRNA in the absence of other viral proteins.

Elgadi *et al.* (76) also used the RRL system to translate vhs, and then added *in vitro* transcribed substrates to monitor their degradation. Elgadi *et al.* made the following observations. Their *in vitro* stidies corroborated Krikorian & Read's conclusions that vhs requires magnesium, but not an energy-generating system to induce mRNA degradation. Ribosomes are not needed for vhs-induced mRNA degradation to proceed *in vitro*. Using specific end labeling, and primer extension analysis to analyze vhs mediated cleavage events at high resolution, Elgadi *et al.* initially detected 5' and 3' intermediates whose sum roughly yielded the length of intact substrate, suggesting initial endoribonucleolytic cleavage on one analyzed substrate. The initial cleavages of SRPα mRNA clustered at the 5'end of the mRNA. When encephalomyocarditis and poliovirus internal ribosome entry sites (IRESs) were introduced into *in vitro* target mRNA, initial degradation events were targeted directly 3' to the IRES sequences, as well as to the 5' end of the substrates, if IRESs were placed internally (76). While IRESs contain extensive secondary structure, it is not likely that extensive secondary structure is in and of itself effective in directing vhs cleavage as rRNA also has extensive secondary structure but is not similarly targeted by vhs.

Lu *et al.* (182) examined the *in vitro* activity of the vhs1 (T214I) mutant to further study the targeting of vhs to substrates. Vhs1 is unable to mediate initial cleavages on IRES–free substrates. Initial cleavage of mRNAs 3' of IRESes, however, still occurs with this mutant. Further degradation of mRNA 3' of the IRES, which occurs with WT

vhs, does not occur readily with vhs1. Thus, Lu *et al.* demonstrated a functional segregation of IRES-directed, and non-IRES-directed vhs activity. As well, the inability of vhs1 to mediate secondary cleavages to yield low molecular weight products, indicates that secondary cleavages, which have been postulated to be performed by ribonucleases other that vhs, show vhs dependence *in vitro*.

Given that vhs degrades mRNA, but not transfer or ribosomal RNA, Elgadi *et al.* (76) sought to determine if distinguishing features of mRNA such as 5' capping or polyadenylation served to direct vhs activity to mRNAs. Neither structural element was required for vhs recognition of mRNA in RRL *in vitro* assays. In mapping initial cleavages, Elgadi *et al.* did not observe any strongly selective sequence specificity. Thus far, ribonucleoprotein association is the only remaining feature associated with mRNAs that may be responsible for their selective degradation.

Krikorian & Read (161) suggested that one possible reason that they could not copurify nuclease activity from isolated virions (unpublished data) was that tegument vhs needs to associate with a cofactor protein in the host cytoplasm in order to function. Lu *et al.* (181) made observations that were consistent with this postulate. Vhs synthesized in yeast extracts is not able to induce mRNA degradation. Yeast-extract vhs is, however, functional when supplemented with RRL, which does not independently mediate mRNA degradation. RRL is able to complement the yeast extract vhs and therefore likely contains a cofactor or additional nuclease component to induce vhs nuclease activity. Feng *et al.* (88) found determined that the translation initiation factor, eIF4H may be a vhs cofactor. Vhs and eIF4H associate with each other as determined by coimmunoprecipitation of vhs and GST-tagged eIF4H in the yeast two-hybrid system. Some forms of vhs that have mutations that abolish vhs mRNA degradation activity *in vivo*, do not associate with eIF4H. Given that eIF4H associates with other translation initiation factors, such as eIF4A, eIF4G, and eIF4E, it is possible that these other proteins are relevant to supporting vhs activity. Rosalyn Doepker *et al.* (73) demonstrated that both partially purified eIF4H and partially purified eIF4B (a homologue of eIF4H) can complement vhs activity in *in vitro* assays. Given that no obvious mRNA sequence elements serve to direct vhs to their degradation, translation initiation – associated

proteins are alternative markers that vhs may use to target mRNAs. Translation initiation factors may therefore be relevant for vhs substrate specificity, as well as processivity.

1.5.2.1.3 VP16 tempering of vhs activity

Vhs and VP16 associate with each other *in vitro* as determined by co-immunoprecipitation with αvhs antibody, yeast-two-hybrid system analysis, and reciprocal solid-phase capture of vhs and VP16 using protein A fusion proteins (303).

A functional significance of the vhs/VP16 interaction was suggested by the following discoveries. VP16$^-$ infection initiates normally, but then undergoes a dramatic decline as viral protein synthesis is arrested at early and late times post infection (165). The abnormal and extensive destabilization of gB (L) mRNA in VP16 knockout infection suggested that downregulation of viral gene expression was occurring at the mRNA level, and therefore, arguably through vhs (165). VP16 influence on vhs function was demonstrated in tissue culture (165). A VP16 mutant that is unable to transactivate IE genes, but is able to bind vhs, completes the infection cycle, and does not show excessive viral translational arrest. Infection with virus defective in both VP16 and vhs genes proceeds readily (where there is obviously no vhs activity to downregulate). Cells transfected with a VP16-expressing plasmid were resistant to translational arrest induced by incoming virions in the context of ActD. Collectively, these studies illustrated the functional repression of vhs activity by VP16, and that this function could occur independently of IE gene transactivation. In the absence of VP16, vhs activity is more extensive, and excessive relative to its activity in WT infection.

The ΔSma mutant vhs protein, which lacks required sequence for vhs-VP16 interaction, failed to be packaged into virions (256). Therefore, Smibert *et al.* (303) proposed that VP16 may be required for proper vhs tegument localization.

The domains of vhs and VP16 that are sufficient for their interaction have been described. Monitoring vhs-VP16 interactions with the yeast two hybrid system demonstrated that vhs amino acids 310 to 330 were sufficient to mediate its association with VP16 (286). This minimal binding domain is conserved in HSV-2, but not other alphaherpesviruses, indicating that vhs activities present in other alphaherpesviruses may

be tempered by a protein other than VP16, or may be less catalytically potent (as for pseudorabies virus) and do not need to be downregulated for the infection course to proceed. The 369 N-terminal amino acids of VP16 are sufficient for vhs-VP16 interaction (303). The minimal VP16 amino-terminal subfragment necessary to mediate association with vhs is VP16 amino acids 1 to 345 (156). VP16 sites for interaction with vhs and sites for transactivation complex formation overlap. Vhs could block formation of the VP16 transactivation complex, but only if vhs was first bound with pre-incubation, indicating that vhs would likely be displaced by transactivation complex elements during infection initiation (303).

1.5.2.2 Vhs requirements *in vivo*

Vhs has been implicated in the neurotropic character of alphaherpesviruses. Five alphaherpesviruses: HSV-1, HSV-2, VZV, equine herpesvirus and pseudorabies virus have vhs homologues (18). Non-neurotropic β and γ herpesviruses do not. Perhaps vhs is necessary to mediate neuroinvasion during infection. The neuroinvasiveness putatively mediated by vhs may not correlate with its nuclease activity since HSV-1, HSV-2, and pseudorabies virus (76) vhs' are all involved in mediating neuroinvasiveness even though pseudorabies vhs is somewhat less potent *in vitro*. It would be interesting to determine if neuroinvasiveness, and vhs's capacity to induce degradation of mRNA are consistently associated.

A study conducted by Strelow & Leib exemplified the reduced neuroinvasiveness of vhs$^-$ HSV-1(329). In *in vivo* mouse studies, viral titers of vhs$^-$ HSV-1 infection were much lower in brain, cornea, and ganglia tissue. Vhs- infection was confined to areas of the cornea that were scarified prior to infection (328). Vhs$^-$ infections caused little clinical disease, and were impaired in their ability to establish latency and reactivate (329).

The idea that vhs is immunomodulatory has been put forward (reviewed in (305)). HSV-2 specific CD8$^+$ cytotoxic T-lymphocytes were increasingly able to target HSV-2 infected fibroblasts when fibroblasts were infected with vhs-defective (vhs mutant 333

vhsB) HSV-2 (338). Two groups reported that bovine herpes virus 1 (BHV-1) vhs contributed to the downregulation of MHC class I molecule synthesis and suggested that a BHV-1 vhs$^-$ mutant would have reduced pathogenicity, enhanced immunogenicity, and would serve as a good vaccination candidate (45, 110). Vhs facilitates evasion of non-specific host defense mechanisms through suppression of cytokine production and suppression of the interferon-α and interferon-β antiviral effects (331). Vhs is also reported to reduce levels of MHC class II (339). In the same study, γ34.5 was found to be even more important in the downregulation of MHC class II surface presentation. One could argue that viral immunomodulatory proteins, like γ34.5, are expressed in an untimely fashion in the retarded viral gene expression cascade of vhs$^-$ infections, such that they do not mediate their activities efficiently *in vivo*. In this scenario, vhs immunomodulatory effects are indirect. In contrast, vhs was sufficient to mediate immunomodulatory effects on dendritic cells in the context of minimal viral gene expression (276). Activation of some dendritic cell types was abrogated by vhs.

Are vhs$^-$ HSV-1 strains appropriate for use as vaccines? When replication incompetent (ICP8$^-$) vhs$^+$ and vhs$^-$ strains were compared, vhs$^-$ HSV-1 was found to be more immunostimulatory for both the humoral and cell-mediated immunity responses in the mouse model (102). Perhaps additional mutations in ICP47 and γ34.5 would further improve a vaccine candidate.

1.5.3 Secondary host shutoff

De novo viral protein synthesis initiates a second wave of host shutoff effects including: arrest of host transcription, inhibition of mRNA splicing and arrest of host translation. These processes and the viral proteins thought to mediate them are described below.

1.5.3.1 Arrest of host transcription

Activities of host RNA polymerases I, II, and III have all been shown to decrease to less than 50% of the levels observed in uninfected cells by 5 hours post HSV-1 infection (249). As virions did not trigger the arrest of host mRNA transcription, and as

E and L genes were not required to elicit transcription arrest, Spencer *et al.* (316) and Kemp and Latchman (148) both deduced that a viral IE protein(s) mediates the effect. The two investigator groups did not agree, however, on which IE protein(s) was responsible for the effect. Kemp *et al.* concluded that ICP22 was necessary for the transcriptional arrest of the 8 unidentified mRNAs that were examined. ICP0, ICP4, ICP27 and ICP47 did not contribute to host transcriptional arrest in their hands. Spencer *et al.*, however, found that ICP0, ICP4, and ICP27 each contributed to the transcriptional arrest of at least one mRNA that was examined, but that, contrary to expectation, ICP22 was not involved in the process. ICP0, ICP4 and ICP27 each contributed to the transcriptional arrest of a different subset of the mRNAs monitored. The transcriptional arrest of some mRNAs could be partially impaired in infections with several single IE knockout viruses. Spencer *et al.* acknowledged that differences in cell type and virus strains used may explain the conflicting observations in their work and the work of Kemp and Latchman.

How is the transcriptional arrest process directed to host, but not viral, mRNAs? Since HSV-1 E and L genes do not have recognizable unique sequences in their promoter regions to distinguish them from host genes (reviewed in Smiley *et al.*, 1991), it is thought that sequence differences do not serve to direct viral and host transcription to different fates. Changes in the post-translational modification of host RNA polymerase II may account for the selectivity of transcriptional arrest. As described in section 1.3.4.30, the phosphorylation state of the C-terminal domain of RNA polymerase II is modified during infection, and some of those modifications are mediated by ICP22. If considering the work by Kemp and Latchman (148), one logically concludes that the RNA polymerase modifications mediated by ICP22 likely manifest in the selective repression of host transcription. However, if considering the work conducted by Spencer *et al.* (316), then one would predict that the RNA polymerase modifications mediated by ICP22 are not responsible for arrest of host transcription. Consistent with this postulate, there are additional RNA polymerase modifications that occur in infection that have not been determined to depend uniquely on ICP22, but rather, are mediated redundantly by two or more IE proteins (141). During infection, the RNA polymerase II holoenzyme is

modified such that the essential general transcription factor, TFIIE is no longer associated with it. TFIIE is thought to be required for RNA polymerase II C-terminal domain phosphorylation. One can envision a scenario where several IE proteins can induce the removal of TFIIE from the RNA polymerase holoenzyme, inhibiting host transcription which requires this general transcription factor, and where ICP22 mediates the formation of RNA polymerase IIi which is capable of transcribing viral RNA.

1.5.3.2 ICP27-mediated splicing inhibition

Among the other defects noted for ICP27 mutants, Sacks *et al.* (274) noted that ICP27 mutants were unable to induce the shutoff of host protein synthesis. A large body of research supports the idea that ICP27 mediates host shutoff by inhibiting mRNA splicing, and hence, maturation of host mRNAs.

Martin *et al.* (186) first noticed a relationship between infection and splicing when they observed that small nuclear ribonuclear proteins (snRNPs), components of the splicing apparatus, were relocalized from their nuclear speckled dispersion, excluding the nucleoli, to cluster dispersion in interchromatin granules. The clusters progressively localized to the periphery of the nucleus. Phelan *et al.* (240) determined that snRNP relocalization during infection depended on ICP27, and that transfected ICP27 was sufficient to mediate the effect. ICP27 colocalized with the redistributed snRNPs.

Hardwicke & Sandri-Goldin (118) confirmed that the ICP27-dependent reduction of 3 spliced host mRNAs occurres post-transcriptionally and independently of virion-vhs. Hardy *et al.* suggested that pre-mRNA accumulation is indicative of splicing inhibition (119). They did not observe accumulation of host pre-mRNAs, but did observe the accumulation of viral ICP0 and UL15 pre-mRNA upon KOS infection. In ICP27 infection, no ICP0 or UL15 pre-mRNA accumulation was evident. Hardy *et al.* conducted ICP0/ICP27 cotransfection experiments to investigate the activities of ICP27 on ICP0 mRNA in the absence of ICP27-induced viral proteins. While the level of total ICP0 mRNA decreased in these cotransfections, the ratio of pre-mRNA to mature ICP0 mRNA increased.

Consistent with the idea that ICP27 is involved in inhibition of splicing, ICP27 associates with and modifies the phosphorylation state of several splicing proteins. ICP27 coimuunoprecipitates with highly conserved splicing factors termed SR proteins (279). The phosphorylation of U170K and an unidentified spliceosome-associated 85kDa protein is modified in the presence of ICP27 (281).

Recently, Lindberg & Krievi (175) also reported ICP27's ability to inhibit mRNA splicing *in vitro*, in a context where no other HSV-1 proteins were expressed. ICP27 was expressed in HeLa cells from a recombinant adenovirus where the E1A and E1B genes were removed, and replaced with the gene encoding ICP27 protein under the control of a CMV progesterone promoter. ICP27 was induced by the addition of activating virus, and progesterone agonist. Nuclear extracts were taken from these transfected cells, uninfected cells, and infected but non-induced cells. Input β-globin pre-mRNA and adenovirus pre-mRNAs were added to the nuclear extracts, and pre mRNA stability, as well as formation of splicing products was monitored. In ICP27-expressing extracts, 80-100% reduction in splicing activity was observed relative to control extracts. This difference in mRNA processivity was specific to splicing as RNA polymerase II activity was verified to be roughly equivalent in different extracts. The ability of ICP27-containing nuclear extract to confer pre-mRNA induction activity on ICP27$^-$ nuclear extracts was examined. ICP27-containing nuclear extract confers its ability to induce the accumulation of pre-mRNA on ICP27$^-$ extract, but a preincubation at 30^0 before splicing is assessed is required for the effect to be noted, implying that ICP27 has an enzymatic activity that acts over time to somehow alter the splicing apparatus.

Lindberg & Kreivi (175) also monitored the progressive formation of the spliceosome complex in ICP27-containing nuclear extracts, and noted that two stages in spliceosome complex formation are affected by ICP27. Briefly, the serial spliceosome complex stages are complexes E, A, B, and finally, the mature complex, C. Formation of the A complex is delayed in the presence of ICP27. The most striking ICP27-dependent effect on spliceosome complex formation is the strongly inhibited transition from the B to C complex, which involves protein rearrangements, and ATP hydrolysis. A, H, and B spliceosomal complexes isolated from ICP27 expressing cells migrate faster in native

PAGE, indicating that these complexes are somehow altered in the presence of ICP27 in an undetermined way.

Cheung *et al.* (50) reported that host α-globin (one of the small subset of host mRNAs that increase over infection) pre-mRNA accumulation depended on ICP27. In contrast to what was reported for other mRNAs however, concomitant reduction in the amount of spliced α-globin mRNA was not observed, nor was there inhibition of transport of pre-mRNA in infection. (As ICP27 facilitates the transport of unspliced viral mRNA, it is not surprising to see unspliced host mRNAs exported to the cytoplasm in the presence of ICP27.) Thus, ICP27's effects on pre-mRNA accumulation did not appear to actually reduce the availability of mature mRNAs, and would not therefore be responsible for protein level shutoff effects downstream. This work indicates that ICP27 likely mediates host shutoff by a mechanism independent of its effects on pre-mRNA levels.

How do we reconcile the contrasting results of Cheung *et al.* (50) and Lindberg *et al.* (175)? Both groups conducted their studies in Hela cells. It is possible however, that α-globin (monitored by Cheung *et al.*) and β-globin (monitored by Lindberg *et al.*) pre-mRNAs and mRNAs are differentially influenced by ICP27.

1.5.3.3 Host translation arrest

Sydiskis & Roizman (333) were the first investigators to examine polyribosome profiles, and their correlation with translation levels over infection. They reported a transient decrease, transient increase, and then gradual decrease, both in the number of polyribosomes, and the amount of translation activity over infection. They also noted that polyribosomes formed after infection sediment more uniformly and slightly faster in sucrose density gradients (were more uniformly sized and larger). The mechanism by which the polyribosomes are disrupted was not known. Nishioka & Silverstein (227) corroborated the results with respect to the presence of polyribosome disruption over infection, and determined that infection with UV-inactivated virus, and therefore a virion component, was sufficient to mediate the disruption. In cells transfected with a vhs-expressing plasmid, the amount of polyribosomes decreases while the amount of free 40S

ribosomal subunits increases (168). Vhs-dependent mRNA degradation which, as described above, is mediated by the virion, causes disruption of polyribosomes by destroying the template mRNA on which polyribosomes are assembled.

If all degraded mRNAs are similarly dissociated from polyribosomes, we would conclude that vhs degradation of RNA is the sole mediator of polyribosome alterations in infection. However, mRNAs that decrease to similar levels over infection are not all affected the same translationally, and by inference, are not in the same polyribosome complexes. Greco *et al.* (114) reported that while β-actin and ribosomal protein-encoding mRNAs are similarly degraded over infection, only the synthesis of β-actin protein is arrested. Greco *et al.* attribute these differences to differential association of mRNAs with polyribosomes. β-actin mRNA is less frequently associated with large polysomes, and more frequently associated with 40S ribosomal subunits during infection. In contrast, during infection, ribosomal protein-encoding mRNAs are increasingly associated with large polysomes, which are associated with efficient translation. Selective translational arrest occurred on a subset of mRNAs examined.

Laurent *et al.* (168) extended the above analysis to viral mRNAs, and determined that when viral mRNAs are translated, they are preferentially associated with large polyribosomes. However, even viral mRNA translation ceases, and viral mRNAs are eventually associated with the 40S ribosomal subunit as infection progresses. Perhaps viral mRNAs preferentially associate with polyribosomes at least transially, and are therefore preferentially translated.

How does HSV-1 infection modify the translational apparatus of a host cell to cause preferential translation of viral mRNA? During HSV-1 infection, several ribosomal subunits: S6, Sa, S2, and S3A become phosphorylated (189). These ribosomal modifications may potentiate the selectivity of ribosomes for associating with and/or translating viral mRNA. Several viral proteins are associated with ribosomes during infection, and may modify them in such a way as to mediate host translational shutoff, namely: US11, VP19C, and VP26 (113).

1.5.4 Indirect shutoff effecter mechanisms: Modulators of other shutoff processes

As described above, ICP22 has been implicated in host shutoff through host transcription arrest. Ng *et al.* (225) proposed an additional mechanism whereby ICP22 contributes to the mRNA degradation, and resultant host protein translational arrest components of host shutoff. They propose an indirect contribution of ICP22 to shutoff through ICP22 effects on vhs. Ng *et al.* observed a decrease in both the mRNA degradation and translational arrest components of host shutoff in ICP22$^-$ infection. They attributed these observations to concurrent decreases in vhs mRNA and protein synthesis as well as decreased incorporation of vhs into tegument observed in ICP22$^-$ infection. I.e., ICP22 is necessary for adequate amounts of vhs to be synthesized, packaged and delivered into an infected cell to mediate primary shutoff. Ng *et al.* found that a UL13 kinase knockout virus has the same shutoff defects that are observed in ICP22 KO infections, and suggest that UL13 kinase likely acts upstream of ICP22 in this same pathway.

Overton *et al.* (235) suggested that UL13 kinase directly increases vhs function through post-translational modification of vhs, and did not recognize an intermediary-acting protein. They did not note any differences in the amount of tegument vhs in UL13$^-$ infection. However, the indications that host shutoff was impaired in the absence of UL13 kinase in their study were quite poor. The only signal discussed as an index of host shutoff was a metabolic labeling band that migrated at the same position as actin. The metabolic labeling smear representing the multitude of host proteins was not clearly displayed, nor clearly shown to be maintained or dissipated in the relevant studies illustrated. Their work does not strongly argue for the contribution of UL13 kinase to shutoff. Overton *et al.* used a truncated UL13 kinase that may actually be shutoff competent, and capable of facilitating normal vhs packaging.

As described above, UL 13 kinase has been implicated in many ICP22-associated processes: alleviation of IE promoter inhibition, stabilization of cdk1 and destabilization of cyclin B, RNA polymerase II modification, and as described here, optimal packaging

of vhs in the tegument. ICP22 and UL13 kinase have been implicated commonly in at least two shutoff pathways, as well as many others, illustrating a mechanistic linkage between UL13 kinase, a virion structural protein, and ICP22. Purves & Roizman (253) have determined that UL13 kinase modifies the phosphorylation state of ICP22. This post translational modification may be the medium through which UL13 kinase mediates host shutoff and other activities.

1.5.5 Early studies of host mRNA levels during HSV infection

With Northern analysis of individual mRNAs, it has been found that several host mRNA decrease in abundance over HSV-1 infection. Globin mRNA decreased over infection of murine erythroid cells with the HSV-1 F strain (226). Smibert *et al.* (304) demonstrated that β-globin mRNA decreased over transcriptionally arrested (actD) and transcriptionally competent L7/14 infection of murine erythroleukemia cells. β-globin mRNA loss was dependent on expression of functional vhs (304). Human cytoplasmic β-actin mRNA decreased over infection in HeLa cells (114). Several mRNAs homologous to: human keratinocyte α-tubulin, human cytoplasmic β-actin and human heat shock protein (HSP) 70 mRNAs decreased during transcriptionally arrested (actD) HSV-1 & HSV-2 infections in Vero cells (330). These losses were reported relative to mock infection, which had also been transcriptionally arrested, and were reported to be dependent on functional vhs. Homologues of human fibroblast β-tubulin, 2.5 & 1.8kb mRNAs, human fibroblast β-actin, human fibroblast γ-actin, and histones H3 and H4 mRNAs decreased in abundance during both transcriptionally competent and transcriptionally arrested infection in comparison to respective mock infections in Vero cells (283). Inglis (133) determined that GAPDH and β-actin mRNA levels decrease over infection of BHK cells. Becker *et al.* (17) determined that β-actin, fibronectin, glucose transporter-1 and docking protein mRNAs were markedly reduced during infection. All 12 of the above mRNAs were shown to decrease over HSV-1 infection.

It is thus evident that the mRNA loss patterns of only a restricted subset of host mRNAs have been examined. mRNA profiles were studied in very few cell types,

frequently in non-human cell lines. Additionally, the mRNAs studied encode proteins representing only a few cellular processes. Four of the mRNAs analyzed encode cytoskeletal proteins, β and γ actin, and α and β tubulin. Histones H3 and H4 are both components of the nucleosome core used for DNA packaging. All mRNAs studied are highly expressed. mRNA profiles for genes that are expressed at low levels had not been examined.

Our lab chose to initiate an analysis of a broader spectrum of host mRNAs over infection in human host cells in hopes of verifying the extent to which previous results applied. We elected to look for subsets of host mRNAs whose expression might differ from mRNAs previously studied. Our lab pursued these questions with the technique of microarray analysis. The technique is summarized below. Microarray analysis of HSV-1 infection has been undertaken by and published from other labs since we initiated this work, and results from these works are summarized below.

1.6 Study of global effects on mRNA levels with microarray analysis

Microarray analysis (reviewed in (121, 129)) has greatly expanded the surveying ability of molecular biology, as it allows biologists to monitor the profiles of thousands of mRNAs simultaneously in comparative studies. Briefly, in a process analogous to slot-blotting, DNA sequences that each bind specifically to a unique RNA or cDNA sequence are immobilized discretely onto a glass slide in an ordered array. Current technologies allow tens of thousands of genes to be arrayed and assessed together. The RNA samples undergoing comparison can themselves be labeled for detection, but generally, mRNA-representative fluorescent cDNA is generated by one round of reverse transcription of the RNA. Hybridization reactions between immobilized unique cDNAs and sample-representative cDNA yields a fluorescent signal for each cDNA spot which serves as in index of the expression of that gene. These gene specific signals are quantitated, normalized, and interpreted in order to reveal information about gene expression patterns in a given study. There are alternate approaches to some of the procedures in microarray

experimental design that are relevant in the assessment of work presented here. Some of these procedural steps are described in more detail below.

Samples can be hybridized simultaneously on the same slide for optimal comparison, and be distinguished through the use of different fluorophore labels that absorb and emit light at different wavelengths (284). Cy3 and Cy5 labels are often used for two samples being compared within the same hybridization reaction (284). Fluorophore-labeled nucleotides cannot be used *in vivo* to synthesize fluorescent RNA directly because the fluorophores act as rather bulky side groups on nucleotides, inhibiting complete transcription elongation. Rather, a mRNA-representing cDNA sample is generated by one round of reverse transcription of the sample RNA. In order to selectively reverse transcribe mRNA from the total RNA isolate, reverse transcription is primed with polyT oligonucleotides. Fluorescent cDNA synthesis is only initiated within mRNA poly A tails. Like mRNA elongation, the bulk of fluorescently labeled nucleotides impairs complete cDNA elongation, generally resulting in frequently incomplete cDNAs with an average length of 500 nucleotides.

When fluorescent cDNA samples are hybridized simultaneously to microarrays, their signals need to be normalized to account for variability in other parameters within the experiment (reviewed in (2, 20, 111, 162, 254)). Efficiency of the reverse transcription reaction to synthesize mRNA-representative fluorescent cDNA may vary between samples because of variance in reaction temperature and reagent concentrations (361). Cy3 and Cy5 are incorporated into cDNA with different efficiencies (361). Additionally, the absolute values of fluorescence emissions vary between samples as fluorophores emit signal with variable intensity (361).

Several frames of reference can be used to normalize samples. Some normalization methods only function in biological systems where biological phenomena under examination achieve a stable steady state. These normalization methods are inappropriate in biological systems where massive changes of many genes occur, or when cell homeostasis is extensively disrupted. Some normalization protocols are described below.

Normalization protocols that use housekeeping genes operate under the assumption that housekeeping gene expression levels are likely stable in the experimental condition being tested if they are involved in basic cell metabolism and are stably expressed in many other experimental scenarios. This normalization practice is coming under challenge more recently, as variability in expression of "housekeeping genes" is increasingly observed (169).

Another normalization method that requires a generally stable state of the biological system under investigation is the method of constant majority, which operates under the assumption that the majority of genes expressed in a given system do not have a different transcription profile within a given study. Goryachev *et al.* (111) claim that the method of constant majority is valid when up to 50% of the genes are differentially expressed. The quantitative readout of mRNAs from one sample is "tuned up", retaining intra-sample ratios, until most mRNA species are reported as equal intensity between samples.

The normalization method of integral balance also requires that gene expression is not generally disrupted in the biological process under observation, and operates under the assumption that the total mRNA-representing cDNA signal is the same for samples being compared. The total array fluorescence emissions are equalized between samples after background correction. Signal intensities are effectively reported as a fraction of total intra-sample signal. This normalization method is inappropriate when a significant change in total mRNA is suspect in the test condition.

In analysis of biological phenomena where changes of high magnitude are expected in the transcription profiles of a large number of genes and where cell homeostasis is not expected to be conserved, the normalization method used is the method of control spots (111). Equivalent amounts of external reference mRNAs (not present in the samples analyzed) can be added to the total RNA samples after biological treatments and RNA harvesting. These external reference mRNAs undergo reverse transcription, hybridization, and detection, and are influenced by all the sources of data variability throughout these procedures. Normalization of samples to each other based on

these external reference mRNAs serves to control for these variables, regardless of the extent by which compared samples differ.

As a large volume of raw quantitation is obtained in microarray analysis, it is necessary to organize the quantitation is a meaningful way, with bioinformatics tools (reviewed in (301)). Genes that are differentially expressed can be designated as such based on a specified minimal fold increase or decrease. Pattern discovery can be done where similar RNA profiles are grouped into a specified number of clusters with the help of computer algorithms. Alternatively, class prediction can be done in which test RNAs, for which transcription profiles are known to be similar, are used to generate known classes. Genes of unknown classes are then sorted into these pre-defined groups, often adding new genes to a previously recognized coregulated gene cohort.

As microarray analysis interpretation can involve extensive variability and normalization, it is necessary to validate the results (reviewed in (53)). RNA profiles reported with microarray analysis should be confirmed with Northern analysis, RT-PCR, RNAse protection assays, *in situ* hybridization, etc. In order to evaluate the significance of the microarray results, it is helpful to monitor genes of interest at the protein level, to verify that RNA profile differences manifest in significant translation profile differences as well.

1.7 Herpes microarray studies

Microarray analysis has been used to monitor transcription profiles of infection with several herpesviruses other than HSV-1: KSHV (142, 217), HHV-6 (194), CMV (109, 149), VZV (147), EBV (41).

Generally speaking, microarray and macroarray analyses of HSV-1 infection have focused on monitoring viral gene expression in different cell types and different virus mutants. These studies also contained analysis of an albeit limited subset of host genes. Most microarray studies of HSV-1 infection indicated that host mRNA levels are generally downregulated. Each of these studies also determined that a subset of host genes is upregulated during infection. Some genes were found to be upregulated during HSV-1 infection in several studies.

The first array study of HSV-1 infection (151) was done by macroarray analysis, which differs from microarray analysis in the following ways. Hybridization is done on membranes with radioactive mRNA-representing cDNAs. This method has reduced resolution, and was used to assess the transcription profile of 588 human genes. As the radioactive cDNA could not be distinguished between samples, hybridization of different samples was conducted on different membranes, and in separate reactions. Within this study, mRNA-representing cDNA was primed with a cocktail of gene-specific primers (provided by the macroarray manufacturer), rather than with polyT oligonucleotides. Consistent with Northern analysis of most host mRNAs examined so far, Khodarev *et al.* determined that there was an overall decrease in the total amount of host mRNA over F-strain HSV-1 infection in HEL cells, as well as in two isogenic glioma cell lines, U87-lux.8 and U87-175.4. Khodarev *et al.* also found that six transcripts that encode regulatory proteins, transcription factors and one stress response protein, GADD45, were upregulated during infection. The upregulation varied with cell type and viral strain.

Stingley *et al.* (325) conducted an oligonucleotide-based microarray analysis to monitor the levels of all viral transcripts and the levels of 57 human stress response gene transcripts over KOS and *27lacZ* (ICP 27$^-$) infections of HeLa cells. Microarray results were strongly consistent with what is known about transcription profiles of viral RNAs analyzed by other methods. Stingley *et al.* (325), like Khodarev *et al.* (151), also found a general decrease in abundance of host transcripts, along with an increase in abundance of a small subset of stress response and transcription regulation genes. In microarray analysis of viral and host transcript profile in ICP27$^-$ infection, Stingley *et al.* determined that 10 of the viral transcripts analyzed are present at levels similar to those seen during KOS infection. One viral transcript (ICP4) is present at higher levels than those seen during KOS infection. Thirty-nine of the 52 viral transcripts monitored (including the UL41/vhs transcript) are present at reduced levels relative to wildtype infection, 21 of which are reduced by more than a factor of 5. ICP27 therefore affects the levels of many HSV-1 transcripts. The levels of 7 of the 57 stress response host genes monitored over KOS infection either do not change, or increase. The expression level of all the other host stress response genes monitored decreases. Stingley *et al.* reported that there is no

general decrease in host mRNA abundance by 6 hours post *27lacZ* infection. Indeed, some host mRNAs increase in abundance during *27lacZ* infection.

Taddeo *et al.* (334) monitored RNA-level expression of 12626 human gene transcripts in microarray analysis of mock, wildtype and vhs$^-$ infections. They also concluded that most host mRNAs decrease in abundance over wildtype infection, and that a small subset of host mRNA increase in abundance over infection. Four hundred and seventy-five transcripts increased in abundance 3 fold in HSV-1 F strain infection relative to mock infection. In comparing the host transcript levels in vhs$^-$ and KOS infections, Taddeo *et al.* determined the following. The number of host transcripts upregulated at early times post vhs$^-$ infection was higher. The number of host transcripts downregulated at late times post vhs$^-$ infection was lower. Downregulation of some host transcripts was delayed in vhs$^-$ infection.

Wagner *et al.* (349) monitored viral transcript abundance in microarray analysis of HSV-1 infection in various cell types. They concluded that the viral transcription profile does vary somewhat from infected cell type to infected cell type. Wagner *et al.* note that the differences in HSV-1 pathogenesis in various cell types may be due to these variances in viral transcription profiles.

Kramer *et al.* (160) monitored KOS latent infection in mouse trigeminal ganglia using mouse macroarrays. They observed changes in the expression of genes involved in immune response, transcription regulation and neural transmission.

In our laboratory, Mossman *et al.* (218) monitored the expression of approximately 19,000 human transcripts in microarray analysis of mock and KM110 infections. KM110 bears lesions that eliminate the transactivation functions of ICP0 and VP16 proteins, and thus does not express viral genes in the absence of complementation by VP16. KM110 infection induced the expression of a small set of cellular genes, many of which are also upregulated by interferon α in the same cell type. The increase in expression of one of these RNAs was confirmed qualitatively by Northern analysis. Northern analysis also confirmed the observation in UV-irradiated KOS and V422 (VP16$^-$) infections.. Mossman *et al.* allude to comparative studies between mock and KOS infection conducted using the same experimental methodologies, and state that the

results will be discussed elsewhere. As the results from this microarray analysis led to my research, and as they have not been published, they are described below.

Microarray analysis was conducted by Aled Edwards' laboratory at the Banting and Best Research Institute, to examine the expression patterns of approximately 19,000 human expressed sequence tags (ESTs) (supplied by Genetic Systems) over the course of KOS infection by methods previously described (218). Holly Saffran, in our lab, conducted a mock infection and infections with KOS at a multiplicity of infection (MOI) of 10. Holly Saffran harvested RNA from the mock infection at 3 hours post infection (h.p.i.), and from the KOS infections at 3, 6, and 12 h.p.i. with Trizol® Reagent. The RNA was sent to the Edwards laboratory for further manipulations. Isolated RNA was reversed transcribed, enriching for reverse transcription of mRNA with the use of AncT (polyT oligonucleotide) primers, and incorporating fluorescent nucleotides to yield fluorescent mRNA-representing cDNA. To differentiate fluorescent signal between samples, Cy3-containing nucleotides were incorporated into one sample while Cy5-containing nucleotides were incorporated into the other. Specific detection of RNA species was achieved by allowing binding of fluorescent cDNAs from both samples simultaneously to previously characterized EST cDNAs immobilized on a glass slide. Bound cDNAs were detected with fluorescence microscopy and absolute fluorescence intensities were reported. Fluorescent signal for each EST was quantified. Local background signals were obtained from the perimeter of each EST signal. Background correction factors were calculated (excluding microarray slide defect regions with spurious background) and were duly subtracted from reported signal intensities for each EST examined. Samples were compared pairwise, mock with 3 hour infection, mock with 6 hour infection, and mock with 12 hour infection. Dye swapping, which entails repeating the experiment such that fluorophores used in each pairwise comparison are switched, was done to account for differential Cy3 and Cy5 incorporation. mRNAs for which Cy3 and Cy5 analyses were in disagreement were excluded from further analysis. The normalization method of constant majority was used.

1.8 Interpretation of fluorescence intensities from our microarray analysis

An algorithm developed by Andrew B. Goryachev was used in a pattern discovery protocol to assign the mRNA-representing signals into an arbitrarily selected number of 20 cohorts, based on the rate and magnitude of increase or decrease in their levels over the infection course. Figure 1 illustrates the categorization of mRNAs into these cohorts.

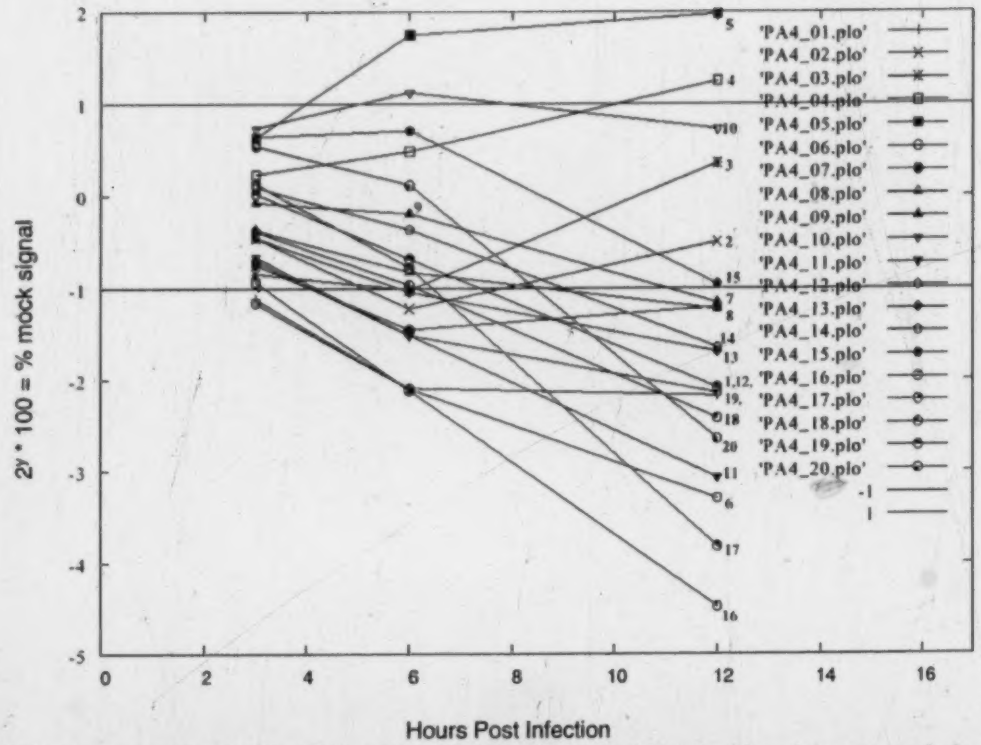

Figure 1. Patterns of mRNA level expression for 20 mRNA cohorts during infection as determined by microarray analysis. HEL cells were either mock infected, or infected with KOS at an MOI of 10. The mock infection was harvested at 3 h.p.i. with Trizol® Reagent. Infection RNA was similarly harvested at 3, 6, 9, and 12 h.p.i.. Fluorescently labeled cDNA, which selectively represented mRNA, was generated by conducting one round of RT PCR with AncT as primer. The cDNA was then hybridized to microarray chips with 20,000 EST cDNAs discretely immobilized on the array, and fluorescence emissions were analyzed to determine the levels of mRNAs, identified by their ability to hybridize to specific cDNA sequences. A computer algorithm was used to assign ESTs to 20 different cohorts which distinguish them in terms of their levels of expression over infection. The horizontal lines denote the cutoff values used to define mRNAs as increased or decreased over infection. Cluster PA4_16.plo', hereafter referred to as cluster 16, was the most severely downregulated cohort of mRNAs.

The array results, normalized with the method of constant majority, can be summarized as follows. Of the approximately 19,000 ESTs analyzed, approximately 10,000 were detectably expressed in mock-infected HEL cells, and were relevant to further comparisons. Approximately 900 (clusters 1, 6, 7, 8, 9, 11, 12, 13, 14, 16, 17, 18, 19 and 20) of these ESTs were characterized as downregulated as defined by a minimum decrease to 50% of initial levels by 12 h.p.i. Eighty-seven ESTs (clusters 4 and 5) were characterized as upregulated ocer infection, as defined by a minimum increase to 200% of initial levels by 12 h.p.i. The majority of the ESTs, approximately 9000 (clusters 2, 3, 10, and 15), or approximately 90% of the genes expressed in mock-infected HEL cells, were characterized as unchanged, as defined by no alteration in expression, or an alteration in expression by a factor less than 2.

These results are in stark contrast to what is currently understood to occur to host mRNA profiles over infection. These data suggest that, in contrast to literature reports cited above, host mRNA loss is not a general process in wildtype HSV-1 infection, but rather, occurs with only approximately 9% of host mRNAs.

ESTs in the most severely downregulated cohort of genes, cluster 16, are listed in Table 1. We observed that many of the genes (6 out of the 17 genes listed) encode components of, or proteins that stimulate the synthesis of, the extracellular matrix (ECM). ESTs with identity to the following ECM mRNAs are included in cluster 16: connective tissue growth factor (CTGF), exostoses 1, fibronectin 1 (detected by two I.M.A.G.E. clones listed in the cluster), the $\alpha 2$ subunit of type I collagen, and the $\alpha 1$ subunit of type III collagen. The extensive downregulation of ECM gene RNA-level expression observed was intriguing, as it might potentially be involved in the cytopathology observed during HSV-1 infection *in vitro*, in which cells lose their adhesion to neighbouring cells, and the culture surface. As the coordinate regulation of ECM genes during infection may have biological significance, and as their expression over infection was examined in more detail in work presented here, a brief introduction to the EDM, and the ECM genes analyzed further in this work is in order.

Table 1. Most extensively downregulated mRNAs : cluster 16.
The mRNAs of cluster 16 (reported by microarray analysis to be most extensively downregulated during infection) are listed here, specified by their Genbank accession numbers, and their gene products, or homologies, as annotated by the I.M.A.G.E. Consortium. The relative amount of these mRNAs over infection was reported as a fraction of mock infection signal. ECM protein-encoding mRNAs are shown in italics. Type I, α2 collagen, examined extensively in studies here, is shown in boldface.

Genbank accession number	Fraction of mock signal at specified h.p.i.			Gene product or homologies noted
	3 hr	6 hr	12 hr	
N74271	0.8265	0.3091	0.0539	site-1 protease (subtilisin-like, sterol-regulated, cleaves sterol regulatory element binding proteins)
AA115261	*0.6439*	*0.1731*	*0.0253*	*connective tissue growth factor*
AA210803	0.643	0.4044	0.0154	ESTs, [a] homology to H.sapiens glutaminase C ,UniGene cluster Hs.128410
W02072	0.6303	0.2728	0.0536	ESTs, Highly similar to CGI-121 protein [H.sapiens]
W61134	0.613	0.3171	0.0615	brain acid-soluble protein 1
N67818	*0.5808*	*0.4008*	*0.0485*	*exostoses (multiple) 1*
N90769	*0.5668*	*0.3104*	*0.0471*	*fibronectin 1*
N36862	0.5641	0.2643	0.0643	ESTs, [a] homology to UniGene cluster Hs. 269908 H. Sapiens on chromosome 11
R43785	0.5598	0.1739	0.069	ESTs, [a] homology with H.Sapiens phospholipid scramblase 1, UniGene cluster Hs. 348478
AA195589	*0.5583*	*0.3129*	*0.05*	*fibronectin 1*
AA135667	0.5559	0.2289	0.0686	ESTs, [a] Homology with H.Sapiens polyhomeotic-like 2, UniGene cluster Hs. 165263, BLAST alignment shows homology is very weak
N30461	***0.499***	***0.29***	***0.0486***	***collagen, type I, alpha 2***
N32802	*0.4444*	*0.1824*	*0.0262*	*collagen, type III, alpha 1 (Ehlers-Danlos syndrome type IV, autosomal dominant)*
AA043451	0.4138	0.1882	0.0567	platelet-derived growth factor receptor, alpha polypeptide
R66525	0.3506	0.1284	0.0334	ESTs, [a] homology to UniGene cluster Hs. 445715: human transcribed sequence that is weakly similar to protein ref:NP_071431.1 (H.sapiens) cytokine receptor-like factor 2, cytokine receptor CRL2, BLAST alignment shows homology is very weak
R34020	0.3444	0.1282	0.0463	ESTs, [a] BLAST alignment shows homology to H. Sapiens p21 (CDKN1A)-activated kinase 2 (Genbank acc. BC046197)
R66533	0.3413	0.1157	0.0433	ESTs, [a] homology toUniGene cluster Hs. 419195: hypothetical protein FLJ35954 which has 28% homology to H. Sapiens metastasis-associated protein 2

[a] Not official clone designations, relationships found through NCBI website searches and BLAST alignments

1.9 Extracellular matrix

The ECM (reviewed in (153, 242)) constitutes the structure surrounding and supporting cells. The ECM also serves as a medium for communication between neighbouring cells by allowing the following molecules to traverse between them: nutrients, hormones, cytokines, and other signaling molecules. The structure is dynamically responsive to growth stimulus, injury, and other forces of remodeling. Some of the main extracellular matrix proteins are described below. ECM proteins, many of which are in cluster 16, ar described below. Other cluster 16 ECM proteins are also described.

mRNAs coding for two collagen subunits, the α2 subunit of type I collagen and the α1 subunit of type III collagen are included in the list of mRNAs in cluster 16. Collagen, predominantly synthesized by fibroblasts, is the most abundant protein in the body, and the most prominent structural unit of the ECM. Thus far, 11 types of collagen have been identified. Collagen monomers form triple helix fibers upon secretion from the cell. Both collagen types I & III form fibrillar structures of the ECM. Type I collagen is a heterotrimer composed of two α1 subunits and one α2 subunit. Type III collagen is a homotrimer composed of three α1 subunits.

The mRNA coding for the α2 subunit of type I collagen was monitored extensively in infection studies presented in this work. It is therefore relevant to provide information on its structure. There are four polyadenylation sites in collagen mRNA (annotated in NCBI file code # NM_000089). There are 5 transcript variants of the mRNA coding for the α2 subunit of type I collagen, 5.1, 4.9, 4.6, 4.5, and 4.3 kilobases long. The collagen RNAs resolved into 3 bands in Northern analysis. There are 52 exons in the mRNA coding for the α2 subunit of type I collagen (60).

Collagen mRNAs contain regulatory sequences in their 5' and 3' UTRs. Within the 5'UTR of the mRNA coding for the α2 subunit of type I collagen, 115 bases downstream of the transcription start site, there is a 5' stem loop structure (NCBI code

J03464). Homologous stem loop structures are also found in the mRNAs coding for the α1 subunit of type III collagen (which is also in cluster 16) and the α1 subunit of type I collagen. The stem loop has been implicated in collagen mRNA stability dynamics. The stem loop of collagen α1 subunit type I mRNA decreases the stability of reporter RNAs when not complexed to proteins, more so in quiescent than active hepatic stellate cells (321). This indicated that, unless otherwise regulated, the stem loop structure may somehow actually target mRNA for destruction in quiescent cells. When bound to an unknown 120kDa protein in activated hepatic stellate cells, however, the stem loop containing reporter RNA is greatly stabilized (321). The reporter RNAs were further stabilized by addition of the 3'UTR of collagen α1subunit type I mRNA (321).

The mRNA coding for the α1 subunit of type I collagen mRNA contains a binding site for αCP_2, which is implicated in increasing the stability of this mRNA (322). The binding of αCP_2 was only observed in activated, and not quiescent hepatic stellate cells (322). αCP_2 has since been purported to stabilize collagen and α-globin mRNAs by binding polyA binding protein (PABP), thus stabilizing the binding of PABP to the polyA tail, or to eIF4G (51, 176). Lindquist *et al.* (176) propose that the 5'stem loop and αCP_2 binding activity of collagen mRNA may act synergistically. The stabilized mRNA molecule may be circularized through binding of αCP_2, or its associated proteins, with the 120kDa protein that binds the 5' stem loop structure in activated hepatic stellate cells. While a similar αCP_2 binding sequence has not been noted in the mRNA coding for the α2 subunit of type I collagen, it is possible that one may be present in this mRNA, also affording it stability.

Two cluster 16 I.M.A.G.E. clones are reported to detect fibronectin 1 mRNA. It is interesting to note that fibronectin is reported to be codistributed with collagen types I and III in the ECM, which are also in cluster 16. Fibronectins (reviewed in (96, 131)) are extracellular matrix glycoproteins that promote cell adhesion by connecting integrin cell surface receptors to cell matrices through interactions with collagen, heparan sulfate, and fibrin. Polymerization of fibronectin is required for deposition and maintenance of collagen type I and thrombospondin in the ECM, and is also required for maintaining the

localization of α5β1 integrins in cell-matrix fibrillar adhesions (312). Thus, fibronectin polymerization globally controls the composition and stability of the extracellular matrix and of cell-matrix adhesion sites. Fibronectin mRNA is spliced in three regions. There are at least 20 spliced variants of the fibronectin gene. The full sequences of only two of them are known. Other than a recognized need for fibronectins with differential affinity for various integrins, the reasons for the high number of fibronectin variants are not well understood.

Laminin attaches the basal lamina matrix (containing type IV collagen, heparan sulfate proteoglycans and entactin) to the cell surface.

Connective tissue growth factor (CTGF) (reviewed in (27, 228)), a heparin-binding growth factor and a member of the CCN family, is important for wound repair and stimulates cell proliferation, chemotaxis, adhesion and ECM formation. CTGF stimulates the expression of several extracellular matrix genes: α1 and α2 subunits of type I collagen, fibronectin, and α5 integrin. Promoter sequences of the gene encoding the alpha 2 subunit of type I collagen conferred CTGF responsiveness on a reporter gene, indicating that CTGF responsive elements are located within the first 376 b.p.'s of the collagen type 1 alpha 2 subunit promoter region (295). One I.M.A.G.E clone in cluster 16 is specific to CTGF mRNA. Notably, collagen and fibronectin genes, whose expression is reported to be regulated by CTGF, appear to be coordinately regulated with CTGF during infection.

Exostoses 1 mRNA codes for the exostoses 1 protein. A heterodimer formed from exostoses 1 and 2 proteins catalyses the glycosyltransferase reaction necessary for the polymerization of heparan sulfate, a component of the ECM (196). One I.M.A.G.E. clone in cluster 16 is specific to exostoses mRNA.

While some of the ECM genes discussed here are coregulated, BLAST alignments and literature search indicated that there are no universally common secondary structures or homologous sequences among all cluster 16 mRNAs.

1.10 Project rationale

The microarray analysis conducted by our lab suggested a general stability of host mRNA profiles, with only a minor subset of host mRNA profiles changing over wildtype HSV-1 infection. This result is contrasted by results from Northern analyses of host mRNAs, as well as published microarray results from other groups which reported extensive downregulation of most host mRNAs studied. My initial research goal was to confirm our microarray observations with an alternate method, Northern analysis. I first investigated the mRNA profiles of several cluster 16 ECM mRNAs, as the coregulation of ECM genes indicated by our microarray analysis was of interest.

2 MATERIALS AND METHODS

2.1 Cell and virus culture

Cell culture methods were adapted from Brown & MacLean's "Herpes simplex virus protocols" (29) unless otherwise specified.

2.1.1 Cell lines

Vero cells (American Type Culture Collection (ATCC) #CCL-81 (1)) are an African green monkey kidney cell line, reported by the ATCC to be the best Vero cell line for the propagation of HSV-1. CCL-81 cells will hereafter be referred to as Vero cells.

V27 cells are a Vero-derived cell line that is stably transfected with the gene which encodes for ICP27 under control of the native promoter (259). V27 cells do not constitutively express ICP27. Rather, induction of ICP27 gene expression in V27 cells occurs upon transcriptional activation by VP16 during infection.

E5 cells, developed by De Luca *et al.* (63) are another Vero-derived cell line, stably transfected with the gene which encodes ICP4 under control of the native promoter. E5 cells do not constitutively express ICP4. Rather, induction of ICP4 gene expression in E5 cells occurs upon transcriptional activation by VP16 during infection.

The HEL-299 line of human embryonic lung cells, (ATCC, cat. #CCL-137, Lot #1375933 (1) are not immortalized, and have not been extensively passaged.

Telomerase 12 cells (25) are life-extended derivatives of primary diploid human foreskin fibroblast (HFF) cells. Telomerase 12 cells have been engineered to express the catalytic subunit of telomerase and thus their chromosomes do not undergo truncation. A gene encoding puromycin resistance was also stably transfected via the same plasmid, and served as a selectable marker to indicate marker transfer. Initially developed as a prototype cell line for the generation of stable complementing cell lines for CMV, we have found that HFF cells are capable of supporting HSV-1 replication.

2.1.2 Cell maintenance

All cells were cultured in an incubator at 37°C and 5%CO_2, generally in 150^{2}cm (T-150) cell culture flasks. All cell types used were cultured in approximately 30ml Dulbecco's Modified Eagle Medium (Life Technologies™, cat. # 12100-061) (DMEM) with 2mM glutamine added. Vero cells were cultured with 5% heat-inactivated fetal bovine serum (Sigma Chemical Co., cat. #F-4135) (HI-FBS). Vero-derived cell types, V27 and E5, were also cultured with 5% HI-FBS, as well as 100µg/ml active G418 Sulfate / Genetecin® (Life Technologies™, cat. #11811-031) for selection of G418 resistance. HEL cells and HFF cells were cultured in 10% HI-FBS.

All cell types were subcultured by the following method at confluence every 3-4 days, Vero and Vero-derived cells at a ratio of 1:10, and HEL cells and HFF cells at a ratio of 1:4. Confluent cell monolayers were washed twice with 10ml autoclave-sterilized PBS (137mM NaCl, 1.66mM KH_2PO_4, 2.68mM KCl, 8.34M Na_2HPO_4•7H2O). Cells were then trypsinized in 5ml 1X Trypsin-EDTA (Invitrogen Corporation, cat. # 25300-062) until the monolayer lifted with tapping of the flask. Trypsinization was arrested with addition of medium. An appropriate fraction of cells was reseeded into 30ml of medium for further culture.

2.1.3 Cryopreservation of cells

Cells were frozen using the following protocol provided by James Stone (personal communication). Cells designated for harvesting were cultured in T-150 flasks until confluence. Cells were trypsinized as described in section 2.1.2. Seven ml of medium were added to arrest trypsinization and to resuspend cells. Cells were transferred to 50ml conical centrifuge tubes, and spun in a tabletop centrifuge (BECKMAN, model# CS-6R) at 4°C, 2000rpm for 10 minutes. Cells were resuspended in 750µl of medium / flask of cells harvested, and incubated on ice for 10 minutes. Pre-chilled freezing solution (80% HI-FBS, 20% dimethyl sulfoxide (DMSO)) was added dropwise, while vortexing in a 1:1 ratio to the cell suspension. Cell aliquots (1.5ml or one flask's worth of cells) were placed into pre-chilled cryovials. The vials were cooled gradually in a –80°C freezer

using an ethanol-saturated Cryo 1°C Freezing Container (Nalgene, cat. #5100-0001) overnight, and were then transferred to liquid nitrogen for long-term storage.

2.1.4 Virus strains

KOS is a wildtype HSV-1 strain.

5dl1.2 is an ICP27 null mutant viral strain, in which promoter sequences, the transcriptional start site, and sequences encoding 262 N-terminal amino acids of the ICP27 gene have been deleted (195). Infection with 5dl1.2 does not result in production of detectable ICP27 transcripts nor does it result in production of detectable partial ICP27 proteins (195). As 5dl1.2 is replication-defective, 5dl1.2 stocks were propagated on a complementing cell line which synthesizes ICP27, V27 cells.

ΔSma (256) is a vhs truncation mutant strain which contains a deletion of about one third of the vhs gene from amino acid 149 to amino acid 344. Infection with ΔSma produces a truncated vhs protein 31kDa in size.

VhsA (304) is a vhs insertion mutant which has a *lacZ* cassette under the control of the ICP6 promoter inserted into the vhs locus. The *lacZ* open reading frame interrupts the vhs gene, UL41, such that the sequences predicted to encode amino acids 22 to179 are deleted, and amino acids downstream of amino acid 179 are separated from the vhs promoter.

d120 (63) is an ICP4 truncation mutant which has a 4.1kb deletion of the 3'ends of both copies of the ICP4 gene. ICP4 mRNA is not detectable during d120 infection. d120 infection does, however, produce a putative truncated ICP4 protein, 40kDa in size, which is recognized by an ICP4 polyclonal antibody. The size of this product is consistent with that predicted by the remaining ICP4 amino-terminal sequence present in d120. d120 infection, therefore, produces a truncated ICP4 product during infection. (Full length ICP4 has a molecular mass of 170kDa.)

d22-lacZ (180) is an ICP22 insertion mutant which has the *lacZ* open reading frame inserted in frame after the first 6 codons of the ICP22 gene. d22-lacZ, therefore, does not synthesize ICP22, but rather, synthesizes a fusion protein of the first 6 amino acids of ICP22 fused to the *Escherichia coli* β-galactosidase enzyme.

n212 (36) is an ICP0 nonsense mutant which has a nonsense mutation in the codon coding for the 212th amino acid in ICP0. This genetic structure is predictive of a truncated ICP0 protein, containing only the 212 amino acid N-terminal portion of the full length 775 amino acid ICP0.

2.1.5 Generation of virus stocks: Isolation of cell-associated virus

Virus stocks were generated on Vero cells, or on the appropriate complementing cell line, V27 cells for ICP27$^-$ 5dl1.2 virus and E5 cells for ICP4$^-$ d120 virus. Cells were subcultured 1:2 12-24 hours before infection. V27 and E5 cells were subcultured at this stage in the absence of G418. Confluent cell layers were infected at an approximate multiplicity of infection (MOI) of 0.01 for 1hr in serum free (SF) DMEM, at 34°C (37°C for 5dl1.2 and d120 virus), 5% CO_2, with gentle rocking every 10 minutes. The innoculum was removed from the flasks and 20ml of 199 medium (GibcoBRL, cat. #31100-035) with 5% HI-FBS was added. Infection was allowed to proceed at 34°C (37°C for 5dl1.2 and d120 virus), 5% CO_2 until most or all cells were rounded and could be lifted off with one hit of the flask (2-4 days). The cell suspension was transferred to 50ml conical centrifuge tubes and spun down at 2000rpm for 10 minutes at 4°C. Supernatant was discarded. The cells were resuspended in 1ml SF DMEM/ T-150 source flask. Cells were disrupted by freezing and thawing them 3 times at -80°C and 37°C respectively. Samples were then sonicated 3 times for 30 seconds over ice water at power 7 in a sonicator (Fisher Scientific, model: 550 Sonic Dismembrator). Cell particulates and nuclei were spun down at 2000rpm for 10 minutes at 4°C. The supernatant / virus isolate was aliquoted in 100-200µl aliquots and stored at –80°C.

Mock lysates were generated by incubation of Vero cells in SF-DMEM for 1 hour followed by incubation in 199 medium under the conditions specified above, for three days. Mock-infected cells had to be scraped into resuspension, and were treated as infected cells above with respect to spins, freeze-thaws, sonication, and aliquoting to generate mock infection stocks.

2.1.6 Titration of virus stocks

Virus stocks were serially diluted in SF-DMEM. Four hundred or 500µl of diluted virus from each dilution was used to infect a 3.5cm well of confluent cells for 1 hour at 37°C, 5% CO_2 with gentle rocking every 10 minutes. Innoculum was then replaced by 2ml of 199 medium with human serum / well and the infection was allowed to proceed until plaques were visible. (Batches of human serum were tested to determine the amount of serum necessary to restrict viral growth to plaque formation. Generally, 1-2% human serum was required.)

Plaques were stained for counting with modified Giemsa stain (Sigma Diagnostics, cat. # GS-1L). Culture medium was aspirated off, and cells were fixed for 5-7 minutes with 2ml methanol per 3.5cm well. Methanol was replaced with 1X Giemsa stain for several hours. Plates were gently rinsed with tap water and dried. Plaques were counted, and plaque-forming units (p.f.u.) determined for the inoculating virus stock, accounting for dilution factor and the innoculum volumes.

2.1.7 Experimental infection

Cells were seeded into wells or plates 12-24 hours before infection so as to have a confluent or almost confluent monolayer to infect within 24 hours. Cells were infected at an MOI of 10 unless otherwise specified. Medium was aspirated off, and wells were infected with innoculum for 1 hour at 37°C, 5% CO_2 with gentle rocking every 10 minutes. The innoculum volume was 400-500µl, 1ml, and 2ml for 3.5cm wells, 6cm dishes, and 10cm dishes respectively. Medium was aspirated off, and cells were harvested as specified below, depending on the analysis that was conducted.

Mock infections were conducted as with full infections, but with mock lysate. The mock lysate volume used was equivalent to the largest viral stock volume used within the same experiment.

In cell incubations or infections in the presence of actinomycin D (actD) (Sigma, cat. #A-1410), actD was used at a concentration of 10 µg/ml in both SF-DMEM innoculum, and further incubation. Stock actD solutions were made with 95% ethanol as

solvent, to a concentration of 4.4mg/ml. ActD concentration was verified spectrophotometrically as described in Sambrook *et al.* (277).

Viral stocks designated for ultraviolet (UV) irradiation were first diluted to their final concentration in SF-DMEM. Aliquots (3-5ml) were transferred to 10cm dishes to be irradiated. Virus suspensions were irradiated for 1 minute in a UV crosslinker (Stratagene, model: UV Stratalinker ™ 2400) and then immediately used in infection protocols.

In order to verify that UV-irradiation of virus, and actD treatment successfully prevented viral mRNA synthesis during infection, Northern analysis was done to monitor ICP27 mRNA levels under these conditions. Northern analysis indicated that ICP27 mRNA was not detectable after infection with UV-irradiated KOS nor was ICP27 mRNA detectable when infections were done in the presence of actD (10μg/ml). (See Figure 8.) We therefore surmise that the DNA damage induced by the UV-irradiation and intercalation of actD into DNA are both sufficient to render the viral genome virtually transcriptionally inactive.

2.1.8 Monitoring viral plaque growth

Viral plaques were grown as for virus titering, using human serum to restrict viral growth to plaque formation. Viral plaques were viewed in unfixed cell cultures, still immersed in medium. Plaques were viewed under light microscopy at 200 fold magnification with a Leica DM IRB inverted fluorescent / light microscope from Leica Microsystems. Photographs of plaques were taken with a camera from SPOT Diagnostic Instruments Inc., and viewed using SPOT Advanced software, also developed by Diagnostic Instruments Inc.

2.2 Molecular biology techniques

Methods were adapted from Sambrook *et al.* (277), unless otherwise specified.

2.2.1 Electrophoresis of DNA

DNA samples were mixed with 10X loading buffer and dye (1mM EDTA, 50% glycerol v/v, 0.25% xylene cyanol w/v, 0.25% bromophenol blue w/v), and loaded into wells of a 1% agarose TAE-buffered gel (0.04M Tris-acetate, 0.001M EDTA (pH. 8.0)). For size comparison, DNA samples were run alongside *Bst*EII–digested λ phage DNA. Gels were electrophoresed at 90-120 Volts. Gels were either electrophoresed in the presence of, or were post-electrophoresis stained in 0.5mg/ml ethidium bromide. DNA luminescence was then visualized and photographed on the UV Transilluminator.

2.2.2 Monitoring mRNA levels with Northern analysis

Aqueous solutions made in house, for use with RNA in solution, were treated with diethylpyrocarbonate (DEPC) to inactivate RNAses. DEPC was added to the solutions at a ratio of 1:1000. The solutions were shaken vigourously, left at 37°C overnight, and then autoclaved.

2.2.2.1 Isolation and quantitation of total RNA

Trizol® Reagent (Life Technologies, cat. #15596) was used to isolate total RNA from cell monolayers as per the manufacturer's instructions with some modifications. Unless otherwise specified, total RNA isolation was conducted with Trizol® Reagent. Medium was aspirated from infected monolayers and the appropriate amount of Trizol® Reagent was added (1ml for a 10cm dish of cells, 500µl for a 6cm dish of cells). Cells were scraped into the Trizol® Reagent, and pipetted up and down several times to homogenize samples. Samples were then incubated at room temperature for 5 minutes to allow complete homogenization. Two hundred µl of chloroform / ml of Trizol® Reagent were added. Samples were then shaken vigorously for at least 15 seconds. Centrifugation steps were conducted in an Eppendorf 5415C or 5417C centrifuge. Samples were spun for 15 minutes at 14000rpm. The top aqueous phase, which contained the isolated RNA, was collected and transferred to a new tube. The RNA was precipitated with 0.5ml isopropanol / ml Trizol® Reagent, and after a 10 minute room

temperature incubation, was spun down at 14000rpm for 15 minutes. The supernatant was removed, and the samples were washed with 1ml 75% ethanol / ml Trizol® Reagent. Pellets were spun down at 8000rpm for 5 minutes. The supernatant was removed. The pellets were resolubilized in DEPC-treated water by pipetting, followed by warming samples at 55°C for 10 minutes.

RNA was quantified spectrophotometrically using a spectrophotometer (Ultrospec® 3000, Pharmacia Biotech) and quartz cuvettes. RNA was diluted in DEPC-treated water to a volume of 800µl, followed by measurement of its A_{260} and A_{280}. An optical density (O.D.) of 1 at 260 nm corresponds to a concentration of 40µg/ml of RNA, and this extinction coefficient, accounting for the dilution factor, was used to calculate the concentration of RNA. The A_{260}/A_{280} ratio is used as an estimate of RNA purity. Pure RNA in unbuffered water has an A_{260}/A_{280} ratio of 1.5-1.9. Generally, the A_{260}/A_{280} ratio of RNA obtained was in the range of 1.4-1.6.

2.2.2.2 Isolation of the poly A^+ fraction from total RNA

Total RNA was used as a source of poly A^+ RNA. Poly A^+ RNA was isolated by affinity chromatography with the Oligotex™ system from Quiagen (cat. #70022) using the Oligotex™ mRNA Spin-Column Protocol specified by the manufacturer. The Oligotex™ system is based upon the affinity of polystyrene-latex particles coated with $dC_{10}T_{30}$ oligonucleotides for the poly A^+ RNA in the sample. Briefly, Oligotex™ beads and total RNA were mixed and warmed. The oligonucleotides on the polystyrene-latex particles and the polyA^+ RNA were allowed to hybridize upon cooling. After association of poly A^+ RNA with the beads, the beads were washed. Elution of polyA^+ RNA was done with rewarming of the mixture, as well as with the use of an elution buffer with low salt concentration to disrupt the oligonucleotide – poly A^+ RNA interaction. Two elutions were done to maximize poly A^+ RNA yield. To account for an expected 10% loss of sample in the poly A^+ enrichment process, samples were eluted into a volume equivalent to 90% of the original volume loaded onto the column.

2.2.2.3 Electrophoresis, transfer, and immobilization of RNA

RNA, prepared as indicated above, was mixed with loading buffer (10X Northern MOPS (0.2M 3-(N-Morpholino) propanesulfonic acid (MOPS), 50mM sodium acetate, 5μM EDTA, brought to pH 7, DEPC treated (NMOPS)), 37% formaldehyde, formamide, 3:5:15) and resolved through a formaldehyde agarose gel (1% agarose, 1X NMOPS (made with DEPC water), 0.666% formaldehyde (made with DEPC water)) in 1X NMOPS buffer towards the anode. RNA was stained during electophoresis with 0.5mg/ml ethidium bromide, then visualized with the UV Transilluminator and photographed with a The Imager ™ camera from Appligene. Alternatively, the gel was stained post-electorphoresis with SyberGold™ (Molecular Probes, cat. #S-11494) for 30 minutes to 1 hour in 1X NMOPS buffer and was visualized by blue fluorescence imaging on a phosphorimager (STORM 860 model, Molecular Dynamics). Ethidium bromide and SyberGold™ could both confirm approximate equivalent loading. Where SyberGold™ staining appeared uniform, 28s rRNA signal was quantified with ImageQuant software (Amersham Biosciences), and Northern blot RNA probe signal was reported relative to 28s rRNA signal to account for differential loading.

To determine the size of detected RNAs, RNA markers of known size were run alongside the samples. One μg / lane of high range RNA ladder markers (MBI Fermentas, cat. #SM0421) were used, with RNA fragment sizes of 6000, 4000, 3000, 2000, 1500, 1000, 500, and 200 bases. Alternatively, 2μg / lane of RNA Millenium™ size markers (Ambion®, cat. #7150) were used, with RNA fragment sizes of 9, 6, 5, 4, 3, 2.5, 2.0, 1.5, 1.0, and 0.5 kilobases.

RNA was transferred to nylon-based GeneScreen Plus® by capillary action, using 10X SSC (1.5M NaCl, 0.15M NaCitrate) as solvent. RNA was then immobilized onto the membrane by UV cross-linking using 2 X 120 000 μJoules / cm^2 doses from the UV Stratalinker™ from Stratagene.

2.2.2.4 Detection of specific mRNAs

2.2.2.4.1 Generation and use of random prim- labeled probes

Plasmids containing desired probe sequences (I.M.A.G.E. clone ID numbers 291622, 491711, 665126, 40813, 188381, 190904, 193313, 382693, 291057, 264960), were obtained from the I.M.A.G.E. Consortium public clone repository, which is managed by the Biology and Biotechnology Research Program. The clone stocks were distributed through Research Genetics Invitrogen Corporation. *E. coli* strain DH10B (amp^r) was used as the host for the EST-containing plasmids.

Three rounds of bacterial colony purification were done by streaking clone cultures on agar plates with 100µg/ml ampicillin to yield single colonies. Diagnostic digests at sites flanking I.M.A.G.E. clone insert sequences were done with *Not*I and *Eco*RI, followed by electrophoresis alongside size markers, to confirm expected insert sizes where possible. Plasmids were sequence verified by an external sequencing facility. I.M.A.G.E clone inserts destined for use as probes were first amplified from the clones using the polymerase chain reaction (PCR). Reactions were done in a PTC-100™ Programmable Thermal Controller (MJ Research, Inc.). One hundred µl PCR reactions were set up as follows (1X PCR buffer, 1.5mM $MgCl_2$, 0.2mM dATP, dCTP, dGTP, and dTTP, 0.25µM primer 1 mp19-P1 (M13/pUC Forward): 5'-CCC AGT CAC GAC GTT GTA AAA CG, 0.25µM primer 2 mp19-p2 (M13/pUC Reverse): 5'-AGC GGA TAA CAA TTT CAC ACA GG , 2.5 units *Taq* polymerase, 1µl DNA template). The PCR amplification cycle used was as follows: (step 1) 5 minutes at 94°C to lyse bacteria if whole cells were used and initially separate reaction components, (step 2) 45 seconds at 94°C to denature double-stranded DNA, (step 3) 45 seconds at 50°C to allow primers to anneal, (step 4) 45 seconds at 72°C to allow elongation of PCR products, (step 5) loop back to step 2 30 times, totaling 31 amplifications, (step 6) 2 minutes at 72°C to complete remaining elongation reactions, and (step7) 4°C refrigeration in the reactor for sample storage. PCR products were purified with the Quiaquick™ Nucleotide Removal Kit (Quiagen cat. #28306) according to the manufacturer's instructions. Purified PCR product was eluted into 50µl water. PCR-amplified insert sequences were then used as random-prime labeling templates

Probe fragments were radioactively labeled by random priming as follows. Approximately 2µg of DNA was boiled with 2µg of 6 base random sequence oligonucleotides (made by the DNA Core facility in house) in a 35µl volume. Seven µl oligo labeling buffer (315mM Tris pH 8.0, 31.5mM $MgCl_2$, 7.2µl β-mercaptoethanol, 126µM dGTP, 126µM dATP, 126µM dTTP, 1.29M HEPES pH 6.6), 2µl of 10µg/ml BSA, 5µl α^{32}P-d-CTP (Amersham Biosciences, cat. # AA0005, 3000Ci/mmol, 10mCi/ml at reference date), and 1µl of 3-9units/µl large fragment of DNA polymerase I were then added. The polymerase reaction was allowed to proceed at 37°C for 30 minutes or at room temperature for several hours. Fifty µl TE (10mM Tris buffer to pH 8, 1mM EDTA) was added to the reaction. The probe was phenol-chloroform extracted with 100µl phenol-chloroform-isoamyl alcohol (25:24:1) to remove protein from the reaction. The sample was spun, and the supernatant that contained the probe was loaded onto a size exlusion NICK™ column (Sephadex ™ G-50 DNA grade by Amersham Pharmacia Biotech, cat. #17-0855-02) for elimination of unincorporated nucleotides. The NICK™ column was prepared by passage of 3ml of TE through the column. The aqueous phase of the probe sample was loaded onto the column. Passage of 400µl of TE through the column, followed by passage and collection of 500µl of TE through the column yielded purified probe. Two µl of probe was counted in Ready Safe™ Scintillation fluid (Beckman, cat. #534547-A).

Random prime-labeled probes were used in Church buffer hybridization (54) or the ExpressHyb (Clonetech, cat. # 636832) system.

Blots to be probed with Church buffer (0.25M sodium phosphate buffer pH 7.2, 7% SDS w/v, 1mM EDTA, 1% BSA w/v) were prehybridized in Church buffer for 1 hour at 65°C in a hybridization oven (Tyler Research Instruments, HI-16000). Church buffer was replaced. Random prime-labeled probe was boiled for 3-5 minutes and was then added to the Church buffer for blot hybridization overnight at 65°C. All washes were done at 68°C. Blots were washed twice with 2X SSC, 0.1% SDS w/v and twice with 0.1X SSC, 0.1%SDS w/v.

The ExpressHyb hybridization system was used as per the manufacturer's instructions. Two 20 minute washes each were conducted with both ExpressHyb wash 1 and wash 2.

2.2.2.4.2 Generation and use of 5'end-labeled oligonucleotide probes

Oligonucleotide probes were 5'end-labeled in the following 50µl reaction (1µl substrate oligonucleotides at 1 OD/ml, 1X forward reaction buffer (Gibco BRL, cat. # 18004-010), 20 units T4 polynucleotide kinase, 5µl γ-^{32}P-ATP (Amersham Biosciences, cat. # AA0068, 3000Ci/mmol, 10mCi/ml)) at 37°C for 1-2 hours. The reaction was arrested with 200µl 2.5M ammonium acetate, and 100µg tRNA was added as a carrier to facilitate probe precipitation. Probe was precipitated with 1ml of 95% ethanol, spun down, and redissolved in 400µl 0.3M sodium acetate. Another round of precipitation in 1ml ethanol was performed, followed by a wash in 70% ethanol to remove salts. The probe was then washed with 95% ethanol to facilitate drying, dried in a speed vacuum (Savant, model #SC110A), and resuspended in 60µl TE. One µl of probe was counted in the scintillation counter.

Blots were hybridized to the probe by the Modified Westneat method. Blots were rehydrated in 2X SSC, then prehybridized in modified Westneat (6.6% SDS w/v, 0.25M MOPS, 10% Denhardts reagent v/v (1% Ficoll w/v, 1% polyvinylpyrolidene w/v, 1% low grade BSA w/v), 1mM EDTA) for a minimum of 1 hour at 55°C. One million cpm / 5ml Westneat hybridization, or all available 5'end-labeled probe was added to 0.5ml Westneat solution to generate a label mixture. Sonicated and denatured salmon sperm DNA was added to the label mixture at a concentration of 100µg/ml label mixture. The label mixture was heated at 95-100°C for 10 minutes and was then added to the Westneat solution incubated with the pre-hybridized blot. Hybridization was allowed to proceed for 2 days at 55°C. Membranes were washed twice for 5 minutes at room temperature with Westneat wash solution 1 (2X SSC, 0.2%SDS), and twice for 20 minutes at 55°C with Westneat wash solution 2 (0.2X SSC, 0.2% SDS).

2.2.2.5 Imaging and quantitation of mRNA signal

Northern blot ^{32}P signals were visualized following exposure to Kodak BioMax film and/or by phosphorimager (STORM 860 model, Molecular Dynamics) analysis with ImageQuant™ software from Amersham Biosciences. In ImageQuant, uniformly sized boxes encompassing the signals were selected, and the object average of each was calculated. Object averages were transferred to Microsoft Excel for analysis. The object average value of one background signal for each blot was subtracted, and signals were reported relative to the first mock time point unless otherwise specified.

2.2.3 Monitoring protein levels with Western analysis

2.2.3.1 Preparation of cell extracts for SDS-PAGE

At the appropriate harvest time, medium was aspirated off the cell monolayer, and 2X SDS-PAGE lysis buffer (125mM Tris, 20% glycerol, 2% SDS w/v, 0.025% bromophenol blue w/v, brought to pH 6.8 w/ 1N HCl, 20mM Dithiothreitol (DTT) added right before use) was added to the infected wells or plates. Cells were scraped into the lysis buffer and samples were passed several times through a 23-gauge needle to shear DNA, making samples less viscous. Samples were boiled for 5 minutes, and stored at 80°C until use.

2.2.3.2 Electrophoresis and transfer of total protein

SDS-PAGE samples prepared as noted above were boiled for 5 minutes again and electophoresed through two consecutive gel layers. Samples were first run through a 5% acrylamide stacking gel (5% acrylamide / bisacrylamide 29:1, 0.125M Tris pH 6.8, 0.1% SDS, 0.066% TEMED, 0.1% ammonium persulfate (APS)) at 100 Volts and then resolved in a 10% acrylamide resolving gel (10% acrylamide / bisacrylamide 29:1, 0.4M Tris pH 8.8, 0.1% SDS, 0.066% TEMED, 0.1% APS) at 100-200 Volts through SDS-PAGE running buffer (25mM Tris, 0.19M glycine, 0.1% SDS w/v). Electrophoresis was done in a Hoefer electrophoresis unit (SE 600 series). For sizing of proteins, pre-stained

SDS-PAGE standards were run alongside the protein samples (Bio-Rad, high range markers, cat. #161-0309, low range markers, cat. #161-0305).

The gel, Hybond™ ECL™ nitrocellulose membrane (Amersham Pharmacia Biotech, cat. #RPN303D), and Whatmann filter paper (cut to the size of the gel) were soaked in semi-dry gel transfer buffer (25mM Tris, 0.19M glycine, 20% methanol w/v). They were then layered on the cathode of a semi-dry transfer apparatus in the following order: 3 pieces of filter paper, gel, membrane, 3 pieces of filter paper. The anode was fastened on, and the transfer set to run at 300mA for 1 hour. Transfer was confirmed with movement of pre-stained molecular weight markers.

2.2.3.3 Detection of vhs by Western blot

2.2.3.3.1 Pre-clearing the vhs antiserum

The S2 polyclonal rabbit anti-vhs antiserum (303) (generated using a vhs-proteinA fusion protein) was used to monitor vhs levels over infection. As the background signal obtained was quite high, pre-clearing of the antibody was attempted to improve the specificity of the signal. Twenty ml of a 1 in 750 dilution of the S2 antiserum in Western solution 1 (23mM Tris.HCl pH 7.5, 150mM NaCl, 0.5% Carnation® skim milk, 0.05% NP40, 0.1% SDS) was incubated with a blot containing at least 10 maximally loaded lanes of mock infected cell lysate overnight. This blot removed antibodies that had cross-reaction with cellular proteins from the polyclonal αvhs antibody mixture. The cell type used to make mock lysate for the pre-clearing was the same as the cell type infected in a given study.

2.2.3.3.2 Western blot analysis

Incubations and washes were done with gentle rocking. Blots to be probed for vhs protein were blocked in Western solution 1 in the cold room at 4°C overnight. They were then placed in 20ml of the appropriately pre-cleared αvhs in Western solution 1 for 12-24 hours. Blots were washed twice for 5 minutes in Western solution 1, then washed twice for 5 minutes in Western solution 2 (25mM Tris.HCl pH 7.5, 150mM NaCl, 0.5%

Carnation® skim milk, 0.5% NP40, 0.1% SDS). Secondary horseradish peroxidase - coupled goat anti-rabbit antibody was incubated with the blot at a dilution of 1 in 3000 in Western solution 1 for 2 hours at room temperature, or in the cold room overnight. Two 5 minute washes were done with Western solution 1, and then two more were done with Western solution 2. ECL plus ™ (Amersham Pharmacia Biotech, cat.# RPN 2132) was used as per manufacturer's instructions to visualize the vhs signal. Briefly, the blot was incubated with ECL plus ™, which contains Lumigen PS-3. In the presence of horseradish peroxidase (which is localized to product we wish to detect through association with the secondary antibody), and peroxide, Lumigen PS-3 is oxidized and yields a luminescent signal which is detected on film. FUJI medial x-ray film was used to detect ECL luminescent signal.

2.2.4 Analysis of metabolically labeled proteins

Metabolic labeling was done with confluent 3.5cm wells. Fifteen minutes before the time point under investigation, medium was aspirated off and cells were washed serially with 1ml PBS and 1ml labeling medium (9:1 mixture of SF-DMEM and methionine$^-$ cysteine$^-$ glutamine$^-$ SF-DMEM ((ICN, cat.#1642449), 200mM glutamine added). Five hundred µl labeling medium and 2.5µl of ^{35}S labeled methionine (Easy Tag express-(^{35}S) protein labeling mix, from Perkin Elmer, cat. # NEG-772, 1175.0 Ci/mmol, 11.05µCi/µl at reference date) was incubated with each sample for 30 minutes, with gentle rocking every 10 minutes. Cells were washed with 1ml chilled PBS, and samples were harvested into 100 µl 2X SDS-PAGE lysis buffer as described above.

SDS-PAGE samples prepared as noted above were boiled for 5 minutes, and were electrophoresed through two consecutive gel layers. Samples were first run through a 5% acrylamide stacking gel as described in section 2.2.3.2 and then resolved in a 12% acrylamide resolving gel (12% acrylamide / bisacrylamide 29:1, 0.4M Tris pH 8.8, 0.1% SDS, 0.033% APS, 0.066% TEMED) at 100-200 Volts.

Labeled proteins were detected by fluorography using EN^{3}HANCE® autoradiography enhancer (NEN Life Science Products, cat. #NEF981) according to manufacturer's instructions. Briefly, SDS-PAGE gels were fixed in 10% glacial acetic

acid, 30% methanol with gentle agitation for 1 hour. The gel was then gently agitated in EN^{3}HANCE® for one hour to allow impregnation of the solution. EN^{3}HANCE® was precipitated inside the gel by gentle agitation of the gel in water for 30 minutes. Gels were then dried onto Whatmann filter paper with a slab gel dryer (Hoefer Scientific Instruments, model #SE160) for 2 hours at 60°C. Luminescent signal was detected and visualized on FUJI MEDICAL X-RAY film.

2.3 Generation of a vhs$^-$/ICP27$^-$ HSV-1 double mutant

A mutant isolate of HSV-1 KOS bearing inactivating mutations in both the vhs and ICP27 genes was constructed *in vivo by* homologous recombination between singly mutant parental strains, followed by screening for the desired doubly mutant recombinant. Two parental strain combinations were used. The first coinfection used ICP27$^-$ 5dl1.2 and vhs$^-$ vhsA viruses as parental strains. 5dl1.2 is an ICP27 null mutant viral strain, in which promoter sequences, the transcriptional start site, and sequences encoding 262 N-terminal amino acids of the ICP27 gene have been deleted (195). Infection with 5dl1.2 does not result in production of detectable ICP27 transcripts nor does it result in production of detectable partial ICP27 proteins (195). VhsA (304) has a *lacZ* cassette under the control of the ICP6 promoter inserted into the vhs locus. The *lacZ* open reading frame interrupts the vhs gene, such that the sequences predicted to encode amino acids 22 to179 are deleted, and amino acids downstream of amino acid 179 are separated from the vhs promoter. Expression of the β-galactosidase gene in the vhs locus allows for colour selection of the vhs deletion. As described below, I was unable to isolate a vhs$^-$/ICP27$^-$ recombinant using this combination of parental strains.

The second (and ultimately successful) coinfection also used 5dl1.2, but used ΔSma as the vhs$^-$ parental strain. ΔSma (256) has a deletion of about one third of the vhs gene from amino acid 149 to amino acid 344. Infection with ΔSma produces a truncated vhs protein 31kDa in size.

2.3.1 Coinfection

Four independent coinfections were conducted for each of the parental combinations described above. Both of the parental strains were used to infect 3.5cm wells of V27 cells at an MOI of 5 in 500µl of SF-DMEM for 1 hour at 37°C, 5% CO_2. Innoculum was replaced with 5% HI-FBS DMEM and incubated at 37°C, 5% CO_2 for approximately 24 hours. Coinfections were scraped into the medium, freeze-thawed, sonicated and had particulates spun out and removed as described above for other virus stock preparations. Viral stocks were then filtered through sterile 13mm diameter, 0.45µm pore size PVDF membranes (Millipore, catalogue #SLV013SL) to eliminate aggregates of virus particles.

2.3.1.1 Screening for the vhs$^-$/ICP27$^-$ double mutant from 5dl1.2 / vhsA coinfection

Progeny were first screened for the expression of β-galactosidase, which flags the vhsA mutation. Then, vhsA mutation-containing plaques were further screened for the ICP27$^-$ phenotype, characteristic of the 5dl1.2 mutation by searching for isolates incapable of growth on non-complementing Vero cells. To identify *lacZ*$^+$ plaques, appropriate dilutions of coinfections were plated onto V27 cells. After plaques had developed, growth medium was aspirated off, and wells were overlayed with 1% agar 15% HI-FBS 100-200µg/ml x-gal DMEM (made from mixing 2% agarose boiled and pre-cooled to 50°C right before overlay with 2X DMEM, FBS, and x-gal mixture). β-galactosidase-expressing virus generates blue plaques by metabolism of x-gal present in the medium to a blue product. Thus, after further incubation overnight, blue plaques were selected for further analysis. Blue plaques were picked by stabbing a pipette tip into the agar, and resuspending plugs in 500µl SF-DMEM. Plugs were freeze-thawed 3 times and vigorously vortexed directly before further screening.

LacZ$^+$ plaques were then scored for the ICP27$^-$ phenotype. Half (250µl) of each plug resuspension was placed on a 2.2cm well of Vero cells, while the other half was placed on V27 cells. Viruses that grew on V27 cells and not Vero cells were harvested

and rescreened. No plaques were obtained that had the desired characteristics for both screening steps. Additionally, the growth of *lacZ*$^+$ virus from vhsA / 5dl1.2 coinfection plaques was very inefficient. We therefore pursued the coinfection combination described below.

2.3.1.2 Screening for the vhs$^-$/ICP27$^-$ double mutant from 5dl1.2/ΔSma coinfection

The vhs mutation in ΔSma is not flagged by a *lacZ* expression cassette. Hence, an alternate screening strategy was required. Coinfection progeny were first screened for the 5dl1.2 mutation by searching for isolates incapable of growth on non-complementing Vero cells. Well-spaced plaques were generated on V27 cells. When plaques were visible, medium was aspirated, wells were overlayed with 1% agarose, and plaques were picked after agar hardened. Agar plugs were processed and screened for dependence on ICP27 complementation as described above. Viral DNA was harvested for further screening from coinfection progeny that were phenotypically ICP27$^-$.

Viral DNA was harvested as follows. Infections in screening wells with the desired ICP27$^-$ phenotype were allowed to proceed until cells were rounded up and started to detatch from the culture wells, in order to maximize viral DNA yield for further analysis. Infected cells were then scraped up, harvested into their growth medium (1ml), and transferred to microfuge tubes. Cells were spun down in a microcentrifuge at 2700rpm for 1 minute, and the supernatant was removed. Cell pellets were vortexed in 500µl urea/SDS buffer (6.3M urea, 315mM NaCl, 9mM Tris-HCl pH 7.5, 18mM EDTA, 1% SDS w/v)), and the mixture was left on ice for 1 minute to lyse cells. This mixture was vortexed with 500µl buffer saturated phenol-chloroform (phenol-chloroform-isoamyl alcohol (25:24:1)). Samples were spun at 4°C and 14000rpm for 15 minutes. The aqueous phase of each sample was transferred to a new tube. The phenol-chloroform extraction, spin, and aqueous phase transfer was repeated. DNA was precipitated with 1ml ethanol, left at –80°C for at least 15 minutes, vortexed, and spun at 4°C, 14000rpm for 20 minutes. The resultant pellet was resolubilized in 250µl 0.3M sodium acetate. The pellet was

precipitated with 750µl ethanol, and spun down again, washed with 1ml 75% ethanol, dried and resuspended in 40µl water.

The viral DNA isolated from the phenotypically ICP27$^-$ coinfection progeny was used as template for PCR amplification of the vhs locus. The reduced size of the amplified product was indicative of the ΔSma genotype. One hundred µl PCR reactions were set up with reagents added in the following order (63.5µl water, 10µl 10X GC-rich PCR buffer (300mM Tricine pH8.4, 20mM $MgCl_2$, 50mM β-mercaptoethanol, 1% thesit w/v), 3µl 50mM $MgCl_2$, 2µl of dNTP mix containing 10mM each of dATP, dCTP, dGTP, and dTTP, 5µl of 5µM primer 1 (8maVvhs5: 5'-CGC TAC ACT GCC TCT GTC GC-3'), 5µl of 5µM primer 2 (8maVvhs3: 5'-CCT GGG TCC GCA ACT GCT CC-3'), 2.5 units *Taq* polymerase, 1µl viral DNA template as prepared as described above, 10µl DMSO). Reactions were done in a PTC-100™ Programmable Thermal Controller (MJ Research, Inc.). The PCR cycle used was as follows: (step 1) 1 minute at 94°C, (step 2) 30 seconds at 92°C, (step 3) 30 seconds at 52.8°C, (step 4) 45 seconds at 72°C, (step 5) loop back to step 2 29 times, totaling 30 amplifications, (step 6) 7 minutes at 72°C, (step7) 4°C refrigeration in the reactor. Ten µl of the PCR reaction was visualized by DNA electrophoresis to detect the desired ΔSma deletion.

Prospective double mutants with the desired ICP27$^-$ phenotype and the desired vhs$^-$ genotype underwent 3 rounds of plaque purification where successive plaque plugs were picked and regrown under growth restriction of human serum as in titrations above. After purification, growth on V27 cells and not on Vero cells was reconfirmed.

In preparation for use in Southern analysis to verify the vhs$^-$/ICP27$^-$ genotype, viral DNA was digested as follows. Sixteen µl aliquots of viral DNA harvested as described above were used in diagnostic digests with *Bst*EII for vhs gene analysis and *Nru*I for ICP27 gene analysis.

Diagnostic DNA digests were electrophoresed in 0.9% agarose gels in preparation for Southern blotting. Gels were rinsed and soaked for 15 minute intervals with gentle rocking in 0.25M HCl, 0.5M NaOH, 1M Tris/1.5M NaCl, and 10X SSC successively.

Blots were transferred, UV-cross linked and stored as specified for Northern blots in Materials and Methods section 2.2.2.3 until probing.

To reconfirm the ΔSma deletion in the desired vhs⁻/ICP27⁻ progeny strains, Southern blot analysis with *Bst*EII-digested DNA was done by the Church method. The PCR product amplified from 5dl1.2 DNA with primers 8maVvhs5: (5'-CGC TAC ACT GCC TCT GTC GC-3') and 8maVvhs3: (5'-CCT GGG TCC GCA ACT GCT CC-3') includes sequences which flank the ΔSma deletion and was therefore used as a template for random-prime labeled probe to detect the ΔSma deletion in ljs1. To reconfirm the ICP27 deletion in the desired vhs⁻/ICP27⁻ progeny strains, Southern blot analysis with *Nru*I-digested DNA was done by the Westneat. The oligonucleotide sequence of the probe for detection of the ICP27 mutation is (5' CCG CCA GGA GTG TTC GAG TCG TGT CTG CGA G 3'). BLAST analysis was done to verify that this oligonucleotide has no known homology to any human gene, nor to any viral gene other than ICP27.

3 RESULTS

3.1 Northern analysis of cluster 16 mRNAs

As described in the Introduction, it is vital to validate microarray results with alternate methodologies. The following experiments were conducted for the purpose of verifying the quantitative reports of our microarray analysis and included the Northern analysis of mRNAs from different cohorts in our microarray study.

I first undertook to validate the results for a subset of mRNAs from cluster 16, as the prominence of ECM genes therein was of interest. I conducted infection with the same methodology used to generate sample RNA for our microarray analysis. HEL cells were either mock infected with serum free medium or infected with KOS at an MOI of 10. Mock samples were harvested at 3 h.p.i. Total RNA was isolated from infections harvested at 0 (media change, followed by immediate harvest), 3, 6, 9, and 12 h.p.i. and was used for Northern analysis. Probes for Northern analyses were generated from the same I.M.A.G.E. clones used in microarray analysis: cluster 16 clones 291622, 491711 and 665126. These clones have identity to exostoses 1, CTGF, and fibronectin 1 mRNAs respectively. Insert sequence from these clones was PCR amplified with M13 primers. These PCR products were then used as templates to generate random prime-labeled probes. These probes were used in Church hybridizations to conduct the Northern analyses that are illustrated in Figure 2.

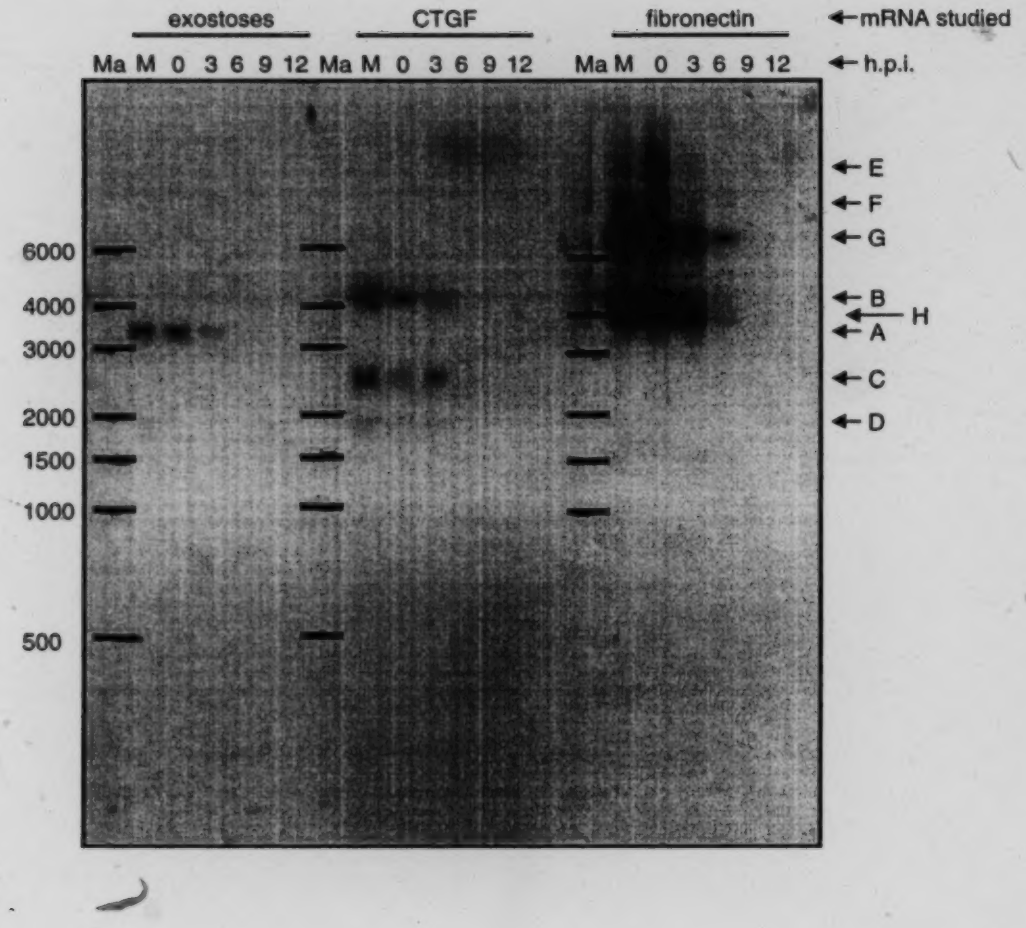

Figure 2. Northern analysis of cluster 16 mRNAs.
HEL cells were mock infected with serum free medium, or were infected with KOS. Mock RNA (M) was harvested at 3 h.p.i. Total RNA was isolated from infections harvested at 0, 3, 6, 9, and 12 h.p.i. Northern analysis was done with random prime labeled probes using the Church method and was detected on film. The levels of exostoses, CTGF, and fibronectin mRNAs all decreased extensively over infection. RNA marker (Ma) fragment sizes are indicated on the left hand side of the figure. Bands A to H are described in the text.

Below, I have described the sizes of the bands detected by cluster 16 clones, and denoted the putative identity of these bands, based on size similarity with homologous mRNA sequences. It would not have been unreasonable for us to have observed additional bands representing RNAs with partial homology to the clone insert sequences. The bands observed in Figure 2 are discussed below.

Band A, detected by clone 291622 whose insert sequence has identity to exostoses 1 mRNA, migrated slightly above the 3000 base marker. The size of the RNA product observed is consistent with reported exostoses 1 mRNA sizes of 3304 and 3183 bases (NCBI codes NM_000127.1 and S79639.1 respectively). The signal detected by clone 291622 insert sequence will hereafter be referred to as exostoses 1 mRNA.

The bands detected by clone 491711, whose insert sequence has identity to CTGF mRNA, migrated beside the 4000 base marker (band B), between the 2000 and 3000 base markers (band C) and slightly below the 2000 base marker (band D). One human CTGF mRNA was reported to be 2312 bases long (NCBI code NM_001901.1) and is likely represented by band C. One human CTGF mRNA was reported to be 1814 bases long (NCBI code AY395801) and is likely represented by band D. No homologous human mRNA of approximately 4000 base length was found by BLAST searching of Genbank with known 5' and 3' insert sequences of clone 491711, nor with the human CTGF mRNA sequence (NCBI code NM_001901.1). A CTGF precursor of *Bos taurus* was reported to be 4176 bases long (NCBI code AF 309555.1). Perhaps band B represents an unrecognized human CTGF pre mRNA. Band B may alternatively represent an unknown mRNA that has some homology to the clone. For the sake of simplicity of nomenclature, all three signals will hereafter be referred to as CTGF mRNAs.

The bands detected by clone 665126, whose insert sequence has identity to fibronectin 1 mRNA, migrated beside the 4000 base marker (band H), and above the 6000 base top marker (bands E, F, and G). As described in the Introduction, there are 20 transcript variants of fibronectin, only two of which have been completely sequenced. We therefore do not expect to be able to definitively identify the fibronectin splice variants detected by 665126. Transcript variant 1 of fibronectin 1 mRNA was recorded

to be 8027 bases long (NCBI code NM_002026). A human mRNA which codes for a fibronectin precursor was recorded to be 7680 bases long (NCBI code X02761.1). Both of these RNAs have identity to known portions of 665126 insert sequence, and thus may be represented by bands E and/or F and/or G. BLAST alignment of the terminal sequences of 665126 did not reveal an alignment with a known, completely sequenced, mRNA of 4000 base length. Thus the identity of the 4000 base length band was not determined. For the sake of simplicity of nomenclature, all four signals will hereafter be referred to as fibronectin 1 mRNAs.

The quantitation of cluster 16 mRNAs from both microarray and Northern analyses is presented in Table 2. Bands from Northern analysis presented in Figure 2 are presented as percentages of mock signal intensities, alongside the % mock signal intensities reported from microarray analysis. Quantitation of individual bands from Northern analysis is presented. Microarray analysis does not resolve different RNAs that hybridize to one cDNA slide spot (bind one probe), but rather, measures them cumulatively. As total lane signals most accurately parallel this scenario, total lane signals are also presented. Comparison of microarray data with total lane signals did not indicate a significant difference between results from microarray and Northern methodologies. The microarray and Northern analyses of cluster 16 mRNA profiles were consistent with each other and suggested that the microarray quantitation was valid. Both methods evinced extensive downregulation of cluster 16 mRNAs.

Table 2. Quantitation of cluster 16 mRNAs over the course of infection
The quantitation of bands from Northern analyses in Figure 2 is presented below as percentages of mock signal intensities, alongside the % mock signal intensities reported from microarray analysis. (- = not applicable) Comparison of microarray with total lane signals did not indicate a significant difference in the reporting of mRNA levels over infection from microarray and Northern methodologies. The microarray assessment of cluster 16 mRNA levels over infection appeared reasonable.

Mock (M) / h.p.i.	% mock (microarray)	% mock (total lane)	Uppermost band	2nd band from top	3rd band from top	4th band from top
Exostoses						
M	100	100	100	-	-	-
0	-	69.2	69.2	-	-	-
3	58.08	34.3	34.3	-	-	-
6	40.08	11.5	11.5	-	-	-
9	-	2.57	2.57	-	-	-
12	4.85	3.64	3.64	-	-	-
CTGF						
M	100	100	100	100	100	-
0	-	58.5	55.7	47.5	91.5	-
3	64.39	55.8	40.7	56.7	78.5	-
6	17.31	9.89	0	5.23	22.8	-
9	-	4.58	0	1.19	16.4	-
12	4.53	10.45	9.47	1.01	10.0	-
Fibronectin						
M	100	100	100	100	100	100
0	-	126	137	140	142	104
3	55.83	63.7	37.7	53.0	67.0	63.3
6	31.29	17.0	9.34	14.1	18.6	18.5
9	-	6.10	14.1	6.05	3.95	4.03
12	5	6.49	32.8	2.27	1.87	1.32

3.2 Northern analysis of "highly expressed and unchanged" group A mRNAs

In order to properly verify the categorization of RNAs by our microarray analysis, it was necessary to validate the quantitation for a cluster that was very distinct from cluster 16. I therefore attempted to verify the quantitation for I.M.A.G.E. clones within group A, defined as highly expressed and unchanged over infection by microarray analysis. For group A clones, high expression was defined by an average (between dye-swaps for each sample) absolute fluorescent intensity over 20000. Group A clones were designated as "unchanged" if their signal intensity decreased by no more than 33% of initial values or increased to no more than 1.5 times initial values over the infection. If the array quantitative analysis was valid, we expected Northern analysis with group A clones to detect RNAs whose signal intensity would either remain the same over the course of infection, or would differ within the narrow range specified above.

HEL cells were treated with mock lysate (generated as described in Materials and Methods) or infected with KOS. Total RNA was harvested at 12 h.p.i. Initial results with some of the group A clone probes indicated that group A mRNAs decrease in abundance over infection (data not shown, replicates shown in more extensive experiments below).

We reasoned that Northern analysis and microarray analysis might have produced different quantitative results because the methods detect different subsets of RNA. PolyA$^-$ RNA can present a signal in Northern analysis. In contrast, polyA$^-$ RNA is not represented in microarray analysis. (Recall the selective representation of polyadenylated RNA in microarray analysis.) Perhaps a large portion of the mock signal detected in Northern analysis was actually from polyA$^-$ RNA, thereby inflating the mock frame of reference in Northern analysis, relative to microarray analysis. To test for this, we analysed both total and poly A+ RNA over infection. We anticipated that polyA$^+$ group A RNA would appear to be relatively stable over infection in Northern analysis, in agreement with our microarray data.

HEL cells were treated with mock lysate, or infected at an MOI of 20, and total RNA was harvested at 12 h.p.i. The poly A^+ component of each sample was isolated from 1/2 of the total RNA pool with oligo dT columns, and was resuspended in 90% original volume, assuming 10% loss in yield. Northern analyses, illustrated in Figures 3 and 4, were done using random prime-labeled probe made from four of the group A clones by ExpressHyb hybridization: 40813, 188381, 190904, 193313, as well as with a PCR product specific for HSV-1 VP16.

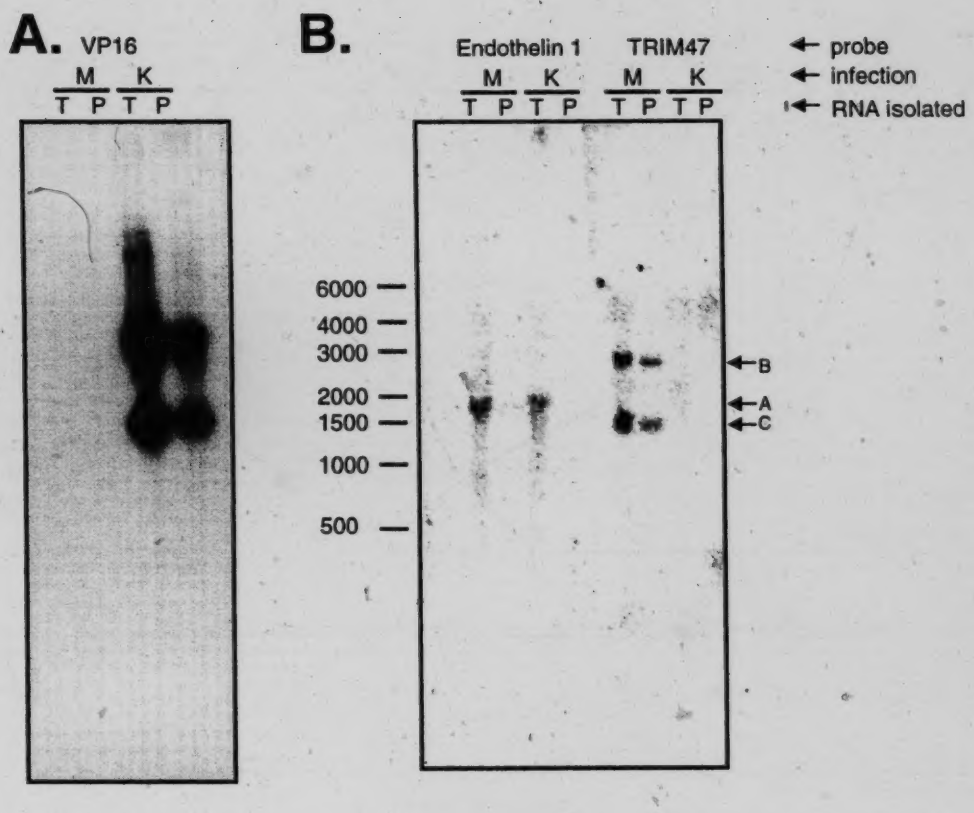

Figure 3. Northern analysis of group A mRNAs.
HEL cells were treated with mock lysate, or were infected with KOS at an MOI of 20. Mock (M) and KOS infection (K) total RNA (T) was harvested at 12 h.p.i. The poly A^+ component (P) of the sample was isolated from 1/2 of the total RNA pool using oligo dT columns, and was resuspended in 90% original volume, assuming 10% loss in yield. A) A PCR product containing sequence homologous to the VP16 gene was used as a template for random prime labeling. Northern analysis was done with this random prime labeled probe using the ExpressHyb system and was visualized on film. Northern analysis for VP16 served as a positive control that showed VP16's expected expression during infection, and successful oligo dT column purification of VP16 polyA$^+$ mRNA. B) Insert sequences from I.M.A.G.E. clones 40813 (detects endothelin 1) and 188381 (detects tripartite motif containing 47 (TRIM47)), previously used in microarray analysis, were used as templates for random prime labeling. Northern analysis was done with these random prime labeled probes using the ExpressHyb system and was visualized by phosphorimager analysis. Both endothelin 1 specific and TRIM47 specific probes detected distinct polyA$^+$ mRNAs that were degraded extensively over infection. A polyA$^-$ component of the endothelin 1 signal did not completely dissipate over infection. Bands indicated by arrows A, B and C are discussed in the text.

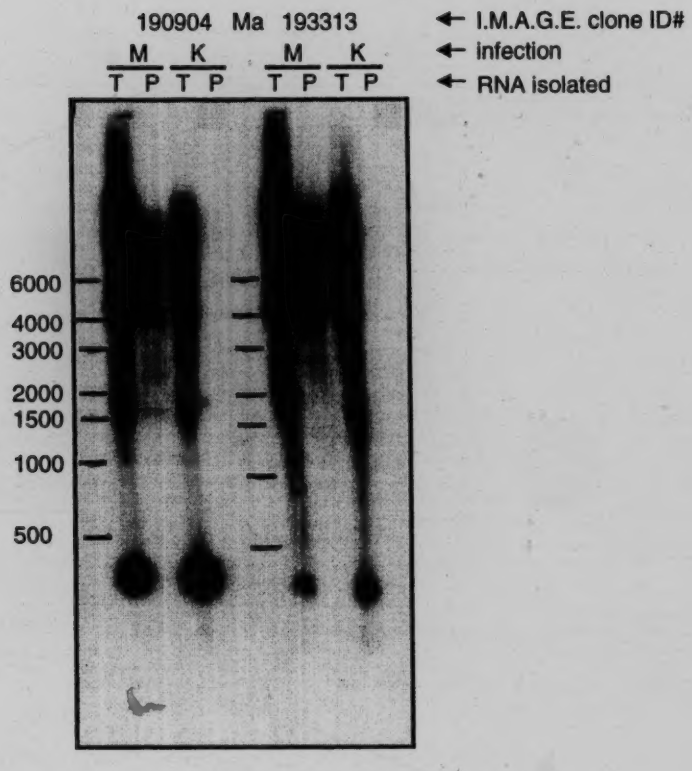

Figure 4. Northern analysis of *Alu* element containing group A mRNAs.
HEL cells were treated with mock lysate, or infected with KOS at an MOI of 20. Mock (M) and KOS infection (K) total RNA (T) was harvested at 12 h.p.i. Insert sequences from I.M.A.G.E. clones 190904 and 193313, previously used in microarray analysis, were used as templates for random prime labeling. Northern analysis was done with these random prime labeled probes using the ExpressHyb system and was visualized on film. (P) Poly A^+ RNA

Northern analysis of VP16 RNA, illustrated in Figure 3A, was conducted to verify successful poly A^+ mRNA purification, and detection in this experiment.. The VP16 mRNA signal was detectable only in infection and was retained after oligo dT column purification, as expected. Quantitation of the total VP16 signal, however, indicated that only 40% of the total signal was recovered after oligo dT column purification, as opposed to the 90% recovery expected for this generally polyadenylated RNA species. Forty % recovery of polyadenylated RNA was therefore used as a frame of reference in assessing the relative proportion of polyadenylated : unpolyadenylated RNA fractions of other RNA species. RNA recovery in the polyadenylated fraction significantly below 40% (here, arbitrarily designated as a minimum 10% difference in the absence of statistically significant multiple trials) was considered suggestive of a significant unpolyadenylated RNA species fraction in the total RNA isolate.

Figure 3B illustrates the Northern analysis conducted with group A clones 40813 and 188381 by ExpressHyb hybridization. Clones 40813 and 188381 group A clones detected distinct mRNAs that are described below.

IMAGE Consortium clone 188381 detected two distinct mRNAs indicated by bands B and C in Figure 3B. Band B migrated between the 2000 and 3000 base markers. Band C migrated between the 1000 and 1500 base markers. Clone 188381 has identity with one known human mRNA which encodes for a human tripartitite motif containing protein (TRIM 47) (NCBI code XM_290731), reported to be 2261 bases long. Band B may represent TRIM 47 mRNA. Band C remains unidentified. For simplicity of nomenclature, both bands detected by clone 188381 will hereafter be referred to as TRIM 47 mRNAs. As for VP16 RNA, approximately 40% of total RNA mock treatment signal was recovered with the oligo dT column purification for TRIM 47 RNAs (48% and 49% for bands B and C respectively). It is likely, therefore, that most of the detected TRIM 47 RNA was polyadenylated. Using total RNA as a measure, TRIM 47 RNA species were degraded extensively to 15% and 13% of mock levels for bands B and C, respectively. Contrary to microarray results, Northern analysis indicated that TRIM 47 mRNAs were extensively downregulated during infection.

I.M.A.G.E. clone 40813 detected one RNA species (band A in Figure 3B). Band A migrated between the 1500 base and 2000 base markers. Clone 40813 has identity to human endothelin 1 mRNA (NCBI code NM_001955), which is reported to be 1334 bases long. With variable polyadenylation, a band representing a mRNA product over 1500 bases is consistent with a putative endothelin 1 mRNA identity. The band detected by clone 40813 will hereafter be referred to as endothelin 1 mRNA. Band A appeared to be of lower molecular weight in the polyadenylated RNA fraction, as compared to the total RNA fraction. We do not know the reason why this putative polyadenylated RNA appeared to be shorter than its homologue(s) in total RNA. Only 19% of the endothelin 1 signal was recovered from the mock infection sample with the oligo dT column. This recovery was much less than the 40% recovery of a "mostly polyadenylated" species, VP16. Significant portions of the endothelin 1 RNA in mock infection were, therefore, likely not polyadenylated. A very high fraction of mock total endothelin 1 RNA remained after infection (88%). However, a very small portion of the endothelin 1 RNA which remained after infection was polyadenylated, as only 3.8% of endothelin 1 polyA$^+$ mRNA signal remained after the infection. Even if we account for incomplete polyA$^+$ RNA recovery by multiplication of this value by the factor of 2.5 (inverse of 40%), the polyA$^+$ RNA is still a minor portion of total RNA remaining after infection (9.4% of 88%). Northern analysis illustrated that polyadenylated endothelin 1 RNA is destabilized over infection. This component of the endothelin 1 RNA signal parallels the microarray analysis most closely with respect to RNA species represented. Contrary to the microarray analysis, this result suggested that polyadenylated endothelin 1 mRNA decreased in abundance extensively over infection. Also noteworthy, the above Northern analysis suggested that a high proportion of endothelin1 RNA species that remained after infection was not polyadenylated, and that the unpolyadenylated endothelin RNA may have been relatively more stable over infection.

We had expected microarray clones to be specific for either a singular mRNA or perhaps a narrow subset of host mRNAs with strong homology. Contrary to this expectation, Northern analyses with two group A clones, 190904 and 193313, illustrated

in Figure 4, suggested that both of these clones detected a multitude of RNA species, and quite possibly, a similar set of RNA species.

The features of the Northern signals for probes 190904 and 193313 are described below. The mock infection total RNA signals included a smear which extended to the top of the gel. The smears represented a multitude of RNA species with a maximal length of more than 6000 bases. The mock infection total RNA signal for both clones also included an intense band that migrated below the 500 base marker. The polyA$^+$ component of the smears detected by clones 190904 and 193313 dissipated extensively over infection (to 4.4% and 4.3% of mock total RNA levels, respectively) while the total RNA signals in the smears dissipated only moderately under the same conditions (to 39% and 46% of mock total RNA levels, respectively). It is possible that, like endothelin 1 RNA, a significant portion of RNAs detected by clones 190904 and 193313 are unpolyadenylated and relatively stable over infection. Consistent with this postulate, only 23%, and 28% of the 190904 and 193313 smear signals, respectively, were recovered from the mock infection sample with the oligo dT column. (These recoveries were lower than the 40% recovery of a "mostly polyadenylated" species, VP16.) The band below the 500 base marker increased moderately over infection (to 118% and 161% of mock values over infection for 190904 and 193313 clones, respectively). This band was not part of the polyA$^+$ fraction. These results suggested that the multitude of polyadenylated RNAs detected by clones 190904 and 193313 dissipated to virtually undetectable levels over infection. A portion of the RNAs detected by these clones was relatively stable over infection and may be enriched for unpolyadenylated RNA.

We thought that 190904 and 193313 may have detected a multitude of RNAs through specificity for some genetic repeat element and therefore did *in silico* sequence analysis of the clone insert sequences to determine if this was the case. Sequence analysis of clones 190904 and 193313 verified that they did indeed contain *Alu* repeat element sequences, and would thus likely detect *Alu* element-containing RNAs. Because of the unusually high frequency (two out of four clones tested) of *Alu* element-containing I.M.A.G.E. clones in my random selection of group A clones, we decided to determine the prevalence of *Alu* elements among group A clones. Alignment of the known 5' and

3' terminal sequences of the group A clones with a canonical *Alu* element from the BLUR8 plasmid (GI accession # 337596) was conducted using BLAST 2 Sequences software, available at the NCBI homepage. (BLUR8 (62, 139, 272) (*Bam* linked ubiquitous repeat 8) is a pBR322 plasmid containing an *Alu* family sequence cloned at the *Bam*HI site. There is a 22% mismatch between BLUR8 and the average *Alu* family sequence.) As listed in Table 3, 20 of 39 group A clones, were determined to contain *Alu* element sequence, as defined by their strong homology to BLUR8. (Many group A clones were also reported to contain other kinds of repeat elements. These additional repeat element designations from Genbank are also shown in Table 3.) *Alu* element-containing RNAs, and how they are influenced over infection is thus briefly reviewed below.

Table 3. Prevalence of *Alu* repeat element sequences in group A clones

Group A genes, defined as higly expressed and unchanged, are listed below. *In silico* analysis, in combination with Northern analysis where specified, showed that a minimum of 20 out of 39 group A genes contained *Alu* sequences. A small portion (6/39) of the group A genes were determined to not contain *Alu* sequences. The presence or absence of *Alu* sequences in 13 of the 39 clones could not be verified, due to sequence unavailability. Many clones that contained *Alu* sequences were found to contain sequences of other repeat elements as well.

I.M.A.G.E. clone	*Alu* element prevalence	Comments / additional repeat elements
199705	+	
190904	+	• Northern analysis indicated the presence of *Alu* repeat sequences in this clone
193313	+	• Northern analysis indicated the presence of *Alu* repeat sequences in this clone • 3'end listed as having LTR2 repetitive element
172447	+	• 5' end listed as having L1 repeat element
194512	+	• Clone annotation is wrong. *Alu* element is in 3', not 5' end of insert sequence.
178118	+	
138505	+	
665105	+	• 3'end has TAR1 element
241224	+	
247073	+	
245828	+	• 3'end has MER 22 element
283446	+	• 3'end listed as "*Alu* Classic C Warning Entry!!!!"
428492	+	
488164	+	• 5'end has L1.b3 L1 repeat element • 3'end has MER1 element
416095	+	• 3'end has MER36 element
504224	+	• 5'end has MSR1 repeat element
471477	+	• 5'end has MER9 repeat element • 3'end has L1.b2 L1 repeat element
327657	+	
430183	+	
328284	+	• BLAST alignment of both 5' and 3' ends shows that the clone insert sequence is from one Alu^+ exon of islet amyloid polypeptide mRNA.
166016	?	• 5' or 3'end of clone sequence unavailable for verification
222642	?	"
176039	?	"
381680	?	"
491783	?	"
269067	?	"
255331	?	"
175815	?	• An internal portion of the clone's sequence is unavailable for verification
198693	?	"
470567	?	"
415201	?	"
270365	?	"
268217	?	"
40813	-	• reported to be specific for endothelin 1 mRNA • Northern analysis signal is specific to 1 RNA species, not to repeat sequences present in many RNAs.
188381	-	• Northern analysis signal is specific to 2 RNA species, not to repeat sequences present in many RNAs. • strong homology to and therefore likely detects TRIM 47 mRNA
429928	-	
251543	-	

382693		• reported to be specific for glial fibrillary acidic protein • Northern analysis signal is specific to 1 or 2 RNA species, not to repeat sequences present in many RNAs.
291057	-	• reported to be specific to cyclin dependent kinase inhibitor 2C • Northern analysis signal is specific to 1 mRNA species, not to repeat sequences present in many mRNAs

Alu elements (reviewed in (16, 61, 271)) are a type of short interspersed repeat element in the human genome. There are somewhere in the range of five hundred thousand to one million copies in the genome, such that *Alu* repeat elements comprise approximately 10% of the mass of the human genome. They are inserted approximately once every five kilobasepairs in the genome. *Alu* elements consist of a tandem arrangement of 2 monomers, each derived from 7SL RNA sequence. Each *Alu* element transcript has an internal polyA tract and a polyA tail.

Alu sequences are transcribed by RNA polymerase III in human cells, albeit at low levels. RNA polymerase III *Alu* transcripts are initiated within the *Alu* element, but are polymorphic in length, as the signal for their termination is outside of the element at a variable distance. *Alu* elements are transcribed more readily in cells with RNA polymerase II as part of transcripts into which they have been internally retrotransposed, usually as part of an intron, or part of the 5' or 3' UTR. RNA polymerase II *Alu* transcripts are also polymorphic in length, as the mRNA length is defined by the mRNA into which *Alu* sequence has retrotransposed.

Jang *et al.* (137) conducted Northern analysis of total mRNA from HSV-1 infection of HeLa cells with a probe specific to *Alu* sequence and observed a high molecular weight smear decreasing somewhat over infection, and a band approximately 200-300 bases in size, increasing 5 fold over infection. Our results, illustrated in Figure 4, are consistent with those observed by Jang et al. with respect to smear dissipation and a low molecular weight band that increases in intensity over infection. It is worthwhile to note that the low molecular band increase was less extreme in our hands. This may be due to differential specificity of the *Alu* probes used in these studies, or perhaps may be due to differences in cell types used.

Upon infection with adenovirus and HSV-1, RNA polymerase III transcription of *Alu* elements greatly increases (137, 236-238). For example, in a primer extension analysis of *Alu* element–containing cytoplasmic RNA in infection, Panning *et al.* (237) observed that a primer extension product of 120 nucleotides, representing *Alu* element transcription from the *Alu* RNA polymerase III promoter, increased in abundance 30 to

50 fold. In the same primer extension analysis of *Alu* element – containing cytoplasmic RNA in infection, Panning *et al.* (237) observed that a smear that represents RNA polymerase II transcribed *Alu* transcripts dissipated extensively over infection. Thus, upon infection with HSV-1, RNA polymerase II-transcribed *Alu* element-containing RNAs decrease in abundance.

As *Alu* repeat element-containing clones bind many RNAs, and lack unique RNA species specificity, they are inappropriate for use in detection of specific mRNA species in microarray analyses. *Alu* element-containing clones immobilized on the microarray slide hybridized to repeat elements present in a multitude of fluorescent cDNA species. The slide spot was likely saturated. Accurate sample comparison with these clones is therefore not possible.

In summary, our analysis of group A mRNAs thus far suggested the following. Results from microarray and Northern analyses of "highly expressed and unchanged" group A RNAs were not found to be consistent with each other. Group A clone 188381, which detected two polyadenylated TRIM 47 mRNAs, was the only clone that was specific enough to be appropriate for use in microarray analysis and was specific to mRNA species that were polyadenylated. Contrary to microarray results, Northern analysis indicated that this mRNA was extensively downregulated during infection. Group A clone 40813 detected a unique endothelin 1 mRNA species. Endothelin 1 mRNA seemed to be an atypical RNA, however, as a minor fraction of it was polyadenylated. While total RNA quantitation indicated that endothelin 1 mRNA was stable over infection, the polyadenylated component of its signal dissipated during infection. As the polyadenylated mRNA measure more accurately reflects RNA species detected in microarray analysis, and as polyA$^+$ endothelin 1 mRNA decreased in abundance during infection, we conclude that Northern results were contrary to what the microarray analysis reported for clone 40813. Many group A clones were not specific to unique RNA species, but rather, detected a multitude of RNAs containing *Alu* element and other repeat sequences. Their quantitation in microarray analysis was likely faulty due to slide spot saturation, as described above. In the end, the Northern analysis of a multitude of polyadenylated RNAs conducted with Alu element-containing probes

illustrated that a multitude of host mRNAs do indeed decrease in abundance over infection. The microarray analysis quantitation was incorrect in reporting the stability of group A clone mRNA levels over infection. Whether cluster 16 and group A mRNAs were still distinct in the rates at which they were downregulated during infection is addressed further below.

Unpolyadenylated RNAs may be significantly more stable than polyadenylated RNA species over infection. This was suggested by observations made for RNA with homology to the endothelin 1 mRNA sequence, as well as a multitude of RNAs detected by clones 190904 and 193313. The nature of these RNA species (other than their possession of *Alu* element sequence), as well as their subcellular localization, was not determined in work presented here. Quantitation of the smears for clones 190904 and 193313 as well as quantitation for all the bands in Figure 3 is presented in Figure 5, in order to compare total RNA and polyA$^+$ RNA samples and display this trend. Repetition of this study with improved polyA$^+$ RNA isolation is warranted.

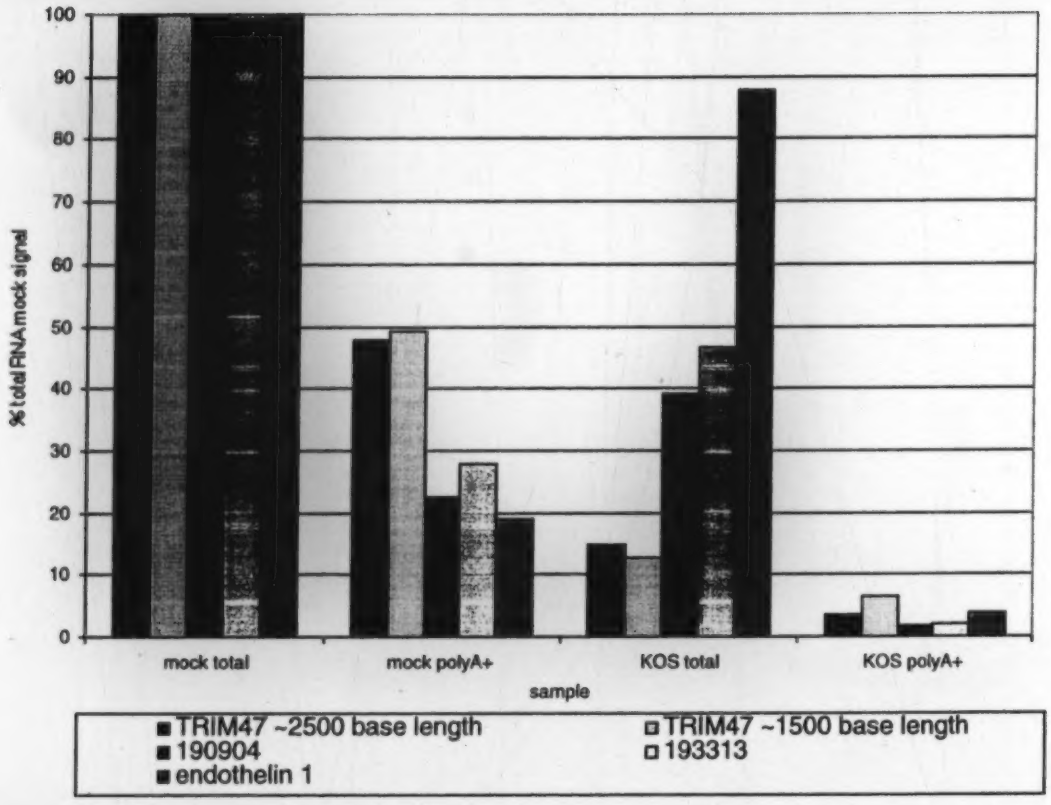

Figure 5. Total and polyA⁺ RNA signal intensities of group A RNAs over infection.
The smears for 190904 and 193313 clone- detected signals, as well as the bands for endothelin 1 and TRIM47 RNAs, from Northern analyses presented in Figures 3 & 4, were quantified from phosphorimager analysis. The quantitation, reported as a percentage of the total RNA mock infection signal, is presented above.

3.3 Attempt to adjust microarray calibration

Northern analysis with group A clones was unusual in that a significant portion of unpolyadenylated RNA was sometimes detected and/or some clones were determined to be specific for *Alu* repeat element sequence and detected a multitude of RNAs. Only one of the 4 group A clones monitored thus far had the expected specificity for a limited set (in this case, 2) of polyadenylated RNAs. However, all of the polyadenylated RNAs, whether they were detected within typical or within atypical Northern patterns, had diminished over infection. This observation contrasted the microarray assessment of these mRNAs, which described these mRNAs as unchanged over infection. We hoped that these group A mRNA loss patterns might still be clearly distinguishable from cluster 16 mRNA loss patterns. Distinction between group A and cluster 16 mRNA loss patterns would have indicated that while the actual relative values reported for the different cohorts were inaccurate, the sorting of the mRNAs into cohorts was still statistically significant.

In the following experiment, the profiles of more group A clones were monitored alongside cluster 16 clones in order to determine if there was a difference in the rate at which they dissipated during infection and if, perhaps, a correction factor could be calculated for the microarray analysis, based on the differences in these decay rates. Two cluster 16 clones and two group A clones were examined over a 12 hour infection time course by Northern analysis. (We ensured that the group A clones used were *Alu* element negative by analyzing their insert sequences. See Table 3.) Briefly, HEL cells were treated with mock lysate for 3 hours, or were infected with KOS for 3, 6, 9 and 12 hours. After mock treatment or infection, total RNA was isolated from the cells. Recall that only polyadenylated RNAs (or RNAs with some polyA tract within the sequence) can be represented in microarray analysis. As we were aware that some RNAs in our studies were not polyadenylated, we elected to isolate and quantitate polyA$^+$ RNA species from the total RNA isolates as a more accurate reflection of microarray quantitative measures and to identify polyA$^+$ RNA species that should be included in quantitation. The

Northern analysis of this study is illustrated in Figure 6. The RNA species detected are described below.

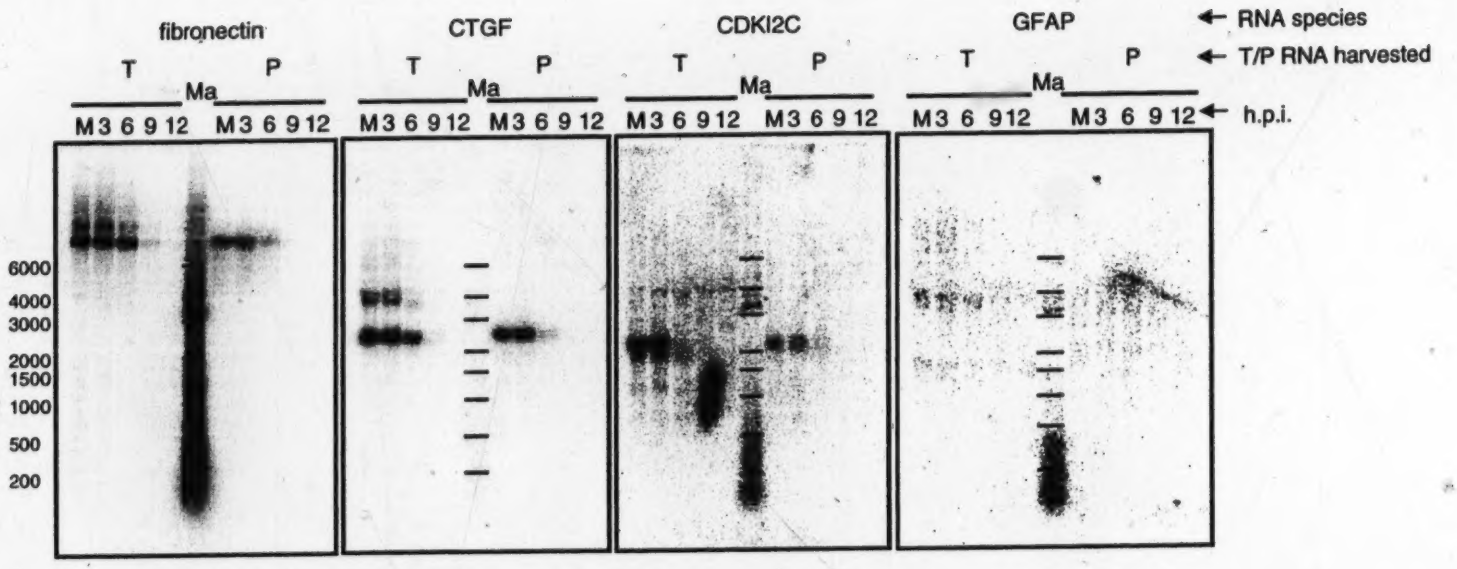

Figure 6. Northern analysis of total and polyA⁺ RNA for cluster 16 and group A mRNAs.
HEL cells were infected with mock lysate or infected at an MOI of 10 with KOS. Mock RNA (M) was harvested at 3 h.p.i. Infections were harvested at 3, 6, 9, and 12 h.p.i. Insert sequences from I.M.A.G.E. clones, previously used in microarray analysis, were used as templates for random prime labeling. Northern analysis was done with random prime labeled probes using the Church method in order to detect fibronectin (665126), CTGF (491711), cylin dependent kinase inhibitor 2C (CDKI2C) (291057), and glial fibrillary acidic protein (GFAP) (382693) mRNAs, and was visualized by phosphorimager analysis. Marker (Ma) was run between the total and polyA⁺ RNA time courses for each mRNA, for which there are some cross reacting bands in the fibronectin, CDKI2C, and GFAP Northern blots. (T) total RNA, (P) PolyA⁺ RNA

Clone 382693 is in group A. Two faint bands detected by clone 382693 migrated between the 3000 and 4000 base markers and between the 1500 and 2000 base markers, respectively. Neither band was detected after polyA$^+$ RNA purification. This could have simply been due to the extreme weakness of the signal. Clone 382693 aligns with a 3033 base mRNA which encodes a glial fibrillary acidic protein (GFAP) (NCBI code S40719.1). The size of the top mRNA band was consistent with that predicted for GFAP. The lower band remains unidentified. Probing with clone 382693 yielded very weak signal, a low signal:noise ratio, and non-uniform background, for which quantitation of mRNA was inappropriate. For simplicity of nomenclature, both bands detected by clone 382693 will hereafter be referred to as GFAP mRNAs.

Clone 291057 is in group A. Three bands were detected by clone 291057: one (which was very faint) that migrated between the 3000 and 4000 base markers, one that migrated between the 2000 and 3000 base markers, and one (which was very faint) that migrated just above the 1000 base marker. Only the middle band was detected within the polyA$^+$ RNA fraction. The other two bands may have been undetectable in the polyA$^+$ fraction because of their very weak signal. There are two transcript variants of cyclin-dependent kinase inhibitor 2C (CDKI2C) that have identity to clone 291057, and that are possibly represented in our Northern analysis. Transcript variant 1 is 2104 bases long (NCBI code NM_001262.2), and transcript variant 2 (NCBI code NM_078626.1) is reported to be 1315 bases long.

Fibronectin (clone 665126 from cluster 16) probe detected the same bands seen in Figure 2 (verified in high exposure, data not shown), except that the band immediately above the 4000 base marker decreased drastically in intensity. Perusal of three experiments in which fibronectin RNA was monitored in HEL cells showed that this band varied in intensity from study to study and may have decreased gradually with cell passage number. Only one observed fibronectin RNA species, equivalent to band G in Figure 2, was detected within the polyA$^+$ fraction.

CTGF (clone 291622 from cluster 16) probe detected the same bands as in Figure 2. Only one observed CTGF RNA species, equivalent to band C in Figure 2, was detected within the poly A^+ fraction.

A quantitative comparison of the mRNA loss patterns for fibronectin, CTGF, and CDKI2C mRNAs is shown in Figure 7. As stated above, Northern analysis of polyA$^+$ RNA species is a better approximation of microarray analysis than Northern analysis of total RNA species. The singular band for each RNA containing polyA$^+$ RNA products in Figure 6 was quantified from the phosphorimager analysis. For each polyA$^+$ RNA–containing band, both total and polyA$^+$ RNA quantitations are presented. The mRNA profile of group A CDKI2C mRNA cannot be clearly distinguished from cluster 16 fibronectin and CTGF mRNAs. Figure 6 shows that GFAP was also strongly downregulated during infection, even though accurate quantitation was not possible. These results indicate that mRNA loss profiles of cluster 16 and group A members could not be distinguished quantitatively and are very similar. We could not calculate a correction factor for the microarray results.

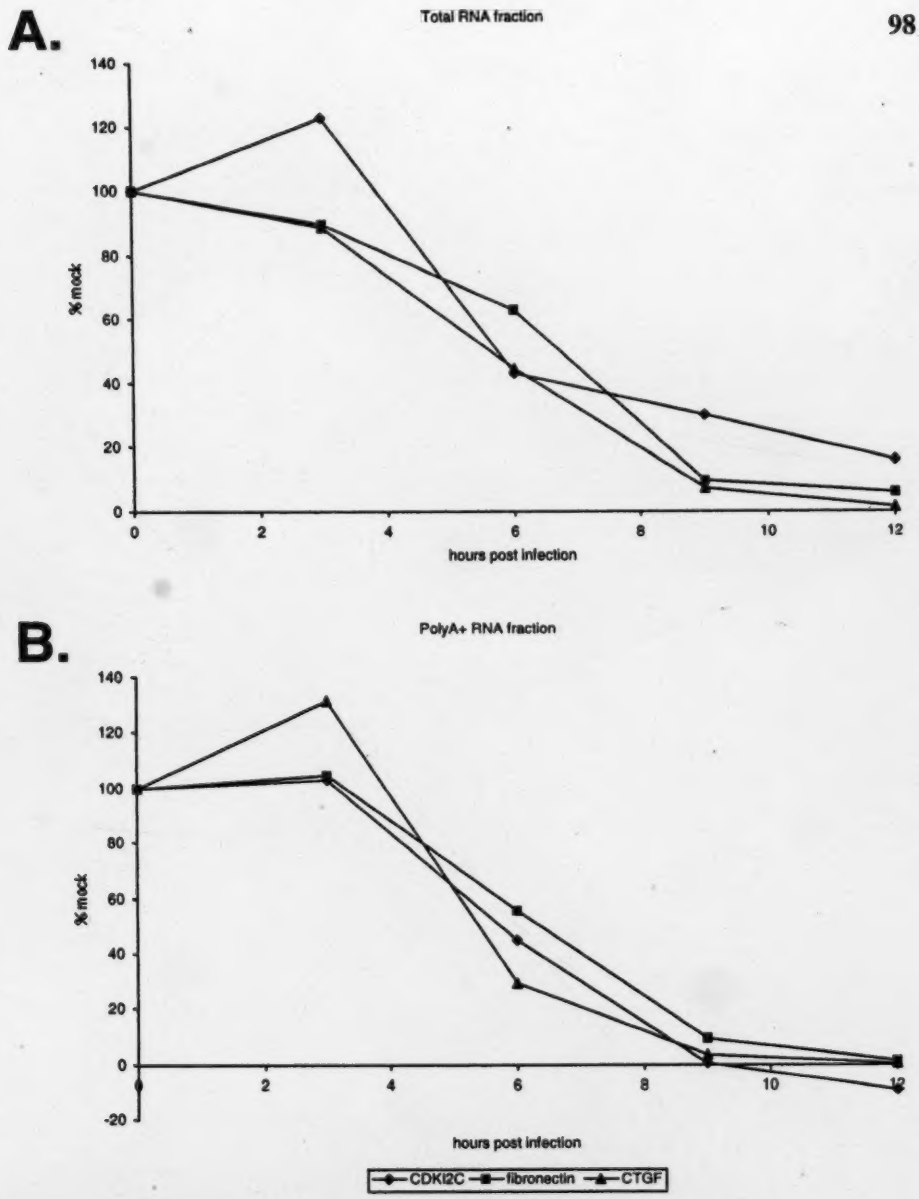

Figure 7. mRNA profiles for two cluster 16 mRNAs and one group A RNA.
The bands containing polyA$^+$ products for CDKI2C, fibronectin, and CTGF mRNAs were quantified by phosphorimager analysis. The quantitation, reported as % mock infection signal from the total RNA isolation (A) or from the poly A$^+$ RNA isolation (B), is presented above. The CDKI2C mRNA profile did not appear to be distinct from the fibronectin and CTGF mRNA profiles. CDKI2C mRNA, as measured in the polyA$^+$ RNA isolate, appeared to have decreased to levels below background by 12 hours post infection. This anomalous result was observed for the following reasons. The background signal in the CDKI2C Northern analysis was non uniform, and therefore, difficult to measure. The background signal was also high, relative to measured bands.

In summary, we conclude that the microarray quantitation was inaccurate. Group A polyadenylated RNAs were not stable, but were actually degraded over infection. The profiles of Group A and cluster 16 mRNAs were not distinguishable in Northern analysis. The distinction of the microarray cohorts could not be verified. As described later in the Discussion, the errors in quantitation of our microarray analysis may be due to our use of an inappropriate normalization protocol. We still felt that the co-sorting of ECM mRNAs into cluster 16 might stem from a real distinction in their RNA profiles over infection. We examined the RNA profiles of some of the cluster 16 ECM mRNAs in more detail for this reason as well as for the general purpose of monitoring previously uninvestigated mRNAs over infection.

3.4 Host mRNA profile in HSV-1 infection of HEL cells

Most of the experiments in this work monitored mRNA profiles in HEL cells and employed the following treatments. Actinomycin D was used to block ongoing transcription in order to assess the stability of the remaining mRNAs. UV-inactivated / UV-irradiated viruses were used to determine the shutoff effects of virion components in various infections. The following experiment was intended to verify that the dose of pre-infection UV irradiation of HSV-1 virus used effectively rendered the virus transcriptionally inactive during infection of HEL cells, and that the 10 μg/ml actD treatment successfully mediated global transcriptional arrest during infection in HEL cells. ICP27 mRNA synthesis was monitored as an index of transcriptional activity for both tests during infection. HEL cells were mock infected, infected with KOS, infected with UV-irradiated KOS, or infected with KOS in the presence of actD. We expected that ICP27 mRNA would be transcribed in KOS infection, but not from UV-irradiated KOS genomes, nor from normal KOS virus entering actD treated cells. Northern analysis of this study is shown in Figure 8. ICP27 mRNA was expressed in KOS infection, as expected. The band indicated by arrow A in Figure 8 migrated between the 1500 and 2000 base markers and was consistent with the expected band for the ICP27 transcript, reported to be 1687 bases long. UV-irradiation of virus, at the dose used in studies

presented in this work, was effective in arresting viral transcription, as was evinced by the lack of expression of ICP27 mRNA in UV-irradiated KOS infection. ActD, at the concentration used in studies presented in this work, was effective in arresting transcription, as was evinced by the lack of expression of ICP27 mRNA in KOS infection conducted in the presence of this drug.

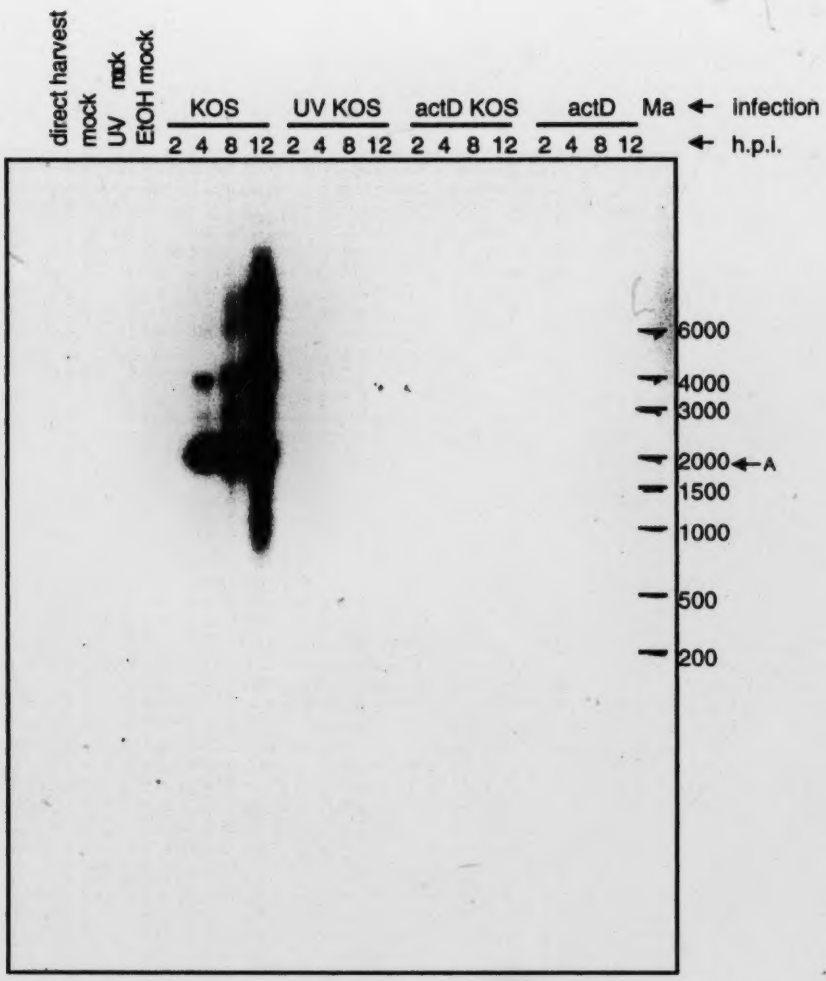

Figure 8. Northern analysis of ICP27 mRNA to verify transcriptional arrest in UV irradiated and actD treated infections.

HEL cells were directly harvested, treated with mock lysate, treated with UV irradiated mock lysate, or treated with serum free medium containing 0.2% ethanol. HEL cells were also infected with KOS, UV irratiated KOS, and KOS in the presence of actD. Mock treated HEL cell RNA was harvested at 12 h.p..i. Total RNA was isolated from infections harvested at 2, 4, 8, and 12 h.p.i. Northern analysis was done with a random prime labeled probe specific for ICP27 using the Church method and was visualized on film. RNA marker (Ma) fragment sizes are indicated on the right hand side of the figure. Arrow A indicates the position of the ICP27 transcript. The bands above band A are frequently detected by ICP27 probes in Northern analyses, but have not been definitively identified. These RNAs of higher molecular weight may be ICP27 run through transcripts.

We suspected that mRNAs coding for a cytoskeletal protein such as β-actin and an extracellular matrix protein such as collagen (two mRNAs monitored in work presented below) might have differential expression over the duration of some of the longer time courses, as their expression can vary with changing cell density. Therefore, I conducted mock time series in order to determine if expression of these genes (and others) fluctuated over the duration of studies presented below. These mock series can be viewed within each of these respective studies.

For the quantitation of Northern data, signal intensity of the earliest mock infection harvest was used as the frame of reference against which all other values for a given RNA in a given study were measured. All other values were reported as a percentage of the signal of that first mock infection harvest.

In the graphs presented in this work, the value for the zero time point in all time courses did not come from an instantaneous harvest of a given experimental treatment, unless otherwise specified. The zero time point value is 100%, represented by the common frame of reference of the first mock infection measured.

3.5 GAPDH, β-actin & collagen mRNA profiles over HSV-1 infection.

While it was not possible to distinguish the microarray cohorts by Northern analysis, the sorting of ECM genes into cluster 16 appeared to be a non-random event. We elected to monitor, in infection of HEL cells, one of the cluster 16 ECM mRNAs, which encodes the α2 subunit of type I collagen, alongside two other mRNAs that have been previously examined: one coding for glyceraldehyde–3–phosphate dehydrogenase (GAPDH), and one coding for β-actin. This investigation had multiple purposes.

First, we wanted to determine if the mRNA profiles of GAPDH and β-actin in HEL cell infection were similar to the profiles observed in other cell types in previous studies. We wished to determine if KOS infection caused extensive loss of both mRNAs,

determine if UV irradiated KOS caused partial loss of both mRNAs and determine the extent of loss of both mRNAs in the absence of vhs (ΔSma infection) in HEL cels.

Secondly, we wished to determine if the infection mRNA profile of collagen had any distinguishing attributes. Would the collagen mRNA profile be similar to the profiles of β-actin and/or GAPDH mRNAs under the test conditions described above? We planned to expand this study to other cluster 16 mRNAs if collagen mRNA profiles proved to be distinct.

Thirdly, we considered the benefits of analyzing an mRNA with very high stability, such as collagen. As described in the Introduction, collagen mRNA is highly stable. Collagen mRNA did not significantly decay in HEL cell actD incubations for the duration of infection studies in this work, thus demonstrating that collagen mRNA was indeed highly stable in our hands. Decreases in collagen RNA levels over infection of HEL cells had to include some kind of active RNA degradation or destabilization activity in order to account for the loss of pre-existing collagen mRNA. We hoped that the ability to define some RNA destabilization or degradation events might allow us to elucidate more details about the mechanisms operating to reduce collagen mRNA levels over infection.

In Figure 9, Northern analysis of collagen and GAPDH RNAs is illustrated to show the sizing of the bands seen and to indicate the bands selected for quantitation in the series of experiments that follow. The GAPDH, collagen and β-actin RNA bands are discussed below.

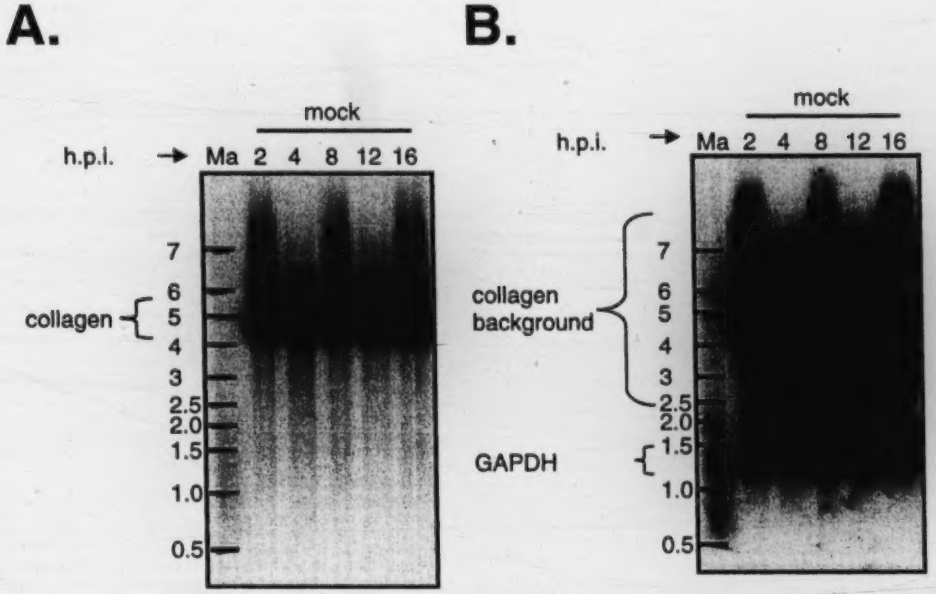

Figure 9. Northern analysis showing size determination for bands detected by probes for collagen and GAPDH mRNAs.

HEL cells were mock infected. Total RNA was harvested at 2, 4, 8, 12, and 16 hours post mock infection. Collagen mRNA was detected with a random prime labeled probe specific for the α1 subunit of type II collagen by the Church method. (The template for the probe was a PCR amplified insert sequence from I.M.A.G.E. clone 264960). Collagen mRNA was visualized on film (A). GAPDH mRNA was detected with a 5'end labeled oligonucleotide probe using the Westneat method, directly after collagen probing, without stripping, and was also visualized on film (B). RNA marker (Ma) fragment sizes are indicated, in kilobases, on the left hnd side of part A and part B in the figure. The bracketed signals in parts A and B were used for quantitation of these RNA species in this work.

The singular band detected by the GAPDH probe migrated between the 1000 and 1500 base pair markers. GAPDH mRNAs have been reported to be 1283 and 1237 base pairs in length (NCBI codes NM_002046 and M17851). The band observed was thus an expected signal, likely representing GAPDH mRNA.

Collagen RNA signal migrated as a doublet between the 4000 and 6000 base pair markers, a band above the 6000 base pair marker, and a band that ran alongside the 7000 base pair marker. BLAST alignment with the insert sequence of I.M.A.G.E. clone 264960 shows alignment with mRNAs coding for the α2 subunit of type I collagen. These mRNAs are reported to be 5060, 5084, 5416 and 5086 base pairs in length (NCBI codes BC054498, NM000089, J034641, Z74616 respectively). The lower band within the doublet was smaller in size than what is expected for collagen mRNAs. Nonetheless, the entire doublet was selected for quantitation in Northern analyses presented in this work, as the bands within could not be resolved from each other.

In experiments where β-actin mRNA was monitored, RNA markers were lacking, due to the number of samples that were simultaneously compared on one gel. Thus, the precise position of the singular band detected was not determined. On blots on which collagen, β-actin and GAPDH mRNAs were monitored, β-actin was determined to run between collagen and GAPDH mRNAs, slightly above the GAPDH band. This band position was consistent with the expected size of β-actin mRNA, which is reported to be 1729-1849 bases long (NCBI codes NM_001101.2, BC002409, BC001301, BC004251, BC012854, BC013380).

GAPDH and β-actin signals contained unique RNA species, which were specific to expected mature mRNAs. As there were multiple RNA species detected for collagen RNA, some of which were unexpected, we decided to verify that the collagen doublet signal represented polyadenylated mature collagen mRNA, and not pre mRNA species. Figure 10, lane A, shows Northern analysis of polyA$^+$ collagen RNA. Both collagen RNA doublet species were detected in this sample, confirming that both RNAs in the collagen doublet signal were polyadenylated. Notably, the poly A$^+$ collagen doublet

migrated somewhat differently, as the bands in the doublet were somewhat sharper and migrated slightly higher on the gel. The reasons for this observation are uncertain. One possible source of the variation may be reduced amounts of salt in the oligo dT column-purified sample, which had undergone both Trizol® Reagent and oligo dT column purification.

A=direct harvest & polyA+ RNA isolation (48.5%)
B=direct harvest (85.7%)
C=mock treatment with mock lysate (100%)
D=mock treatment with UV irradiated mock lysate (111%)
E=actD solvent (ethanol) treatment (82.5%)

Figure 10. Northern analysis identifying polyadenylated collagen mRNA species and monitoring mock treatment effects

HEL cells were directly harvested (A&B), mock infected with untreated (C) or UV irradiated (D) mock lysate, or were incubated with the actD solvent, ethanol (E). Total RNA was harvested 16 hours post treatment. PolyA+ RNA was purified from the direct harvest with an oligo dT column (A). Collagen mRNA was detected with a random prime labeled probe specific for the α1 subunit of type II collagen by the Church method. (The template for the probe was a PCR amplified insert sequence from I.M.A.G.E. clone 264960.) The bands within the characteristic doublet of the collagen signal (which are used in quantitation) are polyadenylated RNA species. The signal intensities of various mock treatments are reported relative to the mock lysate treatment (C) to the right of the blot.

We wished to determine if any of several mock treatments, including direct harvest, infection with mock lysate, infection with UV-irradiated mock lysate, or mock infection in the presence of actD solvent, would cause diverse effects on collagen mRNA levels. This series of mock treatments was therefore performed in HEL cells and monitored by Northern analysis to assess treament effects. The mock treatment with mock lysate, used throughout most of the studies presented in this work, is used as the frame of reference to which all other mock treatments were compared. No mock treatment tested altered the quantity of collagen mRNA obtained by more than 20%. None of the treatments applied caused major effects on collagen mRNA levels. Thus, direct harvest of cells (lane B) and the standard mock infection protocol used in this work (lane C) do not cause significantly differential collagen RNA expression. UV-irradiated mock lysate (lane D), when used in mock treatment, yielded similar collagen mRNA expression to mock treatment with unirradiated mock lysate (lane C). Therefore, effects observed with UV-irradiated virus infection are due to the virus particles, and not changes in the host proteins in the lysate. Ethanol (0.2%, added to cells as solvent for actD) did not significantly alter collagen mRNA levels in mock infection (lane E). Effects observed during actD treatment are therefore due to the actD, and not the actD solvent, ethanol.

Now that transcriptional arrest treatments were determined to be effective, mRNA bands were identified, and mock treatments were determined to not have significantly differential effects, we proceeded with an infection study of GAPDH, β-actin and collagen mRNAs. Four experiments that included the following treatments were conducted. HEL cells were infected with mock lysate, KOS, UV-irradiated KOS, and vhs$^-$ ΔSma. Cells were also incubated with actinomycin D (actD) to induce universal transcriptional arrest. We predicted the following RNA profiles, based on the HSV-1 infection RNA profile trends demonstrated in literature described in the Introduction.

We expected KOS infection to cause extensive degradation of most host mRNAs, via processes summarized below. Initially delivered vhs is thought to cause host mRNA degradation and/or destabilization at early times in infection. Newly synthesized IE viral

gene products arrest or greatly reduce transcription of host mRNAs, as well as inhibit the processing of pre mRNAs into mature mRNAs.

We expected UV-irradiated KOS infection to cause a portion of the mRNA loss observed in KOS infection, presumably via initially delivered vhs activities. We did not expect UV-irradiated KOS infection to cause the full extent of mRNA loss observed in KOS infection, as IE viral gene products are not synthesized, and their shutoff activities are not manifested.

For stable mRNAs with slow intrinsic decay rates, we predicted that ΔSma infection would be deficient in causing mRNA loss, as vhs is not present to mediate degradation of pre-existing mRNAs. Even if synthesis of new mature mRNA transcripts was abrogated via the activities of viral IE proteins, this pre-existing mRNA would remain. For less stable mRNAs with fast intrinsic decay rates, we predicted that ΔSma might be defective in causing the extent of mRNA loss observed in KOS infection, as vhs would not be present to induce degradation of pre-existing mRNAs. We also expected that there would still be a detectable decline in these transcripts because, while IE proteins could still prevent mature mRNA biogenesis (which we expect), the pre-existing mRNA molecules would detectably decay due to their inherent instability.

GAPDH, β-actin and collagen mRNAs were all monitored in one of the experimental trials of this study. Collagen mRNA was monitored in all four trials. Northern analysis for each mRNA, along with its quantitation, is shown in Figures 11, 12, and 13. As distortion in the blot within the region where collagen mRNA signal resided made quantitation of the collagen signal difficult for Figure 13A, quantitation is presented from other Northern analyses of similar series of cell treatments and infections in 13B, 13C, and 13D.

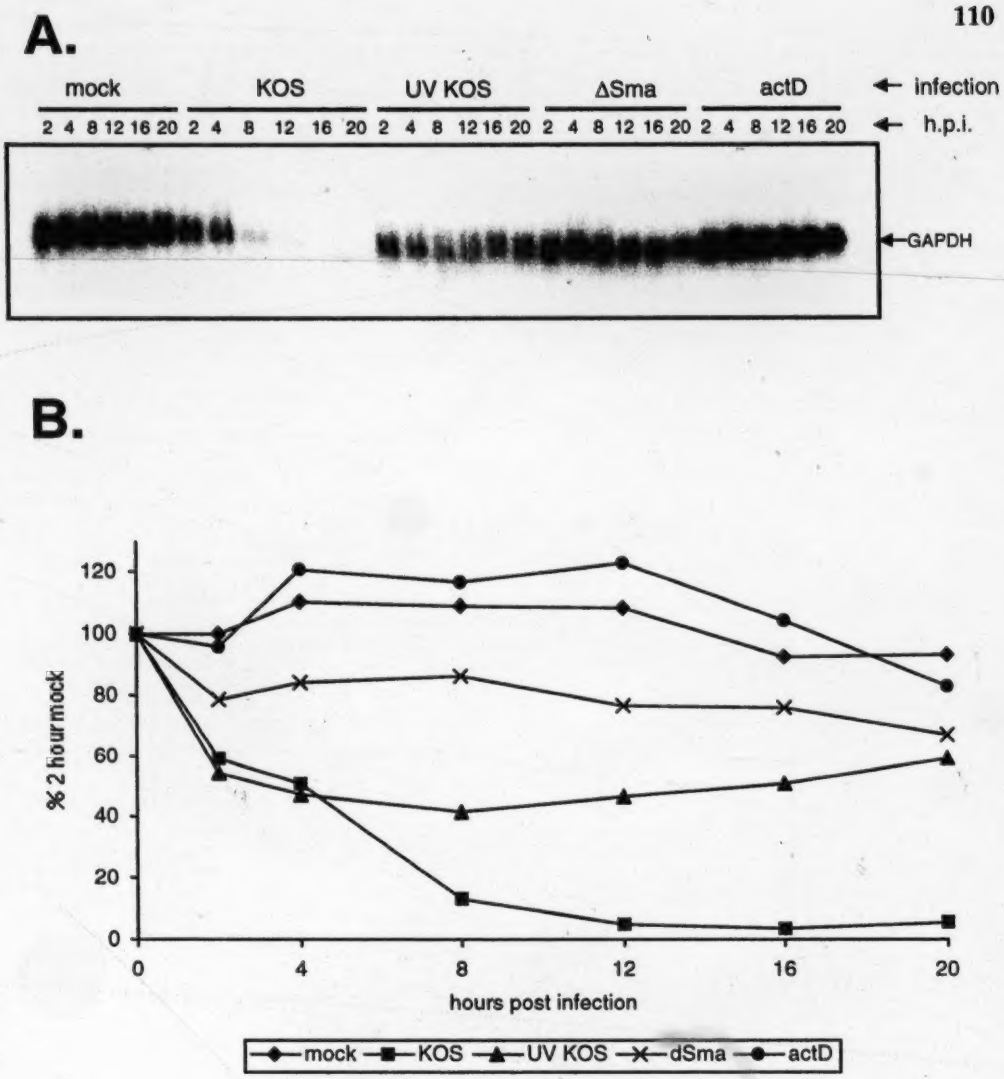

Figure 11. Northern analysis of GAPDH mRNA over the course of infection.
HEL cells were either mock infected, infected with KOS, UV irradiated KOS, or ΔSma viruses, or were incubated with actinomycin D. Total RNA was harvested at 2, 4, 8, 12, 16, and 20 h.p.i. Northern analysis was done with 5' end labeled oligonucleotide probe specific for GAPDH mRNA using the Westneat hybridization method and was visualized by phosphorimager analysis (A). Part B shows the quantitation for GAPDH mRNA in the Northern analysis presented in Figure 11A.

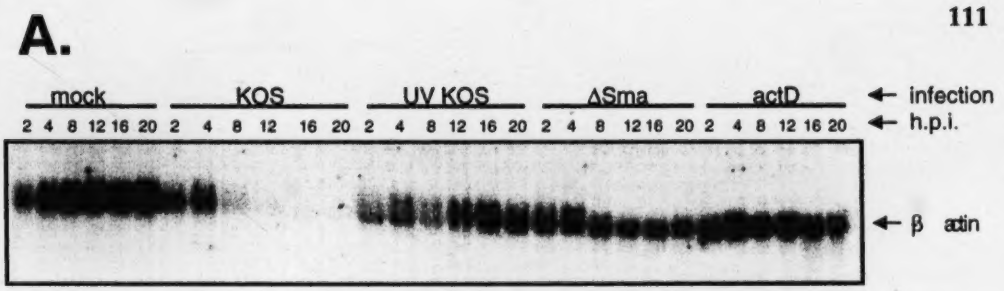

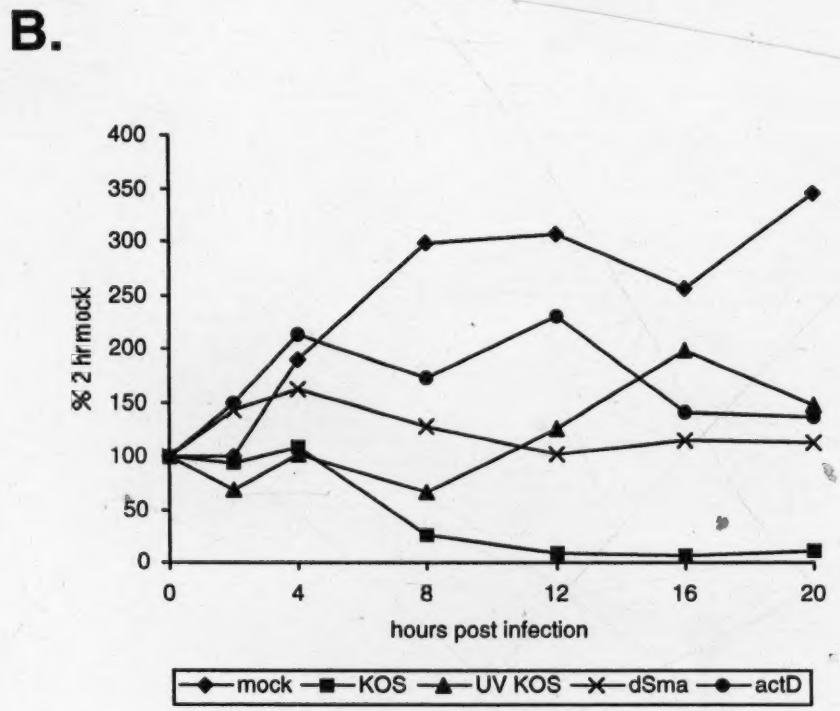

Figure 12. Northern analysis of β actin mRNA over the course of infection.
HEL cells were either mock infected, infected with KOS, UV irradiated KOS, or ΔSma viruses, or were incubated with actinomycin D. Total RNA was harvested at 2, 4, 8, 12, 16, and 20 h.p.i. Northern analysis was done with 5' end labeled oligonucleotide probe specific for β actin mRNA using the Westneat hybridization method and was visualized by phosphorimager analysis (A). Part B shows the quantitation for the β actin mRNA in the Northern analysis presented in Figure 12A.

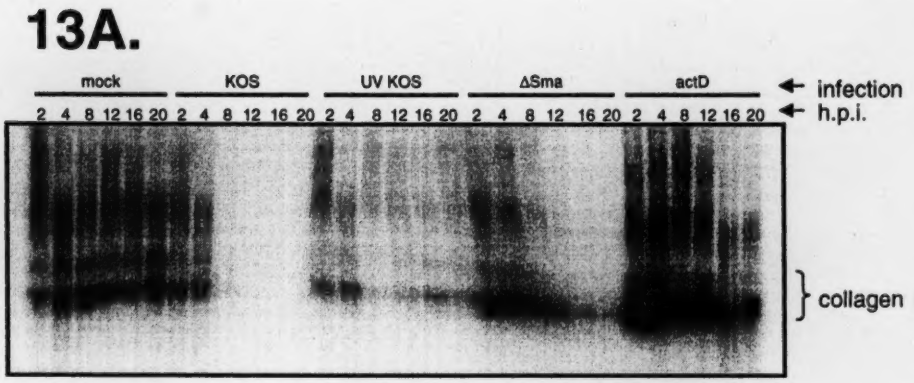

Figure 13. Northern analysis of collagen mRNA over the course of infection.
HEL cells were mock infected, infected with KOS, UV irradiated KOS, or ΔSma virus, or were incubated with actinomycin D. Total RNA was harvested at 2, 4, 8, 12, 16, and 20 h.p.i. Insert sequence from I.M.A.G.E. clone 264960 (detects collagen type I (α2 subunit) mRNA) was used as a template for random prime labeling. Northern analysis was done with this random prime labeled probe using the Church method and was visualized by phosphorimager analysis. The collagen probe detected a doublet signal, as indicated by the brackets, which was quantified. Each subfigure A Dshows a trial of this study Part ii shows the quantitation for collagen mRNA in the Northern analysis presented in Part i for each subfigure.
Figure 13A shows the detection of collagen mRNA done on the same blot used to monitor GAPDH and β actin mRNAs. Quantitation was not possible due to band distortion. Figure13B shows an experiment that was monitored only until 16 h.p.i. Additionally, RNA was directly harvested, and further purified with an RNeasy column. Further purification of the RNA with this column did not change the migration pattern of collagen RNA. Figure 13C does not contain a mock time series, but rather, contains a series of mock conditions as described in Figure 10. Figure 13D does not contain a 20 hour mock harvest.

13Bi.

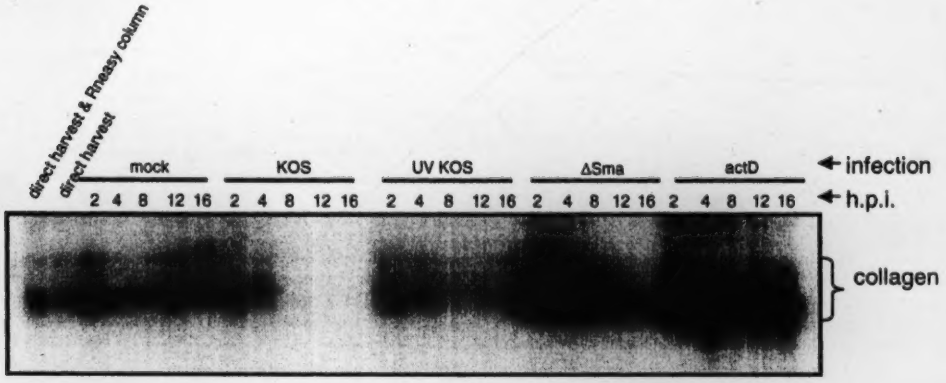
direct harvest & Rneasy column
direct harvest
mock
KOS
UV KOS
ΔSma
actD
2 4 8 12 16 2 4 8 12 16 2 4 8 12 16 2 4 8 12 16 2 4 8 12 16
infection
h.p.i.
collagen

13Bii.

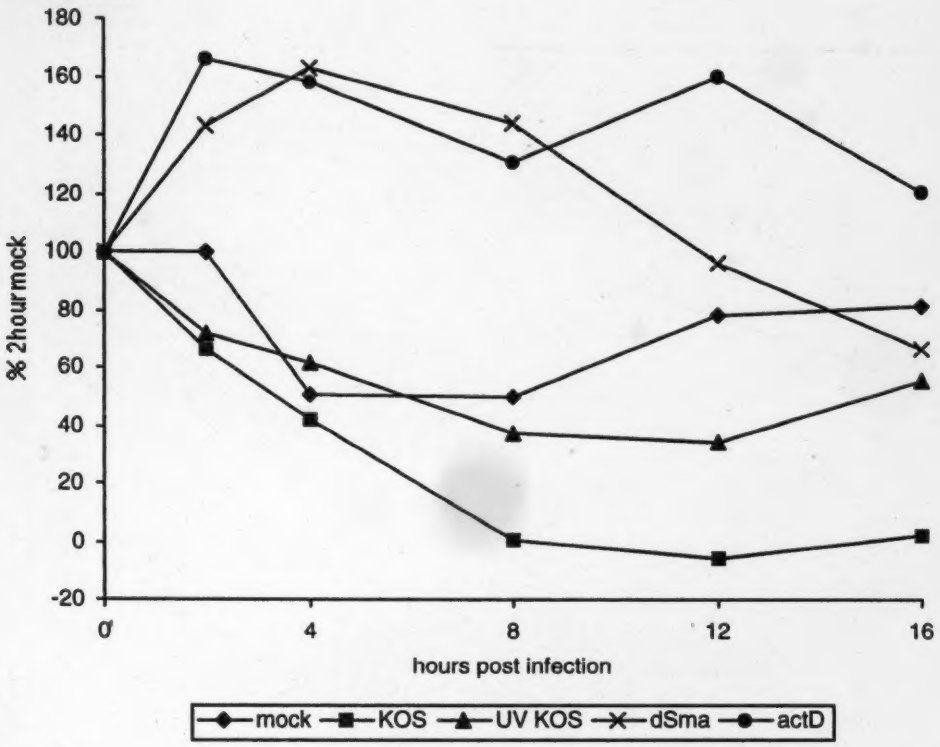
180
160
140
120
100
80
60
40
20
0
-20
% 2hour mock
0
4
8
12
16
hours post infection
mock
KOS
UV KOS
dSma
actD

13Ci.

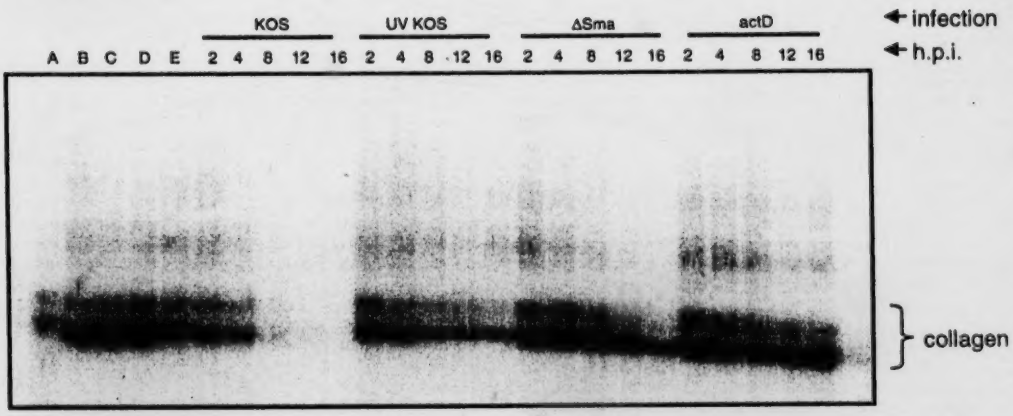

A=direct harvest & polyA+ RNA isolation
B=direct harvest
C=mock treatment
D=mock treatment with UV irradiated mock lysate
E=actD solvent (EtOH) treatment

13Cii.

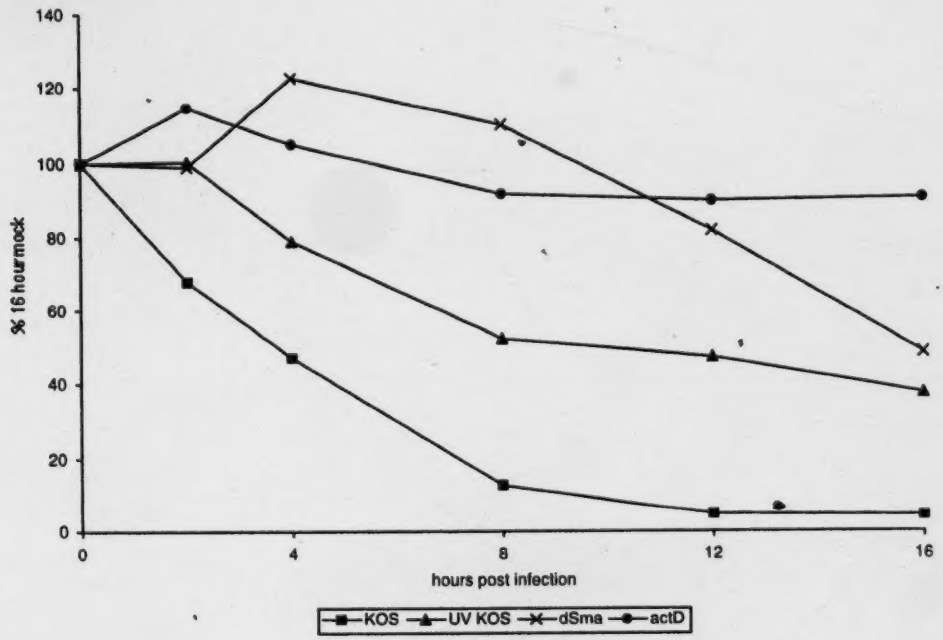

13Di.

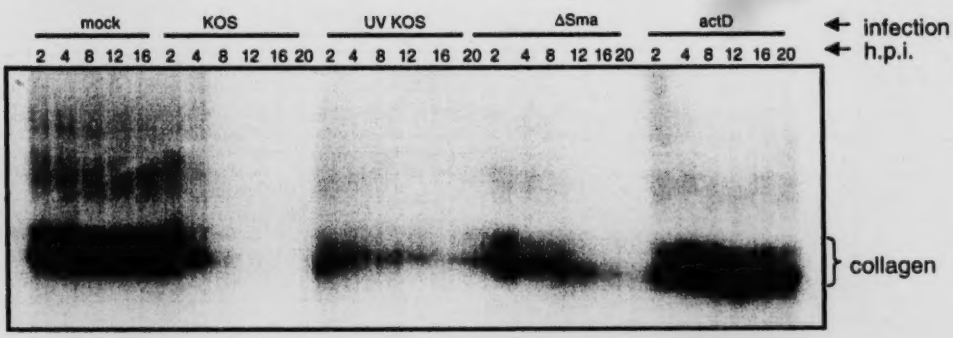
mock
KOS
UV KOS
ΔSma
actD
2 4 8 12 16 2 4 8 12 16 20 2 4 8 12 16 20 2 4 8 12 16 20 2 4 8 12 16 20
infection
h.p.i.
collagen

13Dii.

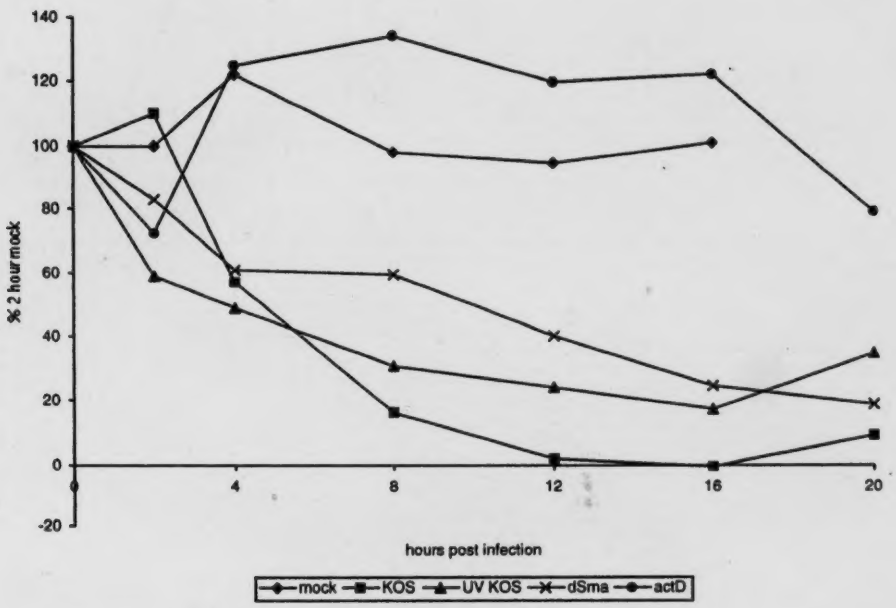
140
120
100
80
60
40
20
0
-20
% 2 hour mock
0
4
8
12
16
20
hours post infection
mock
KOS
UV KOS
dSma
actD

GAPDH mRNA profiles over mock treatment, actD treatment, KOS infection, UV-irradiated KOS infection, and ΔSma infection are illustrated in Figure 11. GAPDH mRNA levels did not fluctuate greatly over the mock infection time course; thus, GAPDH's expression appeared to be stable. As GAPDH is frequently defined as a housekeeping gene, this result was expected. Eighty-three % of the GAPDH mock signal remained after incubation of HEL cells for 20 hours with actD, evincing GAPDH mRNA's high stability and half-life exceeding 20 hours. GAPDH mRNA levels decreased to 5.5% of mock levels by 20 hours post KOS infection, evincing the very extensive GAPDH mRNA loss expected. UV-irradiated KOS infection caused partial mRNA loss, as expected, reducing GAPDH mRNA levels to 59% of mock levels by 20 h.p.i. Since GAPDH mRNA had a slow intrinsic decay rate, we predicted that ΔSma infection would be deficient in causing mRNA loss. Vhs was not present to mediate degradation of pre-existing mRNAs, and no other viral protein is known to mediate the destabilization or degradation of pre-existing mRNAs. A minimum of 76% of GAPDH mRNA remained through the first 16 hours of ΔSma infection. GAPDH mRNA decreased in abundance to 67% by 20 h.p.i. GAPDH mRNA remained intact for most of the ΔSma infection, implicating vhs as the major mediator of GAPDH mRNA loss. There may have been some mRNA loss, but the result is statistically indeterminate in this respect, as the mRNA loss was only observed at very late times post infection. As GAPDH mRNA is highly stable over the 20 hour time course analyzed, we can conclude that the mRNA loss observed in KOS infection included an active mRNA destabilization process that eliminated ~78% of the pre-existing GAPDH RNA molecules, at a minimum. (At 20 h.p.i. 83% of GAPDH pre-existing mRNA was stable. Subtract the 5.5% of GAPDH mRNA that remained after 20 hours of KOS infection to determine the approximate minimum fraction of GAPDH mRNA that was destabilized over KOS infection.) The results showing that vhs is a major mediator of GAPDH mRNA loss and that a majority of pre-existing mRNA is actively destabilized or degraded by the virus over infection are consistent with each other, as vhs is thought to function through destabilization of mRNA molecules. The above trends in GAPDH mRNA profiles over

this infection were observed in two other studies. Due to high variance from study to study, the simultaneous presentation of the data with error bars was inappropriate. The sae rank order was, however, consistently observed for the treatment described for all three experiments.

β-actin mRNA profiles over mock treatment, actD treatment, KOS infection, UV-irradiated KOS infection, and ΔSma infection are illustrated in Figure 12. The β-actin mRNA profile over the mock infection time course showed a strong increasing trend to 345% of the 2 hour mock level by 20 h.p.i. This result is not likely due to loading error, as GAPDH RNA, quantified from the same blot as shown above, did not show this increasing trend. (The β-actin mock series in Figure 20 did not show an increasing trend, thus this observation is not consistent from experiment to experiment.) It is possible that β-actin mRNA profiles differed with HEL cell passage number, which was not consistent from experiment to experiment. Conclusions cannot be made about β-actin mRNA stability from this experiment. (In Figure 20, ~74% of the β-actin mRNA mock signal was present after a 20 hour incubation of HEL cells with actD. Based on this result, we concluded that β-actin does have a half life exceeding 20 hours.) It was very difficult to interpret the trends in this Northern analysis quantitatively. Within this study, mock values increased more than three fold. Therefore, the appropriate mock value to which all other measures should be compared was not obvious. WT infection caused extensive β-actin mRNA loss, such that β-actin mRNA levels decreased to 10.9% of the amount present in the 2 hour mock sample. β-actin mRNA loss which occurred with UV-irradiated KOS infection was less extensive than with full KOS infection. Transcriptionally competent infection was therefore necessary to mediate the β-actin mRNA loss seen in wildtype infection, as expected. RNA loss which occurred with ΔSma infection was less extensive than with full KOS infection. Thus, vhs appeared to be necessary to mediate the β-actin mRNA loss seen in wildtype infection. Two other similar experiments were done with β-actin but could not be quantified due to speckles on the blot. Overall trends for β-actin mRNA in KOS^+ UV irradiated KOS infections appeared to be consistent.

Collagen mRNA profiles over mock treatment, actD treatment, KOS infection, UV-irradiated KOS infection, and ΔSma infection are illustrated in Figure 13.

In the mock time courses, collagen mRNA profiles were not identical from study to study. The study shown in Figure 13A showed some fluctuation in collagen mRNA levels over the time course. In the study shown in Figure 13B, collagen mRNA levels decreased to 50% of 2 hour mock levels at 4 and 8 hours post treatment. The collagen mRNA levels were ~80% of 2 hour mock levels for 12 and 16 hours post treatment. In the study shown in Figure 13D, collagen mRNA levels increased to 122% of 2 hour mock levels by 4 hours post treatment, and then appeared to steady within a 6% range of the 2 hour RNA level for 8, 12, and 16 hours post treatment. Generally, there was no consistent increasing or decreasing trend in collagen mRNA levels over mock series. The observed variation in collagen mRNA levels in these studies may be due to experimental error in RNA quantitation, gel loading precision or collagen mRNA signal quantitation from the blots. It is also possible that collagen mRNA profiles differed with HEL cell passage number, which was not consistent from experiment to experiment.

In the actD treatment time courses, collagen mRNA profiles were generally more similar. The study shown in Figure 13A showed a late decrease in collagen RNA levels at 16 hours post treatment. In the study shown in Figure 13B, collagen mRNA levels did not apparently decrease over the duration of the 16 hour actD treatment. In the study shown in Figure 13C, collagen mRNA levels decreased slightly to ~90% of mock levels for 12 and 16 hours post treatment. In the study shown in Figure 13D, collagen mRNA levels appeared to be 72% of mock levels at 2 hours post actD treatment, and 79% of mock levels at 20 hours post actD treatment. At all other time points, no decreases were observed in this trial. Even conservatively, we can deduce that collagen mRNA has a half life exceeding 20 hours.

In all trials shown in Figure 13, KOS infection caused extensive collagen mRNA loss. As shown in Figures 13B, 13C, and 13D, 1.6%, 4.5%, and 9.2% of mock collagen mRNA levels remained after 16, 16, and 20 hours of KOS infection respectively.

Collagen mRNA levels decreased partially during UV-irradiated KOS infections shown in Figure 13, as expected. The lowest collagen mRNA levels observed during

UV-irradiated KOS infections were 34%, 38%, and 17% of mock collagen mRNA levels at 12, 16, and 16 h.p.i., in Figures 13B, 13C, and 13D respectively. While the amount of RNA that remained after infection with UV-irradiated KOS was not uniform, within each experiment, collagen mRNA levels consistently decreased less than they did in transcriptionally competent KOS infection. Within each UV-irradiated KOS infection, collagen mRNA levels decreased and then plateaud, or decreased and then slowly increased afterward.

ΔSma infection resulted in variable collagen mRNA loss, which, if it occurred, occurred at late times post infection. In the study shown in Figure 13B, collagen mRNA levels did not decrease until 16 h.p.i., whereupon collagen mRNA levels decreased to 67% of mock levels. In the study shown in Figure 13C, collagen mRNA levels did not decrease until 12 h.p.i. Collagen mRNA levels decreased to 82% and 49% of mock levels by 12 and 16 h.p.i., respectively. In the study shown in Figure 13D, collagen mRNA levels appeared to decrease more rapidly than in the other trials, with a decrease to 61% of mock levels by 4 h.p.i, followed by a continuous decrease to 19% of mock levels by 20 h.p.i. In all three quantified studies of ΔSma infection, some collagen mRNA loss did occur. When compared to the collagen mRNA loss which occurred in actD incubation within each experiment, collagen mRNA loss with ΔSma was more extensive. The late collagen mRNA loss that occurred in ΔSma infection therefore included destabilization and/or degradation of pre-existing collagen mRNA. When compared to the collagen mRNA loss that occurred in ΔSma infection, within each experiment, the collagen mRNA loss that occurred with UV-irradiated KOS infection was more extensive, and generally occurred at earlier time points.

As discussed in the Introduction, previous studies have demonstrated that KOS / wildtype infection causes virtually complete loss of mRNAs studied. This trend was true for GAPDH, β-actin and collagen RNAs in work presented above. Previous studies have also demonstrated that infection with UV-irradiated KOS, which includes initially delivered vhs, mediates only a portion of the mRNA loss observed in KOS infection. Results presented above for GAPDH and collagen RNAs were consistent with this

finding. The results for β-actin mRNA are inconclusive in this respect. In UV-irradiated KOS infections where GAPDH and β-actin mRNAs were monitored, and for 2 out of 3 UV-irradiated KOS infections where collagen mRNA was monitored, a small increase in RNA levels was observed at late times post infection. These increases suggest that a transcriptionally competent host cell may be able to partially recover from the RNA losses that are incurred during UV-irradiated KOS infection. A minor amount of GAPDH mRNA was lost during ΔSma infection. As GAPDH mRNA was shown to be highly stable, this result was expected. As suggested above, IE viral products may have arrested GAPDH mRNA transcription and GAPDH mRNA maturation. However, in the absence of the mRNA destablization activity of vhs, pre-existing GAPDH may have remained. β-actin mRNA degradation was not observed in ΔSma infection, and therefore, vhs is necessary to mediate β-actin mRNA loss. Very little, if any, collagen mRNA loss occurred in the absence of vhs at early times in infection. In some studies, at later times in ΔSma infection, however, some collagen mRNA loss was observed. As described above, arrest of mRNA transcription and inhibition of mRNA maturation would not cause a decrease in levels of pre-existing stable collagen mRNA in the absence of vhs. Therefore, given that collagen mRNA is highly stable, and vhs was absent in ΔSma infection, it was surprising to see collagen mRNA loss in this context.

Collagen mRNA profiles in KOS and UV-irradiated KOS infections were generally similar to those observed for GAPDH and β-actin RNAs. The only unique character implicated for the cluster 16 mRNA coding for the α2 subunit of type I collagen thus far, is that in some studies of ΔSma infection, late vhs-independent RNA destabilization was observed.

Recall that the current understanding of host mRNA loss during infection implicates initially-delivered vhs in RNA destabilization activities at early times post infection, before the synthesis of new viral products, and ICP27 and other IE proteins in transcriptional arrest and pre mRNA maturation inhibition at later times post infection. UV-irradiated virus infection, which contains initially-delivered vhs, does not mediate complete shutoff at the RNA level. According to current literature perspectives, this

occurs because new host mRNA biogenesis is still occurring in the absence of IE gene products, and vhs mRNA destabilization activities are presumably catalytically inadequate to cause complete RNA level shutoff when new mRNAs are being made.

It is possible to explain the above results with a different perspective on the role of vhs in inducing mRNA loss. Newly-synthesized vhs may contribute to host mRNA destabilization during infection. This postulate could also explain the necessity for vhs for host mRNA loss throughout infection. Partial mRNA loss observed during UV-irradiated virus infection could reflect the lack of new vhs synthesis. As described in the Introduction, vhs activity is tempered by VP16 at late times post infection. This does not, however, indicate that vhs has absolutely no catalytic activity at these times.

3.6 Vhs levels in KOS and 5dl1.2 infections

We've proposed above that newly-synthesized vhs may be catalytically relevant at late times in infection. ICP27 is an IE protein that is likely required for optimal late vhs gene expression. Therefore, some RNA level shutoff activities that are reported to depend on ICP27 may actually be occurring via upregulation of vhs expression.

In consideration of the above postulate, the following experiment was conducted to verify that efficient late vhs expression did indeed require the expression of ICP27. Vhs protein expression in KOS and 5dl1.2 (ICP27$^-$) infections was compared by Western blot analysis. Infections were monitored in HEL cells and Vero cells. The Western blot analysis is illustrated in Figure 14. The size of the singular band detected in HEL cells is consistent with the size reported for vhs protein of 58kDa (302). The vhs band in the Vero cell Western was observed in the context of background bands, which could be identified as non-vhs species, as they were present in mock infected samples. The vhs band in the Vero cell Western also appeared to be the correct size. In ΔSma infection of HEL cells, no truncated vhs product was detected. The antibody used was generated with the full vhs ORF and could possibly have detected the expected putative truncated vhs protein (303). Perhaps the truncated protein was not synthesized at significant levels in our study, or perhaps the polyclonal antibody preparation did not have many antibodies that effectively targeted epitopes of the truncated protein.. In KOS infected HEL cells,

vhs was detectably and consistently expressed from 8 until 16 h.p.i. The vhs expression decreased by 20 h.p.i. This late vhs protein decrease may be an artifact due to loss of cells over infection. Vhs protein expression was not detectable in 5dl1.2 (ICP27$^-$) infected HEL cells. In KOS infected Vero cells, vhs was detectably and strongly expressed from 8 – 20 h.p.i. The long exposure of the Vero cell Western showed a low level of vhs protein expression in KOS infected cells at 2 and 4 h.pi., and throughout the full 20 hour time course in 5dl1.2 (ICP27$^-$) infection. Our results did not determine if the low levels of vhs detected in ICP27$^-$ infection are initially delivered vhs or "leaking" newly synthesized vhs molecules. This study was repeated once with similar results. In summary, these results indicate that ICP27 was required for wildtype robust vhs protein levels to manifest in infection. The requirement for ICP27 to induce robust vhs expression is consistent with the postulate that some of ICP27's RNA shutoff activities may occur through upregulation of vhs.

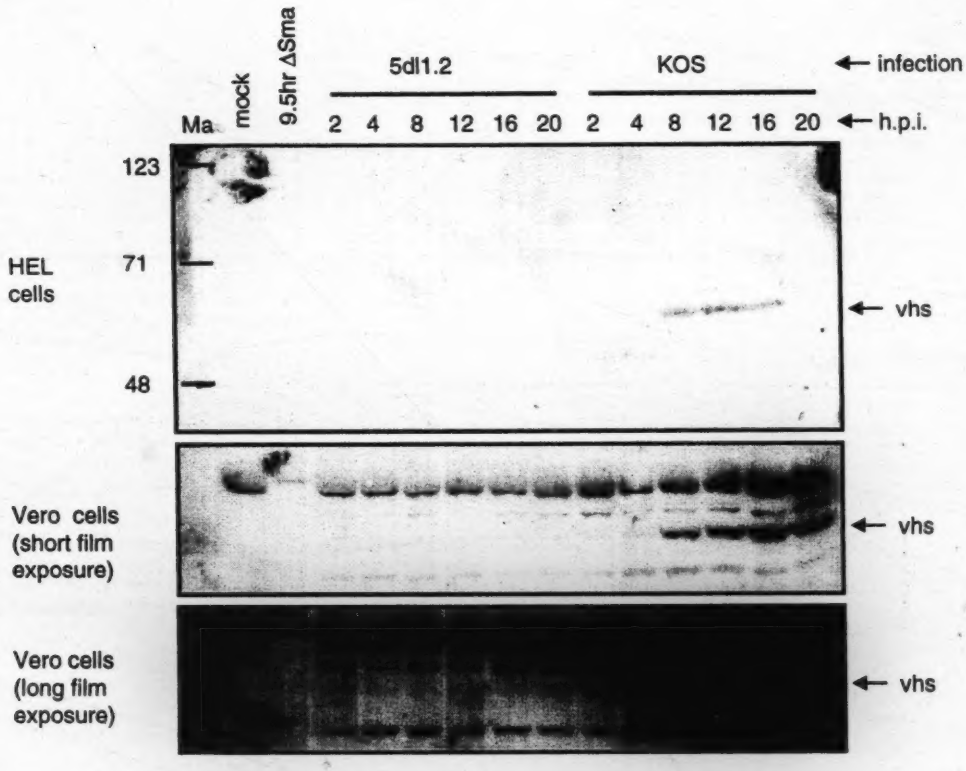

Figure 14. Western analysis illustrating vhs protein levels in 5dl1.2 and KOS infections.
Both HEL cells and Vero cells were either mock infected or infected with KOS and 5dl1.2 viruses. The mock infections were harvested at 2 h.p.i. KOS and 5dl1.2 infections were harvested at 2, 4, 8, 12, 16, and 20 h.p.i. The ΔSma infection was harvested during a previous experiment in which HEL cells were infected with ΔSma and were harvested at 9.5 h.p.i. All samples were harvested into SDS PAGE lysis buffer and cells equivalents for each cell type were resolved on 10% SDS PAGE gels. Western analysis was conducted with rabbit polyclonal antibody specific for vhs, precleared with mock lysate from the infected cell type.

3.7 Collagen, GAPDH, β-actin, fibronectin & exostoses mRNA profiles over IE mutant and UV-irradiated IE mutant infections

As described in the Introduction, viral immediate early proteins ICP0, ICP4, ICP22 and ICP27 have been implicated in RNA-level host shutoff through inhibition of host transcription. ICP27 has been implicated in RNA-level host shutoff through inhibition of mRNA processing. The following experiment was intended to determine if these IE proteins exterted their expected influence on profiles of RNAs that have been examined previously as well as on cluster 16 ECM mRNA profiles that have not been studied in this respect (and that may be differentially affected by IE proteins). We reasoned that RNA-level shutoff would be compromised in infections lacking a given IE protein if that IE protein was necessary for the shutoff of the mRNA under study. We therefore studied the RNA-level shutoff profiles of cluster 16 collagen, fibronectin and exostoses mRNA profiles alongside those of GAPDH and β-actin mRNAs over n212 (ICP0$^-$), d120 (ICP4$^-$), d22lacZ (ICP22$^-$), and 5dl1.2 (ICP27$^-$) infections in order to determine which IE proteins were critical for the shutoff of these mRNAs. Mock series were done in order to determine if expression of these genes fluctuated over the duration of this study. ActD incubations were included to monitor the stability of mRNAs in this study. UV-irradiated IE knockout infections were done as well, in order to compare the RNA-level shutoff activities of initially-delivered proteins from each mutant studied. Northern analysis of the above study is illustrated in Figure 15. Quantitation of data in Figure 15 is presented graphically in Figures 16, 17, 18, 19 and 20. Table 4 includes all of the quantitation from this study, so that any further comparative analysis can be done. As there were no repeat trials with which standard deviations could be calculated in this study, we arbitrarily chose to discuss differences greater than 10% of 2 hour mock levels for each mRNA.

15A. collagen & GAPDH mRNA

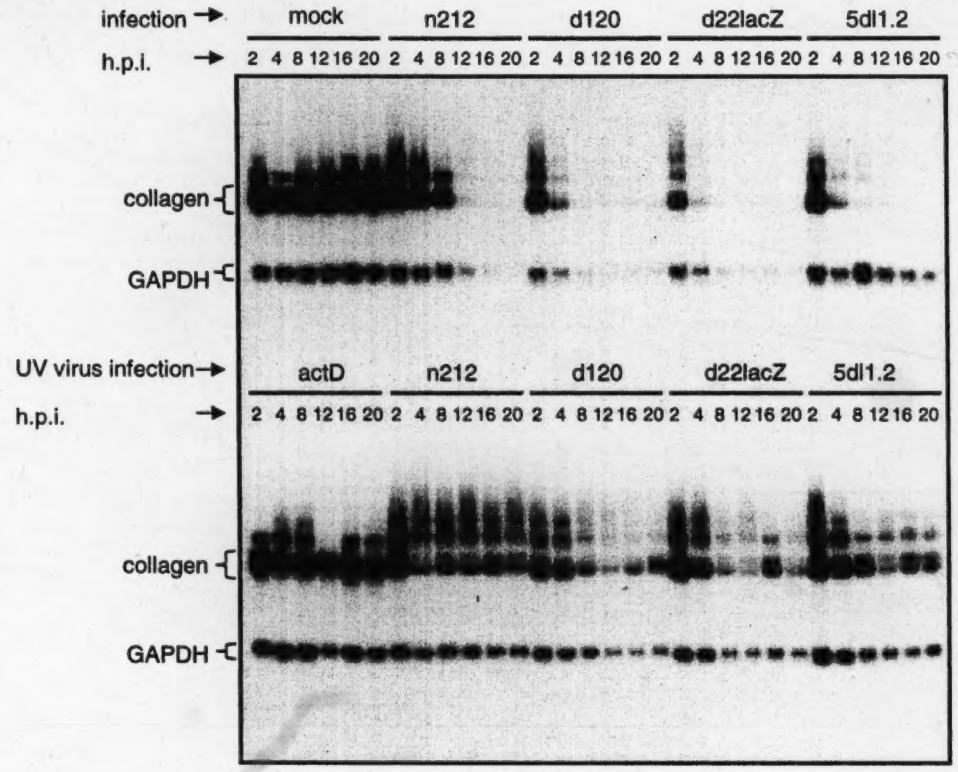

15B. β actin mRNA

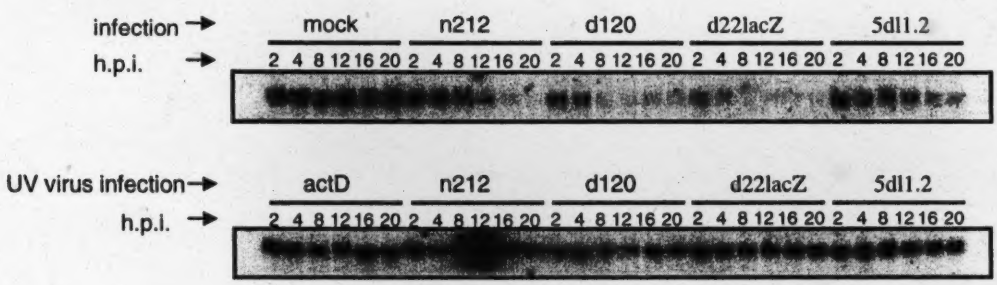

15C. fibronectin mRNA

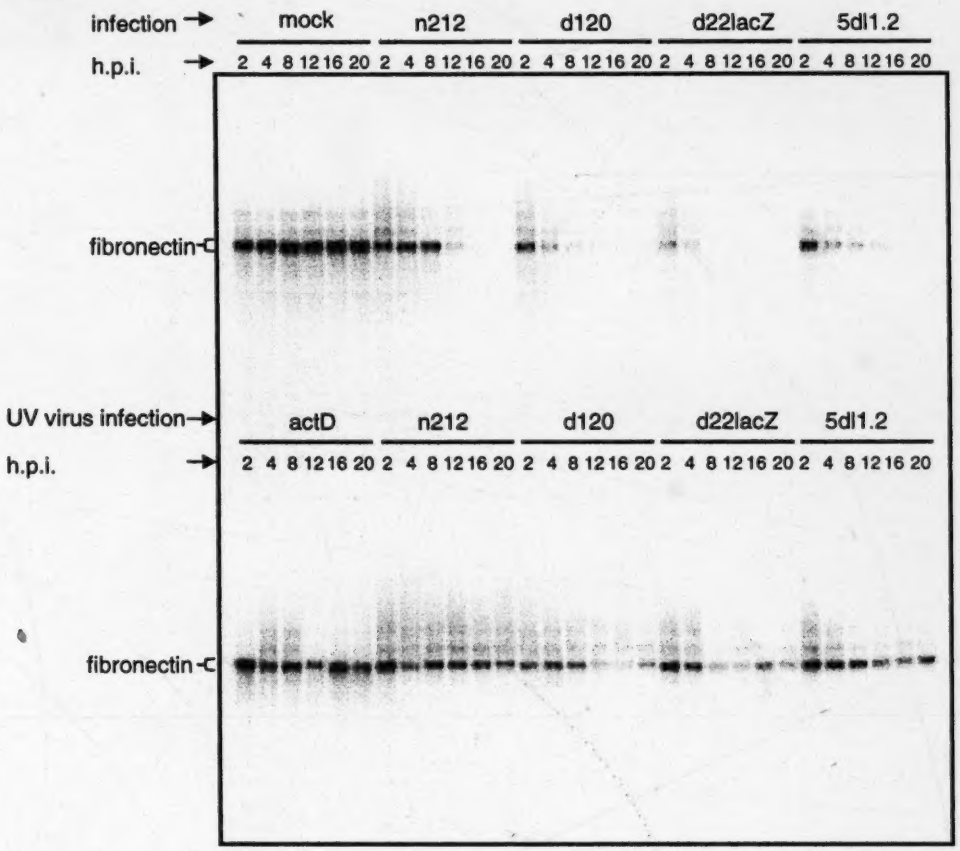

15D. exostoses mRNA

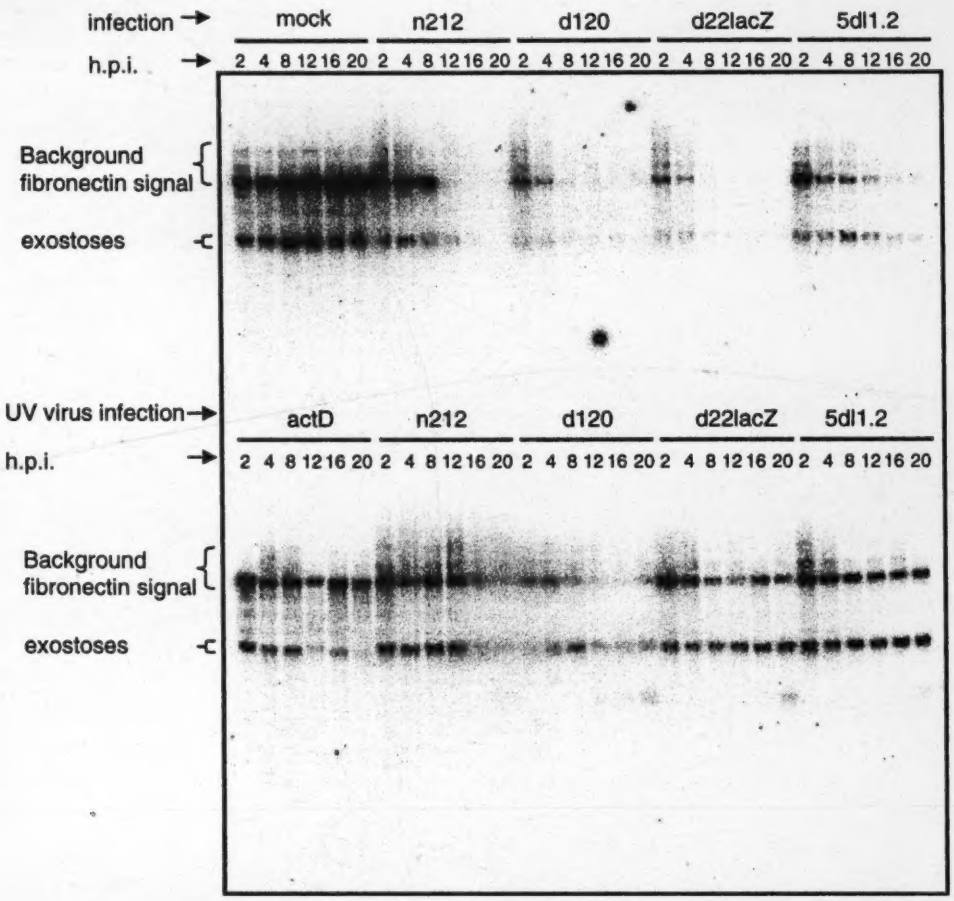
infection
mock
n212
d120
d22lacZ
5dl1.2
h.p.i.
2 4 8 12 16 20 2 4 8 12 16 20 2 4 8 12 16 20 2 4 8 12 16 20 2 4 8 12 16 20
Background fibronectin signal
exostoses
UV virus infection
actD
n212
d120
d22lacZ
5dl1.2
h.p.i.
2 4 8 12 16 20 2 4 8 12 16 20 2 4 8 12 16 20 2 4 8 12 16 20 2 4 8 12 16 20
Background fibronectin signal
exostoses

Figure 15. Northern analysis of a series of mRNAs over mock, IE mutant infections, and UV irradiated IE mutant infections.

HEL cells were mock infected, were infected with both transcriptionally competent, and UV irradiated n212 (ICP0$^-$), d120 (ICP4$^-$) , d22lacZ (ICP22$^-$), and 5dl1.2 (ICP27$^-$) viruses, or were incubated with actinomycin D. Total RNA was harvested at 2, 4, 8, 12, 16, and 20 h.p.i. Collagen mRNA was detected with a random prime- labeled probe specific for the α2 subunit of type I collagen by the Church method. GAPDH mRNA was detected with 5' end labeled oligonucleotide probe using the Westneat method, directly after collagen probing, without stripping of the blot. Collagen and GAPDH were visualized together on film (A). The Northern blot was stripped. Northern analysis of β actin mRNA was done with 5'end labeled oligonucleotides using the Westneat method and was visualized by phosphorimager analysis (B). The blot was stripped again. Northern analysis of fibronectin mRNA was done with random prime labeled probe by the Church method and visualized by phosphorimager analysis (C). The radioactive signal was allowed to decay. Northern analysis was done for exostoses mRNA with random prime labeled probe using the Church method and was visualized by phosphorimager analysis (D). Background fibronectin signal is still visible (D). Bands used in quantiatative analysis (shown in other figures) are indicated with brackets to the left of the figure.

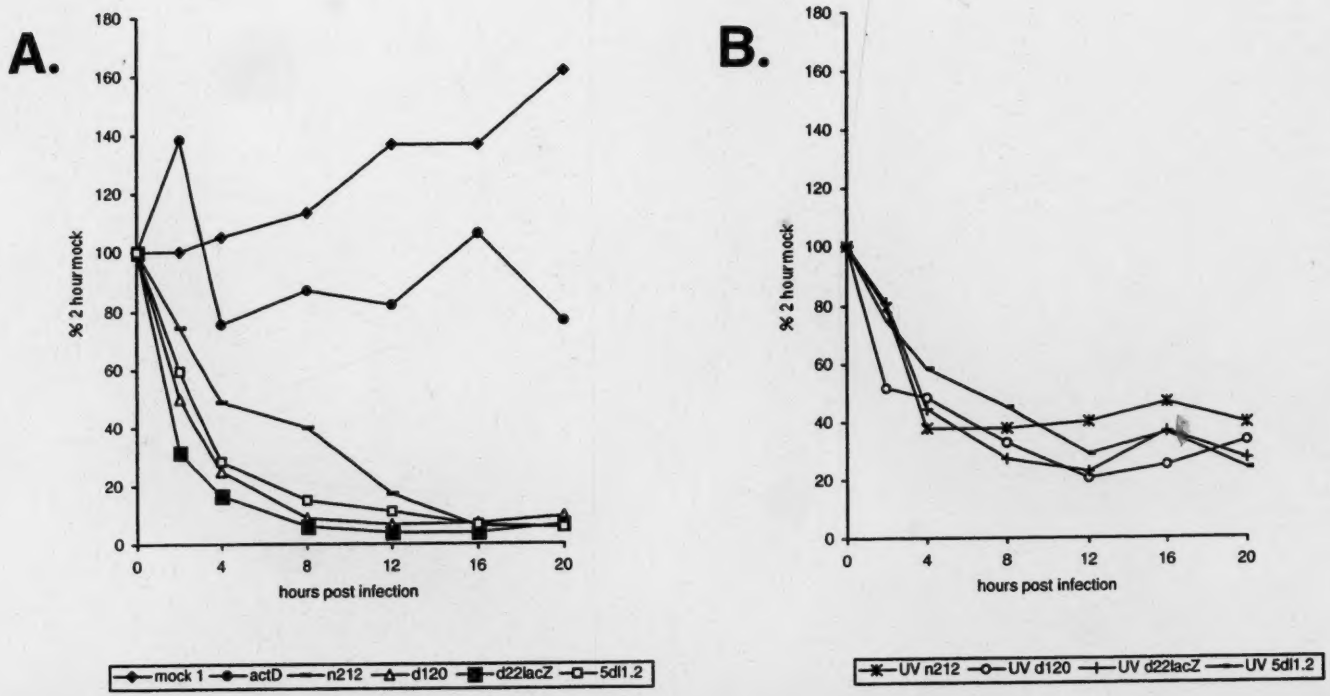

Figure 16. Collagen mRNA profiles over IE mutant infections and UV irradiated IE mutant infections.
The doublet for collagen mRNA indicated by brackets in Figure 15 was quantified by phosphorimager analysis. Part A shows the RNA profiles of the mock treatment, actD treatment, and infections with n212, d120, d22lacZ, and 5dl1.2. Part B shows the RNA profiles of infections with UV irradiated n212, d120, d22lacZ, and 5dl1.2.

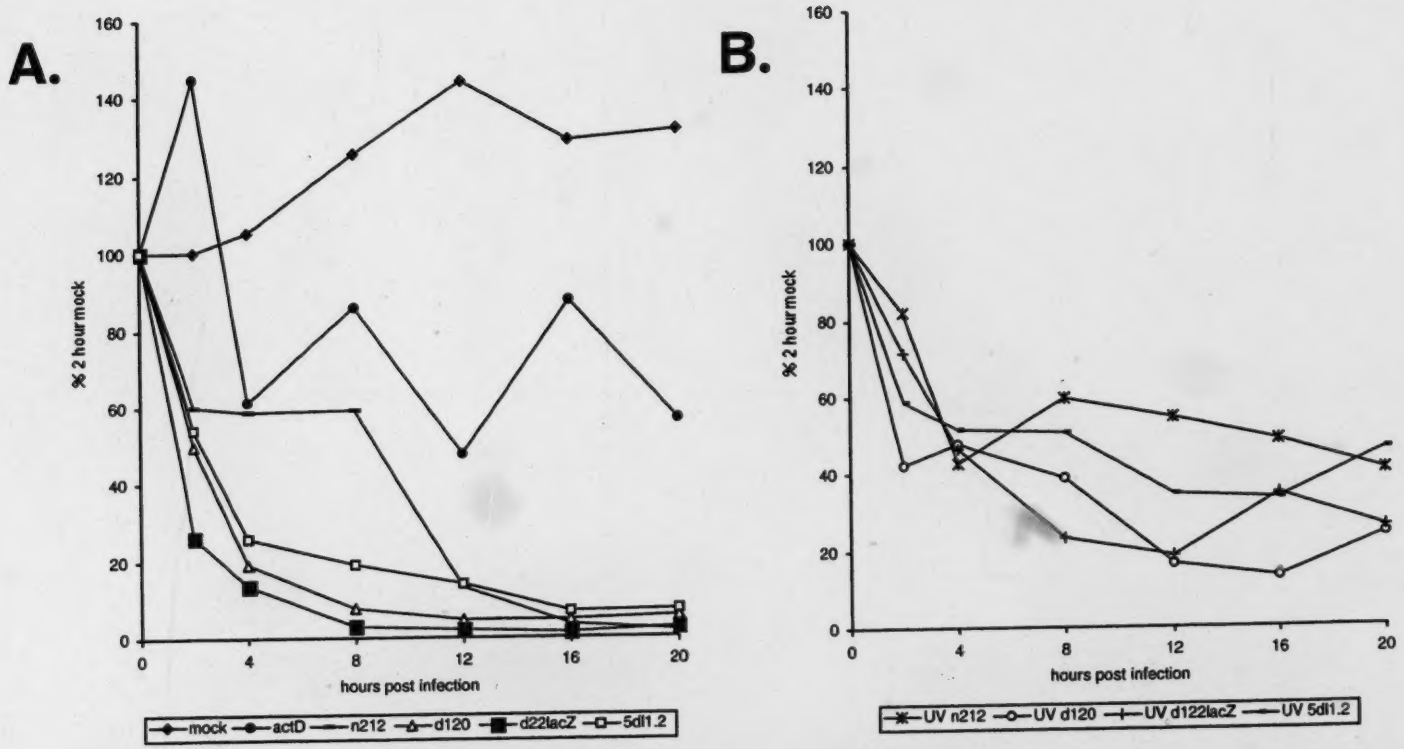

Figure 17. Fibronectin mRNA profiles over IE mutant infections and UV irradiated IE mutant infections.
The fibronectin mRNA band from Figure 15 was quantified by phosphorimager analysis. Part A shows the RNA profiles of the mock treatment, actD treatment, and infections with n212, d120, d22lacZ, and 5dl1.2. Part B shows the RNA profiles of infections with UV irradiated n212, d120, d22lacZ, and 5dl1.2.

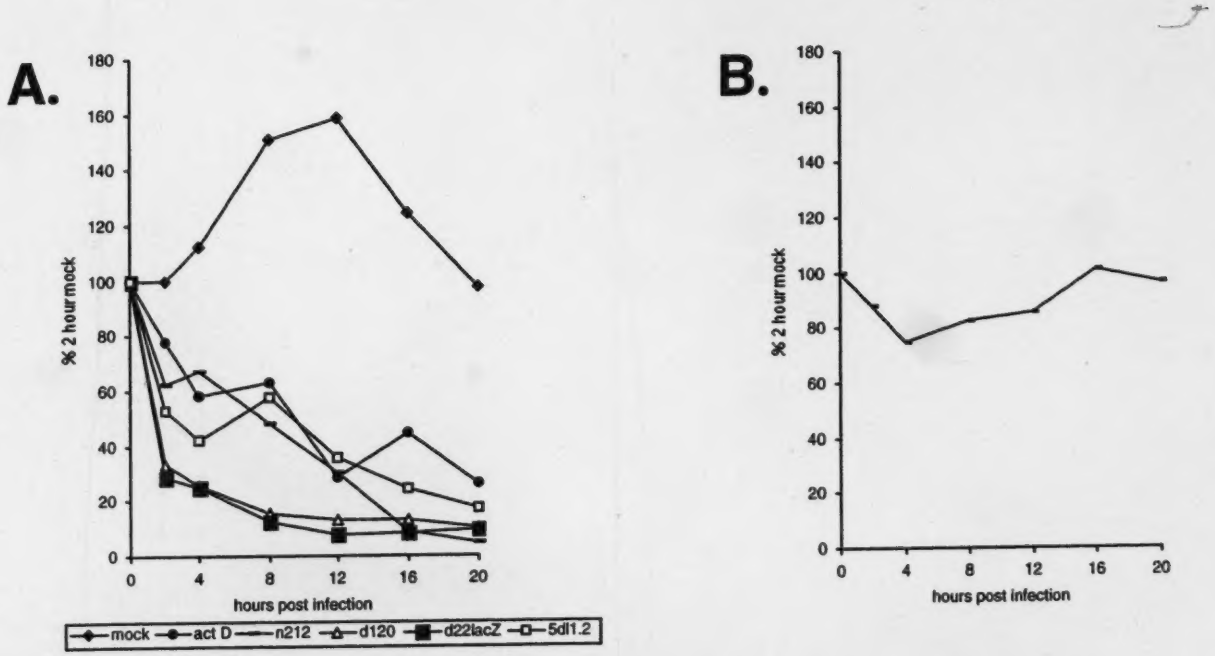

Figure 18. Exostoses mRNA profiles over IE mutant infections and UV irradiated 5dl1.2 (ICP 27⁻) infections.
The band for exostoses mRNA from Figure 15 was quantified by phosphorimager analysis. Part A shows the RNA profiles of the mock treatment, actD treatment and infections with n212, d120, d22lacZ, and 5dl1.2. Part B shows the RNA profile of infection with UV irradiated 5dl1.2. The quantitation of the RNA profiles for UV irradiated n212, d120 and d22lacZ infections are not presented, due to apparent damage of the Northern blot where these profiles were monitored.

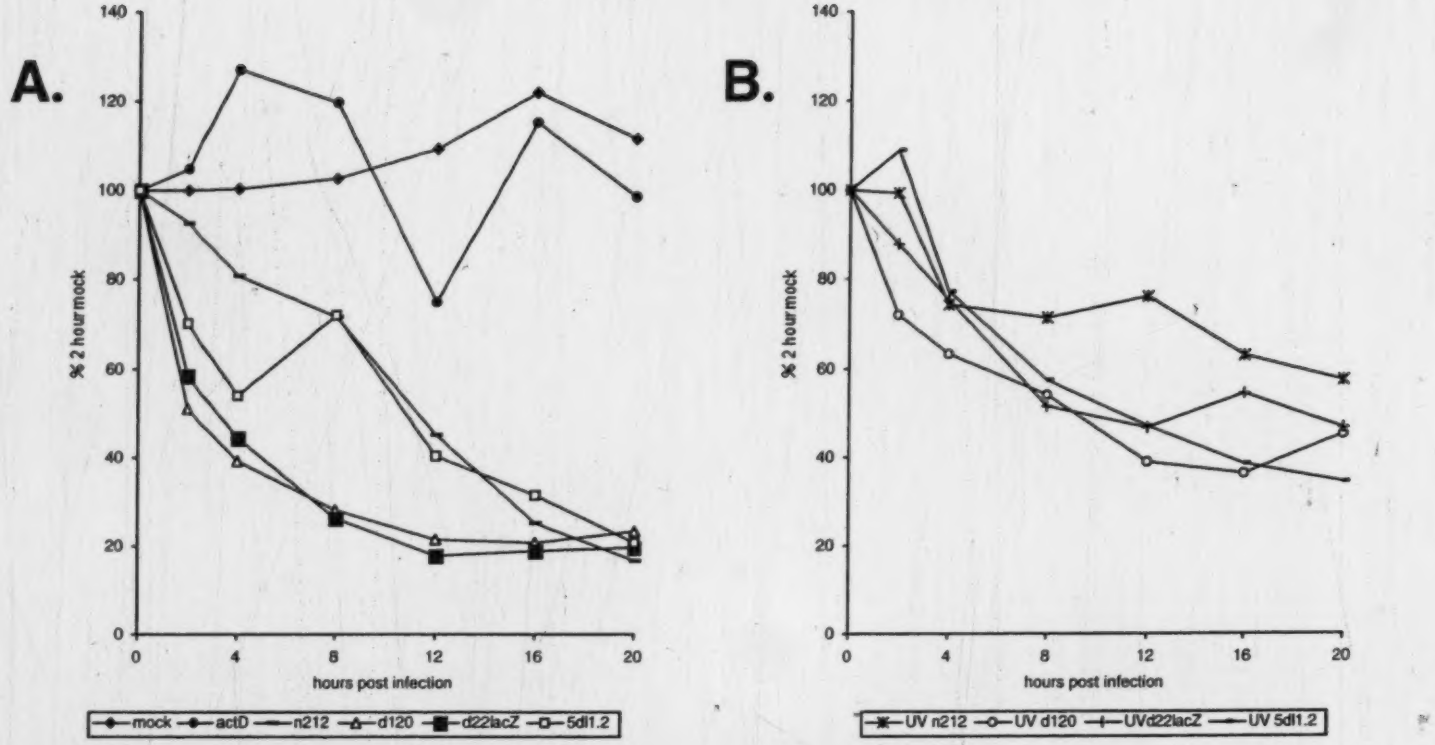

Figure 19. GAPDH mRNA profiles over IE mutant infections and UV irradiated IE mutant infections.
The band for GAPDH mRNA from Figure 15 was quantified by phosphorimager analysis. Part A shows the RNA profiles of the mock treatment, actD treatment, and infections with n212, d120, d22lacZ, and 5dl1.2. Part B shows the RNA profiles of infections with UV irradiated n212, d120, d22lacZ, and 5dl1.2.

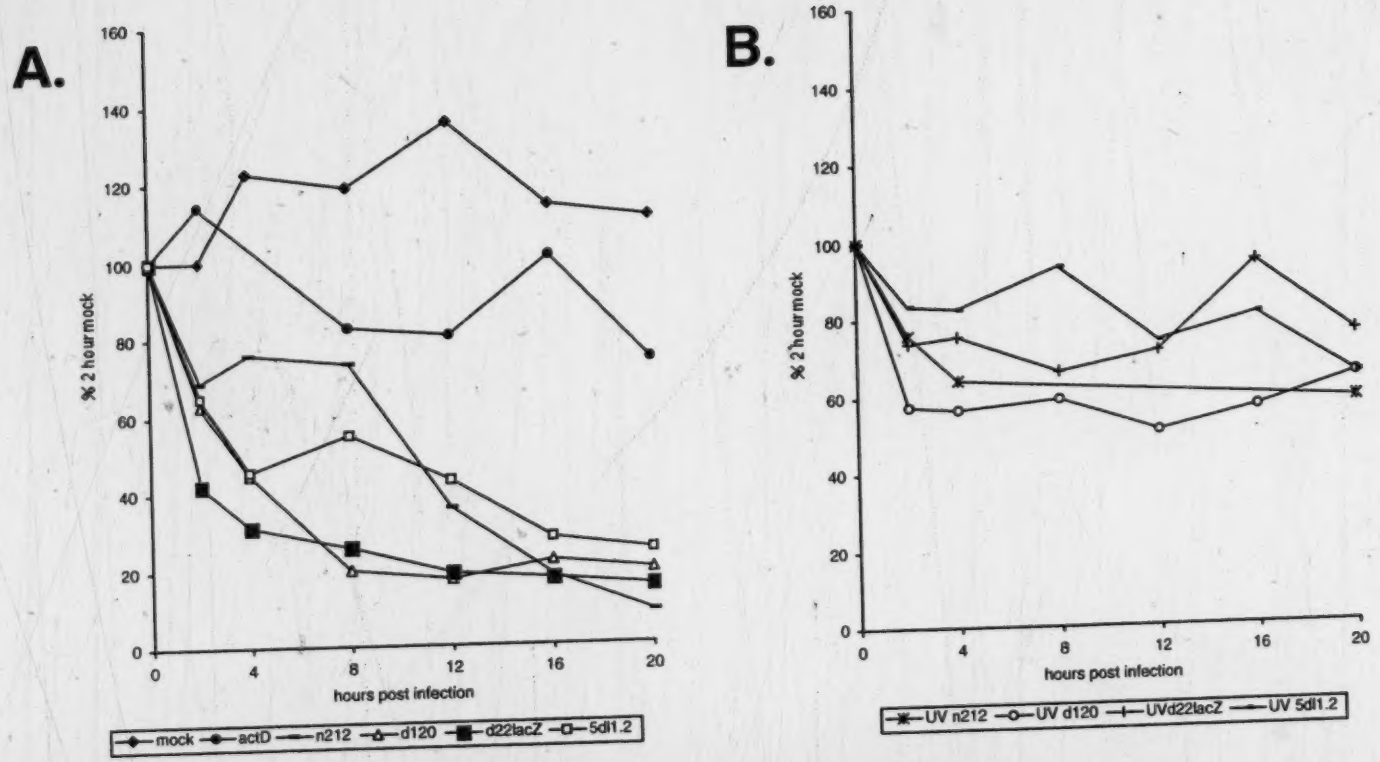

Figure 20. β actin mRNA profiles over IE mutant infections and UV irradiated IE mutant infections.
The band for β actin mRNA from Figure 15 was quantified by phosphorimager analysis. Part A shows the RNA profiles of the mock treatment, actD treatment, and infections with n212, d120, d22lacZ, and 5dl1.2. Part B shows the RNA profiles of infections with UV irradiated n212, d120, d22lacZ, and 5dl1.2. The β actin mRNA bands for the 4 hour time point in actD incubation, as well as the 8, 12 and 16 hour time points for UV irradiated n212 infection, were not included in quantitation, due to spurious background.

Table 4. Quantitation of a series of mRNAs over mock, IE deletion mutant infections, and UV-irradiated IE deletion mutant infections. Quantiation of the Northern analyses shown in Figure 15 was done with phosphorimager analysis using ImageQuant software and is presented below. The bands shown in brackets in Figure 14 were quantified, and % 2 hour mock values for each mRNA species are reported. Results are also shown graphically in Figures 16, 17, 18, 19, 20.

RNA	h.p.i.	mock	act D	n212	d120	d22lacZ	5dl1.2	UV n212	UV d120	UV d22lacZ	UV 5dl1.2
collagen	0	100	100	100	100	100	100	100	100	100	100
	2	100	138	74	50	32	60	79	51	81	75
	4	105	75	49	25	17	28	38	48	44	58
	8	114	87	40	9	6.1	15	38	33	27	45
	12	137	82	17	6.4	4.1	11	40	21	23	29
	16	137	107	6.3	7.1	3.7	6.7	46	25	36	36
	20	162	76	5.3	9.5	6.4	5.6	39	33	27	24
fibronectin	0	100	100	100	100	100	100	100	100	100	100
	2	100	145	60	50	26	54	82	42	71	59
	4	105	61	59	19	13	26	43	48	47	52
	8	125	86	59	7.5	3.1	19	60	39	23	51
	12	144	47	13	4.8	2.2	14	55	17	19	34
	16	129	87	3.5	4.4	1.3	6.7	49	13	34	33
	20	131	57	1.8	5.5	2.5	7.1	40	24	26	46
exostoses	0	100	100	100	100	100	100	-	-	-	100
	2	100	78	63	33	29	53	-	-	-	88
	4	112	58	67	25	25	42	-	-	-	75
	8	151	63	48	15	12	58	-	-	-	82
	12	158	28	30	13	8	35	-	-	-	86
	16	124	45	9	13	8	24	-	-	-	101
	20	97	26	4.5	10	9.8	17	-	-	-	96
GAPDH	0	100	100	100	100	100	100	100	100	100	100
	2	100	105	93	51	59	70	99	72	88	109
	4	101	127	81	39	44	54	74	63	76	77
	8	103	120	72	28	26	72	71	54	51	57
	12	109	75	45	22	18	40	76	39	47	47
	16	122	115	25	21	19	31	63	36	54	38
	20	111	99	17	23	20	21	57	45	46	34
β-actin	0	100	100	100	100	100	100	100	100	100	100
	2	100	114	69	63	42	65	76	57	74	83
	4	122	-	76	44	31	45	64	57	76	83
	8	119	82	73	20	26	55	-	59	66	93
	12	135	81	36	17	19	43	-	50	71	74
	16	114	100	18	22	17	28	-	56	94	80
	20	111	74	8.6	19	15	24	58	65	76	64

The mRNA profiles in mock infection are described below. GAPDH mRNA levels were generally stable. β-actin and exostoses mRNA levels fluctuated. Collagen and fibronectin mRNA levels gradually increased to 162% and 131% of the 2 hour mock levels respectively. (An increase in collagen mRNA levels over mock infection was not seen in every study in which it was monitored, but was also seen in Figure 31 where, in an averaging of 4 repeat trials, mRNA levels increased to 148% of 8 hour mock levels by 16 h.p.i.). We did therefore observe variability in mRNA profiles over the 20 hour mock time course, as well as an increasing trend for some mRNAs. These differences are not likely due to gel loading variables, as mRNA profiles for different mRNA species varied within analysis of the same mock treatment on the same Northern blot.

The stability of the mRNAs over actD treatment is described below. At 20 hours post actD treatment, levels of collagen, fibronectin, exostoses, GAPDH, and β-actin mRNAs were 76.3%, 56.7%, 26.1%, 98.7%, and 73.5% of 2 hour mock levels, respectively. Thus, collagen and GAPDH mRNA were again found to be very stable, with half lives exceeding 20 hours. β-actin and fibronectin mRNAs were similarly found to be quite stable. Exostoses mRNA degraded considerably over the 20 hour actD treatment.

Ideally, we would like to have been able to compare the mRNA profiles of IE deletion mutant infections to those of KOS infection. We would have been able to assess the extent of mRNA loss that occurred with these mutants relative to wildtype infection. Unfortunately, the KOS infection trial that had been conducted for this study had been done at an incorrect MOI. The KOS infection mRNA profiles therefore had to be omitted from the analysis.

We expected vhs to be present in the teguments of the ICP0$^-$ (n212), ICP4$^-$ (d120), and ICP27$^-$ (5dl1.2) mutant viruses used in infection. We therefore expected these IE mutant viruses to be capable of mediating some RNA level shutoff in both transcriptionally competent and UV-irradiated virus infections. We recognize that the UV-irradiated virus RNA level shutoff activities may vary with the virus strain used.

Varying particle to p.f.u. ratios for each mutant could result in different numbers of virus particles, and therefore, different amounts of vhs, delivered at the same MOI.

As described in the Introduction, ICP22 has been implicated in RNA level host shutoff via it's purported effects on vhs function and packaging. We therefore expected that infection with UV-irradiated d22lacZ and/or d22lacZ might result in comparatively less RNA-level shutoff, as less vhs may be delivered upon infection, and the vhs that is delivered may be modified to a less active form.

As described in the Introduction, ICP0, ICP4, ICP22 and ICP27 have been implicated in the arrest of host transcription. Each of these viral proteins had a variable influence on the transcriptional arrest of different RNAs. Spencer *et al.* (316) reported that ICP27 was critical for GAPDH mRNA loss. We therefore expected infection with ICP27$^-$ HSV-1 (5dl1.2) to be compromised in RNA-level shutoff activity. We had not done nuclear run-on assays to assess the extent of transcriptional arrest mediated by the different IE proteins. We still hoped, however, to determine if any IE proteins appeared to be particularly important for mediating the loss of specific RNA species under study.

Several trends were observed for each of the mRNAs analyzed and are described below. Transcriptionally competent IE mutant infections caused more mRNA loss than their respective UV-irradiated IE mutant counterparts. (Quantitation with UV-irradiated n212, d120, and d22lacZ infections could not be done with exostoses RNA. Therefore, this trend was only verified for exostoses mRNA in 5dl1.2 mutant infection.) Therefore, in each IE mutant infection, at least one newly synthesized viral product was capable of inducing additional mRNA-level shutoff. Contrary to literature reports, UV-irradiated ICP22$^-$ (d22lacZ) infection had an RNA profile which was similar to those observed with the other UV-irradiated viruses. No compromise of initially-delivered vhs activity was evident.

Some trends in comparing the RNA profiles of the transcriptionally competent IE mutant infections to each other were also found to be valid for each of the mRNAs studied. These comparisons were done in one experimental trial comparing infections with different viruses and, therefore, with possible variability in MOI. The results described below need to be repeatedly observed in additional experimental trials with

independently titered viral preparations in order to be validated. RNA profiles of d120 and d22lacZ infection were similar. d120 and d22lacZ RNA profiles also showed the most extensive decreases across infection. Contrary to literature reports, our results do not indicate that ICP22 is a significant contributor to RNA level shutoff. The mRNA loss that occurred in n212 infection was delayed relative to the mRNA loss observed in d120 and d22lacZ infections. However, net loss of mRNA by the end of n212 infection was similar to that seen in d120 and d22lacZ infections.

5dl1.2 infection caused variable mRNA loss, as is shown in Figure 21. Collagen and fibronectin mRNA levels decreased more quickly, and more extensively than exostoses, GAPDH and β-actin mRNA levels within one infection trial. A second experimental trial showed a similar trend, where collagen mRNA levels again decreased more quickly, and more extensively than GAPDH mRNA. (A third trial, which monitored the profile of collagen mRNA in 5dl1.2 infection, demonstrated that collagen mRNA decreased to less than 10% of mock levels by 20 h.p.i. in the absence of ICP27.) Our results suggested that dependence on ICP27 for mediating extensive host mRNA loss was not universal. (In future, it would be ideal to repeat this study and include a comparison of KOS and ICP27$^-$ infection RNA profiles.) Exostoses, β-actin and GAPDH mRNA-level shutoff appeared to be compromised in 5dl1.2 infection. Cluster 16 mRNAs did not share the same RNA profile in this respect and were not coregulated in this respect.

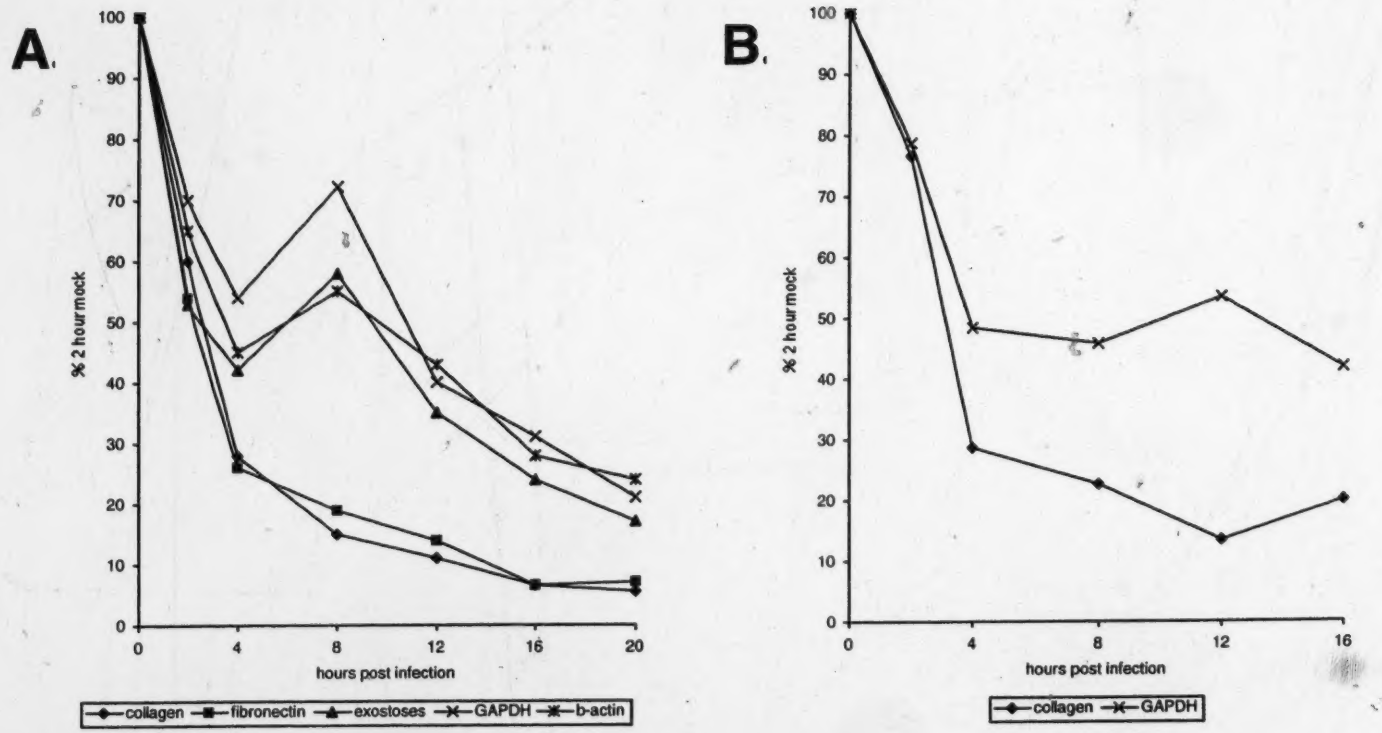

Figure 21. RNA profiles for different RNA species are distinct in 5dl1.2 (ICP27$^-$) infection
Part A shows the quantitation of collagen, fibronectin, exostoses, GAPDH, and β actin mRNA profiles from the Northern analyses shown in Figure 14. Part B shows the quantitation of collagen and GAPDH mRNA profiles from Northern analyses shown in Figure 29.

Remarkably little, if any exostoses mRNA loss occurred in UV-irradiated ICP27⁻ infection, where 96% of mock mRNA levels remained at 20 h.p.i.

In summary, these results suggest that ICP0, ICP4 and ICP22 are not necessary for the shutoff of collagen, fibronectin, exostoses, GAPDH and β-actin mRNAs, though ICP0 may be important for timely shutoff of these mRNAs. We observed, in two trials shown, that dependence on the expression of ICP27 for mRNA loss is variable from RNA species to RNA species and that dependence on ICP27 for mediating the majority of host mRNA loss is not universal. Results from the IE knockout study described above do not indicate that there are RNA profile characteristics that consistently distinguish cluster 16 from non-cluster 16 mRNAs.

3.8 Generation of a vhs⁻/ICP27⁻ double mutant of HSV-1

The following experiments were intended to elucidate the relative contributions of vhs, ICP27, and other viral proteins to various elements of the host shutoff process. We hoped to determine if vhs and ICP27 do contribute to host shutoff independently at both the RNA and protein level, or if, perhaps, some shutoff effects attributed to ICP27 are actually directly mediated by vhs. We also hoped to determine if, in the absence of vhs and ICP27, other viral proteins could independently mediate significant shutoff effects at the RNA and protein level. Towards these purposes, a vhs⁻/ICP27⁻ double mutant (ljs1) was generated. We hoped that comparison of RNA and protein synthesis profiles of ljs1 infection and infections with WT, vhs⁻, and ICP27⁻ viruses would facilitate answering these questions, based on the predictions describe below.

I predicted that when vhs and ICP27 contributed to a particular shutoff effect independently, shutoff effects would be more compromised in ljs1 than with either parental strain. I suspected that some of the shutoff effects attributed to ICP27 were actually due to ICP27's effects on vhs levels, as ICP27 is required for normal levels of vhs synthesis (shown in Figure 14). I therefore looked for shutoff effects that appeared to occur to similar extents in both ΔSma (vhs⁻) and ljs1 infection, suggesting that some of ICP27's effects on shutoff were actually directly mediated by vhs.

Aside from the extent of independence of vhs and ICP27 RNA level shutoff activities, I also considered the extent of RNA and protein level shutoff abrogation in ljs1 infection. Complete abrogation of a shutoff effect in ljs1 infection would indicate that only vhs and/or ICP27 and/or other ICP27-dependent proteins could be possible mediators of protein level shutoff. Incomplete abrogation of a host shutoff effect in ljs1 infection would indicate that a viral protein(s) expressed in the absence of vhs and ICP27 was partially responsible for the shutoff effect.

The generation and genetic screening of ljs1 is described below. Figure 22 illustrates the relative position of the vhs and ICP27 genes in the HSV-1 genome. They are approximately 21 kilobasepairs apart and are present in opposite orientations, with ICP27 being transcribed from left to right in the prototype arrangement of the viral genome. Neither vhs nor ICP27 overlap with other viral genes.

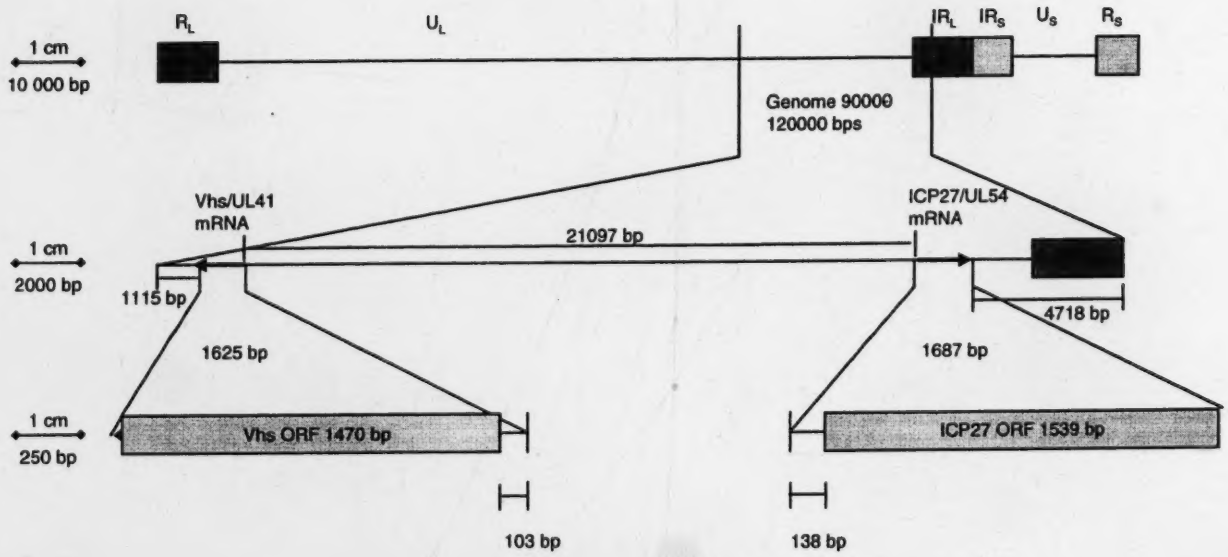

Figure 22. Scaled diagram illustrating vhs and ICP27 genes in the HSV 1genome.
Both vhs and ICP27 genes are located in the unique long segment (U_L) of the genome. As both genes do not contain introns, their gene and mRNA sequences are contiguous. The vhs and ICP27 gene orientations are depicted through directional arrows. Neither vhs nor ICP27 genes overlap with other genes. The open reading frames of vhs (NCBI code Z72338) and ICP27 (NCBI code AF220940) are 1470 and 1539 base pairs long, respectively. Reported mRNA lengths for vhs (NCBI code NC_001806) and ICP27 (NCBI code NC_001806) are 1625 and 1687 bases long, respectively. The transcriptional start site for the vhs locus is approximate. The scale of each section of the diagram is indicated on the left. Long repeat region (R_L), internal copy of long repeat region (IR_L), internal copy of short repeat region (IR_S), unique short segment (U_S), short repeat region (R_S)

A mutant isolate of HSV-1 KOS bearing inactivating mutations in both the vhs and ICP27 genes was successfully constructed *in vivo* by homologous recombination between singly mutant parental strains ΔSma and 5dl1.2, followed by screening for the desired doubly mutant recombinant, as described in Materials and Methods section 2.3.1. Briefly, ICP27$^-$ coinfection progeny were selected, based on their requirement for ICP27 complementation on V27 cells for growth. Phenotypically ICP27$^-$ progeny were then further screened by PCR analysis to identify progeny that contained the ΔSma truncation. A schematic diagram illustrating the desired crossover event is shown in Figure 23.

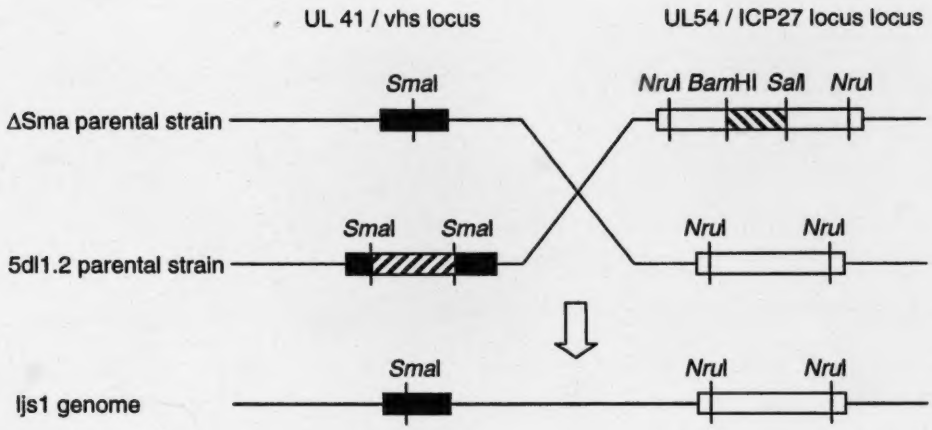

Figure 23. Schematic diagram (not to scale) of desired crossover event to generate vhs⁻ / ICP27⁻ HSV 1double mutant (ljs1) from ΔSma and 5dl1.2 parental strains.
The generation of ljs1 required a single crossover event to occur between the UL41 and UL54 loci. Cross hatched bars indicate regions of viral genes deleted in mutant parental strains and ljs1.

3.8.1 Screening for the vhs⁻/ICP27⁻ double mutant from 5dl1.2/ΔSma coinfection

PCR analysis was done, as described in Materials and Methods, to identify viral recombinants with the ΔSma vhs truncation, as illustrated in Figure 24. The ΔSma truncation is apparent in ljs1.

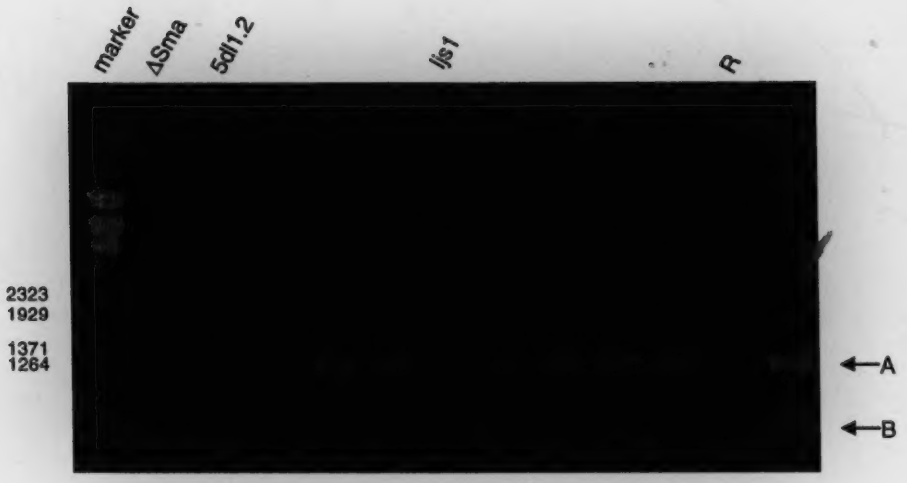

Figure 24. PCR analysis used in screening for vhs ΔSma truncation in potential vhs⁻/5dl1.2⁻ HSV 1 strains.

Infection DNA was harvested, when full c.p.e. was evident, from isolates that displayed a requirement for ICP27 complementation. Oligonucleotides flanking the ΔSma deletion (Primer 1 is homologous to vhs transcript bases 278 297. Primer 2 is homologous to vhs transcript bases 1500 1519.) were used to PCR amplify a region of the vhs locus from these DNA samples. PCR products were resolved on 1% TAE agarose gels, and stained during electrophoresis with EtBr. The WT PCR product, indicated by arrow A on the right side of the figure, was predicted to be a length of 1242 bases. The ΔSma deletion PCR product, indicated by arrow B on the right side of the figure, was predicted to be a length of 654 bases. The marker (Ma) sizes are indicated to the left of the figure. (R) rejected screen progeny

Prospective double mutants with the desired ICP27$^-$ phenotype and the desired vhs$^-$ genotype (according to PCR analysis) underwent 3 rounds of plaque purification. After purification, growth on V27 cells and lack of growth on Vero cells was reconfirmed.

To verify the vhs truncation in ljs1, viral DNA was digested with *Bst*EII and subjected to Southern analysis. As illustrated in Figure 25, the ljs1 track shows a band approximately 1500 base pairs length, consistent with the 1588 base pair DNA fragment expected. To verify the mutation of the ICP27 locus in ljs1, viral DNA was digested with *Nru*I and subjected to Southern analysis. As illustrated in Figure 26, the ljs1 lane shows a band of approximately 3800 base pair length, consistent with the 3780 base pair DNA fragment expected.

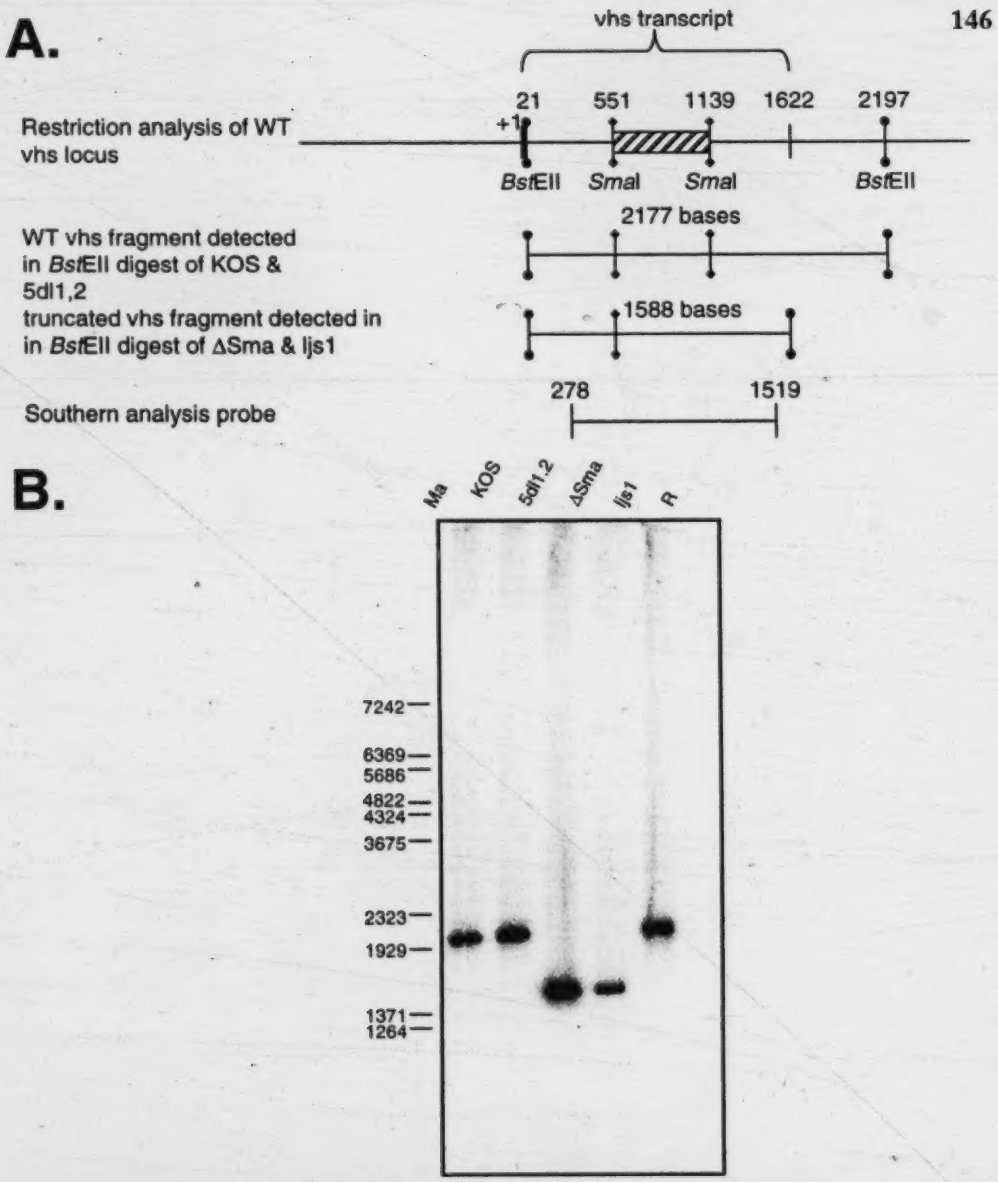

Figure 25. Southern analysis of the vhs locus in ljs1 and parental strains.
KOS, 5dl1.2, ΔSma, and ljs1 viruses were grown on V27 cells until full c.p.e. was evident. Total infection DNA was harvested and was digested with *Bst*EII enzyme. Digested DNA was electrophoresed through a 0.9% TAE agarose gel, and was then transferred for Southern analysis. A random prime labeled probe, specific to bases 278 - 519 of the vhs transcript was used to verify the ΔSma truncation in ΔSma and ljs1. Part A is a scaled diagram (1cm = 400bp) of the restriction analysis for the vhs locus in ljs1 and parental strains. The ΔSma truncation is indicated by a cross hatched bar. The barbells with the circular and diamond shaped heads represent *Bst*EII and *Sma*I restriction sites, respectively. Part B shows the Southern analysis in which the expected DNA restriction fragments were detected. (R) rejected screen progeny

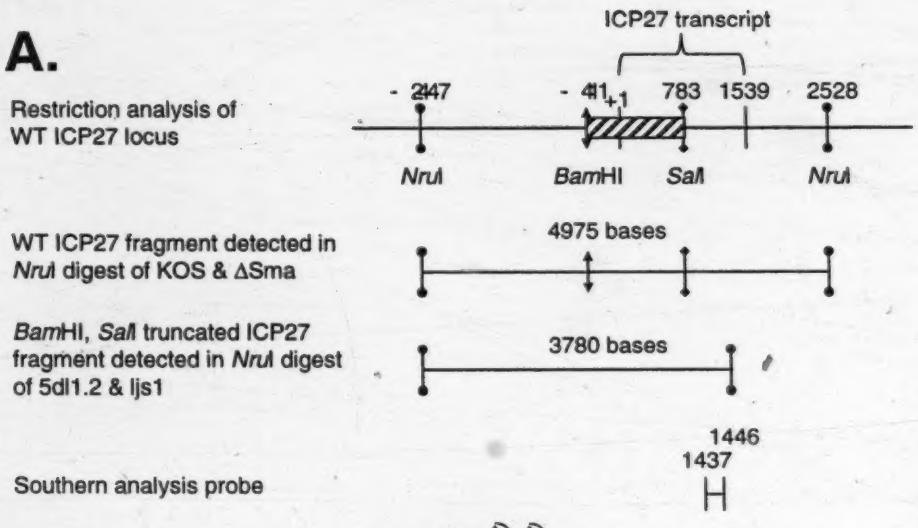

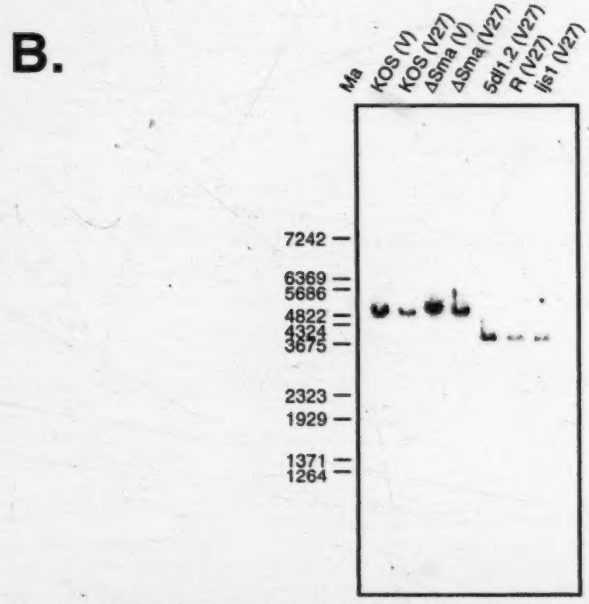

Figure 26. Southern analysis of the ICP27 locus in ljs1 and parental strains.
KOS, 5dl1.2, ΔSma, and ljs1 viruses were grown on V27 (V27) cells until full c.p.e. was evident. Similarly, KOS and ΔSma viruses were also grown on Vero (V) cells. Total infection DNA was harvested and was digested with *Nru*I enzyme. Digested DNA was electrophoresed through a 0.9% TAE agarose gel, and was then transferred for Southern analysis. A 5'end labeled oligonuceotide probe, specific to bases 1347- 1446 of the ICP27 transcript, was used to verify the *Bam*HI *Sal*I truncation in 5dl1.2 and ljs1. Part A is a scaled diagram (1cm = 800bp) (Southern probe not shown to scale) of the restriction analysis for the ICP27 locus in ljs1 and parental strains. The *Bam*HI *Sal*I truncation in 5dl1.2 is indicated by a cross hatched bar. The barbells with the circular, diamond shaped, and triangular heads represent *Nru*I, *Sal*I and *Bam*HI restriction sites, respectively. Part B shows the Southern analysis in which the expected DNA restriction fragments were detected.(R) rejected screen progeny

3.9 Comparison of ljs1 with with parental strains ΔSma and 5dl1.2

3.9.1 Growth of ljs1 on V27 cells

The following experiment was intended to determine the growth phenotype of ljs1 and compare it to the growth phenotype of wildtype and parental strains. The growth of ljs1, KOS, ΔSma, and 5dl1.2 viral strains was monitored on V27 cells. Generously spaced plaques were grown for 4 days, in order for differences in plaque size to be maximally apparent. Photographs were taken of 5 plaques for the each of the viral strains, as illustrated in Figure 27. With ICP27 complementation on V27 cells, KOS and 5dl1.2 plaques appeared to be approximately the same size. ΔSma and ljs1 plaques were similar to each other in size and smaller than KOS and 5dl1.2 plaques. Ljs1 appeared to have a growth phenotype similar to that of ΔSma on V27 cells.

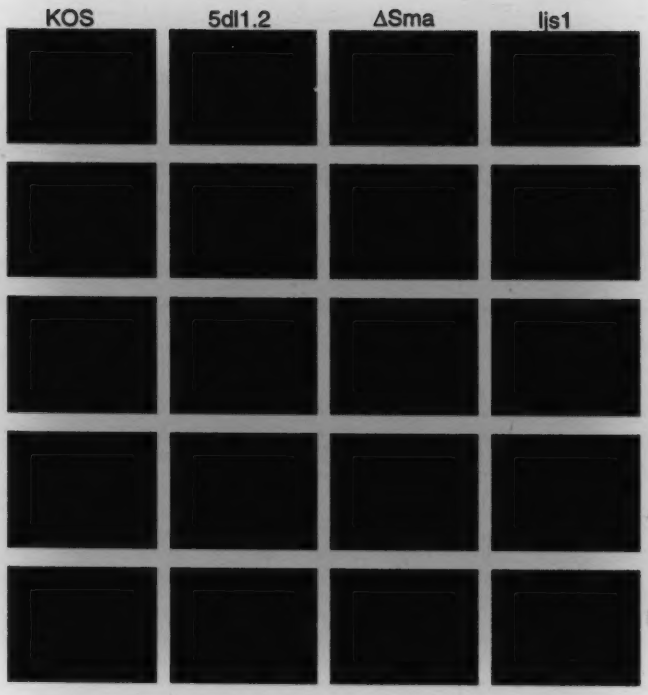

Figure 27. Comparison of ljs1 plaque size with that of KOS and with parental strains, ΔSma and 5dl1.2.

The growth of ljs1 was monitored alongside the growth of KOS, ΔSma, and 5dl1.2 on V27 cells. Photographs were taken of 5 randomly selected plaques of each strain at 200X magnification while they were still in cell medium. No fixing or staining of infected cells was performed.

3.9.2 Collagen and GAPDH mRNA profiles over ljs1, ΔSma, 5dl1.2, and KOS infections

Using the predictions described above, we wished to study the independence of vhs and ICP27 RNA level shutoff effects as well as determine if other viral proteins could contribute to RNA level shutoff in the absence of ICP27 and vhs. Two Northern analyses were therefore conducted to compare RNA profiles in infection with vhs$^-$ / ICP27$^-$ ljs1 to RNA profiles from infections with parental strains and KOS. The first of two such studies included a 5 point time course, and included analysis of collagen and GAPDH mRNAs. HEL cells were either mock-infected, infected with KOS, UV-irradiated KOS, ΔSma, 5dl1.2, or ljs1, or were incubated with actinomycin D. Total RNA was harvested from the infections and actD treatment and used in the Northern analyses. The Northern analyses are illustrated in Figure 28. Quantitation for the Northern analyses presented in Figure 28 is shown in Figure 29.

28A.

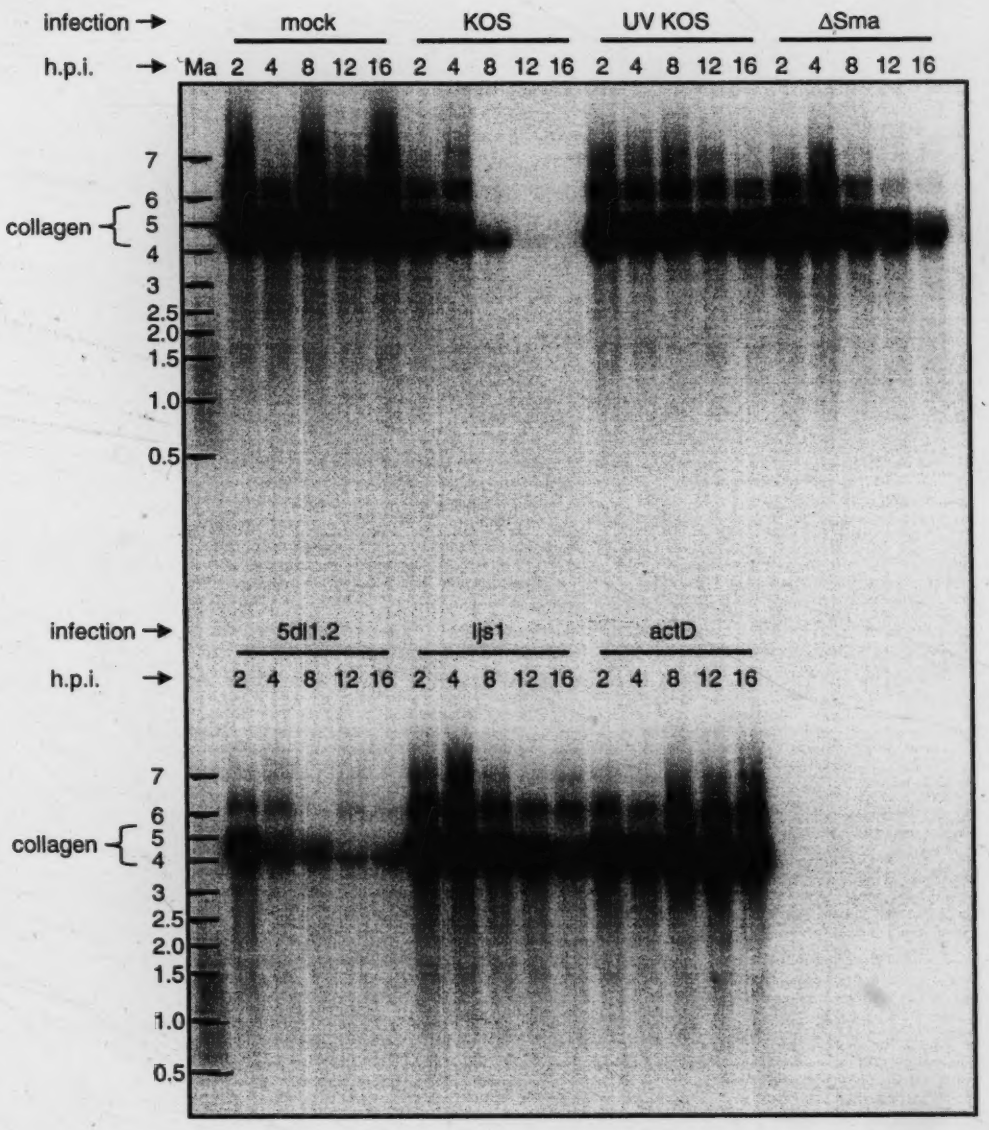
infection
mock
KOS
UV KOS
ΔSma
h.p.i.
Ma 2 4 8 12 16 2 4 8 12 16 2 4 8 12 16 2 4 8 12 16
7
6
collagen
5
4
3
2.5
2.0
1.5
1.0
0.5
infection
5dl1.2
ljs1
actD
h.p.i.
2 4 8 12 16 2 4 8 12 16 2 4 8 12 16
7
6
collagen
5
4
3
2.5
2.0
1.5
1.0
0.5

28B.

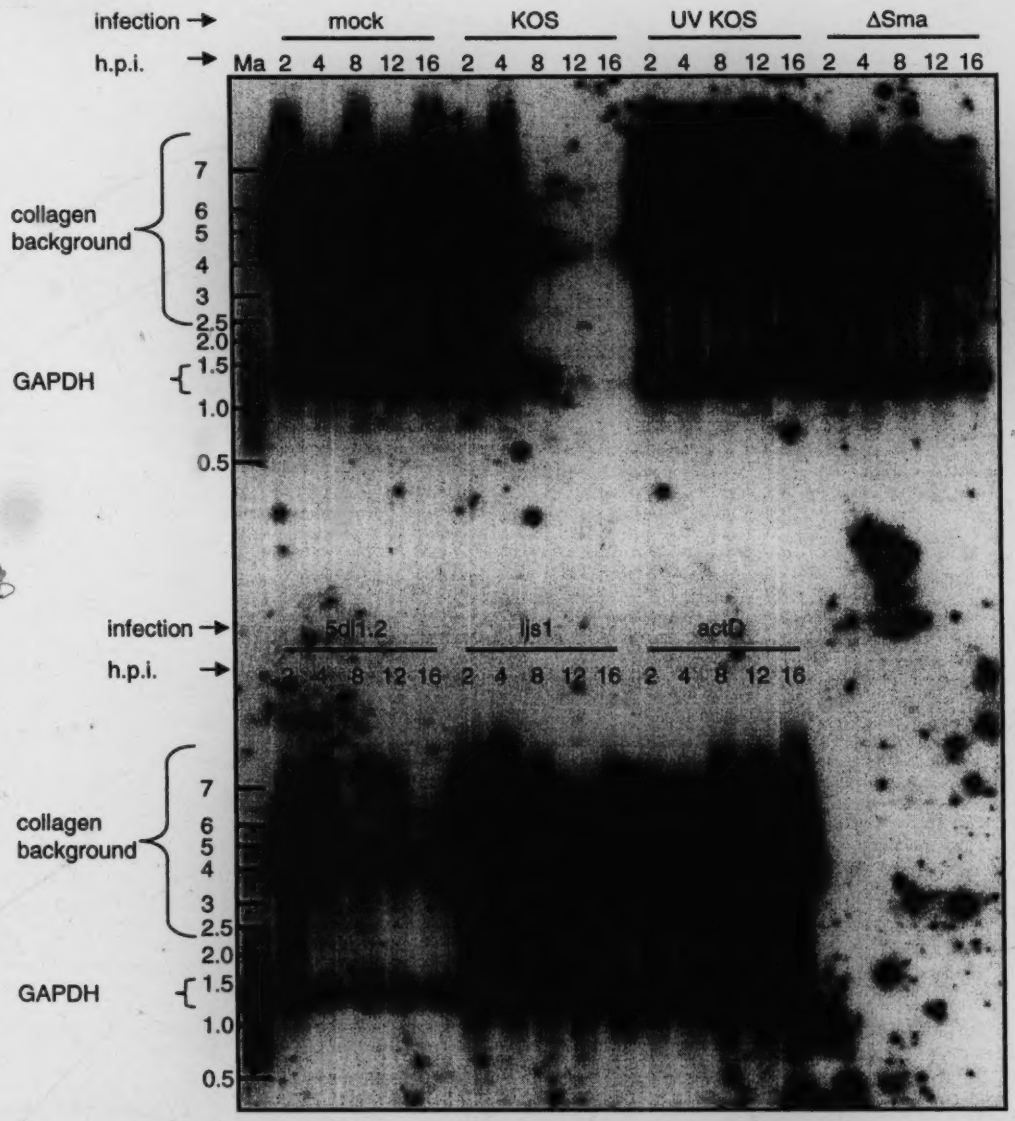

Figure 28. Northern analysis of collagen and GAPDH mRNA over UV irradiated KOS, KOS, ΔSma, 5dl1.2, and ljs1 infections.

HEL cells were mock infected, were infected with UV irradiated KOS, KOS, ΔSma, 5dl1.2, and ljs1 viruses, or were incubated with actinomycin D. Total RNA was harvested at 2, 4, 8, 12, and 16 h.p.i. Collagen mRNA was detected with a random prime labeled probe specific for the α2 subunit of type I collagen by the Church method. Collagen mRNA was visualized on film (A). GAPDH mRNA was detected with a 5'end labeled oligonucleotide probe using the Westneat method, directly after collagen probing, without stripping, and was also visualized on film (B). RNA marker (Ma) fragment sizes are indicated, in kilobases, on the left hand side of the figure. The bracketed signals in parts A and B were used for quantitation presented in Figure 27.

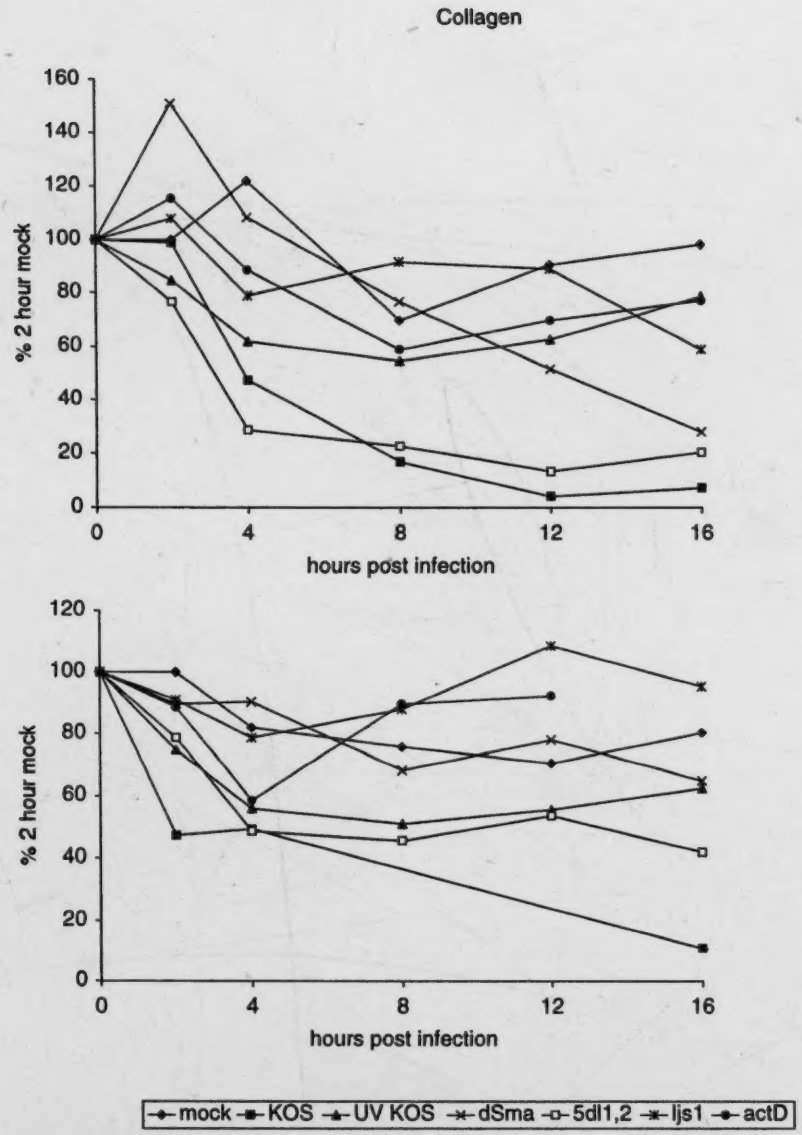

Figure 29. Quantitation of collagen and GAPDH mRNA over UV irradiated KOS, KOS, ΔSma, 5dl1.2, and ljs1 infections.

Northern analyses presented in Figure 28 were also visualized by phosphorimager analysis, and quantified, as presented above. Signal intensities are reported as a percentage of 2 hour mock infection signal. Quantitation for GAPDH signals at 8 h.p.i. with KOS virus, and 16 hours of actinomycin D incubation was excluded, due to spurious background.

Many principles described and demonstrated previously in this work were shown again within this study. Both collagen and GAPDH mRNAs were very stable in actD incubations in this study, with 77% and 92% of mock levels remaining after 16 and 12 hours of actD incubation, respectively. Collagen and GAPDH mRNA levels decreased to 7.4% and 11% of mock levels by 16 hours post KOS infection. The degradation of these mRNAs over KOS infection must have included destabilization and/or degradation of approximately 70% (77% stable pre-existing collagen mRNA - 7.4% collagen remaining after KOS infection) and approximately 81% (92% stable pre-existing GAPDH mRNA - 11% GAPDH remaining after KOS infection) of the pre-existing collagen and GAPDH mRNAs, respectively. As seen before, GAPDH mRNA levels decreased partially over UV-irradiated KOS infection, relative to KOS infection, to 63% of mock levels. Collagen mRNA levels had decreased to 54% of mock levels by 8 hours post UV-irradiated KOS infection, and then steadily increased to 79% of mock levels by 20 h.p.i. In ΔSma infection, collagen mRNA loss again appeared to occur more extensively for collagen than GAPDH mRNA. Also, as demonstrated before, collagen mRNA loss occurred more extensively than GAPDH mRNA loss in ICP27$^-$ infection (Shown in Figure 21.)

GAPDH mRNA levels did not go below 79% of mock levels during a 16 hour ljs1 infection. Therefore, infection with vhs$^-$/ICP27$^-$ (ljs1) virus did not cause notable GAPDH mRNA loss. Some collagen mRNA loss (decrease to 59% of mock levels) was observed late in ljs1 infection. Collagen and GAPDH RNA-level shutoff appeared to occur less extensively for ljs1 than for either parental strain. This result is consistent with literature reports indicating ICP27 and vhs mediate at least some independent mRNA level shutoff activities.

It was difficult to assess the statistical significance of RNA profile differences shown in Figure 29. We therefore elected to do a similar infection Northern analysis of 4 repeat trials over only 2 time points. With 4 repeat trials, standard deviations could be used to assess the significance of the RNA profile differences observed. The same series of experimental conditions shown in Figures 28 & 29 were used in this study. Four

independent virus suspensions were used to infect HEL cell plate series from the same cell pool on the same day. Total RNA was harvested at 8 and 16 h.p.i. Northern analysis that shows the RNA profile of collagen within this experiment is illustrated in Figure 30. Northern analysis of the GAPDH mRNA profile was unsuccessful on this blot. Quantitation and standard deviations calculated from the Northern analysis in Figure 30 are shown in Figure 31.

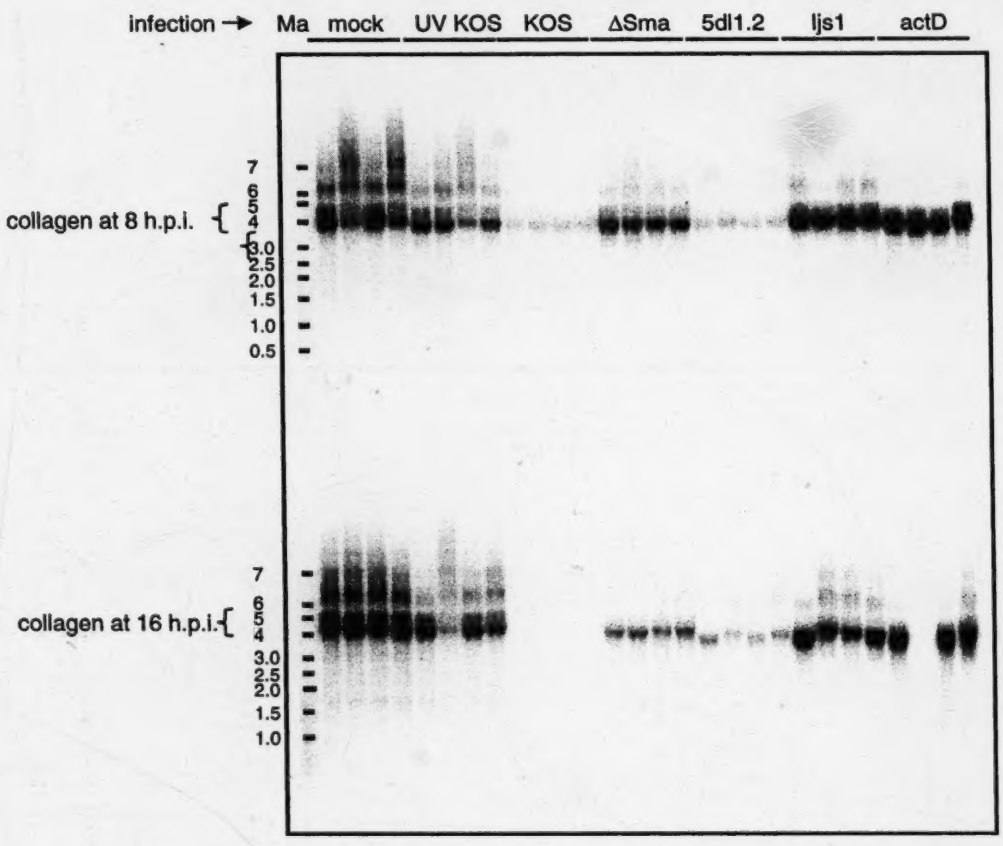

Figure 30. Northern analysis of collagen mRNA over UV irradiated KOS, KOS, ΔSma, 5dl1.2, and ljs1 infections.

HEL cells were mock infected, were infected with UV irradiated KOS, KOS, ΔSma 5dl1.2 and ljs1 viruses, or were incubated with actinomycin D. Total RNA was harvested from four independently infected samples at 8 and 16 h.p.i. Collagen mRNA was detected with a random prime labeled probe specific for the α2 subunit of type I collagen by the Church method. Collagen mRNA was visualized by phosphorimager analysis. RNA marker (Ma) fragment sizes are indicated, in kilobases, on the left hand side of the figure. The bracketed collagen signal was used for quantitation.

A.

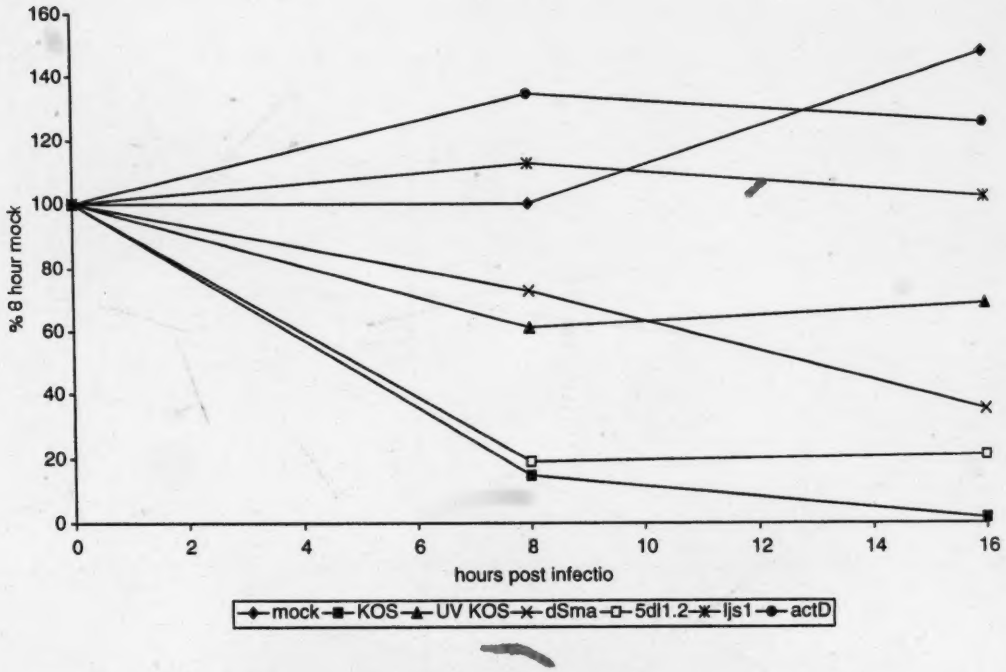

B.

Treatment	h.p.i.	%mock ± std. dev.
mock	8	100±24
	16	148±8.3
KOS	8	15±1.9
	16	1.6±0.97
UV KOS	8	61±20
	16	69±25
ΔSma	8	73±8.4
	16	35.±3.8
5dl1.2	8	19±2.1
	16	21±4.6
ljs1	8	113±3.8
	16	102±23
act D	8	135±17
	16	125±12

Figure 31. Quantitation of collagen mRNA over ljs1 and parental strain infections.
Northern analysis presented in Figure 30 was quantified, as shown above (A). Signal intensities were reported as a percentage of 8 hour mock infection signal. Standard deviations are presented with an n=4 (B). (N=3 for the actinomycin D treatment at 16 h.p.i.)

Consistent with previous results, collagen mRNA levels decreased to 1.6 +/- 0.97% of mock levels by 16 hours post KOS infection. UV irradiated KOS infection collagen mRNA levels decreased to 61% +/- 20% of mock levels by 8 h.p.i., and increased back up to 69 +/- 25% of mock levels by 16 h.p.i. We have observed similar trends of a decrease, followed by a small increase in UV-irradiated virus infection in other experiments. (See Figures 11, 12, 13B and 13D.) In ΔSma, and 5dl1.2 infections, collagen mRNA levels decreased to 35% +/- 3.8% and 21% +/- 4.6% of mock levels by 16 h.p.i., respectively. Compared to UV-irradiated virus infection, both ΔSma and 5dl1.2 infection induced more extensive collagen mRNA loss than that induced by tegument-delivered products in UV-irradiated KOS infection. Using the standard deviations provided, it can be seen that the above observations are statistically significant (using 95% confidence interval, ΔSma and UV-irradiated KOS p=0.0361, 5dl1.2 and UV-irradiated KOS p=0.00092). The rates of collagen mRNA loss are also statistically significantly different between ΔSma and 5dl1.2 infections, with mRNA loss occurring earlier and more extensively in 5dl1.2 infection (using 95% confidence interval, ΔSma and 5dl1.2 p= 0.0034).

Transcriptional arrest with actD did not induce collagen mRNA loss in this study, where collagen mRNA levels were 125 +/- 12% of mock levels at 16 hours post treatment. At 16 hours post ljs1 infection, 102 +/- 23% of mock collagen mRNA levels remained. Ljs1 infection did not apparently cause collagen mRNA loss. Viral proteins other than vhs, ICP27, and other ICP27-induced viral proteins, therefore, did not appear to be necessary to mediate collagen mRNA loss.

The most significant observation from the study shown in Figure 30 and 31 is found in the comparison of collagen mRNA loss patterns over infection with ΔSma, 5dl1.2, and ljs1. Collagen mRNA level shutoff was more impaired in ljs1 infection than in either parental ΔSma or 5dl1.2 infections. These comparisons are statistically significant (using 95% confidence interval, ljs1 and ΔSma p=0.0012, ljs1 and 5dl1.2 p=0.0005). Recall the postulate that a portion of ICP27's contribution to host shutoff at

the mRNA level occurs through the induction of new vhs synthesis. The newly synthesized vhs could be catalytically significant, and directly responsible for late mRNA loss. Had this postulate been correct, ljs1 mRNA loss would have proceeded to the same extent as in ΔSma, since vhs would have been the downstream mediator for all mRNA loss influence. However, ljs1 was further impaired than either parental strain, indicating that at least some of vhs and ICP27's influence on collagen mRNA levels occurs by independent mechanisms. This result does not preclude the possibility that ICP27 is necessary for optimal full infection vhs activity. The result indicated that an additional independent ICP27 RNA- level shutoff activity exists, consistent with current literature reports.

3.9.3 HSV-1 induced host protein level shutoff by ljs1, ΔSma, 5dl1,2, and KOS

In addition to our analysis of RNA level shutoff effects of ljs1, we wished to assess the protein level shutoff effects of this virus as well. To what extent do vhs and ICP27 contribute independently to shutoff at the protein level? Do other viral proteins contribute to host shutoff at the protein level in the absence of vhs and ICP27? A metabolic labeling study was done to address these questions through comparison of protein-level host shutoff activities of UV-irradiated KOS, KOS, ΔSma, 5dl1.2, and ljs1 infections, using the predictions described above. HEL cells were infected with UV-irradiated KOS, KOS, ΔSma, 5dl1.2, and ljs1 viruses. Mock infection was also done, as well as incubation of cells with actD. Metabolic labeling was done for 30 minute intervals initiated at 2, 4, 8, 12, and 16 h.p.i. After 30 minutes of metabolic labeling, samples were harvested into SDS-PAGE lysis buffer. Cell equivalents of each sample were simultaneously electrophoresed on 2 12% SDS-PAGE gels, and were EN^{3}HANCE®ed. In the metabolic labeling study illustrated in Figure 32, the following observations were made.

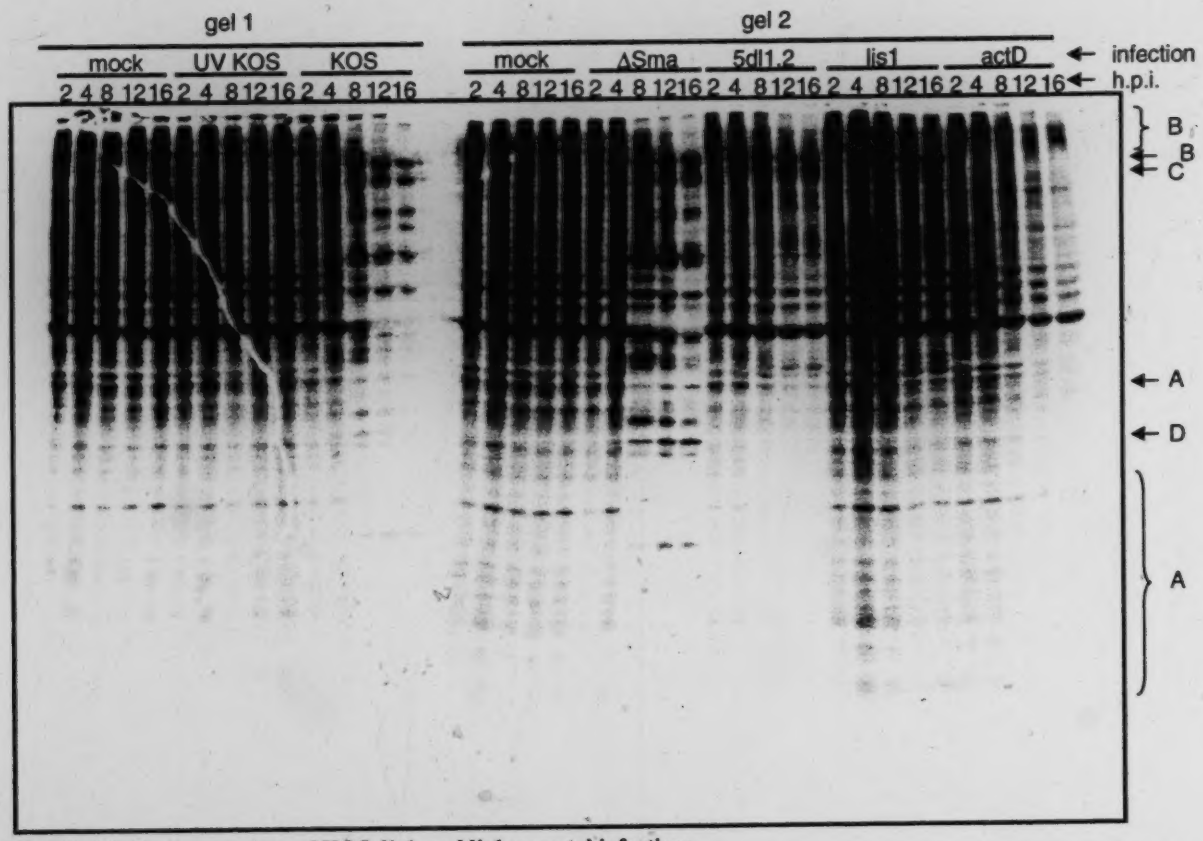

Figure 32. Metabolic labeling comparison of KOS, ljs1, and ljs1 parental infections.
HEL cells were infected at an MOI of 10 with UV irradiated KOS, KOS, Δsma, 5dl1.2, and ljs1 viruses. Mock infection was also done, as well as incubation of cells with actD. Metabolic labeling was done for 30 minute intervals initiated at 2, 4, 8, 12 and 16 h.p.i. After 30 minutes of metabolic labeling, samples were harvested into SDS PAGE lysis buffer. Cell equivalents of each sample were simultaneously electrophoresed on 2 12% SDS PAGE gels, and were EN^{3}HANCE®ed. Bands A to D and brackets A and B are described in the text.

Mock infection had consistent labeling of a panel of cell proteins throughout the time course illustrated. Therefore, there were no obvious changes in the protein synthesis profile over a 16-hour time course, despite potential increases in cell density.

UV-irradiated infection demonstrated a protein synthesis profile that was indistinguishable from mock infection. While initially-delivered vhs induces partial mRNA-level shutoff, this did not appear to detectably manifest at the protein level in this study. This result was not surprising. In the literature, vhs's RNA-level shutoff has only been shown to manifest at the protein level in metabolic labeling studies of UV-irradiated HSV-1 infections conducted in the presence of actD (127).

KOS infection showed the expected metabolic labeling pattern characteristic of HSV-1-induced host shutoff, which included a general loss of protein signals accompanied with the appearance of punctate bands representing the expression of viral proteins in a cascade.

ΔSma infection resulted in a protein-level shutoff pattern similar to that observed in KOS infection. There was a general loss of protein signals, accompanied with the appearance of discrete bands representing the expression of viral proteins. General host translational arrest was evident for KOS and ΔSma infection by the same time of 8 h.p.i. Recall from the Introduction, that vhs contributes to the temporal regulation of viral genes. The expected delayed appearance of some viral proteins, indicated by arrow A in Figure 32, and the expected delayed dissipation of some viral protein bands, as indicated by arrows B, C, and D in Figure 32, was observed. Because virtually complete host translational arrest occurred in the absence of vhs, one can surmise that vhs was not necessary for translational arrest in HEL cell culture.

Host translational arrest was impaired in 5dl1.2 infection, as was evinced by the presence of host metabolically labeled proteins throughout infection. Note the presence of low molecular weight host proteins specified by bracket A in 5dl1.2 infection and the lack of a similar protein profile specified by bracket A in KOS infection. This contrast is indicative of host translational arrest impairment in 5dl1.2 (ICP27$^-$ infection). ICP27 is therefore, as expected, required for full host translational arrest in HEL cells. It is also

worthwhile to note that the host protein profiles in mock and 5dl1.2 infections are not identical. Examination of regions of the gel, such as that specified by bracket B, indicate that some host translational shutoff occurred in ICP27⁻ infection.

First, it is worthwhile to consider the viral protein synthesis profile of ljs1. Viral proteins that are indicated by bands B and C in Figure 32 appear to be synthesized in ljs1 infection. Like in ΔSma infection, the viral protein indicated by band B appears to be synthesized in a delayed and sustained fashion.

Ljs1 infection did display a very minor amount of host translational arrest, as demonstrated for high molecular weight proteins specified by bracket B, indicating that viral proteins other than vhs and ICP27, expressed in infection with ljs1, have the capacity to contribute to a minor portion of host translational arrest. Host translational arrest is impaired even further in ljs1 infection than in 5dl1.2 infection. While initially-delivered vhs did not manifest a protein-level shutoff effect on its own in UV-irradiated KOS infection, as shown above, deletion of the vhs gene did manifest as a further impairment of shutoff in the context of an ICP27⁻ genetic background. Therefore, vhs may contribute to host shutoff at the translational level, in the context of the activities of other host shutoff proteins.

Cell incubation with actD demonstrated the expected result of gradual, partial dissipation of host protein synthesis as no new mRNA was synthesized. The host translational arrest in ΔSma infection was more extensive than that observed in act D incubation, particularly evinced by examining the levels of low molecular weight host proteins specified by bracket A.

In summary, the experiments which studied the shutoff effects of ljs1 relative to those of parentals strains and KOS suggested the following. Ljs1 was largely impaired in causing shutoff of collagen and GAPDH mRNAs as well as protein level shutoff in general. Viral proteins expressed in ljs1⁻ are therefore not major contributers to the overall shutoff of host cell protein synthesis during infection. If the proteins expressed in ljs1 do contribute to host shutoff, their contribution is minor. Ljs1 was more impaired than either parental strain in mediating shutoff for both collagen and GAPDH mRNAs as

well as in mediating shutoff at the protein level. Thus, vhs and ICP27 do appear to contribute to host shutoff independently.

4 DISCUSSION

4.1 Evaluating the quantitation of our microarray analysis

HSV-1 proteins cause downregulation of host mRNAs through inhibition of host mRNA transcription and maturation as well as through mRNA degradation. These RNA level host shutoff mechanisms are a major research focus of our laboratory, but have only been shown to occur with a limited set of host mRNAs. Our laboratory wished to determine if most, or if only a few host mRNAs are downregulated during HSV-1 infection. We elected to conduct a study of RNA level host shutoff in which we could monitor a broad spectrum of host mRNA species. Our laboratory, in collaboration with Aled Edward's laboratory, attempted a microarray analysis of HSV-1 infection, in which a panel of 20 000 human ESTs was monitored.

At around the same time, other laboratories were similarly using microarray analysis to study changes in gene expression during HSV-1 infection. As described in the Introduction, these microarray analyses corroborated the conclusions from previous works, and indicated that host mRNAs do indeed generally decrease in abundance over HSV-1 infection. In contrast, our microarray study suggested that most host mRNA profiles do not change during infection. Indeed, only a minor fraction of host mRNAs was reported to decrease and an even smaller fraction of host mRNAs was reported to increase in abundance.

My initial experimental goal was to verify the results of our microarray analysis by an alternate method, Northern analysis. I examined mRNAs that were downregulated (cluster 16 mRNAs) and I also examined mRNAs that were allegedly highly expressed and unchanged over infection (group A mRNAs). My work corroborated microarray results for cluster 16 mRNAs. (See Figure 2.) A significant portion of the RNA detected by some group A clones was polyA$^-$. As only polyA$^+$ RNAs could be detected in microarray quantitation, only polyA$^+$ RNAs observed in group A Northern analyses were quantified for comparison with microarray data. Contrary to our microarray results, all polyA$^+$ group A mRNAs decreased in abundance extensively over infection. (See

Figures 3 & 4.) The suggestion that most host mRNAs do not change in abundance over infection was therefore incorrect. In the end, our work also supported the concept of general host mRNA downregulation during infection.

We asked why infection mRNA profiles were inaccurately reported in the microarray study. One likely source of the discrepancy was the use of an inappropriate microarray normalization protocol. The method of constant majority, described in the Introduction, was used to normalize the quantitation from our microarray study. Recall that this normalization procedure operates on the premise that the profiles of most mRNA species do not differ between samples compared in a given study. HSV-1 infection is thought to downregulate host mRNAs generally. We therefore expected the RNA profiles of *most* mRNA species to differ *extensively* between mock and infection samples. Clearly, the experimental pretext required for the appropriate use of the method of constant majority did not apply to our experimental scenario. The quantitative interpretation of infection signals had been "tuned up" excessively and inappropriately in their comparison to mock infection signals. The relative measure of different mRNAs *within* a sample was still valid but the inappropriate normalization of the samples distorted comparison between them. As we could not have expected any host mRNAs to remain stable, we should not have used any host mRNA as an internal frame of reference. In retrospect, it is clear that the method of control spots, which uses external RNA references, would have been a more appropriate normalization protocol for our experiment.

4.2 Northern analysis of Alu transcripts & unpolyadenylated RNAs in HSV-1 infection

As stated above, because of improper microarray normalization, group A mRNAs were incorrectly reported to be highly expressed and stable during infection. The inaccurate quantitation of some group A mRNAs was also likely influenced by other mitigating factors. We unexpectedly observed that at least 20 of the 39 group A clones contain *Alu* repeat element sequence. (See Table 3.) A clone that contains this repeat element would not detect one or two mRNA species; rather a multitude of mRNAs would

be detected. Consistent with this rationale, we confirmed that two *Alu*$^+$ group A clones did indeed detect a multitude of RNAs when used as probes in Northern analysis. (See Figure 3.) Even very low levels of the thousands of mRNAs detected by these clones saturated the microarray slide spots and distorted quantitation, such that all these signals were "maximal" and "equivalent".

Clearly, it is not desirable to use clones containing *Alu* element sequence in microarray analysis because the clones do not have their purported specificity. How can we prevent the misuse of these clones in future microarray studies? *In silico* screening for *Alu* sequence would be ineffective, as complete sequencing data for clone inserts is often not available. However, to identify *Alu* element sequence containing clones, microarray slides can be probed with *Alu* DNA. These aberrant clones can then be recognized and removed from further analyses. In fact, Dr. Jim Woodgett (personal communication) performed such a screen with the panel of clones used in our microarray study and has identified the same list of *Alu*$^+$ clones shown in Table 3. From the *Alu*$^+$ clones, subclones that are specific to the actual mRNAs of interest can be generated.

Analysis of polyA$^+$ *Alu* transcripts indicated that most host mRNAs are downregulated in HSV-1 infection. Consider that probes specific for *Alu* elements recognize thousands of different mRNA species in polyA$^+$ RNA isolates. Our results (See Figure 3.) indicated that infection caused this multitude of mRNAs to dissipate to virtually undetectable levels. One can therefore again conclude that thousands of host mRNAs decrease in abundance over infection with HSV-1.

In infection, polyA$^-$ RNAs appeared to be more stable than the polyA$^+$ RNAs detected by the same clones. This observation was made for polyA$^-$ RNAs detected in Northern analysis with *Alu*$^+$ clone probes and with a probe specific to endothelin mRNA, a majority of which was polyA$^-$. We do not know the precise identity of these polyA$^-$ RNAs.

It would be interesting to identify the stable polyA$^-$ RNAs. Determining their subcellular localization may aid in this goal. For example, nuclear localization of stable polyA$^-$ RNAs may suggest that these RNAs are indeed pre mRNAs. An expansion of the

study shown in Figures 3 and 4 which includes nuclear, cytoplasmic, and total RNA fraction analyses might therefore be a worthwhile endeavor

We inferred our conclusions about the stability of polyA$^-$ RNA from comparisons of total and polyA$^+$ RNA isolates. In future, for the sake of thoroughness, it could be helpful to monitor polyA$^-$ RNA directly.

The study shown in Figure 4 was conducted with *Alu*$^+$ probes that were not designed to optimally detect specific *Alu* sequences. An expansion of this study repeated with probes of optimal specificity may have merit. For example, one could conduct Northern analysis with probes that specifically detect or exclude the signal from *Alu* element homologues, such as 7SL RNA. This study would facilitate the proper distinction and quantification of *Alu* transcripts. It is also worthwhile to consider the possibility that some *Alu* families that contain many readily transcribed and recently retrotransposed *Alu* elements may be differentially regulated from *Alu* families that are ancient and not readily transcribed. It may be worthwhile to study subsets of *Alu* transcripts derived from different *Alu* families in HSV-1 infection to determine if this is the case.

4.2.1 Why may polyA$^-$ RNAs not be destabilized by vhs?

As described in the Introduction, vhs destabilizes host mRNAs. *In vitro* studies conducted in rabbit reticulocyte lysate (RRL) indicate that a polyA tail is not required to target mRNA destabilization activities of vhs (76). Why, then, did a multitude of polyA$^-$ RNA species appear to be stable over infection in our hands? Well, our result is not entirely unprecedented. Ribosomal RNAs are not targeted by vhs *in vitro* (161) and are similarly polyA$^-$. Perhaps polyadenylation is necessary *in vivo*, and in cytoplasmic HeLa cell extracts, which were used for the *in vitro* studies of ribosomal RNA. In contrast, perhaps RRL is abnormally permissive for polyA independent vhs activity. Consistent with this possibility, polyA tails are significantly less potent for mediating translation upregulation in RRL than in physiological conditions (208). An unusual cap-independent translation also occurs in rabbit reticulocyte lysate. It is therefore not unreasonable to envision that the lysate may also be abnormally permissive for some polyA independent

vhs activities. The results obtained here for a multitude of mRNAs, as well as results for ribosomal RNAs seen in previous works, are consistent with the idea that polyadenylation, or perhaps protein factors associated with polyadenylation, may be necessary for vhs targeting *in vivo*.

Other works have supported the notion that polyA$^-$ RNAs are stable during infection in at least some experimental conditions.

Nakai *et al.* (222) conducted HSV-1 infections in polyoma virus-transformed BHK cells and observed that polyA$^-$ RNA sequences increase in abundance in infection.

Histone mRNAs are the only known class of conserved metazoan mature RNAs that are not polyadenylated (122). They have been monitored in HSV-1 infection. Mayman and Nishioka (193) observed that histone H3 mRNA is stable and histone protein is continually synthesized over infection of Friend erythroleukemia cells. This observation was made in a background of other mRNAs that decreased in abundance over infection. Schek and Bachenheimer (283), in contrast, observed that histone H3 and H4 mRNAs do decrease in abundance over infection of Vero cells. Perhaps some cell types are permissive for vhs-mediated polyA$^-$ RNA degradation, (just as RRL is) while others are not. Histone mRNAs are able to associate with the translation initiation complex through their 3'-terminal stem loop structure that, in combination with the stem loop binding protein, substitutes for the polyA tail in recruiting PABP and translation initiation factors (177). We therefore expect eIF4H and/or eIF4B to be capable of binding these RNAs and targeting vhs activity to them. One can envision that histone mRNAs not bound to stem loop binding protein would be less efficiently targeted by vhs cofactors, and hence, vhs. Perhaps the ability of vhs to target these RNAs fluctuates according to variabilities in this association.

It is also possible that polyA$^-$ RNAs are protected from vhs activity via isolation in a different subcellular compartment. In an intact cell, vhs activity could conceivably be restricted to the cytoplasm, where TIFs are localized. (This postulate requires the assumption that infection does not induce nuclear transport of vhs TIF cofactors.) The stability of polyA$^-$ *Alu* transcripts can be accounted for, if they are determined to be sequestered from known vhs cofactors through retention in the nucleus. Following this

train of thought, perhaps unpolyadenylated mRNAs are artifactually accessible to vhs *in vitro*, as vhs, its cofactors, and its putative substrate are not compartmentalized from each other as they may be *in vivo*.

4.3 Detailed analysis of collagen, β-actin and GAPDH mRNAs in KOS, UV-irradiated KOS and ΔSma infections

Regardless of the errors in the microarray quantitation, the ECM protein-encoding mRNAs in cluster 16 might still be a cohort of RNAs coregulated in some meaningful, distinguishable way during infection. While cluster 16 and group A mRNA profiles were not distinguishable in KOS infection, we thought that cluster 16 mRNA profiles may prove distinct if infection with a wider panel of HSV-1 strains and infection conditions was examined. We elected to monitor some of the cluster 16 mRNAs, alongside 2 other mRNAs studied in previous works, GAPDH and β-actin, over a series of wildtype and HSV-1 mutant infections. We wished to determine if cluster 16 mRNAs had any novel profiles in these infections and if any distinct profile features would be common to all cluster 16 mRNAs. These mRNAs were also of interest, simply because they had not been monitored over infection previously (with the exception of fibronectin).

Collagen (a cluster 16 member), β-actin and GAPDH mRNA profiles were compared in KOS, UV-irradiated KOS and ΔSma (vhs$^-$) infections. (See Figures 13, 12 and 11, respectively.) Profiles for all three mRNAs similarly demonstrated extensive loss over KOS infection. UV-irradiated KOS infection yielded partial loss of the three mRNAs. Within this study, the only cluster 16 mRNA profile distinction was observed in ΔSma infection. GAPDH mRNA remained stable throughout infection with ΔSma while collagen mRNA levels decreased. Unfortunately, we did not monitor the profiles of other cluster 16 mRNAs in ΔSma infection. Extending ΔSma infection analysis to include other cluster 16 mRNAs may be a worthwhile future endeavor.

4.3.1 Assessing mRNA destabilization/degradation activities of KOS, UV-irradiated KOS, and ΔSma infections

We hoped that the study of very stable mRNAs, like collagen, would allow us to identify RNA destabilization activities mediated by viral proteins. We were able to deduce that in KOS and UV-irradiated KOS infections, collagen mRNA losses may have occurred through some mRNA destabilization/degradation activity. These results were expected, given the presence of vhs in these infections. However, the apparent ability of ΔSma (vhs$^-$) infection to also cause collagen RNA destabilization was not expected and suggested that some active viral vhs-independent RNA destabilization mechanism may exist. It is also possible that there is no viral vhs-independent RNA destabilizing activity. Instead, a host response to infection may somehow cause αCP_2 (which as described in the Introduction, binds and stabilizes collagen mRNA) or the stabilizing 120kDa protein to be released from collagen mRNA, increasing the decay rate of collagen mRNA.

4.4 Detailed analysis of collagen, fibronectin, exostoses, β-actin and GAPDH mRNAs in IE mutant infections

Again, we were looking for RNA profile features that were common to all cluster 16 mRNAs, and yet were distinct from profile features of other mRNAs examined previously. We extended our analysis to include those of IE gene knockouts. Cluster 16 collagen, fibronectin and exostoses mRNAs were monitored alongside β-actin and GAPDH mRNAs over transcriptionally competent and UV irradiated ICP0$^-$, ICP4$^-$, ICP22$^-$, and ICP27$^-$ infections. We did not find any cluster 16-specific profiles. We did, however, observe several interesting trends that were common to all mRNAs studied.

The following profile features were common to all mRNAs monitored. (See Figures 16-20.) ICP4$^-$ and ICP22$^-$ infections similarly induced the most extensive mRNA downregulation of all the IE mutant infections. ICP0$^-$ infection induced mRNA loss that was delayed relative to that induced by ICP4$^-$ and ICP22$^-$ infections, but the net RNA loss was similar with all three viruses. We would like to know if mRNA level shutoff seen in

ICP0$^-$, ICP4$^-$ and ICP22$^-$ infections reflects the extent of the mRNA loss that would occur with wildtype infection. We would like to repeat the study of these viruses alongside KOS infection in order to address this uncertainty. The implied extent of shutoff activities of ICP0, ICP4, and ICP22 are described below.

ICP0 has been implicated in transcriptional arrest of only one host mRNA, c-*fos*, and is therefore thought to possibly minorly contribute to the arrest of host transcription (316). Our results did not contest this idea. Our results indicated that RNA-level shutoff may be delayed in ICP0$^-$ infection, and that the delay that occured may have been general, as it was observed for all 5 mRNAs monitored. Our observations may have been the consequence of decreased synthesis of host shutoff proteins. ICP0$^-$ infection does not proceed normally at low MOIs (275). Everett *et al.* (83) determined that, at restrictive low MOIs, IE gene expression is severely impaired, with ICP4 often being the only IE protein expressed. Low MOI ICP0$^-$ infection does not progress to E and L gene expression. Everett *et al.* determined that non-immortalized fibroblasts are most restrictive for ICP0$^-$ infection, and as HEL cells are of this type, it is quite possible that our ICP0$^-$ infection was somewhat impaired, resulting in delayed or reduced expression of shutoff proteins.

Like ICP0, ICP4 was reported to minorly contribute to host transcription arrest as it was necessary to cause full transcriptional arrest of c-*fos* and histone H2b (316). Our results did not contest this idea. However, the transcriptional arrest activities of ICP4 did not result in a significant compromise in total RNA level shutoff in our hands. (See Figures 16-20) Infection with ICP4$^-$ virus mediates tegument activities, elevated IE gene expression (except that of ICP4), and expression of ICP6. A majority of RNA-level host shutoff occurred in this context. It is tempting to suggest that *de novo* E and L viral proteins are not necessary for extensive RNA level host shutoff. However, this suggestion must be made with caution as abnormally high levels of ICP27, which is known to be a shutoff protein, are present in infection with ICP4$^-$ virus, and may confound clear interpretation.

Primary host shutoff is reported to be compromised in ICP22$^-$ infection because less vhs RNA and protein is produced and because less vhs is packaged into the tegument

(225). Holly Saffran, in our laboratory (personal communication) similarly observed a decrease in vhs mRNA levels in ICP22$^-$ infection relative to KOS infection. UL13 kinase is thought to act upstream of ICP22 in this process. Alternatively, UL13 kinase is proposed to mediate post translational modifications of vhs (present at normal levels) that inhibit its activity (235).

There are conflicting reports with regard to ICP22's contribution to host transcriptional arrest. Spencer *et al.* (316) report a lack of participation of ICP22 in transcriptional arrest, despite ICP22's ability to post-translationally modify host RNA polymerase II. Kemp & Latchman (148) however, reported that ICP22 was necessary for the transcriptional arrest of all 8 host mRNAs analyzed, suggesting that ICP22 was generally important for the process of host transcriptional arrest.

ICP22$^-$ infection was not impaired in inducing shutoff of any of the 5 mRNAs examined in our hands. (See Figures 16-20.) Our work did not monitor host transcription in nuclear run on assays, and hence did not delineate the presence or absence of host transcriptional arrest specifically. However, no change in net RNA level host shutoff was observed in ICP22$^-$ infection. Also, UV-irradiated ICP22$^-$ shutoff effects were not impaired relative to those of other UV-irradiated IE mutant viruses. Initially delivered vhs function was clearly not impaired in our hands. If our ICP22$^-$ infection did cause decreased synthesis of vhs mRNA or protein, or decreased packaging of vhs into the tegument, it did not manifest as a detectable inhibition of RNA level host shutoff. ICP22$^-$ infection was still adequate to mediate shutoff of the mRNAs we monitored.

Our results are not the first ones to dispute UL13 kinase and ICP22 shutoff activities. David Shivak (294), in our laboratory, observed that protein level shutoff occurred in the absence of UL13 kinase. Perhaps UL13 kinase and ICP22 shutoff effects vary according to experimental conditions assayed. Our laboratory (personal communication) tried to replicate the results of Ng. *et al.* (225) using the same cell lines and virus strains, and was unsuccessful. Our ICP22$^-$ preparations efficiently packaged vhs which functioned normally. Perhaps the protocols used in virus preparation were different, such that vhs protein packaging was more efficient in our hands. Consider that

our laboratory conducted d22lacZ preparations at 34°C while other laboratories often conduct virus preparations at 37°C. One can envision a scenario where the kinetics of vhs incorporation in the tegument occur with varying efficiency at different temperatures. Perhaps it would be worthwhile to examine vhs synthesis, tegument incorporation and function from d22lacZ prepared under a series of growth temperatures and conditions to determine if vhs function in d22lacZ is indeed influenced by these variables.

ICP27 mutants are defective in host shutoff; thus ICP27 has been implicated in the host shutoff process (274). Hardy & Goldin (119) reported that ICP27 inhibits RNA splicing and may thus mediate host shutoff by preventing the synthesis of mature mRNA. This process was purported to be general to all spliced mRNAs and was said to likely serve as a mode to selectively allow translation of viral mRNAs, the majority of which are intronless and unspliced. We therefore expected RNA level shutoff of all 5 of the mRNAs analyzed in ICP27$^-$ infection (which are all spliced) to be somewhat impaired. ICP27 also mediates host transcription arrest of at least some host mRNAs, namely GAPDH, c-*fos*, and histone H2b mRNA. GAPDH mRNA loss, as well as the loss of other unknown mRNAs whose transcription arrest depends on ICP27, may be more impaired in ICP27$^-$ infection, as these RNAs are putatively shutoff by ICP27 through this additional mechanism. Consistent with this postulate, Stingley *et al.* (325) did a small-scale microarray analysis of ICP27$^-$ infection and determined that host mRNA profiles were non-uniformly affected in ICP27$^-$ infections. We observed that shutoff of exostoses, GAPDH and β-actin mRNAs was indeed impaired in ICP27$^-$ infection (See Figure 21.), indicating that ICP27 was required to mediate shutoff of these RNAs, as expected. However, we observed that the shutoff of collagen and fibronectin mRNAs, which are both spliced, was not similarly impaired. (See Figure 21.) ICP27 did not appear to be necessary for extensive shutoff of these RNAs. Was the extensive shutoff of fibronectin and collagen mRNA seen in ICP27$^-$ infection reflective of the shutoff that occurs in wildtype infection? Well, fibronectin mRNA profiles of ICP27$^-$ and KOS infection were not compared in our work, but this comparison was done for collagen mRNA and is shown in both Figures 29 & 31. Both studies suggest that collagen mRNA shutoff may be minorly impaired in ICP27$^-$ infection. Overall, our results suggest that ICP27's RNA

level shutoff effects may not be significant for all mRNA species, and may not specifically target all spliced RNAs. It would be interesting to identify other host mRNAs that are extensively degraded independently of ICP27, perhaps by an expanded microarray analysis of ICP27$^-$ infection.

Stingley *et al.* (325) observed that host transcripts generally did not decline at all during ICP27$^-$ infection, and that only a subset of host mRNAs declined to some extent. It seems odd that Stingley *et al.* reported *no* decrease in the levels of most human transcripts when we saw at least some loss of all mRNAs in ICP27$^-$ infection. Why were tegument vhs shutoff activities inapparent for so many mRNAs in their hands?

There may have been some errors in the quantitation performed by Stingley *et al.* that could explain their anomalous result. Differential Cy3 and Cy5 label incorporation was controlled for by equalizing values reported for mock infection and 30-minute virus adsorption samples, externally equating the two processes. Stingley *et al.* did not specify that the adsorption step was done at cold temperatures. Therefore, considerable RNA degradation may have occurred during the first 30 minutes of adsorption that would have been masked in their current quantitation format. The relative differences in abundance of human transcripts in ICP27$^-$ infection reflect an intra-sample variance that is valid, regardless of the above potential quantitation problem. mRNAs described by Stingley *et al.* as decreased during ICP27$^-$ infection may be regulated in a similar fashion to collagen and fibronectin mRNAs in our study, in that their loss is relatively less dependent on ICP27.

Kemp *et al.* (148) investigated whether ICP47, an IE protein, contributes to host transcriptional arrest, and determined that it was not necessary for the process. They did not, however, conduct a direct comparison of KOS and ICP47$^-$ infections to demonstrate that transcriptional arrest was completely uninfluenced by ICP47. IE protein ICP47 has not been tested for its contribution to host shutoff in this work. For the sake of thoroughness, and as IE proteins have been implicated in transcriptional arrest, an ICP47$^-$ mutant may prove a worthy addition to our IE mutant study.

4.5 Host shutoff studies conducted with the vhs⁻/ICP27⁻ double mutant, ljs1

We decided to generate a vhs⁻/ICP27⁻ double mutant of HSV-1 (ljs1) with the goals of determining the relative contributions of vhs and ICP27 to host shutoff and assessing the extent to which their contributions to host shutoff were independent. We studied ljs1 shutoff effects alongside those of KOS and parental strains at the RNA and protein level.

Ljs1 is described briefly below. Ljs1 was generated via homologous recombination in coinfections with parental strains ΔSma (vhs⁻) and 5dl1.2 (ICP27⁻). Ljs1 growth requires complementation of ICP27. Its growth phenotype is similar to that of ΔSma on V27 cells. Two unidentified viral proteins were detectably synthesized in ljs1 infection, as shown in Figure 32. While the viral protein synthesis profile of ljs1 was not examined in detail with Western analysis of specific IE, E, and L viral proteins, we can predict the probable gene expression pattern. As described in the Introduction, vhs⁻ mutants express the full panel of viral proteins (except vhs) in a retarded viral gene expression cascade. A logical predicted viral gene expression pattern would therefore be one similar to that of 5dl1.2, with a retarded gene expression cascade due to the lack of vhs.

Collagen and GAPDH mRNAs, both stable, were monitored in ljs1 studies. We expected ljs1 to be incapable of mediating host shutoff at the RNA level. ICP27 was not available to prevent mRNA maturation through inhibition of splicing. Even if other IE viral proteins had been able to arrest host transcription, pre-existing stable collagen and GAPDH mRNAs would have remained because vhs was not present to induce their degradation. Ljs1 did not appear to cause shutoff of collagen or GAPDH mRNAs, consistent with these predictions.

In order to interpret protein level shutoff effects of ljs1, it is necessary to understand the effects of other HSV mutants on host protein synthesis. The protein level host shutoff effects of UV-irradiated KOS, ΔSma and 5dl1.2 are therefore first described and interpreted.

Virion host shutoff with UV-irradiated HSV-1 infection is only seen in actD treated infections and does not actually occur in transcriptionally competent cells (127). The HSV-1 tegument, which includes initially delivered vhs, does not, therefore, mediate host translational arrest on its own. Consistent with this literature report, our metabolic labeling analysis of UV-irradiated KOS infection illustrated a pattern indistinguishable from mock infection, and evinced no translational host shutoff. It is worthwhile to note that this lack of protein level shutoff in UV-irradiated wildtype HSV-1 infection was observed despite the approximate 2-fold decrease in the levels of several host mRNAs seen over similar time courses, both in our hands and in other works. While this relationship should be confirmed with specific mRNA and encoded protein pairs, the suggested trend is that primary vhs-mediated RNA level shutoff does not actually contribute to net translational arrest on its own. It is still possible that, when coupled to IE viral shutoff activities, the degradation of mRNA caused by vhs can have a significant impact on host translation. Host mRNA degradation may advantageously (to infection) recycle mRNA components such that the supply of RNA synthesis precursors for viral mRNA synthesis is optimal.

Consistent with other work (274), we also found that potent protein level shutoff activity requires ICP27, as 5dl1.2 infection is severely impaired in this respect.

Metabolic labeling studies that established that ΔSma is defective in inducing protein level host shutoff (256) were done in transcriptionally arrested cells. When we assessed ΔSma shutoff activities in transcriptionally competent cells, we found of that ΔSma infection caused extensive translational shutoff. Vhs is therefore not necessary for HSV-1 to induce potent host translational arrest in infection where the host cell and virus are transcriptionally competent.

Kim Ellison, in our laboratory, similarly observed that ΔSma infection was able to mediate potent translational shutoff (personal communication). Based on this result, and results from other experiments described below, she deduced that ICP27 is likely acting to mediate shutoff at the translational level. This is the rationale of her deduction. Consider that ΔSma infection can mediate all known host mRNA biogenesis arrest

mechanisms, including the IE transcriptional arrest activities, as well as the splicing inhibition activities of ICP27. Vhs degradation activities are not present in this mutant infection. If protein level shutoff is mediated through host mRNA downregulation, ΔSma mRNA and protein shutoff activities should have been equivalent to actD incubation of cells, where mRNA biogenesis is similarly arrested. However, Kim Ellison and I both observed that ΔSma infection exhibited *more* protein level shutoff than actD incubation. We can therefore infer that more shutoff activities are occurring in ΔSma infection than inhibition of mRNA biogenesis.

Kim Ellison also showed that translation of GAPDH and actin, as measured by metabolic labeling of proteins, was inhibited more than can be accounted for by loss of cytoplasmic mRNA, suggesting a translational host shutoff mechanism. Her polysome analysis indicated that this translational shutoff was associated with a reduction in the average size of polysomes bearing these mRNAs, and an accumulation of some of the mRNA in complexes that comigrate with 40S ribosomal units. ICP27 was necessary for this dissociation of host mRNAs from larger polysomes, which translate more efficiently.

Kim Ellison's work is corroborated by the work of other investigators. Greco *et al.* similarly attributed differences in host translation efficiency in infection to differential association of mRNAs with polyribosomes (114). Greco *et al.* also found that less-readily translated RNAs are less frequently associated with large polysomes, and more frequently associated with 40S ribosomal subunits during infection. Kim Ellison's results implicate ICP27 in translational arrest, but do not specify whether its effects are mediated directly or indirectly through the induction of synthesis of other proteins. Recall that ICP27 is required for TL gene expression. It is quite possible that ICP27 mediates its translational shutoff effects through TL proteins known to be associated with ribosomes during infection that may modify ribosomes in such a way as to mediate translational shutoff, namely: US11, VP19C, and VP26 (113).

Ljs1 infection mediated a very small amount of host translation arrest. This indicated that vhs, ICP27, and possibly ICP27-dependent proteins are largely responsible for the net observed effects in protein level shutoff. Other viral proteins expressed in ljs1 infection can contribute minorly to translation arrest. To identify these other viral

proteins, we can generate further knockout mutants in the ljs1 genetic background, and determine which mutations further impair host translational arrest.

Ljs1 was more extensively impaired in protein level host shutoff than the parental strain, 5dl1.2. If vhs is the only additional viral protein missing in ljs1, then one would surmise that vhs can indeed minorly contribute to net translational arrest, via its nuclease activity and/or it's regulation of the viral gene expression cascade. While clearly unnecessary for protein level host shutoff, vhs may still be capable of contributing to the process, in the context of other functioning shutoff proteins.

4.6 Do vhs and ICP27 function in host shutoff independently?

Throughout this work, we posed the question: Are a portion of the RNA level shutoff effects attributed to ICP27 actually directly mediated by vhs which is newly synthesized during infection? Were some of ICP27 RNA level effects occurring via induction of vhs?

The current literature reports indicate that vhs and ICP27 function independently. Vhs destabilizes new and pre-existing mRNAs. ICP27 inhibits transcription of some mRNAs and splicing of pre-mRNAs. Indeed, results with ljs1 infection did indicate that vhs and ICP27 do contribute independently to shutoff at both the RNA and protein level, as ljs1 was more impaired in inducing shutoff than either parental strain. However, current information still cannot rule out the possibility that a portion of ICP27's contribution to shutoff at the RNA level is mediated through upregulation of vhs synthesis. ICP27 is necessary for normal amounts of vhs mRNA synthesis (325). Additionally, we have shown that ICP27 was necessary for robust vhs protein synthesis.

One can argue that induction of vhs expression by ICP27 is still irrelevant to shutoff because new vhs has not been proven to be catalytically active and relevant to shutoff at late times post infection. True, some investigation (165) has indicated that VP16 does inhibit vhs at late times post infection. However, while Lam *et al.* did demonstrate that vhs activity was tempered by VP16 at late times post infection, preventing excessive degradation of viral mRNAs by vhs, they did not show that newly

synthesized vhs was completely catalytically irrelevant. Oroskar & Read (233) directly monitored the half-lives of 10 viral mRNAs from among all viral kinetic classes. Functional vhs was necessary for *E and L* gene downregulation at the mRNA level. This result supports the idea that vhs is catalytically relevant at late times post infection. Therefore, it is still possible that newly-synthesized vhs is catalytically relevant at late times post infection, and by corollary, that a portion of ICP27's RNA level shutoff activity may occur through induction of newly-synthesized vhs.

The ICP27$^-$ infection microarray analysis suggested above may be used to determine the extent by which ICP27's RNA level shutoff activities do or do not occur through vhs. We would expect the shutoff of mRNAs that are extremely sensitive to vhs to be less dependent on ICP27, as initially delivered vhs may be sufficient to mediate their degradation. We would expect the shutoff of mRNAs that are less sensitive to vhs to be more dependent on ICP27, as newly synthesized vhs may be required to mediate their degradation. The degradation rates of mRNAs from different cohorts of an ICP27$^-$ infection microarray study can be determined in *in vitro* vhs assays. We could then determine if dependence on ICP27 for complete mRNA loss is indeed reciprocally related to vhs ribonucleolytic potency on those substrates. A caveat of this *in vitro* analysis is that differential sensitivity to vhs may not be accurately reflected in the assay. The presence of vhs cofactors at non-*in vivo* concentrations may alter relative catalytic activity.

4.7 Major conclusions from this work

We refuted the results from our incorrectly normalized microarray analysis. Our results do support the idea that most host mRNAs decrease in abundance during HSV-1 infection. Some clones from the microarray analysis detected polyA$^-$ RNAs. We noted that during infection, polyA$^-$ RNAs may be relatively more stable than polyA$^+$ mRNAs. We suspected that ECM mRNAs had unique profiles over infection and thus pursued analysis of several ECM mRNAs alongside other mRNAs that were examined previously. We did not find any novel host shutoff mRNA profile features that were common to all ECM mRNAs examined. We did, however, observe some unexpected

mRNA profiles in our analyses, which included: a late collagen mRNA destabilization that may have been vhs independent, a lack of dependence on ICP22 for efficient RNA level shutoff, and a variable dependence on ICP27 for the induction of host mRNA loss. In order to assess the contributions of vhs and ICP27 to host shutoff, ljs1, a vhs$^-$/ICP27$^-$ double mutant, was generated. Studies with ljs1 generally indicated that ICP27 and vhs contribute to RNA level and protein level host shutoff with at least some degree of independence.

5 BIBLIOGRAPHY

1. 2003. American Type Culture Collection. [Online.]

2. The MGED Data Transformation and Normalization Working Group. [Online.]

3. 2001. STDGEN Databases. Los Alamos National Library operated by the University of California for the National Nuclear Security Administration. [Online.]

4. **Ace, C. I., M. A. Dalrymple, F. H. Ramsay, V. G. Preston, and C. M. Preston.** 1988. Mutational analysis of the herpes simplex virus type 1 trans-inducing factor Vmw65. Journal of General Virology **69:**2595-2605.

5. **Ace, C. I., T. A. McKee, J. M. Ryan, J. M. Cameron, and C. M. Preston.** 1989. Construction and characterization of a herpes simplex virus type 1 mutant unable to transinduce immediate-early gene expression. Journal of Virology **63:**2260-2269.

6. **Ackermann, M., D. K. Braun, L. Pereira, and B. Roizman.** 1984. Characterization of herpes simplex virus 1 alpha proteins 0, 4, and 27 with monoclonal antibodies. Journal of Virology **52:**108-118.

7. **Addison, C., F. J. Rixon, and V. G. Preston.** 1990. Herpes simplex virus type 1 UL28 gene product is important for the formation of mature capsids. J Gen Virol **71 (Pt 10):**2377-84.

8. **Advani, S. J., R. Brandimarti, R. R. Weichselbaum, and B. Roizman.** 2000. The disappearance of cyclins A and B and the increase in activity of the G2/M-phase cellular kinase cdc2 in herpes simplex virus 1-infected cells require expression of the a22/US1.5 and UL13 viral genes. Journal of Virology **74:**8-15.

9. **Advani, S. J., R. R. Weichselbaum, and B. Roizman.** 2003. Herpes simplex virus 1 activates cdc2 to recruit topoisomerase II alpha for post-DNA synthesis expression of late genes. Proceedings of the National Academy of Sciences **100:**4825-4830.

10. **Advani, S. J., R. R. Weichselbaum, and B. Roizman.** 2000. The role of cdc2 in the expression of herpes simplex virus genes. Proceedings of the National Academy of Sciences **97:**10996-11001.

11. **Albright, A. G., and F. J. Jenkins.** 1993. The herpes simplex virus UL37 protein is phosphorylated in infected cells. Journal of Virology **67:**4842-4847.

12. **Al-Kobaisi, M. F., F. J. Rixon, I. McDougall, and V. G. Preston.** 1991. The herpes simplex virus UL33 gene product is required for the assembly of full capsids. Virology **180:**380-8.

13. **Araujo, T. D., B. Berman, and A. Weinstein.** 2002. Human herpesviruses 6 and 7. Dermatologic Clinics **20**.

14. **Bacchetti, S., M. J. Evelegh, and B. Muirhead.** 1986. Identification and separation of the two subunits of the herpes simplex virus ribonucleotide reductase. Journal of Virology **57:**1177-1181.

15. **Baines, J. D., A. P. W. Poon, J. Rovnak, and B. Roizman.** 1994. The herpes simplex virus 1 UL15 gene encodes two proteins and is required for cleavage of genomic viral DNA. Journal of Virology **68:**8118-8124.

16. **Batzer, M. A., and P. L. Deininger.** 2002. Alu repeats and human genomic diversity. Nature Reviews: Genetics **3:**370-380.

17. **Becker, Y., E. Tavor, Y. Asher, C. Berkowitz, and M. Moyal.** 1993. Effect of herpes simplex virus type-1 UL41 gene on the stability of mRNA from the cellular genes: beta-actin, fibronectin, glucose transporter-1, and docking protein, and on virus intraperitoneal pathogenicity to newborn mice. Virus Genes **7:**133-43.

18. **Berthomme, H., B. Jaquemont, and A. Epstein.** 1993. The pseudorabies virus host-shutoff homolog gene: nucleotide sequences and comparison with alphaherpesvirus protein counterparts. Virology **193:**1028-1032.

19. **Betz, U. A., R. Fischer, G. Kleymann, M. Hendrix, and H. Rubsamen-Waigmann.** 2002. Potent in vivo antiviral activity of the herpes simplex virus primase-helicase inhibitor BAY 57-1293. Antimicrobial Agents and ChemotherapY **46:**1766-1772.

20. **Bilban, M., L. K. Buehler, S. Head, G. Desoye, and V. Quaranta.** 2002. Normalizing DNA microarray data. Curr Issues Mol Biol **4:**57-64.

21. **Bjornberg, O., A. C. Bergman, A. M. Rosengren, R. Persson, I. R. Lehman, and P. O. Nyman.** 1993. dUTPase from herpes simplex virus type 1; purification from infected green monkey kidney (Vero) cells and from an overproducing Escherichia coli strain. Protein Expr Purif **4:**149-159.

22. **Blaho, J. A., C. Mitchell, and B. Roizman.** 1993. Guanylylation and adenylylation of the α regulatory proteins of herpes simplex virus require a viral β or γ function. J. Virol. **67:**3891-3900.

23. **Boehmer, P. E., M. S. Dodson, and I. R. Lehman.** 1993. The herpes simplex virus type-1 origin binding protein. DNA helicase activity. J Biol Chem **1220-1225**.

24. **Boehmer, P. E., and I. R. Lehman.** 1997. Herpes simplex virus DNA replication. Annu. Rev. Biochem. **66:**347-384.

25. **Bresnahan, W. A., G. E. Hultman, and T. Shenk.** 2000. Replication of wild-type and mutant human cytomegalovirus in life-extended human diploid fibroblasts. Journal of Virology **74:**10816-10818.

26. **Brignati, M. J., J. S. Loomis, J. W. Wills, and R. J. Courtney.** 2003. Membrane association of VP22, a herpes simplex virus type 1 tegument protein. Journal of Virology **77:**4888-4898.

27. **Brigstock, D. R.** 1999. The Connective Tissue Growth Factor/Cysteine-Rich 61/Nephroblastoma Overexpressed (CCN) Family. Endocrine Reviews **20:**189-206.

28. **Brown, D. G., R. Visse, G. Sandhu, A. Davies, P. J. Rizkallah, C. Melitz, W. C. Summers, and M. R. Sanderson.** 1995. Crystal structures of the thymidine kinase from herpes simplex virus type-1 in complex with deoxythymidine and ganciclovir. Nat Struct Biol **2:**876-881.

29. **Brown, S. M., and A. R. MacLean.** 1998. Herpes simplex virus protocols. Humana Press, Totowa, N.J.

30. **Brown, Z. A., A. Wald, R. A. Morrow, S. Selke, J. Zeh, and L. Corey.** 2003. Effect of serologic status and cesarean delivery on transmission rates of herpes simplex virus from mother to infant. Journal of the American Medical Association **289:**203-209.

31. **Browne, H., B. Bruun, and T. Minson.** 2001. Plasma membrane requirements for cell fusion induced by herpes simplex virus type 1 glycoproteins gB, gD, gH and gL. Journal of General Virology **82:**1419-1422.

32. **Browne, H., B. Bruun, A. Whiteley, and T. MInson.** 2003. Analysis of the role of the membrane-spanning and cytoplasmic tail domains of herpes simplex virus type 1 glycoprotein D in membrane fusion. Journal of General Virology **85:**1085.

33. **Bruckner, R. C., J. J. Crute, M. S. Dodson, I. R. Lehman, ., and F. 5;266(4):2669-74.** 1991. The herpes simplex virus 1 origin binding protein: a DNA helicase. J Biol Chem **266:**2669-2674.

34. **Bryant, H. E., S. E. Wadd, A. I. Lamond, S. J. Silverstein, and J. B. Clements.** 2001. Herpes simplex virus IE63 (ICP27) protein interacts with spliceosome-associated protein 145 and inhibits splicing prior to the first catalytic step. Journal of Virology **75:**4376-4385.

35. **Cai, W., B. Gu, and S. Person.** 1988. Role of glycoprotein B of herpes simplex virus type 1 in viral entry and cell fusion. J. Virol. **62:**2596-2604.

36. **Cai, W., and P. A. Schaffer.** 1989. Herpes simplex virus type 1 ICPO plays a critical role in the de novo synthesis of infectious virus following transfection of viral DNA. Journal of Virology **63:**4570-4589.

37. **Campbell, M. E. M., L. M. Palfreyman, and C. M. Preston.** 1984. Identification of herpes simplex virus DNA sequences which encode a trans-acting polypeptide responsible for stimulation of immediate early transcription. Journal of Molecular Biology **180:**1-19.

38. **Caradonna, S., D. Worrad, and R. Lirette.** 1987. Isolation of a herpes simplex virus cDNA encoding the DNA repair enzyme uracil-DNA glycosylase. Journal of Virology **61:**3040-3047.

39. **Caradonna, S. J., and D. M. Adamkiewicz.** 1984. Purification and properties of the deoxyuridine triphosphate nucleotidohydrolase enzyme derived from HeLa S3 cells. Comparison to a distinct dUTP nucleotidohydrolase induced in herpes simplex virus-infected HeLa S3 cells. J Biol Chem **259:**5459-5464.

40. **Caradonna, S. J., and Y. C. Cheng.** 1981. Induction of uracil-DNA glycosylase and dUTP nucleotidohydrolase activity in herpes simplex virus-infected human cells. J Biol Chem **256:**9834-9837.

41. **Carter, K. L., E. Cahir-McFarland, and E. Kieff.** 2002. Epstein-barr virus-induced changes in B-lymphocyte gene expression. Journal of Virology **76:**10427-10436.

42. **Carter, K. L., and B. Roizman.** 1995. The promoter and transcriptional unit of a novel herpes simplex virus 1 α gene are contained in, and encode protein in frame with, the open reading frame of the α22 gene. J. Virol. **70:**172-178.

43. **Cassady, K. A., M. Gross, and B. Roizman.** 1998. The second-site mutation in the herpes simplex virus recombinants lacking the gamma134.5 genes precludes shutoff of protein synthesis by blocking the phosphorylation of eIF-2alpha. J Virol **72:**7005-11.

44. **Chang, Y. E., C. Van Sant, P. W. Krug, A. E. Sears, and B. Roizman.** 1997. The null mutant of the UL31 gene of herpes simplex virus 1: construction and phenotype in infected cells. Journal of Virology **71:**8307-8315.

45. **Chatterjee, S., and D. Koppers-Lalic.** 2001. The UL41-encoded virion host shutoff (vhs) protein and vhs-independent mechanisms are responsible for down-regulation of MHC class I molecules by bovine herpesvirus 1. Cancer Gene Therapy **8:**566-572.

46. **Chen, I.-H. B., K. Sciabica, and R. Sandri-Goldin.** 2002. ICP27 interacts with the RNA export factor Aly/Ref to direct herpes simplex viurs type 1 intronless mRNAs to the TAP export pathway. Journal of Virology **76:**12877-12889.

47. **Chen, M. S., and W. H. Prusoff.** 1978. Association of thymidylate kinase activity with pyrimidine deoxyribonucleoside kinase induced by herpes simplex virus. J Biol Chem **253:**1325-1327.

48. **Chen, M. S., W. P. Summers, J. Walker, W. C. Summers, and W. H. Prusoff.** 1979. Characterization of pyrimidine deoxyribonucleoside kinase (thymidine kinase) and thymidylate kinase as a multifunctional enzyme in cells transformed by herpes simplex virus type 1 and in cells infected with mutant strains of herpes simplex virus. Journal of Virology **30:**942-945.

49. **Cheung, P., B. W. Banfield, and F. Tufaro.** 1991. Brefeldin A arrests the maturation and egress of herpes simplex virus particles during infection. J Virol **65:**1893-904.

50. **Cheung, P., K. S. Ellison, R. Verity, and J. R. Smiley.** 2000. Herpes simplex virus ICP27 induces cytoplasmic accumulation of unspliced polyadenylated alpha-globin pre-mRNA in infected HeLa cells. Journal of Virology **74:**2913-2919.

51. **Chkheidze, A. N., D. L. Lyakhov, A. V. Makeyev, J. Morales, J. Kong, and S. A. Leibhaber.** 1999. Assembly of the alpha-globin mRNA stability complex reflects binary interaction between the purimidine-rich 3' untranslated region determinant and poly(C) binding protein alpha CP. Molecular and Cellular Biology **19:**4572-4581.

52. **Chou, J., J. J. Chen, M. Gross, and B. Roizman.** 1995. Association of a M(r) 90,000 phosphoprotein with protein kinase PKR in cells exhibiting enhanced phosphorylation of translation initiation factor eIF-2 alpha and premature shutoff of protein synthesis after infection with gamma 1 34.5 gene of herpes simplex virus. Proceedings of the National Academy of Sciences **92:**10516-10520.

53. **Chuaqui, R. F., R. F. Bonner, C. J. M. Best, J. W. Gillespie, M. J. Flaig, S. M. Hewitt, J. L. Phillips, D. B. Krizman, M. A. Tangrea, M. Ahram, W. M. Linehan, V. Knezevic, and M. R. Emmert-Buck.** 2002. Post-analysis follow-up and validation of microarray experiments. Nature Genetics **32:**509-514.

54. **Church, G. M., and W. Gilbert.** 1984. Genomic sequencing. Proceeding National Academy of Science USA **81:**1991-1995.

55. **Crute, J. J., and I. R. Lehman.** 1989. Herpes simplex-1 DNA polymerase. Identification of an intrinsic 5'----3' exonuclease with ribonuclease H activity. J Biol Chem **264:**19266-19270.

56. **Crute, J. J., E. S. Mocarski, and I. R. Lehman.** 1988. A DNA helicase induced by herpes simplex virus type 1. Nucleic Acids Research **16:**6585-6596.

57. **Crute, J. J., T. Tsurumi, L. A. Zhu, S. K. Weller, P. D. Olivo, M. D. Challberg, E. S. Mocarski, and I. R. Lehman.** 1989. Herpes simplex virus 1 helicase-primase: a complex of three herpes-encoded gene products. Proc Natl Acad Sci U S A **86:**2186-2189.

58. **Dargan, D. J., and J. H. Subak-Sharpe.** 1997. The effects of herpes simplex virus type 1 L-particles on virus entry, replication, and the infectivity of naked herpesvirus DNA. Virology **239:**378-388.

59. **Davison, A. J.** 2002. Evolution of heresviruses. Veterinary Microbiology **86:**69-88.

60. **de Wet, W., M. Bernard, V. Benson-Chanda, M.-L. Chu, L. Dickson, D. Weil, and F. Ramirez.** 1987. Organization of the human pro-alpha2(I) collagen gene. The Journal of Biological Chemistry **262:**16032-16036.

61. **Deininger, P. L., and M. A. Batzer.** 1999. Alu repeats and human disease. Molecular Genetics and Metabolism **67:**183-193.

62. **Deininger, P. L., D. J. Jolly, C. M. Rubin, T. Freidmann, and C. W. Schmid.** 1981. Base sequence studies of 300 nucleotide renatured repeated human DNA clones. Journal of Molecular Biology **151:**17-31.

63. **DeLuca, N. A., A. M. McCarthy, and P. A. Schaffer.** 1985. Isolation and characterization of deletion mutants of herpes simplex virus type 1 in the gene encoding immediate-early regulatory protein ICP4. Journal of Virology **56:**558-570.

64. **Desai, P., N. A. DeLuca, J. C. Glorioso, and S. Person.** 1993. Mutations in herpes simplex virus type 1 genes encoding VP5 and VP23 abrogate capsid formation and cleavage of replicated DNA. J Virol **67:**1357-64.

65. **Desai, P. J.** 2000. A null mutation in the UL36 gene of herpes simplex virus type 1 results in accumulation of unenveloped DNA-filled capsids in the cytoplasm of infected cells. Journal of Virology **74:**11608-11618.

66. **Deshmane, S. L., B. Raengsakulrach, J. F. Berson, and N. W. Fraser.** 1995. The replicating intermediates of herpes simplex virus type 1 DNA are relatively short. J Neurovirol **1:**165-76.

67. **Di Lazzaro, C., G. Campadelli-Fiume, and M. R. Torrisi.** 1995. Intermediate forms of glycoconjugates are present in the envelope of herpes simplex virions during their transport along the exocytic pathway. Virology **214:**619-23.

68. **Dick, J. W., and K. S. Rosenthal.** 1995. A block in glycoprotein processing correlates with small plaque morphology and virion targetting to cell-cell junctions for an oral and an anal strain of herpes simplex virus type-1. Arch Virol **140:**2163-81.

69. **Diefenbach, R. J., M. Miranda-Saksena, E. Diefenbach, D. J. Holland, R. A. Boadle, P. J. Armati, and A. L. Cunningham.** 2002. Herpes simplex virus tegument protein US11 interacts with conventional kinesin heavy chain. Journal of Virology **76:**3282-3291.

70. **Dingwell, K. S., C. R. Brunetti, R. L. Hendricks, Q. Tang, M. Tang, A. J. Rainbow, and D. C. Johnson.** 1994. Herpes simplex virus glycoproteins E and I facilitate cell-to-cell spread in vivo and across junctions of cultured cells. J Virol **68:**834-45.

71. **Dixon, R. A. F., and P. A. Schaffer.** 1980. Fine structure mapping and functional analysis of temperature-sensitive mutants in the gene encoding the herpes simplex virus type 1 immediate early protein VP175. Journal of Virology **36:**189-203.

72. **Dodson, M. S., and I. R. Lehman.** 1993. The herpes simplex virus type I origin binding protein. DNA-dependent nucleoside triphosphatase activity. J Biol Chem **268:**1213-1219.

73. **Doepker, R. C., W. L. Hsu, H. A. Saffran, and J. R. Smiley.** 2004. Herpes simplex virion host shutoff protein is stimulated by translations initiation factors eIF4B and eIF4H. Journal of Virology **78:**4684-4699.

74. **Dohner, K., A. Wolfstein, U. Prank, C. Echeverri, D. Dujardin, R. Valee, and B. Sodeik.** 2002. Function of dynein and dynactin in herpes simplex virus capsid transport. Molecular Biology of the Cell **13:**2795-2809.

75. **Donnelly, M., and G. Elliot.** 2000. Nuclear localization and shuttling of herpes simplex virus tegument protein VP13/14. Journal of Virology **75:**2566-2574.

76. **Elgadi, M. M., C. E. Hayes, and J. R. Smiley.** 1999. The herpes simplex virus vhs protein induces endoribonucleolytic cleavage of target RNAs in cell extracts. Journal of Virology **73:**7153-7164.

77. **Elias, P., and I. R. Lehman.** 1988. Interaction of origin binding protein with an origin of replication of herpes simplex virus 1. Proc Natl Acad Sci U S A **85:**2959-2963.

78. **Elias, P., M. E. O'Donnell, E. S. Mocarski, and I. R. Lehman.** 1986. A DNA binding protein specific for an origin of replication of herpes simplex virus type 1. Proc Natl Acad Sci U S A **83:**6322-6326.

79. **Elliot, G., D. O'Reilly, and P. O'Hare.** 1999. Identification of phosphorylation sites within the herpes simplex virus tegument protein VP22. Journal of Virology **73:**6203-6206.

80. **Enquist, L. W., G. F. Van de Woude, M. J. Wagner, J. R. Smiley, and W. C. Summers.** 1979. Construction and characterization of a recombinant plasmid encoding the gene for the thymidine kinase of herpes simplex type 1 virus. Gene **7:**335-342.

81. **Everett, R.** 1999. A surprising role for the proteasome in the regulation of herpesvirus infection. TIBS **24:**293-295.

82. **Everett, R. D.** 2000. ICP0, a regulator of herpes simplex virus during lytic and latent infection. BioEssays **22:**761-770.

83. **Everett, R. D., C. Boutell, and A. Orr.** 2004. Phenotype of a herpes simplex virus type 1 mutant that fails to express immediate-early regulatory protein ICP0. Journal of Virology **78:**1763-1774.

84. **Everett, R. D., P. Freemont, H. Saitoh, M. Dasso, A. Orr, M. Kathoria, and J. Parkinson.** 1998. The disruption of ND10 during herpes simplex virus infection correlates with the Vmw110- and proteasome-dependent loss of several PML isoforms. J Virol **72:**6581-91.

85. **Everett, R. D., A. Orr, and C. M. Preston.** 1998. A viral activator of gene expression functions via the ubiquitin- proteasome pathway [In Process Citation]. Embo J **17:**7161-9.

86. **Everett, R. D., C. M. Preston, and N. D. Stow.** 1991. Functional and genetic analysis of the role of Vmw110 in herpes simplex virus replication, p. 50-76. *In* E. K. Wagner (ed.), The control of herpes simplex virus gene expression. CRC Press Inc., Boca Raton, Florida.

87. **Everly, D. N., Jr., and G. S. Read.** 1997. Mutational analysis of the virion host shutoff gene (UL41) of herpes simplex virus (HSV): characterization of HSV type 1 (HSV-1)/HSV-2 chimeras. J Virol **71:**7157-66.

88. **Feng, P., D. N. J. Everly, and G. S. Read.** 2001. mRNA decay during herpesvirus infections: interaction between a putative viral nuclease and a cellular translation factor. J Virol **75:**10272-80.

89. **Fenwick, M. L., and J. Clark.** 1982. Early and delayed shut-off of host protein synthesis in cells infected with herpes simplex virus. J. Gen. Virol. **61:**121-125.

90. **Fenwick, M. L., and J. Clark.** 1982. The effect of cycloheximide on the accumulation and stability of functional a-mRNA in cells infected with herpes simplex virus. Journal of General Virology **61:**121-125.

91. **Fenwick, M. L., L. S. Morse, and B. Roizman.** 1979. Anatomy of HSV DNA. XI. Apparent clustering of funcitons effecting rapid inhibition of host DNA and protein synthesis. Journal Virology **29:**825-827.

92. **Fenwick, M. L., and M. J. Walker.** 1978. Suppression of the synthesis of cellular macromolecules by herpes simplex virus. J. Gen. Virol. **41:**37-51.

93. **Fierer, D. S., and M. D. Challberg.** 1992. Purification and characterization of UL9, the herpes simplex virus type 1 origin-binding protein. Journal of Virology **66:**3986-3995.

94. **Flemington, E. K.** 2001. Herpesvirus lytic replication and the cell cycle: arresting new developments. Journal of Virology **75:**4475-4481.

95. **Forrester, A., H. Farrell, G. Wilkinson, J. Kaye, N. Davis-Poynter, and T. Minson.** 1992. Construction and properties of a mutant of herpes simplex virus type 1 with glycoprotein H coding sequences deleted. J. Virol. **66:**341-348.

96. **French-Constant, C.** 1995. Alternative Splicing of Fibronectin-Many Different Proteins but Few Different Functions. Experimental Cell Research **221:**261-271.

97. **Fruh, K., K. Ahn, H. Djaballah, P. Sempe, P. M. Van Endert, R. Tampe, P. A. Peterson, and Y. Yang.** 1995. A viral inhibitor of peptide transporters for antigen presentation. Nature **375:**415.

98. **Fuchs, W., B. G. Klupp, H. Granzow, N. Osterrieder, and T. C. Mettenleiter.** 2002. The interacting UL31 and UL34 gene products of pseudorabies virus are involved in egress from the host-cell nucleus and represent components of primary enveloped but not mature virions. J Virol **76:**364-78.

99. **Furlong, D., H. Swift, and B. Roizman.** 1972. Arrangement of herpesvirus deoxyribonucleic acid in the core. Journal of Virology **10.**

100. **Gallo, M. L., D. H. Jackwood, M. Murphy, H. S. Marsden, and D. S. Parris.** 1988. Purification of the herpes simplex virus type 1 65-kilodalton DNA-binding protein: properties of the protein and evidence of its association with the virus-encoded DNA polymerase. Journal of Virology **62:**2874-2883.

101. **Gao, M., L. Matusick-Kumar, W. Hurlburt, S. F. DiTusa, W. W. Newcomb, J. C. Brown, P. J. McCann, 3rd, I. Deckman, and R. J. Colonno.** 1994. The protease of herpes simplex virus type 1 is essential for functional capsid formation and viral growth. J Virol **68:**3702-12.

102. **Geiss, B. J., T. J. Smith, D. A. Leib, and L. A. Morrison.** 2000. Disruption of virion host shutoff activity improves the immunogenicity and protective capacity of a replication-incompetent herpes simplex virus type 1 vaccine strain. Journal of Virology **74:**11137-11144.

103. **Gelman, I. H., and S. Silverstein.** 1987. Dissection of immediate-early gene promoters from herpes simplex virus: sequences that respond to the virus transcriptional activators. Journal of Virology **61:**3167-3172.

104. **Geraghty, R. J., C. Krummenacher, G. H. Coen, R. J. Eisenberg, and P. G. Spear.** 1998. Entry of alphaherpesviruses mediated by poliovirus receptor-related protein 1 and poliovirus receptor. Science **280:**1618-1620.

105. **Gibson, W.** 1996. Structure and assembly of the virion. Intervirology **39:**389-400.

106. **Gibson, W., and B. Roizman.** 1972. Proteins specified by herpes simplex virus. 8. Characterization and composition of multiple capsid forms of subtypes 1 and 2. J Virol **10:**1044-52.

107. **Gibson, W., and B. Roizman.** 1974. Proteins specified by herpes simplex virus. Staining and radiolabeling properties of B capsid and virion proteins in polyacrylamide gels. J Virol **13:**155-65.

108. **Godowski, P. J., and D. M. Knipe.** 1986. Transcriptional control of herpesvirus gene expression: gene functions required for positive and negative regulation. Proc. Natl. Sci. USA **83:**256-260.

109. **Goodrum, F. D., C. T. Jordan, K. High, and T. Shenk.** 2002. Human cytomegalovirus gene expression during infection of primary hematopoietic progenitor cells: a model for latency. Proceedings of the National Academy of Sciences **99:**16255.

110. **Gopinath, R. S., A. P. Ambagala, S. Hinkley, and S. Srikumaran.** 2002. Effects of virion host shut-off activity of bovine herpesvirus 1 on MHC class I expression. Viral Immunology **15:**595-608.

111. **Goryachev, A. B., P. MacGregor, F., and A. M. Edwards.** 2001. Unfolding of microarray data. Journal of Computational Biology **8:**443-461.

112. **Granzow, H., B. G. Klupp, W. Fuchs, J. Veits, N. Osterrieder, and T. C. Mettenleiter.** 2001. Egress of alphaherpesviruses: comparative ultrastructural study. J Virol **75:**3675-84.

113. **Greco, A., W. Bienvenut, J. C. Sanchez, K. Kindbeiter, D. Hochstrasser, J. J. Madjar, and J. J. Diaz.** 2001. Identification of ribosome-associated viral and cellular basic proteins during the course of infection with herpes simplex virus type 1. Proteomics **1:**545-549.

114. **Greco, A., A. M. Laurent, J. J. Madjar, and J. Mateu.** 1997. Repression of beta-actin synthesis and persistence of ribosomal protein synthesis after infection of HeLa cells by herpes simplex virus type 1 infection are under translational control. Molecular & General Genetics **256:**320-327.

115. **Grondin, B., and N. DeLuca.** 2000. Herpes simplex virus type 1 ICP4 promotes transcription preinitiation complex formation by enhancing the binding of TFIID to DNA. Journal of Virology **72:**11504-11501.

116. **Gu, B., and N. DeLuca.** 1994. Requirements for activation of the herpes simplex virus glycoprotein C promoter in vitro by the viral regulatory protein ICP4. J. Virol. **68:**7953-7965.

117. **Hafner, J., F. Mohammad, D. M. Green, and F. E. Farber.** 1987. In situ detection of alkaline nuclease activity in cells infected with herpes simplex virus type 1 (HSV-1). Biochim. Biophys. Acta **910:**72-84.

118. **Hardwicke, M. A., and R. M. Sandri-Goldin.** 1994. The herpes simplex virus regulatory protein ICP27 contributes to the decrease in cellular mRNA levels during infection. J. Virol. **68:**4797-4810.

119. **Hardy, W. R., and R. M. Sandri-Goldin.** 1994. Herpes simplex virus inhibits host cell splicing, and regulatory protein ICP27 is required for this effect. J. Virol. **68:**7790-7799.

120. **He, B., M. Gross, and B. Roizman.** 1997. The gamma 1 34.5 protein of herpes simplex virus 1 complexes with protein phosphatase 1 alpha to dephosphorylate the alpha subunit of the eukaryotic translation initiation factor 2 and precludes the shutoff of protein synthesis by double-stranded RNA-activated protein kinase. Proceedings of the National Academy of Sciences **94:**843-848.

121. **Hegde, P., R. Qi, K. Abernathy, C. Gay, S. Dharap, R. Gaspard, J. E. Hughes, E. Snesrud, N. Lee, and J. Quackenbush.** 2000. A concise guide to cDNA microarray analysis. Biotechniques **29:**548-50, 552-4, 556 passim.

122. **Hentschel, C. C., and M. L. Birnstiel.** 1981. The organization and expression of histone gene families. Cell **25:**301-313.

123. **Herold, B. C., D. WuDunn, N. Soltys, and P. G. Spear.** 1991. Glycoprotein C of herpes simplex virus type 1 plays a principal role in the adsorption of virus to cells and in infectivity. J. Virol. **65:**1090-1098.

124. **Herr, W.** 1998. The herpes simplex virus VP16-induced complex: mechanisms of combinatorial transcriptional regulation. Quant. Biol. **63:**599-607.

125. **Heymann, J. B., N. Cheng, W. W. Newcomb, L. T. Benes, J. C. Brown, and A. Steven, C.** 2003. Dynamics of herpes simplex virus capsid maturation visualized by time-lapse cryo-electron microscopy. Nat Struct Biol **10:**334-341.

126. **Hill, A., P. Jugovic, I. York, G. Russ, J. Bennink, J. Yewdell, H. Ploegh, and D. Johnson.** 1995. Herpes simplex virus turns off the TAP to evade host immunity. Nature **375:**411-415.

127. **Hill, T. M., R. R. Sinden, and J. R. Sadler.** 1983. Herpes simplex virus types 1 and 2 induce shutoff of host protein synthesis by different mechanisms in Friend erythroleukemia cells. J Virol **45:**241-50.

128. **Hobbs, W. E., 2nd, and N. A. DeLuca.** 1999. Perturbation of cell cycle progression and cellular gene expression as a function of herpes simplex virus ICP0. J Virol **73:**8245-55.

129. **Holloway, A. J., R. K. van Laar, R. W. Tothill, and D. D. L. Bowtell.** 2002. Options available-from start to finish-for obtaining data from DNA microarrays II. Nature Genetics **32:**481-489.

130. **Honess, R. W., and B. Roizman.** 1973. Proteins specified by herpes simplex virus. XI. Identification and relative molar rates of synthesis of structural and nonstructural herpesvirus polypeptides in infected cells. J. Virol. **12:**1346-1365.

131. **Hynes, R. O.** 1990. Fibronectins, 1st ed, vol. 1. Springer-Verlag, New York, New York.

132. **Ingemarson, R., and H. Lankinen.** 1987. The herpes simplex virus type 1 ribonucleotide reductase is a tight complex of the type alpha 2 beta 2 composed of 40K and 140K proteins, of which the latter shows multiple forms due to proteolysis. Virology **156:**417-422.

133. **Inglis, S. C.** 1982. Inhibition of host protein synthesis and degradation of cellular mRNAs during infection by influenza and herpes simplex virus. Molecular and Cellular Biology **2:**1644-1648.

134. **Ishov, A. M., and G. G. Maul.** 1996. The periphery of nuclear domain 10 (ND10) as site of DNA virus deposition. Journal of Cell Biology **134**.

135. **Jackson, M. A., and J. F. Sommerauer.** 2002. Human herpesviruses 6 and 7. Pediatric Infectious Journal **21:**565-566.

136. **Jackson, S. A., and N. A. DeLuca.** 2003. Relationship of herpes simplex virus genome configuration to productive and persistent infections. PNAS **100:**7871-7876.

137. **Jang, K. L., and D. S. Latchman.** 1989. HSV infection induces increased transcription of *Alu* repeated sequences by RNA polymerase III. FEBS Letters **258:**255-258.

138. **Jean, S., K. M. LeVan, B. Song, M. Levine, and D. M. Knipe.** 2001. Herpes simplex virus 1 ICP27 is required for transcription of two viral late (gamma 2) genes in infected cells. Virology **283:**273-284.

139. **Jelinek, W. R., T. P. Toomey, L. Leinwand, C. H. Duncan, P. A. Biro, P. V. Choudary, S. M. Weissman, C. M. Rubin, C. M. Houck, P. L. Deininger, and C. W. Schmid.** 1980. Ubiquitous, interspersed repeated sequences in mammalian genomes. Proceedings of the National Academy of Sciences USA **77:**1398-1402.

140. **Jenkins, F. T., and B. Roizman.** 1986. Herpes simplex virus 1 recombinants with noninverting genomes frozen in different isomeric arrangement are capable of independant replication. Journal of Virology **59:**494-499.

141. **Jenkins, H. L., and C. A. Spencer.** 2001. RNA polymerase II holoenzyme modifications accompany transcription reprogramming in herpes simplex virus type 1-infected cells. Journal of Virology **75:**9872-9884.

142. **Jenner, R. G., K. Maillard, N. Cattini, R. A. Weiss, C. Boshoff, R. Wooster, and P. Kellam.** 2003. Kaposi's sarcoma-associated herpesvirus-infected primary effusion lymphoma has a plasma cel gene expression profile. Proceedings of the National Academy of Sciences **100:**10399-10404.

143. **Jensen, H. L., and B. Norrild.** 2003. The morphogenesis of herpes simplex virus type 1 in infected parental mouse L fibroblasts and mutant gro29 cells. Apmis **111:**1037-52.

144. **Johnson, D. C., and M. T. Huber.** 2002. Directed egress of animal viruses promotes cell-to-cell spread. Journal of Virology **76:**1-8.

145. **Johnson, D. C., M. Webb, T. W. Wisner, and C. Brunetti.** 2001. Herpes Simplex Virus gE/gI Sorts Nascent Virions to Epithelial Cell Junctions, Promoting Virus Spread. Journal of Virology **75:**821-833.

146. **Jones, F. E., C. A. Smibert, and J. R. Smiley.** 1995. Mutational analysis of the herpes simplex virus virion host shutoff protein: evidence that vhs functions in the absence of other viral proteins. Journal of Virology **69:**4863-4871.

147. **Jones, J. O., and A. M. Arvin.** 2003. Microarray analysis of host cell gene transcription in response to varicella-zoster virus infection of human T cels and fibroblasts in vitro and SCIDhu skin xenografts in vivo. Journal of Virology **77:**1268-1280.

148. **Kemp, L. M., and D. S. Latchman.** 1988. Induction and repression of cellular gene transcription during herpes simplex virus infection are mediated by different viral immediate-early gene products. European Journal of Biochemistry **174:**443-449.

149. **Kenzelmann, M., and K. Muhlemann.** 2000. Transcriptome analysis of fibroblast cells imediate-early after human cytomegalovirus infection. Journal of Molecular Biology **304:**741-751.

150. **Kesson, A. M.** 2001. Management of neonatal herpes siimplex virus infection. Paediatric Drugs **3:**81-90.

151. **Khodarev, N. N., S. J. Advani, N. Gupta, B. Roizman, and R. R. Weichselbaum.** 1999. Accumulation of specific RNAs encoding transcripitonal factors and stress response proteins against a background of severe depletion of cellular RNAs in cells infected with herpes simplex virus 1. Proceedings of the National Academy of Sciences **96:**12062-12067.

152. **Kimberlin, D. W.** 2001. Advances in the treatment of neonatal herpes simplex infections. Reviews in Medical Virology **11:**157-163.

153. **King, M. W.** August 18th, 2003, posting date. Extracellular Matrix. [Online.]

154. **Klupp, B. G., W. Fuchs, H. Granzow, R. Nixdorf, and T. C. Mettenleiter.** 2002. Pseudorabies virus UL36 tegument protein physically interacts with the UL37 protein. Journal of Virology **76:**3065-3071.

155. **Klupp, B. G., H. Granzow, and T. C. Mettenleiter.** 2000. Primary envelopment of pseudorabies virus at the nuclear membrane requires the UL34 gene product. J Virol **74:**10063-73.

156. **Knez, J., P. T. Bilan, and J. P. Capone.** 2003. A single amino acid substitution in herpes simplex virus type 1 VP16 inhibits binding to the virion host shutoff protein and is incompatible with virus growth. Journal of Virology **77:**2892-2902.

157. **Koelle, D. M., and L. Corey.** 2003. Recent progress in herpes simplex virus immunobiology and vaccine research. Clinical Microbiology Reviews **16:**96-113.

158. **Koffa, M. D., J. B. Clements, E. Izaurralde, S. Wadd, S. A. Wilson, I. W. Mattaj, and S. Kuersten.** 2001. Herpes simplex virus ICP27 protein provides viral mRNAs with access to the cellular mRNA export pathway. The EMBO Journal **20:**5769-5778.

159. **Kotsakis, A., L. E. Pomeranz, A. Blouin, and J. A. Blaho.** 2001. Microtubule reorganization during herpes simplex virus type 1 infection facilitates the nuclear localization of VP22, a major virion tegument protein. Journal of Virology **75:**8697-8711.

160. **Kramer, M. F., W. J. Cook, F. P. Roth, J. Zhu, H. Holman, D. M. Knipe, and D. M. Coen.** 2003. Latent herpes simplex virus infection of sensory neurons alters neuronal gene expression. Journal of Virology **77:**9533-9541.

161. **Krikorian, C. R., and G. S. Read.** 1991. In vitro mRNA degradation system to study the virion host shutoff function of herpes simplex virus. Journal of Virology **65::**112-122.

162. **Kroll, T. C., and S. Wolfl.** 2002. Ranking: a closer look on globalisation methods for normalisation of gene expression arrays. Nucleic Acids Research **30:**e50.

163. **Kwong, A. D., and N. Frenkel.** 1987. Herpes simplex virus-infected cells contain a function(s) that destabilizes both host and viral mRNAs. Proc. Natl. Acad. Sci. USA **84:**1926-1930.

164. **Kwong, A. D., J. A. Kruper, and N. Frenkel.** 1988. Herpes simplex virus virion host shutoff function. Journal of Virology **62:**912-921.

165. **Lam, Q., C. A. Smibert, K. E. Koop, C. Lavery, J. P. Capone, S. P. Weinheimer, and J. R. Smiley.** 1996. Herpes simplex virus VP16 rescues viral mRNAs from destruction by the virion host shutoff function. EMBO J. **15:**2575-2581.

166. **Lamberti, C., and S. Weller, K.** 1996. The herpes simplex virus type 1 UL6 protein is essential for cleavage and packaging but not for genomic inversion. Virology **226:**403-407.

167. **Lamberti, C., and S. K. Weller.** 1998. The herpes simplex virus type 1 cleavage/packaging protein, UL32, is involved in efficient localization of capsids to replication compartments. J Virol **72:**2463-73.

168. **Laurent, A. M., J. J. Madjar, and A. Greco.** 1998. Translational control of viral and host protein synthesis during the course of herpes simplex virus type 1 infection: evidence that initiation of translation is the limiting step. J Gen Virol **79:**2765-75.

169. **Lee, P. D., R. Sladek, C. M. Greenwood, and T. J. Hudson.** 2002. Control genes and variability: absence of ubiquitous reference transcripts in diverse mammalian expression studies. Genome Res **12:**292-7.

170. **Lee, S. S., and I. R. Lehman.** 1999. The interaction of herpes simplex type 1 virus origin-binding protein (UL9 protein) with Box I, the high affinity element of the viral origin of DNA replication. J Biol Chem **274:**19613-18617.

171. **Lehman, I. R., and P. E. Boehmer.** 1999. Replication of herpes simplex virus DNA. The Journal of Biological Chemistry **274:**28059-28062.

172. **Lemaster, S., and B. Roizman.** 1980. Herpes simplex virus phosphoproteins. II. Characterization of the virion protein kinase and of the polypeptides phosphorylated in the virion. Journal of Virology **35:**798-811.

173. **Lengyel, J., C. Guy, V. Leong, S. Borge, S. A. Rice, and I. H. Chen.** 2002. Mapping of functional regions in the amino-terminal portion of the herpes simplex virus ICP27 regulatory protein: importance of the leucine-rich nuclear export signal and RGG Box RNA-binding domain

ICP27 interacts with the RNA export factor Aly/REF to direct herpes simplex virus type 1 intronless mRNAs to the TAP export pathway. Journal of Virology **76:**11866-11879.

174. **Ligas, M. W., and D. C. Johnson.** 1988. A herpes simplex virus mutant in which glycoprotein D sequences are replaced by β-galactosidase sequences binds to but is unable to penetrate into cells. Journal of VIrology **62:**1486-1494.

175. **Lindberg, A., and J. P. Kreivi.** 2002. Splicing inhibition at the level of spliceosome assembly in the presence of herpes simplex virus protein ICP27. Virology **294:**189-198.

176. **Lindquist, J. N., W. F. Marzluff, and B. Stefanovic.** 2000. Fibrogenesis III. Posttranscriptional regulation of type I collagen. Am. J. Gastrointest. Liver Physiol. **279:**G471-G476.

177. **Ling, J., S. J. Morley, V. M. Pain, W. F. Marzluff, and D. R. Gallie.** 2002. The histone 3'-terminal stem-loop-binding protein enhances translation through a functional and physical interaction with eukaryotic initiation factor 4G (eIF4G) and eIF3. Molecular and Cellular Biology **22:**7853-7867.

178. **Lippelt, L., R. W. Braun, and J. E. Kuhn.** 2002. Genital herpes simplex virus type 1 infection: new fields for an old acquaintance? Intervirology **45:**2-5.

179. **Lomonte, P., and R. D. Everett.** 1999. Herpes simplex virus type 1 immediate-early protein Vmw110 inhibits progression of cells through mitosis and from G(1) into S phase of the cell cycle. J Virol **73:**9456-67.

180. **Long, M. C., V. Leong, P. A. Schaffer, C. A. Spencer, and S. A. Rice.** 1999. ICP22 and the UL13 protein kinase are both required for herpes simplex virus-induced modification of the large subunit of RNA polymerase II [In Process Citation]. J Virol **73:**5593-604.

181. **Lu, P., F. E. Jones, H. A. Saffran, and J. R. Smiley.** 2001. The Herpes Simplex Virus virion host shutoff protein requires a mammalian factor for efficient *in vitro* endoribonuclease activity. Journal of Virology **75:**1172-1185.

182. **Lu, P., H. A. Saffran, and J. R. Smiley.** 2001. The vhs1 mutant form of the Herpes Simplex Virus virion host shutoff protein retains significant internal ribosome entry site-directed RNA cleavage activity. J Virol. **75:**1072-6.

183. **Macsween, K. F., and D. Crawford.** 2003. Epstein-Barr virus-recent advences. The Lancet Infectious Diseases **3:**131-140.

184. **Makhov, A. M., P. E. Boehmer, I. R. Lehman, and J. D. Griffith.** 1996. Visualization of the unwinding of long DNA chains by the herpes simplex virus type 1 UL9 protein and ICP8. J Mol Biol **258:**789-799.

185. **Markert, J. M., M. D. Medlock, S. D. Rabkin, G. Y. Gillespie, T. Todo, W. D. Hunter, C. A. Palmer, F. Feigenbaum, C. Tornatore, F. Tufaro, and R. L. Martuza.** 2000. Conditionally replicating herpes simplex viurs mutant, G207 for the treatment of malignant gliomas:results of a phase I trial. Gene Therapy **7:**867-874.

186. **Martin, T. E., S. C. Barghusen, G. P. Leaser, and P. G. Spear.** 1987. Redistribution of nuclear ribonucleoprotein antigens during herpes simplex virus infection. Journal of Cell Biology **105:**2069-2082.

187. **Martinez, R., R. T. Sarisky, P. C. Weber, and S. K. Weller.** 1996. Herpes simplex virus type 1 alkaline nuclease is required for efficient processing of viral DNA replication intermediates. J Virol **70:**2075-85.

188. **Martuza, R. L., A. Malick, J. M. Markert, K. L. Ruffner, and D. M. Coen.** 1991. Experimental therapy of human glioma by means of a genetically engineered virus mutant. Science **252:**854-856.

189. **Masse, T., D. Garcin, B. Jacquemont, and J. J. Madjar.** 1990. Ribosome and protein synthesis modifications after infection of human epidermoid carcinoma cells with herpes simplex virus type 1. Molecular and General Genetics **220:**377-388.

190. **Matis, J., and M. Kudelova.** 2001. Early shutoff of host protein synthesis in cells infected with herpes simplex viruses. Acta Virologica **45:**269-277.

191. **Maul, G. G., H. H. Guldner, and J. G. Spivack.** 1993. Modification of discrete nuclear domains induced by herpes simplex virus type 1 immediate early gene 1 product (ICP0). J. Gen. Virol. **74:**2679-2690.

192. **Maul, G. G., A. M. Ishov, and R. D. Everett.** 1996. Nuclear domain 10 as preexisting potential replication start sites of herpes simplex virus type-1. Virology **217:**67-75.

193. **Mayman, B. A., and Y. Nishioka.** 1985. Differential stability of host mRNAs in friend erythroleukemia cells infected with herpes simplex virus type 1. Journal of Virology **53:**1-6.

194. **Mayne, M., C. Cheadle, S. S. Soldan, C. Cermelli, Y. Yamano, N. Akhyani, J. E. Nagel, D. D. Taub, K. G. Becker, and S. Jacobson.** 2001. Gene expression profile of herpesvirus-infected T cells obtained using immunomicroarrays: induction of proinflammatory mechanisms. Journal of Virology **75:**11641-11650.

195. **McCarthy, A. M., L. McMahan, and P. A. Schafer.** 1989. Herpes simplex virus type 1 ICP27 deletion mutants exhibit altered patterns of transcription and are DNA deficient. Journal of Virology **63:**18-27.

196. **McCormick, C., G. Duncan, T. Goutsos, and F. Tufaro.** 2000. The putative tumor suppressors EXT1 and EXT2 form a stable complex that accumulates in the Golgi apparatus and catalyzes the synthesis of heparan sulfate. Proceedings of the National Academy of Sciences **97:**668-673.

197. **McGeoch, D. J., M. A. Dalrymple, A. J. Davison, A. Dolan, M. C. Frame, D. McNab, L. J. Perry, J. E. Scott, and P. Taylor.** 1988. The complete sequence of the long unique region in the genome of herpes simplex virus type 1. J. Gen. Virol. **69.:**1531-1574.

198. **McGeoch, D. J., M. A. Dalrymple, A. Dolan, D. McNab, L. J. Perry, P. Taylor, and M. D. Challberg.** 1988. Structures of herpes simplex virus type 1 genes required for replication of virus DNA. Journal of Virology **62:**444-453.

199. **McGregor, F., A. Phelan, J. Dunlop, and J. B. Clements.** 1996. Regulation of herpes simplex virus poly(A) site usage and the action of immediate-early protein IE63 in the early-late switch. J. Virol. **70:**1931-1940.

200. **McLauchlan, J., A. Phelan, C. Loney, R. M. Sandri-Goldin, and J. B. Clements.** 1992. Herpes simplex virus IE63 acts at the posttranscriptional level to stimulate viral mRNA 3' processing. J. Virology **66:**6939-6945.

201. **McLauchlan, J., S. Simpson, and J. B. Clements.** 1989. Herpes simplex virus induces a processing factor that stimulates poly(A) site usage. Cell **59:**1093-1105.

202. **McMillan, T. N., and D. C. Johnson.** 2001. Cytoplasmic domain of herpes simplex virus gE causes accumulation in the trans-Golgi network, a site of virus envelopment and sorting of virions to cell junctions. J Virol **75:**1928-40.

203. **McNab, A. R., P. Desai, S. Person, L. L. Roof, D. R. Thomsen, W. W. Newcomb, J. C. Brown, and F. L. Homa.** 1998. The product of the herpes simplex virus type 1 UL25 gene is required for encapsidation but not for cleavage of replicated viral DNA. J Virol **72:**1060-70.

204. **McNabb, D. S., and R. J. Courtney.** 1992. Analysis of the UL36 open reading frame encoding the large tegument protein (ICP1/2) of herpes simplex virus type 1. J. Virol. **66:**7581-7584.

205. **McNabb, D. S., and R. J. Courtney.** 1992. Characterization of the large tegument protein (ICP1/2) of herpes simplex virus type 1. Virology **190:**221-232.

206. **Mears, W. E., and S. A. Rice.** 1998. The herpes simplex virus immediate-early protein ICP27 shuttles between nucleus and cytoplasm. Virology **242:**128-37.

207. **Mettenleiter, T. C.** 2002. Herpesvirus assembly and egress. Journal of Virology **76:**1537-1547.

208. **Michel, Y. M., D. Poncet, M. Piron, K. M. Kean, and A. M. Borman.** 2000. Cap-poly(A) synergy in mammalian cell-free extracts: Investigation of the requirements for poly (A)-mediated stimulation of translation initiation. Journal of Biological Chemistry **275:**32268-32276.

209. **Mineta, T., S. D. Rabkin, T. Yazaki, W. D. Hunter, and R. L. Martuza.** 1995. Attenuated multi-mutated herpes simplex virus-1 for the treatment of malignant gliomas. Nature Medicine **1:**938-943.

210. **Mitchell, C., J. A. Blaho, and B. Roizman.** 1994. Casein kinase II specifically nucleotidylylates in vitro the amino acid sequence of the protein encoded by the a22 gene of herpes simplex virus 1. Proceedings of the National Academy of Sciences **91:**11864-11868.

211. **Mohr, I., and Y. Gluzman.** 1996. A herpesvirus genetic element which affects translation in the absence of the viral GADD34 function. EMBO J **15:**4759-4766.

212. **Montgomery, R. I., M. S. Warner, B. J. Lum, and P. G. Spear.** 1996. Herpes simplex virus-1 entry into cells mediated by a novel member of the TNF/NGF receptor family. Cell **87:**427-436.

213. **Morfin, F., and D. Thouvenot.** 2003. Herpes simplex virus resistance to antiviral drugs. Journal of Clinical Virology **26:**29-37.

214. **Morrison, E. E., A. J. Stevenson, Y.-F. Wang, and D. M. Meredith.** 1998. Differences in the intracellular localization and fate of herpes simplex virus tegument proteins early in the infection of Vero cells. Journal of General Virology **79:**2517-2528.

215. **Morrison, E. E., Y.-F. Wang, and D. M. Meredith.** 1998. Phosphorylation of structural components promotes dissociation of the herpes simplex virus type 1 tegument. Journal of Virology **72:**7108-7114.

216. **Morse, L. S., L. Pereira, B. Roizman, and P. A. Schaffer.** 1978. Anatomy of HSV DNA. X. Mapping of viral genes by analysis of polypeptides and functions specified by HSV-1 x HSV-2 recombinants. J. Virol. **26:**389-410.

217. **Moses, A. V., M. A. Jarvis, C. Raggo, Y. C. Bell, R. Ruhl, B. G. Mattias Luukkonen, D. J. Griffith, C. L. Wait, B. J. Druker, M. C. Heinrich, J. A. Nelson, and K. Fruh.** 2002. A Functional Approach to Kaposi's Sarcoma. Annals of the New York Academy of Sciences **975:**180-191.

218. **Mossman, K. L., P. F. Macgregor, J. J. Rozmus, A. B. Goryachev, A. M. Edwards, and J. R. Smiley.** 2001. Herpes Simplex Virus Triggers and Then Disarms a Host Antiviral Response. Journal of Virology **75:**750-758.

219. **Mossman, K. L., R. Sherburne, C. Lavery, J. Duncan, and J. R. Smiley.** 2000. Evidence that herpes simplex virus VP16 is required for viral egress downstream of the initial envelopment event. Journal of Virology **74:**6287-6299.

220. **Mossman, K. L., and J. R. Smiley.** 2002. Herpes simplex virus ICP0 and ICP34.5 counteract distinct interferon-induced barriers to virus replication. Journal of Virology **76:**1995-1998.

221. **Mulvey, M., J. Poppers, A. Ladd, and I. Mohr.** 1999. A herpesvirus ribosome-associated, RNA-binding protein confers a growth advantage upon mutants deficient in a GADD34-related function. 73 **4.**

222. **Nakai, H., I. H. Maxwell, and L. I. Pizer.** 1982. Herpesvirus infection alters the steady-state levels of cellular polyadenylated RNA in polyoma virus-transformed BHK cells. Journal of Virology **42:**1131-1134.

223. **Newcomb, W. W., R. Juhas, D. R. Thomsen, F. Homa, L., A. D. Burch, S. K. Weller, and J. C. Brown.** 2001. The UL6 gene product forms the portal of entry of DNA into the herpes simplex virus capsid. Journal of Virology **75:**10923-10932.

224. **Newcomb, W. W., B. L. Trus, F. P. Booy, A. C. Steven, J. S. Wall, and J. C. Brown.** 1993. Structure of the herpes simplex virus capsid. Molecular composition of the pentons and the triplexes. J Mol Biol **232:**499-511.

225. **Ng, T. I., Y. E. Chang, and B. Roizman.** 1997. Infected cell protein 22 of herpes simplex virus 1 regulates the expression of virion host shutoff gene U(L)41. Virology **234:**226-34.

226. **Nishioka, Y., and S. Silverstein.** 1977. Degradation of cellular mRNA during infection by herpes simplex virus. Proc. Natl. Acad. Sci. USA **74:**2370-2374.

227. **Nishioka, Y., and S. Silverstein.** 1978. Requirement of protein synthesis for the degradation of host mRNA in Friend erythroleukemia cells infected with HSV-2. J. Virol. **27:**619-627.

228. **Oemar, B. S., and T. F. Luscher.** 1997. Connective Tissue Growth Factor Friend or Foe? Arteriosclerosis, Thrombosis, and Vascular Biology **17:**1483-1489.

229. **Ogle, W. O., and B. Roizman.** 1996. Functional anatomy of herpes simplex virus 1 overlapping genes encoding infected-cell protein 22 and US1.5 protein. Journal of Virology **70:**172-178.

230. **O'Hare, P., and G. S. Hayward.** 1985. Three trans-acting regulatory proteins of herpes simplex virus modulate immediate-early gene expression in a pathway involving positive and negative feedback regulation. J. Virol. **56:**723-733.

231. **Ojala, P. M., B. Sodeik, M. W. Ebersold, U. Kutay, and A. Helenius.** 2000. Herpes simplex virus type 1 entry into host cells: reconstitution of capsid binding and uncoating at the nuclear pore. Molecular and Cellular Biology **20:**4922-4931.

232. **Olivo, P. D., N. J. Nelson, and M. D. Challberg.** 1988. Herpes simplex virus DNA replication: the UL9 gene encodes an origin-binding protein. Proc Natl Acad Sci U S A **85:**5414-5418.

233. **Oroskar, A. A., and G. S. Read.** 1989. Control of mRNA stability by the virion host shutoff function of herpes simplex virus. Journal of Virology **63:**1897-1906.

234. **Oroskar, A. A., and G. S. Read.** 1987. A mutant of herpes simplex virus type 1 exhibits increased stability of immediate-early (alpha) mRNAs. J. Virol. **61:**604-606.

235. **Overton, H., D. McMillan, L. Hope, and P. Wong-Kai-In.** 1994. Production of host shutoff-defective mutants of herpes simplex virus type 1 by inactivation of the UL13 gene. Virology **202:**97-106.

236. **Panning, B., and J. R. Smiley.** 1995. Activation of expression of multiple subfamilies of human Alu elements by adenovirus type 5 and herpes simplex virus type 1. J. Mol. Biol. **248:**513-524.

237. **Panning, B., and J. R. Smiley.** 1994. Activation of RNA plolymerase III transcription of endogenous cellular Alu elements by herpes simplex virus type 1. Virology **202:**408-417.

238. **Panning, B., and J. R. Smiley.** 1993. Activation of RNA polymerase III transcription of human Alu repetitive elements by adenovirus type 5: requirement for E1B 58-kilodalton protein and the products of E4 open reading frames 3 and 6. Molecular Cellular Biology **13:**3231-3244.

239. **Papavassiliou, A. G., K. W. Wilcox, and S. J. Silverstein.** 1991. The interaction of ICP4 with cell/infected-cell factors and its state of phosphorylation modulate differential recognition of leader sequences in herpes simplex virus DNA. EMBO J. **10:**397-406.

240. **Phelan, A., M. Carmo-Fonseca, J. McLauchlan, A. I. Lamond, and J. B. Clements.** 1993. A herpes simplex virus type-1 immediate early gene product IE63 regulates small ribonucleoprotein distribution. Proc. Natl. Acad. Sci. USA **90:**9056-9060.

241. **Phelan, A., and J. B. Clements.** 1997. Herpes simplex virus type 1 immediate early protein IE63 shuttles between nuclear compartments and the cytoplasm. J. Gen. Virol. **78:**3327-3331.

242. **Piez, K. A., and A. H. Reddi (ed.).** 1984. Extracellular Matrix Biochemistry, 1st ed, vol. 1. Elsevier Science Publishing Co., Inc., New York, New York.

243. **Poffenberger, K. L., and B. Roizman.** 1985. A noninverting genome of a viable herpes simplex virus 1: presence of head-to-tail linkages in packaged genomes and requirements for circularization after infection. J Virol **53:**587-95.

244. **Poffenberger, K. L., E. Tabares, and B. Roizman.** 1983. Characterization of a viable, noninverting herpes simplex virus 1 genome derived by insertion and deletion of sequences at the junction of components L and S. Proceedings of the National Academy of Science **80:**2690-2694.

245. **Pomeranz, L. E., and J. A. Blaho.** 2000. Assembly of infectious Herpes simplex virus type 1 virions in the absence of full-length VP22. Journal of Virology **74:**10041-54.

246. **Pomeranz, L. E., and J. A. Blaho.** 1999. Modified VP22 localizes to the cell nucleus during synchronized herpes simplex virus type 1 infection. Journal of Virology **73:**6769-6781.

247. **Poppers, J., M. Mulvey, C. Perez, D. Khoo, and I. Mohr.** 2003. Identification of a lytic-cycle Epstein-Barr virus gene product that can regulate PKR activation. Journal of Virology **77:**228-236.

248. **Powell, K. L., and R. J. Courtney.** 1975. Polypeptide synthesized in herpes simplex virus type 2-infected HEp-2 cells. Virology **66:**217-28.

249. **Preston, C. M., and A. A. Newton.** 1976. The effects of herpes simplex virus type 1 on cellular DNA-dependant RNA polymerase activities. Journal of General Virology **33:**471-482.

250. **Preston, V. G., J. A. V. Coates, and F. J. Rixon.** 1983. Identification and characterization of a herpes simplex virus gene product required for encapasidation of virus DNA. Journal of Virology **45:**1056-1064.

251. **Prod'hon, C., I. Machuca, H. Berthomme, A. Epstein, and B. Jacquemont.** 1996. Characterization of regulatory functions of the HSV-1 immediately-early protein ICP22. Virology **226:**393-402.

252. **Purves, F. C., W. O. Ogle, and B. Roizman.** 1993. Processing of the herpes simplex virus regulatory protein α22 mediated by the UL13 protein kinase determines the accumulation of a subset of α and γ mRNAs and proteins in infected cells. Proc. Natl. Sci. USA **90:**6701-6705.

253. **Purves, F. C., and B. Roizman.** 1992. The U_L13 gene of herpes simplex virus 1 encodes the functions for posttranslational processing associated with phosphorylation of the regulatory protein α22. Proc. Natl. Acad. Sci. USA **89:**7310-7314.

254. **Quackenbush, J.** 2002. Microarray data normalization and transformation. Nature Genetics **32:**496-501.

255. **Read, G. S., and N. Frenkel.** 1983. Herpes simplex virus mutants defective in the virion-associated shutoff of host polypeptides synthesis and exhibiting abnormal synthesis of α (immediate-early) viral polypeptides. J. Virol. **46:**498-512.

256. **Read, G. S., B. M. Karr, and K. Knight.** 1993. Isolation of a herpes simplex virus type 1 mutant with a deletion in the virion host shutoff gene and identification of multiple forms of the *vhs* (UL41) polypeptide. J. Virol. **67:**7149-7160.

257. **Revello, M. G., and G. Gerna.** 2002. Diagnosis and management of human cytomegalovirus infection in the mother, fetus, and newborn infant. Clinical Microbiology Reviews **15:**680-715.

258. **Reynolds, A. E., B. J. Ryckman, J. D. Baines, Y. Zhou, L. Liang, and R. J. Roller.** 2001. U(L)31 and U(L)34 proteins of herpes simplex virus type 1 form a complex that accumulates at the nuclear rim and is required for envelopment of nucleocapsids. J Virol **75:**8803-17.

259. **Rice, S. A., and D. M. Knipe.** 1990. Genetic evidence for two distinct trans-activation functions of the herpes simplex virus α protein ICP27. J. Virol. **64:**1704-1715.

260. **Rice, S. A., M. C. Long, V. Lam, P. A. Schaffer, and C. A. Spencer.** 1995. Herpes simplex virus immediate-early protein ICP22 is required for viral modification of host RNA polymerase II and establishment of the normal viral transcriptional program. J. Virol. **69:**5550-5559.

261. **Rice, S. A., M. C. Long, V. Lam, and C. A. Spencer.** 1994. RNA polymerase II is aberrantly phosphorylated and localized to viral replication compartments following herpes simplex virus infection. J. Virol. **68:**988-1001.

262. **Rice, S. A., L. Su, and D. M. Knipe.** 1989. Herpes simplex virus alpha protein ICP27 possesses separable positive and negative regulatory activities. Journal of Virology **63:**3399-3407.

263. **Rixon, F. J.** 1993. Structure and assembly of herpesviruses. Semin. Virol. **4.**

264. **Rixon, F. J., C. Addison, and J. McLauchlan.** 1992. Assembly of enveloped tegument structures (L particles) can occur independently of virion maturation in herpes simplex virus type 1-infected cells. J Gen Virol **73 (Pt 2):**277-84.

265. **Rixon, F. J., A. M. Cross, C. Addison, and V. G. Preston.** 1988. The products of herpes simplex virus type 1 gene UL26 which are involved in DNA packaging are strongly associated with empty but not with full capsids. J Gen Virol **69 (Pt 11):**2879-91.

266. **Roberts, M. S., A. Boundy, P. O'Hare, M. C. Pizzorno, D. M. Ciufo, and G. S. Hayward.** 1988. Direct correlation between a negative autoregulatory response element

at the cap site of the herpes simplex virus type 1 IE175 (α4) promoter and a specific binding site for the IE175 (ICP4) protein. J. Virol. **62:**4307-4320.

267. **Roizman, B., and D. Furlong.** 1974. The replication of herpesviruses. *In* H. Fraenkel-Conrat and R. R. Wagner (ed.), Comprehensive Virology, vol. 3. Plenum Press, New York.

268. **Roizman, B., and D. M. Knipe.** 2001. Herpes simplex viruses and their replication, p. 1123-1183. *In* B. N. Fields, D. M. Knipe, P. M. Howley, and e. al. (ed.), Fundamental Virology. Lippincott-Ravan, Philadelphia.

269. **Roizman, B., and P. E. Pellett.** 2001. The Family Herpesviridae: A Brief Introduction, p. 2381-2397. *In* D. M. Knipe, P. M. Howley, D. E. Griffin, R. A. Lamb, M. A. Martin, B. Roizman, and S. E. Straus (ed.), Fields Virology, 4th edition ed, vol. 2. Lippincott Williams & Wilkins, Philadelphia.

270. **Roller, R. J., Y. Zhou, R. Schnetzer, J. Ferguson, and D. DeSalvo.** 2000. Herpes simplex virus type 1 U(L)34 gene product is required for viral envelopment. J Virol **74:**117-29.

271. **Rowold, D. J., and R. J. Herrera.** 2000. Alu elements and the human genome. Genetica **108:**57-72.

272. **Rubin, C. M., C. M. Houck, P. L. Deininger, T. Friedmann, and C. W. Schmid.** 1980. Partial nucleotide sequence of the 300-nucleotide interspersed repeated human DNA sequences. Nature **284:**372-374.

273. **Ruyechan, W. T., and A. C. Weir.** 1984. Interaction with nucleic acids and stimulation of the viral DNA polymerase by the herpes simplex virus type 1 major DNA-binding protein. Journal of Virology **52:**727-733.

274. **Sacks, W. R., C. C. Greene, D. P. Aschman, and P. A. Schaffer.** 1985. Herpes simplex virus type 1 ICP27 is an essential regulatory protein. J. Virol. **55:**796-805.

275. **Sacks, W. R., and P. A. Schaffer.** 1987. Deletion mutants in the gene encoding the herpes simplex virus type 1 immediate-early protein ICPO exhibit impaired growth in cell culture. J. Virol. **61:**829-839.

276. **Samady, L., E. Costigliola, L. MacCormac, Y. McGrath, S. Cleverley, C. E. Lilley, J. Smith, D. S. Latchman, B. Chain, and R. S. Coffin.** 2003. Deletion of the virion host shutoff protein (vhs) relieves the viral block to dendritic cell activation: potential of vhs- HSV vectors for dendritic cell-mediated immunotherapy. Journal of Virology **77:**3768-3776.

277. **Sambrook, J., E. F. Fritsch, and T. Maniatis.** 1989. Molecular Cloning, a Laboratory Manual, 2nd ed. Cold Spring Harbour Laboratory Press, New York.

278. **Sandri-Goldin, R. M.** 1998. ICP27 mediates HSV RNA export by shuttling through a leucine-rich nuclear export signal and binding viral intronless RNAs through an RGG motif. Genes Dev. **12:**868-879.

279. **Sandri-Goldin, R. M.** 1998. Interactions between a herpes simplex virus regulatory protein and cellular mRNA processing pathways. Methods **16:**95-104.

280. **Sandri-Goldin, R. M.** 2003. Replication of the herpes simplex virus genome: Does it really go in circles? PNAS **100:**7428-7429.

281. **Sandri-Goldin, R. M., and M. K. Hibbard.** 1996. The herpes simplex virus type 1 regulatory protein ICP27 coimmunoprecipitates with anti-sm antiserum, and the C terminus appears to be required for this interaction. J. Virol. **70:**108-118.

282. **Sandri-Goldin, R. M., and G. E. Mendoza.** 1992. A herpesvirus regulatory protein appears to act post-transcriptionally by affecting mRNA processing. Genes Dev. **6:**848-863.

283. **Schek, N., and S. L. Bachenheimer.** 1985. Degradation of cellular mRNAs induced by a virion-associated factor during herpes simplex virus infection of vero cells. Journal of Virology **55:**601-610.

284. **Schena, M., D. Shalon, R. Heller, A. Chai, P. O. Brown, and R. W. Davis.** 1996. Parallel human genome analysis: microarray-based expression monitoring of 1000 genes. Proc Natl Acad Sci U S A **93:**10614-9.

285. **Schmader, K.** 2001. Herpes zoster in older adults. Clinical Infectious Diseases **32:**1481-1486.

286. **Schmelter, J., J. Knez, J. R. Smiley, and J. P. Capone.** 1996. Identification and characterization of a small modular domain in the herpes simplex virus host shutoff protein sufficient for interaction with VP16. J. Virol. **70:**2124-2131.

287. **Schulz, T. F., J. Sheldon, and J. Greensill.** 2002. Kaposi's sarcoma associated herpesvirus (KSHV) or human herpesvirus 8 (HHV-8). Virus Research **82:**115-126.

288. **Sears, A. E., I. W. Halliburton, B. Meignier, S. Silver, and B. Roizman.** 1985. Herpes simplex virus 1 mutant deleted in the alpha-22 gene: growth and gene expression in permissive and restrictive cells and establishment of latency in mice. Journal of Virology **55:**338-346.

289. **Shah, A. C., D. Benos, G. Y. Gillespie, and J. Markert, M.** 2003. Oncolytic viruses: clinical applications as vectors for the treatment of malignant gliomas. Journal of Neuro-Oncology **65:**203-226.

290. **Shao, L., L. M. Rapp, and S. K. Weller.** 1993. Herpes simplex virus 1 alkaline nuclease is required for efficient egress of capsids from the nucleus. Virology **196:**146-62.

291. **Sheffield, J. S., L. M. Hollier, J. B. Hill, G. S. Stuart, and G. D. Wendel.** 2003. Acyclovir prophylaxis to prevent herpes simplex virus recurrence at delivery: a systematic review. Obstetrics & Gynecology **102:**1396-1403.

292. **Sherman, G., and S. L. Bachenheimer.** 1988. Characterization of intranuclear capsids made by ts morphogenic mutants of HSV-1. Virology **163:**471-80.

293. **Shieh, M.-T., D. WuDunn, R. I. Montgomery, J. D. Esko, and P. G. Spear.** 1992. Cell surface receptors for herpes simplex virus are heparan sulfate proteoglycans. J. Cell Biol. **116:**1273-1281.

294. **Shivak, D. A.** 1998. Characterization of factors affecting the virion host shutoff function of herpes simplex virus. M. Sc. McMaster University, Hamilton.

295. **Shi-wen, X., D. Pennington, A. Holmes, A. Leask, D. Bradham, J. R. Beauchamp, S. C. Fonseca, R. M. du Bois, G. R. Martin, C. M. Black, and D. J. Abraham.** 2000. Autocrine overexpression of CTGF maintains fibrosis: RDA analysis of fibrosis genes in systemic sclerosis. Experimental Cell Research **259:**213-224.

296. **Shukla, D., J. Liu, P. Blaiklock, N. W. Shworak, X. Bai, J. D. Esko, G. H. Cohen, R. J. Eisenberg, R. D. Rosenberg, and P. G. Spear.** 1999. A novel role for 3-O-sulfated heparan sulfate in herpes simplex virus 1 entry. Cell **99:**13-22.

297. **Shukla, D., and P. G. Spear.** 2001. Herpesviruses and heparan sulfate: an intimate relationship in aid of viral entry. The Journal of Clinical Investigation **108:**503-510.

298. **Siminoff, P., and M. G. Menefee.** 1966. Normal and 5-bromodeoxyuridine-inhibited development of herpes simplex virus. An electron microscope study. Exp Cell Res **44:**241-55.

299. **Skaliter, R., A. M. Makhov, J. D. Griffith, and I. R. Lehman.** 1996. Rolling circle DNA replication by extracts of herpes simplex virus type 1-infected human cells. Journal of Virology **70:**1132-1136.

300. **Skepper, J. N., A. Whiteley, H. Browne, and A. Minson.** 2001. Herpes simplex virus nucleocapsids mature to progeny virions by an envelopment-deenvelopment-reenvelopment pathway. Journal of Virology **75:**5697-5702.

301. **Slonim, D. K.** 2002. From patterns to pathways: gene expression data analysis comes of age. Nature Genetics **32:**502-508.

302. **Smibert, C. A., D. C. Johnson, and J. R. Smiley.** 1992. Identification and characterization of the virion-induced host shutoff product of herpes simplex virus gene UL41. Journal of General Virology **73:**467-470.

303. **Smibert, C. A., B. Popova, P. Xiao, J. P. Capone, and J. R. Smiley.** 1994. Herpes simplex virus VP16 forms a complex with the virion host shutoff protein vhs. Journal of Virology **68:**2339-2346.

304. **Smibert, C. A., and J. R. Smiley.** 1990. Differential regulation of endogenous and transduced beta-globin genes during infection of erythroid cells with a herpes simplex virus type 1 recombinant. J Virol **64:**3882-94.

305. **Smiley, J. R.** 2004. Herpes simplex virus virion host shutoff protein: Immune evasion mediated by a viral RNase? Journal of Virology **78:**1063-1068.

306. **Smiley, J. R., and J. Duncan.** 1997. Truncation of the C-terminal acidic transcriptional activation domain of herpes simplex virus VP16 produces a phenotype similar to that of the in1814 linker insertion mutation. J Virol **71:**6191-3.

307. **Smiley, J. R., M. M. Elgadi, and H. A. Saffran.** 2001. Herpes simplex virus vhs protein. Methods in Enzymology **42:**440-451.

308. **Smith, J. S., and N. J. Robinson.** 2002. Age-specific prevalence of infection with herpes simplex virus types 2 and 1: A global review. The Journal of Infectious Diseases **186:**S3-S28.

309. **Sodeik, B., M. W. Ebersold, and A. Helenius.** 1997. Microtuble-mediated transport of incoming herpes simplex virus 1 capsids to the nucleus. J. Cell Biol. **136:**1007-1021.

310. **Soliman, T. M., R. M. Sandri-Goldin, and S. J. Silverstein.** 1997. Shuttling of the herpes simplex virus type 1 regulatory protein ICP27 between the nucleus and cytoplasm mediates the expression of late proteins. J. Virol. **71:**9188-9197.

311. **Song, B., K. C. Yeh, J. Liu, and D. M. Knipe.** 2001. Herpes simplex virus gene products required for viral inhibition of expression of G1-phase functions. Virology **290:**320-8.

312. **Sottile, J., and D. Hocking.** 2002. Fibronectin Polymerization Regulates the Composition and Stability of Extracellular Matrix Fibrils and Cell-Matrix Adhesions. Molecular Biology of the Cell **13:**3546-3559.

313. **Sourvinos, G., and R. D. Everett.** 2002. Visualization of parental HSV-1 genomes and replication compartments in association with ND10 in live infected cells. The EMBO Journal **21:**4989-4997.

314. **Spear, P. G.** 1993. Entry of alphaherpesviruses into cells. Semin. Virol. **4:**167-180.

315. **Spector, D., F. Purves, and B. Roizman.** 1991. Role of α-traninducing factor (VP16) in the induction of α genes within the context of viral genomes. J. Virol. **65:**3504-3513.

316. **Spencer, C. A., M. E. Dahmus, and S. A. Rice.** 1997. Repression of host RNA polymerase II transcription by herpes simplex virus type 1. J. Virol. **71:**2031-2040.

317. **Spencer, J. V., W. W. Newcomb, D. R. Thomsen, F. L. Homa, and J. C. Brown.** 1998. Assembly of the herpes simplex virus capsid: preformed triplexes bind to the nascent capsid. J Virol **72:**3944-51.

318. **Stagno, S.** 2001. Cytomegalovirus, p. 389-424. *In* J. S. Remington and K. O. Klein (ed.), Infectious diseases and the newborn infant. Saunders Co., Philadelphia, Pa.

319. **Stannard, L. M., A. O. Fuller, and P. G. Spear.** 1987. Herpes simplex virus glycoproteins associated with different morphological entities projecting from the virion envelope. J Gen Virol **68 (Pt 3):**715-25.

320. **Stannard, L. M., S. Himmelhoch, and S. Wynchank.** 1996. Intra-nuclear localization of two envelope proteins, gB and gD, of herpes simplex virus. Arch Virol **141:**505-24.

321. **Stefanovic, B., C. Hellerbrand, and D. A. Brenner.** 1999. Regulatory role of the conserved stem-loop structure t the 5'end of collagen alpha 1 (I) mRNA. Molecular and Cellular Biology **19:**4334-4342.

322. **Stefanovic, B., C. Hellerbrand, M. Holcik, M. Briendl, L. S. A., and D. A. Brenner.** 1997. Postranscriptional regulation of collagen alpha 1 (I) mRNA in hepatic stellate cells. Molecular and Cellular Biology **17:**5201-5209.

323. **Steven, A. C., and P. G. Spear.** 1997. Herpvesvirus capsid assembly and envelopment, p. 312-351. *In* W. Chiu, R. M. Burnett, and R. Garcea (ed.), Structural biology of viruses. Oxford University Press, New York, New York.

324. **Steven, A. C., B. L. Trus, F. P. Booy, N. Cheng, A. Zlotnick, J. R. Caston, and J. F. Conway.** 1997. The making and breaking of symmetry in virus capsid assembly: glimpses of capsid biology from cryoelectron microscopy. FASEB J **11:**733-742.

325. **Stingley, S. W., J. J. Garcia Ramirez, S. A. Aguilar, K. Simmen, R. M. Sandri-Goldin, P. Ghazal, and E. K. Wagner.** 2000. Global analysis of Herpes Simplex Virus Type 1 Transcription Using an Oligonucleotide-Based DNA Microarray. Journal of Virology **74:**9916-9927.

326. **Stow, N. D.** 2001. Packaging of genomic and amplicon DNA by the herpes simplex virus type 1 UL25-null mutant KUL25NS. J Virol **75:**10755-65.

327. **Stow, N. D., and E. C. Stow.** 1986. Isolation and characterization of a herpes simplex virus type 1 mutant containing a deletion within the gene encoding the immediate-early polypeptide Vmw110. J. Gen. Virol. **67:**2571-2585.

328. **Strelow, L., T. Smith, and D. Leib.** 1997. The virion host shutoff function of herpes simplex virus type 1 plays a role in corneal invasion and functions independently of the cell cycle. Virology **231:**28-34.

329. **Strelow, L. I., and D. A. Leib.** 1995. Role of the virion host shutoff (vhs) of herpes simplex virus type 1 in latency and pathogenesis. J. Virol. **69:**6779-6786.

330. **Strom, T., and N. Frenkel.** 1987. Effects of herpes simplex virus on mRNA stability. J. Virol. **61:**2198-2207.

331. **Suzutani, T., M. Nagamine, T. Shibaki, M. Ogasawara, I. Yoshida, T. Daikoku, Y. Nishiyama, and M. Azuma.** 2000. The role of the UL41 gene of herpes simplex virus type 1 in evasion of non-specific host defence mechanisms during primary infection. Journal of General Virology **81:**1763-1771.

332. **Sydiskis, R. J., and B. Roizman.** 1967. The disaggregation of host polyribosomes in productive and abortive infection with herpes simplex virus. Virology **32:**678-686.

333. **Sydiskis, R. J., and B. Roizman.** 1966. Polysomes and protein synthesis in cells infected with a DNA virus. Science **153:**76-78.

334. **Taddeo, B., A. Esclatine, and B. Roizman.** 2002. The patterns of accumulation of cellular RNAs in cells infected with a wild-type and a mutant herpes simplex virus 1 lacking the virion host shutoff gene. Proceedings of the National Academy of Sciences **99:**17031-17036.

335. **Tang, Q., L. Li, A. M. Ishov, V. Revol, A. L. Epstein, and G. G. Maul.** 2003. Detmination of minimum herpes simplex virus type 1 components necessary to localize transcriptionally active DNA to ND10. Journal of Virology **77:**5821-5828.

336. **Taylor, G. H.** 2003. Cytomegalovirus. American Family Physician **67:**519-524.

337. **Tengelsen, L. A., N. E. Pederson, P. R. Shaver, M. W. Wathen, and F. L. Homa.** 1993. Herpes simplex virus type 1 DNA cleavage and encapsidation require the product of the UL28 gene: isolation and characterization of two UL28 deletion mutants. Journal of Virology **67:**3470-3480.

338. **Tigges, M. A., S. Leng, D. C. Johnson, and R. L. Burke.** 1996. Human herpes simplex virus (HSV)-specific CD8+ CTL clones recognize HSV- 2-infected fibroblasts after treatment with IFN-gamma or when virion host shutoff functions are disabled. J Immunol **156:**3901-10.

339. **Trgovcich, J., D. Johnson, and B. Roizman.** 2002. Cell surface major histocompatibility complex class II proteins are regulated by the products of the gamma 34.5 and UL41 genes of herpes simplex virus 1. Journal of Virology **76:**6974-6986.

340. **Trus, B. L., F. P. Booy, W. W. Newcomb, J. C. Brown, F. L. Homa, D. R. Thomsen, and A. C. Steven.** 1996. The herpes simplex virus procapsid: Structure, conformational changes upon maturation, and roles of the triplex proteins VP19c and VP23 in assembly. J. Mol. Biol. **263:**447-462.

341. **Trus, B. L., F. L. Homa, F. P. Booy, W. W. Newcomb, D. R. Thomsen, N. Cheng, J. C. Brown, and A. C. Steven.** 1995. Herpes simplex virus capsids assembled in insect cells infected with recombinant baculoviruses: structural authenticity and localization of VP26. J Virol **69:**7362-6.

342. **Turner, A., B. Bruun, T. Minson, and H. Browne.** 1998. Glycoproteins gB, gD and gHgL of herpes simplex virus type 1 are necessary and sufficient to mediate membrane fusion in a Cos cell transfections system. Journal of Virology **72:**873-875.

343. **Uprichard, S. L., and D. M. Knipe.** 1996. Herpes simplex ICP27 mutant viruses exhibit reduced expression of specific DNA replication genes. J. Virol. **70:**1969-1980.

344. **van Genderen, I. L., R. Brandimarti, M. R. Torrisi, G. Campadelli, and G. van Meer.** 1994. The phospholipid composition of extracellular herpes simplex virions differs from that of host cell nuclei. Virology **200:**831-6.

345. **van Leeuwen, H., M. Okuwaki, R. Hong, D. Chakravarti, K. Nagata, and P. O'Hare.** 2003. Herpes simplex virus type 1 tegument protein VP22 interacts with TAF-I proteins and inhibits nucleosome assembly but not regulation of histone acetylation by INHAT. Journal of General Virology **84:**2501-2510.

346. **Vaughan, P. J., D. J. Purifoy, and K. L. Powell.** 1985. DNA-binding protein associated with herpes simplex virus DNA polymerase. Journal of Virology **53:**501-508.

347. **Vlazny, D., A. Kwong, and N. Frenkel.** 1982. Site-specific cleavage/packaging of herpes simplex virus DNA and the selective muturation of nucleocapsids containing full length viral DNA. Proceedings of the National Academy of Sciences USA **79:**1423-1427.

348. **Wadd, S., H. Bryant, O. Filhol, J. E. Scott, T. Y. Hsieh, R. D. Everett, and J. B. Clements.** 1999. The multifunctional herpes simplex virus IE63 protein interacts with

heterogeneous ribonucleoprotein K and with casein kinase 2. Journal of Biological Chemistry **274:**28991-28998.

349. **Wagner, E. K., J. J. Garcia Ramirez, S. W. Stingley, S. A. Aguilar, L. Buehler, G. B. Devi-Rao, and P. Ghazal.** 2002. Practical Approaches to Long Oligonucleotide-Based DNA Microarray: Lesson from Herpesviruses. Progress in Nucleic Acid Research and Molecular Biology **71:**445-491.

350. **Warner, M. S., R. J. Geraghty, W. M. Martinez, R. I. Montgomery, J. C. Whitbeck, R. Xu, R. J. Eisenberg, G. H. Cohen, and P. G. Spear.** 1998. A cell surface protein with herpesvirus entry activity (HveB) confers susceptibility to infection by mutants of herpes simplex virus type 1, herpes simplex virus type 2 and pseudorabies virus. Virology **246**.

351. **Watson, R. J., and J. B. Clements.** 1980. A herpes virus type 1 function continuously required for early and late virus RNA sythesis. Nature **285:**329-330.

352. **Waugh, S. M. L., D. Pillay, D. Carrington, and W. F. Carman.** 2002. Antiviral prophylaxis and treatment (excluding HIV therapy). Journal of Clinical Virology **25:**241-266.

353. **Weinheimer, S. P., B. A. Boyd, S. K. Durham, J. L. Resnnick, and D. R. O'Boyle.** 1992. Deletion of the VP16 open reading frame of herpes simplex virus type 1. J. Virol. **66:**258-269.

354. **Whitley, R. J.** 2001. Herpes Simplex Viruses, p. 2461-2509. *In* D. M. Knipe, P. M. Howley, D. E. Griffin, R. A. Lamb, M. A. Martin, B. Roizman, and S. E. Straus (ed.), Fields Virology, vol. 2. Lippincott Williams & Wilkins, Philadelphia.

355. **Whitley, R. J., D. W. Kimberlin, and B. Roizman.** 1998. Herpes simplex viruses. Clin Infect Dis **26:**541-53.

356. **Whittaker, G. R., M. P. Riggio, I. W. Halliburton, R. A. Killington, and G. P. Allen.** 1991. Antigenic and protein sequence homology between VP13/14, and herpes simplex virus type 1 tegument protein, and gp10, a glycoprotein of equine herpesvirus 1 and 4. Journal of Virology **65:**2320-2326.

357. **Williams, M. V.** 1984. Deoxyuridine triphosphate nucleotidohydrolase induced by herpes simplex virus type 1. Purification and characterization of induced enzyme. J Biol Chem **259:**10080-10084.

358. **Wu, C. A., N. J. Nelson, D. J. McGeoch, and M. D. Challberg.** 1988. Identification of herpes simplex virus type 1 genes required for origin-dependent DNA synthesis. J. Virol. **62:**435-443.

359. **WuDunn, D., and P. G. Spear.** 1989. Initial interaction of herpes simplex virus with cells is binding to heparan sulfate. J. Virol. **63:**52-58.

360. **Xu, F., J. A. Schillinger, M. R. Sternberg, R. E. Johnson, F. K. Lee, A. J. Nahmias, and L. E. Markowitz.** 2002. Seroprevalence and coinfection with herpes simplex virus type 1 and type 2 in the United States. Journal of Infectious Diseases **185:**1019-1024.

361. **Yang, Y. H., S. Dudoit, P. Luu, D. M. Lin, V. Peng, J. Ngai, and T. P. Speed.** 2002. Normalization for cDNA microarray data: a robust composite method addressing single and multiple slide systematic variation. Nucleic Acids Research **30:**e15.

362. **Yeung-Yue, K. A., G. Torres, M. H. Brentjens, P. C. Lee, and T. S. K.** 2003. Herpes Simplex Virus, p. 165-192. *In* H. Rubsamen-Waigmann, K. Deres, G. Hewlett, and R. Welker (ed.), Viral Infections and Treatment, vol. 30. Marcel Dekker, Inc., New York.

363. **Zelus, B. D., R. S. Stewart, and J. Ross.** 1996. The virion host shutoff protein of herpes simplex virus type 1: messenger ribonucleolytic activity in vitro. J. Virol. **70:**2411-2419.

364. **Zhou, C., and D. M. Knipe.** 2002. Association of hepes simplex virus type 1 ICP8 and ICP27 proteins with cellular RNA polymerase II holoenzyme. JOurnal of Virology **76:**5893-5904.

365. **Zhou, Z. H., D. H. Chen, J. Jakana, F. J. Rixon, and W. Chiu.** 1999. Visualization of tegument-capsid interactions and DNA in intact herpes virus type 1 virions. Journal of Virology **73:**3210-3218.

366. **Zhou, Z. H., B. V. Prasad, J. Jakana, F. J. Rixon, and W. Chiu.** 1994. Protein subunit structures in the herpes simplex virus A-capsid determined from 400 kV spot-scan electron cryomicroscopy. J Mol Biol **242:**456-69.